Investigating Microbial Trace-fossils and Abiotic Alteration in Hydrovolcanic Tuffs of the Fort Rock Volcanic Field, Oregon

by

Matthew Peter Casimir Nikitczuk, Honours. B.Sc.

Brock University

Submitted

in partial fulfillment of the requirements

for the degree

Master of Science in Earth Sciences

Faculty of Mathematics and Science, Brock University

St. Catharines, Ontario

Master of Science (2015) Brock University
(Earth Sciences) St. Catharines, ON, Canada

TITLE: Investigating Microbial Trace-fossils and Abiotic Alteration in Hydrovolcanic Tuffs of the Fort Rock Volcanic Field, Oregon

AUTHOR: Matthew Peter Casimir Nikitczuk, Honours B.Sc.

(Brock University, St. Catharines, Ontario, Canada, 2013)

SUPERVISOR: Professor, Dr. Mariek E. Schmidt

NUMBER OF PAGES: 271

Dedicated in loving memory to Monica Koziej Wowchuk (Babcia).

ABSTRACT

Microbial ichnofossils in volcanic rocks provide a significant record of subsurface microbes and potentially extraterrestrial biosignatures. Here, the textures, mineralogy, and geochemistry of two continental basaltic hydrovolcanic deposits - Reed Rocks and Black Hills - in the Fort Rock Volcanic Field (FRVF) are investigated. Methods include petrographic microscopy, micro and powder X-ray diffraction, SEM/BSE/EDF imaging, energy dispersive spectroscopy, stable isotopes, and X-ray fluorescence. Petrographic analysis revealed granular and tubular textures with biogenic morphologies that include terminal enlargements, septate divisions, branching forms, spiral filaments, and ovoid bodies resembling endolithic microborings described in ocean basalts. They display evidence of behaviour and a geologic context expressing their relative age and syngenicity. Differences in abiotic alteration and the abundance/ morphotype assemblage of putative microborings between the sites indicate that water/rock ratio, fluid composition and flux, temperature and secondary phase formation are influences on microboring formation. This study is the first report of reputed endolithic microborings in basalts erupted in a continental lacustrine setting.

Key words: hydrovolcanism; basaltic glass; palagonite; endolithic microborings; Fort Rock Volcanic Field

ACKNOWLEDGEMENTS

First and foremost, I must praise my supervisor Dr. Mariek Schmidt. Since I began working as Mariek's undergraduate research assistant, I have had many great things come my way. I am grateful that over the course of this project, I've been able to work independently and trusted to produce something acceptable. Thank you for going along with the change in focus credited to, like many great scientific research projects, an unexpected discovery and for always encouraging me and believing in me, even when I did not.

I also thank Dr. Roberta Flemming and Dr. Frank Fueten for being on my committee and for making suggestions that surely improved this document. Much thanks to Dr. Flemming for use of the XRD lab over the past few years, bringing much enthusiasm to the table and for considering me an ASTRO success story. Also, thank you to Dr. Martin Fisk for taking the time to review the early stages of the chapter 2 manuscript, providing valuable feedback and for agreeing to be my external examiner.

A special thanks goes to my parents Christine and Casimir Nikitczuk. Letting me live in that basement throughout my university career has made life so much easier. Thanks mom and dad for loving and supporting me, no matter how long I stayed in school and at home.

Funding for this research was provided by the Canadian Space Agency (CSA) Astromaterials Training and Research Opportunity (ASTRO), Ontario Graduate Scholarship (OGS), and Natural Sciences and Engineering Research Council (NSERC) Canadian Graduate Scholarship-Master`s (CGS-M) to Nikitczuk, as well as NSERC

Discovery Grant to Schmidt. Thank you Nevena Novakovic, Frank Popoli, Jeff Berger, and Rebekka Lee, for assisting in the collection of samples and field observations in Fort Rock, Oregon. Thank you to Marty Oulette of the Brock University petrographic lab for thin section preparation. The support of Alex Rupert, Michael Bramble, and Patrick Shepherd during X-ray diffraction analyses at the University of Western Ontario (Western) is greatly appreciated. For access to and assistance at the Zircon and Accessory Phase Laboratory (ZAPLab) at Western during SEM/EDS analysis, I am grateful to Desmond Moser and Ivan Barker. Thank you Marc Beauchamp for helping with EDF imaging at Western. Thank you to Karen Nygard for assisting me with fluorescence microscopy at Western (Biotron), and Kim Law for stable isotope analysis at Western (LSIS).

Of course, last but not least, one more note of appreciation. I have to thank those tiny little microbes that eat basaltic glass. I know there are more of you out there somewhere, chemically etching away. Keep up the good work contributing to global silicate weathering bacteria...probably.

TABLE OF CONTENTS

APPENDICES

LIST OF TABLES

Chapter 2

Chapter 3

LIST OF FIGURES

Chapter 1

Chapter 2

Chapter 3

Chapter 4

LIST OF ABBREVIATIONS AND SYMBOLS

AIT	Ambient inclusion trail
AM	Authigenic mineral
ASTRO	Astromaterials Training and Research Opportunity
BH	Black Hills - Study Site 2
CGS-M	Canadian Graduate Scholarship - Masters (NSERC)
CSA	Canadian Space Agency
DAPI	4',6-diamidino-2-phenylindole (fluorescent stain)
DNA	Deoxyribonucleic acid
EDF	Enhanced depth of focus
EDS	Energy dispersive spectroscopy
FR-	Fort Rock (sample number)
FG	Fresh glass
FRVF	Fort Rock Volcanic Field/ Fort Rock-Christmas Valley Lake Basin
GADDS	General Area Detector Diffraction system
GT	Granular texture
HREE	Heavy rare earth elements

ICDD	International Center for Diffraction Data
LKT	Low potassium tholeiite
LSIS	Laboratory for Stable Isotope Science (Western)
MSL	Mars Science Laboratory (Curiosity Rover)
NBS	National Bureau of Standards
NSERC	Natural Sciences and Engineering Research Council
OGS	Ontario Graduate Scholarship
P	Palagonite
REE	Rare earth elements
RNA	Ribonucleic acid
RRs	Reed Rocks (Reed Rock and South Reed Rock) - Study Site 1
RR	Reed Rock
SEM	Scanning electron microscope
SRR	South Reed Rock
TT	Tubular texture
UWO	University of Western Ontario
VPDB	Vienna PeeDee Belemnite

VSMOW	Vienna Standard Mean Ocean Water
µXRD	Micro X-ray diffraction
pXRD	Powder X-ray diffraction
WSU	Washington State University
XRF	X-ray fluorescence
ZAPLab	Zircon and Accessory Phase Laboratory

µm: micro-meter (micron)

‰: per mil (parts per thousand)

δ: difference in isotope ratio relative to a standard

Chapter 1

Introduction

One of the most widespread yet least investigated aspects of the ancient and modern biosphere is sub-surface microbial activity (McLoughlin et al., 2007). In sedimentary and biological substrates (e.g., sea shells, stromatolites), studies of traces formed microbes capable of bio-eroding materials (endoliths) are well established (e.g., Bathurst, 1966; Reyment et al., 1966; Margolis and Rex, 1971; Fabricius, 1977; Harris et al., 1979; Olempska, 1986; Zhang and Goloubic, 1987). Ichnofossils formed by microbes that have bio-eroded volcanic glass however, are a relatively new area of investigation. Basaltic glass is prone to alteration and readily forms distinctive alteration textures. Such textures that include palagonite and granular and tubular structures have been explained by physico-chemical processes only (Moore, 1966; Hay and Iijima, 1968; Jakobsson, 1972; Furnes, 1984; Staudigel and Hart, 1983; Crovisier et al., 1987; Thorseth et al., 1991). Several observations however, such as bacteria in altered glass and morphologically similar structures to microbial traces in biological and sedimentary substrates indicate that microbes play a role in the process and that the tubular and granular textures in basaltic glass are microbial ichnofossils. Microbes that inhabit volcanic rock interiors and the trace fossils formed by those that actively penetrate volcanic glass by dissolving it to obtain nutrients and/or energy have now been widely reported in oceanic crust (Thorseth et al., 1992, 1995, 2001, 2003; Furnes et al., 1996, 1999, 2001, 2005, 2007a, 2007b, Fisk et al., 1998a, 2003; Torsvik et al., 1998; McLoughlin et al., 2007; Walton, 2008). Studies detailing these biologically produced

alteration textures have mainly focussed on sub-marine pillow basalt hyaloclastites composed of basaltic glass (sideromelane) clasts formed by non-explosive pillow lava rind spalling and granulation (Rittmann, 1962). Less commonly, studies of volcaniclastic marine tuffs formed by explosive hydrovolcanism, and sub-glacially erupted lavas have also revealed ichnofossils in basaltic glass (Banerjee et al., 2003, 2011; Cousin et al., 2009; Cockell et al., 2009). Even though the presence of endoliths and their body fossils have been described in non-marine continental hydrovolcanics (e.g., Fisk et al., 1998b; McKinley et al., 2000), well preserved ichnofossils in basaltic glass produced by bio-erosion matching the morphologies and distributions of those described in oceanic crust have not been documented in a continental setting.

Although there has been an increase in studies focussing on microbial alteration textures in volcanic glass, the environmental conditions that control their production are still poorly understood. In addition to serving as valuable tracers of subsurface microbes on Earth, these textures also have the potential to be used as extra-terrestrial biosignatures on other planetary bodies, such as Mars (Freidmann and Koriem, 1989; McKay et al., 1992; Fisk et al., 1998; McLoughlin et al., 2007). It is therefore important to quantify a connection between the size, abundance, shape and/or distribution of these micro-textures and relate these to other variables. For example, porosity and permeability, depth in oceanic crust, fluid composition and flux, or temperature could be important factors influencing the biological processes responsible for bioalteration textures (Furnes et al., 1999, 2001; 2007a; Banerjee et al., 2003; McLoughlin et al., 2007; Cousins et al., 2009). Furthermore, proving that these textures are the result of biological processes can be difficult (McLoughlin et al., 2007).

This study primarily aims to: (1) investigate alteration textures believed to be microbial in origin in continental basaltic tuffs that are the product of explosive hydrovolcanism from the Fort Rock Volcanic Field (FRVF), Oregon; (2) compare textures with previous accounts in oceanic basalts and establish an argument for their biogenicity; and (3) determine any connections between microbial alteration textures and abiotic primary or secondary variables to improve our understanding of the biologically important factors governing their formation. In the following sections, the basics of hydrovolcanism will first be summarized, followed by abiotic glass alteration, endolithic microboring formation/occurrence, an introduction to the study sites and a general outline for the subsequent chapters of this thesis.

1.1. HYDROVOLCANISM/ PHREATOMAGMATISM

Hydrovolcanism also called phreatomagmatism, is a form of explosive volcanism that occurs when magma and an external water source (marine, lacustrine, fluvatile, ground, connate water) interact at or near the Earth's surface (Sheridan and Wohletz, 1983; Wohletz, 1983; Fisher and Schmincke, 1984). Originally, the term phreatomagmatic was defined as an interaction only with groundwater (Stearns and Vaksvik, 1935). Because this definition is restrictive, the terminology throughout this document will follow Fisher and Schmincke (1984) and use hydrovolcanic synonymously with phreatomagmatic, to include interactions with water in any type of environment.

Three general forms of hydrovolcanoes (Fig. 1.1) produced in phreatomagmatic/ hydrovolcanic eruptions (Fig. 1.1.) include maars, tuff rings, and tuff cones (Lorenz,

1973). All three hydrovolcano types are found in the FRVF. Their shape depends upon the depth of water (at what depth below, at, or above ground surface) the magma interacts

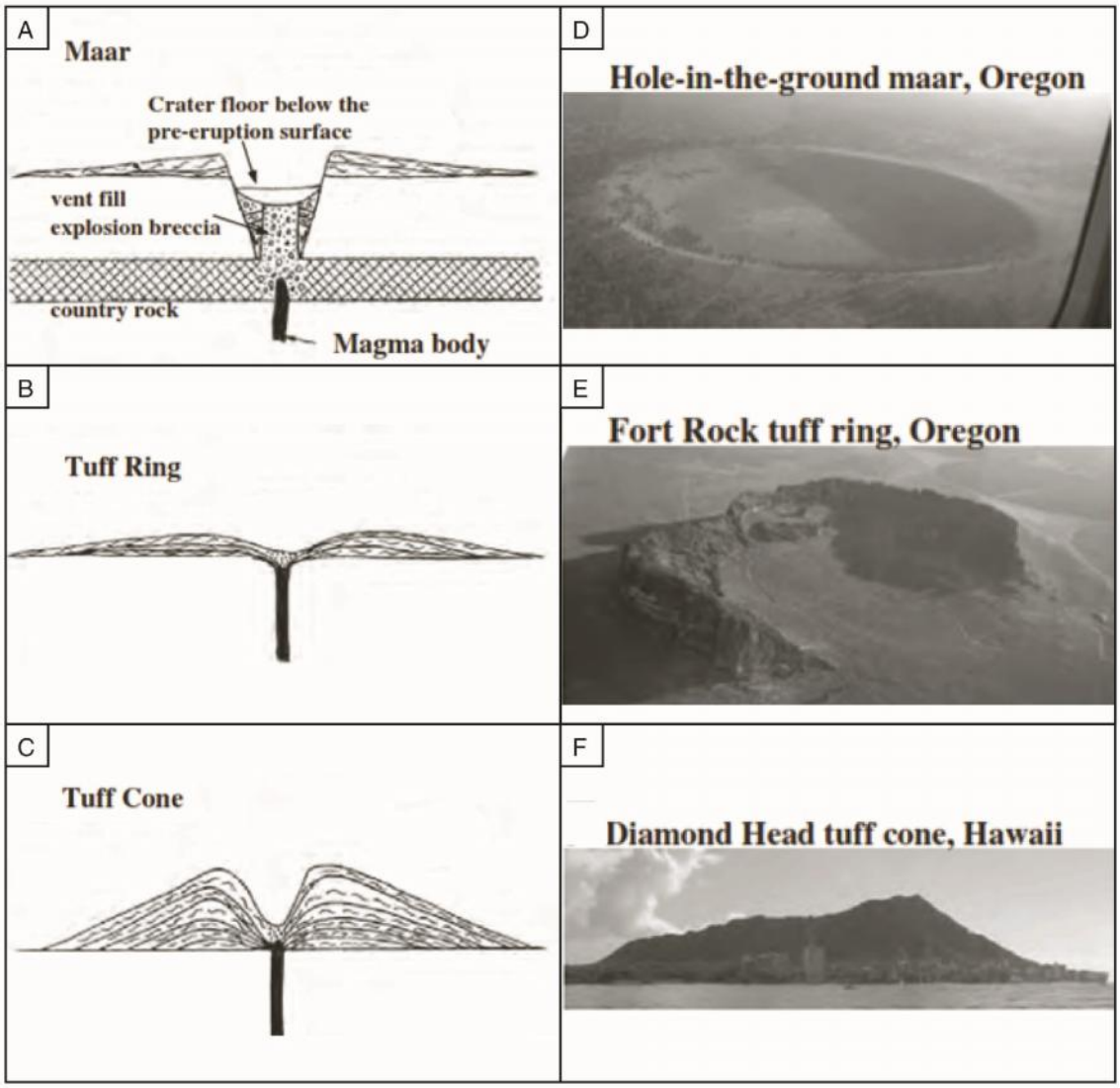

Figure 1.1. Schematic diagrams and examples of different hydrovolcano forms. (A) Maar. (B) Tuff ring. (C) Tuff cone (modified from Cas and Wright, 1988). (D) Hole-in-the-ground maar, ~1.4 km across. (E) Fort Rock tuff ring, ~0.8 km across. (F) Diamond Head tuff cone, ~2.5 km across. (Brand and Heiken, 2009)

with during magmatism. Tuff cones and tuff rings result from magma interacting with relatively shallow (<200 m for basaltic eruptions and tholeiitic islands) standing water either near or at the ground surface. The FRVF hydrovolcanoes, which are the focus of this this study are considered to be tuff rings. They are characterized by large craters enclosed by rims composed of pyroclastic deposits with diameters from 100 - 3000 m (Heiken, 1971; Lorenz, 1973; Heiken and Fisher, 2000). The distinction between tuff rings and cones is that cones have higher rims (up to 300 m) but were basically tuff rings that were volcanically active for longer durations or had interactions between magma and water at greater depths. This difference becomes subjective because in some instances hydrovolcanoes can have one side of the crater rim lower than the other. Maars result from magma interacting with groundwater and have a volcanic crater below or at surface level cut directly into country rock. Their diameters can range from 100 to 3000 m and they can include diatremes from 10 to >500 m in depth with low crater rims (few to ~100 m high) (Heiken, 1971; Lorenz, 1973; Heiken and Fisher, 2000).

When magma and external water come in contact, a rapid transfer of heat from the melt to water occurs that results in superheating, boiling, volatilization, gas pressure build-up of external water, and energetic explosive expansion of gas (vaporization) (Wohletz, 1983; Fisher and Schmincke, 1984; Cas and Wright, 1987; Houghton and Wilson, 1989). The main driving force for magmatic fragmentation is the high energy interaction between water and magma. Depending on magmatic volatile content, fragmentation can secondarily occur by expansion of magmatic volatiles (Houghton and Wilson, 1989; Cole et al., 2001).

Several micro- and macro-textural features in volcanic deposits can indicate factors such as the relative water content and fragmentation or depositional mechanisms. The products of hydrovolcanism consist primarily of fine-grained juvenile (formed directly from magma cooling) ash fragments, or pyroclasts, composed of glass (Fig. 1.2), although many hydrovolcanic eruptions also produce coarse-grained lapilli- and tuff-breccias (Fig. 1.3) inter-bedded with finer grained ash beds (Heiken and Fisher, 2000). Pyroclast formation depends on cooling rate (Fisher and Schmincke, 1984). Rapid cooling rates are the product of the high heat capacity and conductivity of water. During eruption, quenching of silicate melts occurs, initially forming super-cooled liquids, which then quickly transform into a solid amorphous glass material (Ryan and Sammis, 1981). When the glass is basaltic in composition it is termed sideromelane (Fisher and Schmincke 1984). Cooling rates at lava/air contacts are too low for quenching to occur, therefore an important characteristic indicating that basaltic magma was quenched by external water is the large quantity of sideromelane (Fisher and Schmincke, 1984).

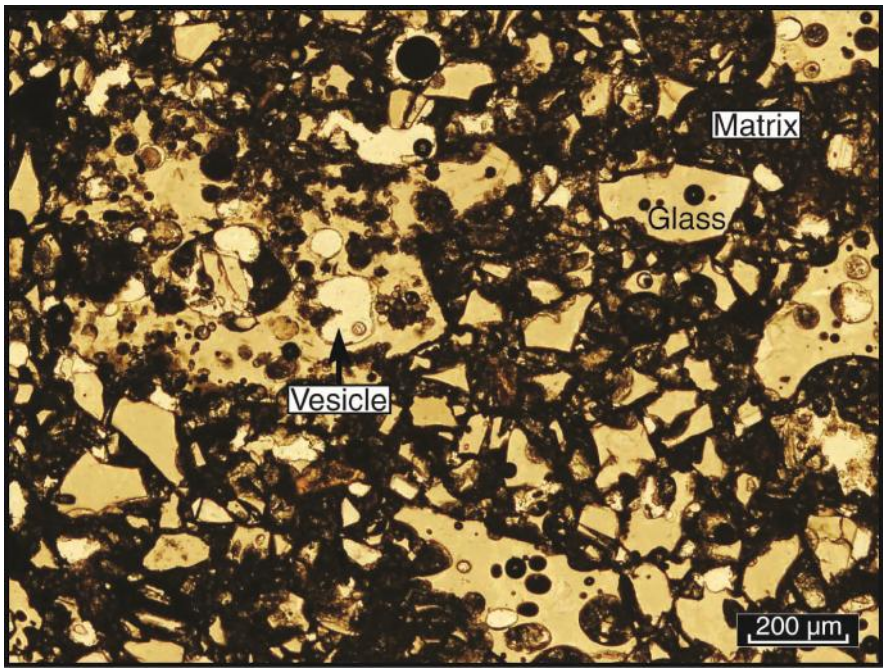

Figure 1.2. Photomicrograph of blocky-angular coarse ash sideromelane pyroclasts from South Reed Rock tuff ring. Most pyroclasts in this thin section do not have vesicles, but some larger ash grains have low vesicularities and a combination of angular and scalloped margins with fractures transecting vesicles and flat to curved surfaces mainly produced by thermal shock cracking.

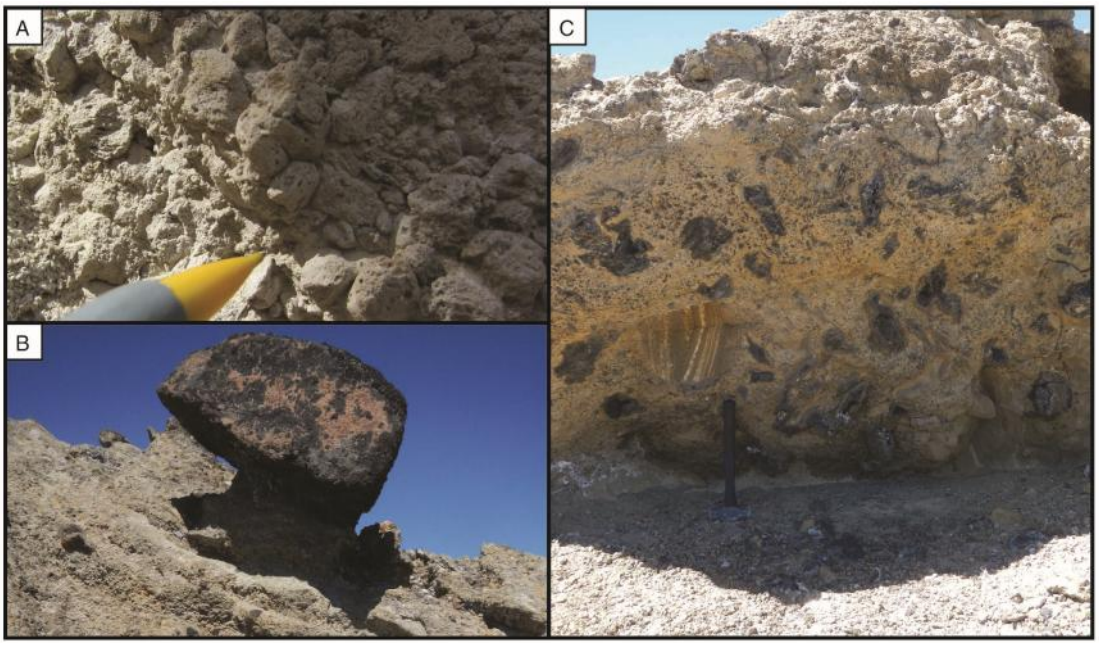

Figure 1.3. (A) Clast rich lapilli-tuff from South Reed Rock, Fort Rock Volcanic Field. Vesicles are visible on individual lapilli pyroclasts that comprise the majority of this tuff layer. Pencil for scale. (B) Large accidental lithic block (~1 m in diameter) embedded in surrounding finer grained tuff at Reed Rock. (C) Hydrovolcanic tuff-breccia with abundant juvenile scoria bombs (dark clasts) and a cognate clast (left of center, above hammer) derived from a diatomite and ash inter-bedded tuff from Black Hills, Fort Rock Volcanic Field.

Pyroclast shapes depend on the fragmentation mechanism acting during hydrovolcanism. Rapid cooling and thermal shock cracking during steam eruptions forms pyroclasts that have blocky non-vesicular shapes with fracture bound surfaces or are slightly vesicular with fracture bound surfaces transecting vesicles (Fig. 1.2). More highly vesicular pyroclasts with scalloped margins result from volatile expansion/magma vesiculation. The combination of these pyroclast shapes are usually indicative of eruption through shallow water (Heiken and Fisher, 2000). Accretionary and armoured lapilli may form when quenched lava or crystal or rock fragments act as a nuclei and become covered in fine or coarse ash, or when moisture and cohesive ash cause the accretion of fine and/or coarse ash in wet spherical balls (Waters and Fisher, 1971). In addition to juvenile clasts, hydrovolcanic tuffs often contain accidental lithic clasts derived from country rock (Fig. 1.3B), cognate clasts (Fig. 1.3C) derived from earlier explosions of the same eruption (Fisher and Schmincke, 1984) and in some cases, ultramafic xenoliths believed to be derived from mantle sources (e.g., White 1966; Jackson and Wright, 1970; Stosch and Seck, 1980). No xenoliths have been identified in the FRVF.

Hydrovolcanic deposits are characterized by well-developed beds dipping radially (quaquaversal) both toward and away from the vent (Figs. 1.1B-C, 1.4). Bed thicknesses range from several millimeters to more than a few tens of centimeters with the majority around 10 cm (Heiken, 1971). Abundant thin millimeter to centimeter scale beds represent a high frequency of short explosive pulses (Fig. 1.4A-B). Thicker (several tens of centimeters or more) beds represent more sustained eruptive pulses (Fig. 1.4C). Bedding features such as soft-sediment deformation are usually present and can indicate the relative wetness of the deposits (Fig. 1.5). Bedding sags (Fig. 1.5A), also referred to

as bomb sags, can form when a ballistically-ejected bomb, block or lapilli clast impacts a bed with a high enough water content to be plastically deformed (Wentworth 1926). The underlying penetrated beds are thinned out and folded as the impacting clast drags downwards, often producing micro-faults (Heiken, 1971). Convolute laminations or folded beds (Fig. 1.5C) may form when water saturated tephra slide down-slope by gravity (Heiken, 1971) or when base surges flow over a water saturated layer causing deformation by shearing (Schmincke, 1970).

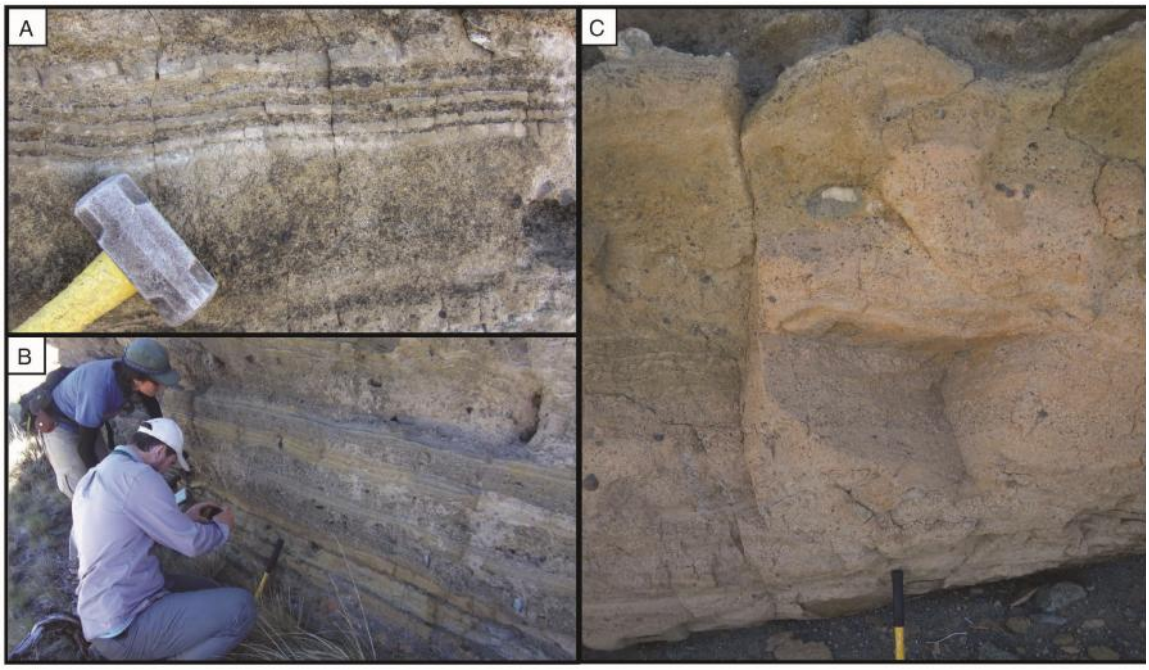

Figure 1.4. Examples of hydrovolcanic bedding characteristics. (A-B) Alternating fine and coarse ash beds representing deposition from individual explosive pulses from Black Hills and Reed Rock, respectively. Hammer and geologists for scale. (C) Massive (> 1 m thick) orange-yellow palagonitized tuff bed bound by darker, coarser tuff layers.

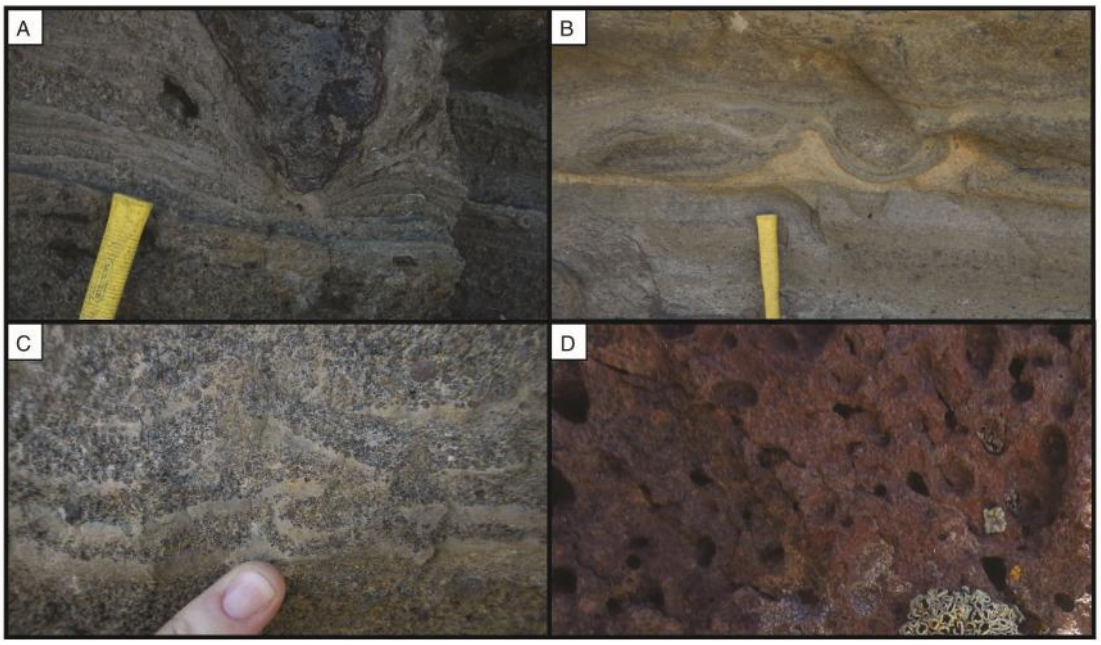

Figure 1.5. Examples of soft sediment deformation that indicate wet pyroclastic deposits. (A) Bedding sag or bomb sag at Reed Rock. The deformed tuff layers have resulted from a ballistic impact of a lava bomb into a water saturated deposit. (B) Orange yellow layer at Black Hills has been deformed by depositing tuff above likely in a base surge causing shearing and bed loading. (C) Convolute bedding at Black Hills caused by shearing either by down slope movement by gravity or base surge deposition. (D) Vesiculated tuff matrix at Reed Rock caused by magma degassing, evaporation of water, rain turned into steam, or hot pyroclast degassing. Vesicle sizes range from 0.5-1.5 cm.

Vesiculation can occur in tuff matrix as a result of gas derived from the magma degassing, evaporation of water or ice beneath hot ash, rain turned into steam, or from degassing of hot pyroclasts (Fig. 1.5D). Matrix vesicles with clay or silt coatings, associations with plastic deformation features or more lithified beds compared to non-vesicular beds are evidence that vesicular tuff contained 15-20% water or vapour when it was deposited (Heiken, 1971). Mud cracks can also form in fine-grained tuffs as a result of desiccation (Lorenz, 1974).

1.2. ALTERATION OF BASALTIC GLASS - PALAGONITE

One method of constraining alteration conditions is to characterize abiotic alteration textures and mineralogy. Basaltic glass, the main component of hydrovolcanic deposits, is readily prone to alteration because it is thermodynamically unstable, especially with respect to the primary igneous minerals. Therefore the various basaltic rocks, including hydrovolcanic pyroclastic deposits and ocean crust contain aqueous (abiotic) hydrothermal or low temperature alteration textures. The most common product of glass alteration is a yellow to orange-brown coloured material known as palagonite (Fig. 1.6) that possesses a wide range of structural and optical properties (Stroncik & Schmincke, 2002). Palagonite occurs along exterior or internal rock surfaces that are exposed to circulating fluids. Planar alteration fronts form along fractures and margins of glassy pyroclasts, pillows and hyaloclastite clasts (Fig. 1.6). Regular banding of palagonite is thought to result from congruent to incongruent dissolution and re-precipitation of insoluble secondary phases. Via congruent dissolution, a solid phase (glass) transitions to a liquid (water) of the same composition whereas during incongruent dissolution, material is converted from a primary solid phase to a secondary solid phase

(Allaby and Allaby, 1999). Secondary phases may include smectites or other mixed layer phyllosilicates, zeolites or iron-oxy-hydroxides (Peacock, 1926; Zhou and Fyfe, 1989; Techer *et al*., 2000, Stroncik and Schmincke, 2001, 2002).

Palagonite can be divided into two varieties. The first is amorphous (Fig. 1.6A) whereas the second is proto- to wholly crystalline (Fig. 1.6B-D). Stroncik and Schmincke (2001) suggested using only the term 'palagonite' to describe the amorphous variety of the glass alteration product but here we distinguish between amorphous gel- palagonite and crystalline fibro-palagonite (Peacock, 1926). Gel-palagonite forms adjacent to fresh unaltered glass and is isotropic, clear, usually yellow and transparent (Fig. 1.6A). Concentric banding of gel-palagonite is common and is often enhanced by differences in alteration ages and in Fe and Ti-oxide contents. Fibro-palagonite is a later alteration product that forms on the exterior surfaces of gel-palagonite (Fig. 1.6B-D) and develops a more translucent, anisotropic, birefringent, fibrous lath-like or granular character (Peacock, 1926; Zhou and Fyfe, 1989). More intensely-coloured than gel-palagonite, fibro-palagonite may be a combination of smectite clay and gel palagonite. These palagonite types likely represent different stages in the alteration evolution from the amorphous gel-palagonite to the later, more crystalline smectite clays (Stroncik and Schmincke, 2002).

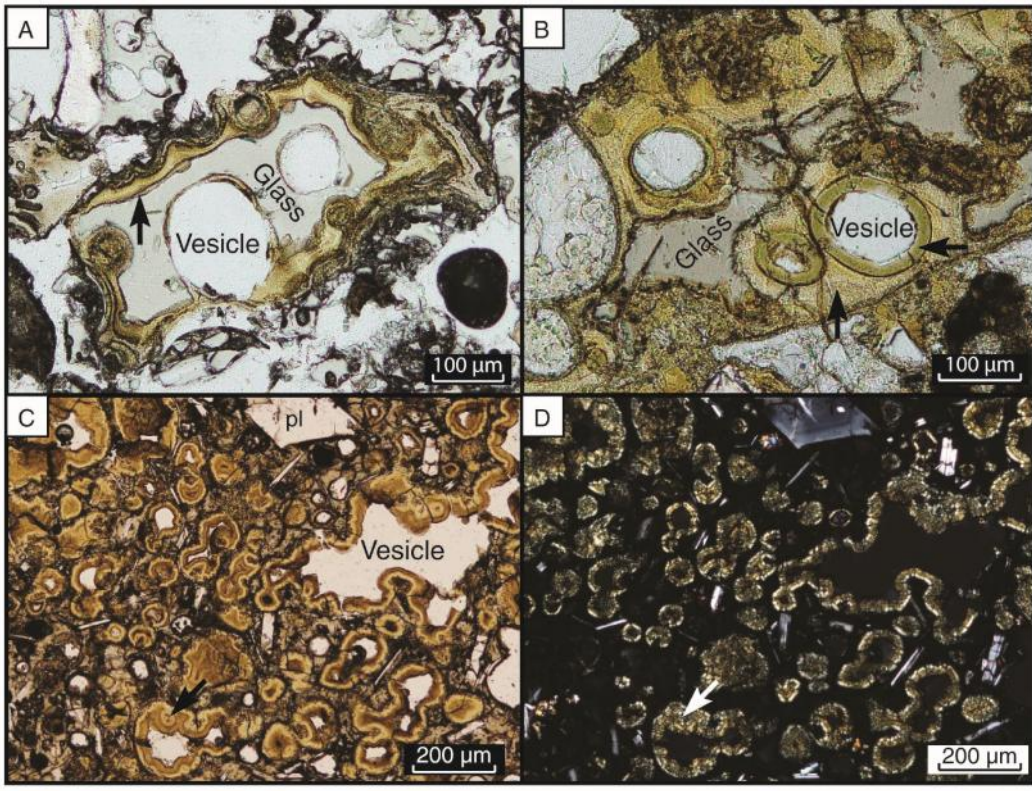

Figure 1.6. Examples of abiotic glass alteration (palagonite). (A) A vesicular, angular basaltic glass (sideromelane) coarse ash pyroclast from South Reed Rock. The clast has a regular banded, amorphous (isotropic) gel-palagonite alteration rim (arrow) around its margin. (B) Vesicular basaltic glass coarse ash pyroclast from South Reed Rock with amorphous gel-palagonite (left arrow) and proto-crystalline fibro-palagonite alteration (right arrow) rimming vesicles. The darker proto-crystalline fibro-palagonite rimming the vesicle (right arrow) has replaced the amorphous gel-palagonite. (C-D) Regular banded crystalline yellow-orange fibro-palagonite alteration rims (arrows) surrounding vesicles in a basaltic glass lapilli pyroclast from Black Hills. Image in C is in plane polarized light whereas D is in cross-polarized light. The distinct crystallinity (anisotropism) is prominently visible in crossed polars.

1.3. ENDOLITHIC MICROBORINGS: FOSSIL EVIDENCE OF MICROBES INHABITING VOLCANIC ROCKS

The main focus of this study is to document putative trace fossils produced by microbes known as endoliths. Endoliths include archaea, bacteria, algae and fungi that live within the interior of rocks (McLoughlin et al., 2007). There are three main types of endoliths including *chasmo-, crypto-* and *eu-endoliths* that are differentiated by the specific endolithic niche they dwell in. *Chasmoendoliths* inhabit cracks and crevices and *cryptoendoliths* reside within the natural pore spaces of rocks. These types only inhabit rocks that are weathered and pervaded by crevices/fissures or possess porous internal structures. *Euendoliths* on the other hand, actively bore into rocks and produce micro-pits and/or tubular micro-cavities (Golubic et al., 1981). An endolithic organism may adopt different habits either in response to external environmental fluxes or at different stages in its lifecycle (e.g., De los Ríos et al., 2005). The micro-pits/tubular micro-cavities left behind by euendoliths in affected rocks, known as *endolithic microborings*, are considered trace-fossils (ichnofossils) because they record the presence or boring behaviour of the organisms that produced them.

1.3.1. Rock Substrates with Evidence of Euendoliths

Endolithic microborings have been most widely documented in carbonate rocks (including oolites), bone and shell substrates, sand grains, and silicate desert rocks (e.g., Margolis and Rex, 1971; Fabricius, 1977; Harris et al., 1979). The most well-known occurrences are of algae, which appear to be the predominant boring organisms in marine carbonate rocks (e.g., Newell et al., 1960). Examples from molluscan shells (Bathurst,

1966), Paleocene and Ordovician ostracod valves (Olempska, 1986; Reyment et al., 1966) and Ordovician trilobite carapaces have also been described. Some of the oldest known preserved endolithic microborings on Earth are found in silicified stromatolites dated at 1.7 Ga (Zhang and Golubic, 1987).

Evidence of endoliths has also been described within glass substrates (sideromelane) of volcanic rocks. Features in natural basaltic glass in the form of grooved etch patterns on grain surfaces were first observed by Ross & Fisher (1986) from Miocene Obispo marine Tuff at Shell Beach, central California and Deep Creek marine Tuff in Miocene John Day Formation, eastern Oregon. In the high silica rhyolite ignimbrite Rattlesnake Tuff in Oregon, Fisk et al. (1998b) found bio-films with rod-shaped microbial colonies covering glass shard surfaces. In the Columbia River basalt lava flows, McKinley et al. (2000) found bacteriomorphs of fossilized microbes. In altered Icelandic hyaloclastites, Thorseth et al. (1992) observed bacteria associated with glass-etched channels, and palagonitic alteration with minute pores matching the dimensions of the bacteria. Experiments by Thorseth et al. (1995) and Staudigel et al. (1995) provided evidence that glass dissolution was biologically mediated. Bacterial attachment and bio-film growth accompanying the production of etch marks, as well as significant surficial corrosion resulting in grooving similar to that observed by Ross and Fisher (1986), respectively, were observed. These earlier findings prompted further investigation focussing on endoliths in volcanic rocks. Endolithic microborings have now been documented in oceanic crust pillow lavas, marine tuffs, subglacial lavas/hyaloclastites and more putatively, metamorphosed greenstone belts and ophiolites (e.g., Furnes et al, 1996; Fisk et al., 1998; Furnes et al., 2004, 2005; Banerjee et al., 2003;

2006, 2007; Cockell et al., 2009; Cousins et al., 2009). This study aims to further expand this set of volcanic rocks to include continental hydrovolcanic tuffs erupted in a lacustrine setting that has not been affected by marine or glacial melt water.

1.3.2. Texture, Morphology, and Distribution of Endolithic Microborings in Volcanic Glass

Two textural types related to microbial bioalteration in volcanic glass that are both texturally and chemically distinct from abiotic palagonitic alteration have been observed. These types termed *tubular* and *granular* are the textures widely observed in oceanic basalts. To characterize the suite of putative bioalteration textures in the basalts of this study, they are compared to those reported in ocean basalts. Tubular and granular textures are always associated with surfaces exposed to water such as fractures, clast or pillow margins, and vesicles. The *granular* type (Fig. 1.7) is characterized by individual globular/spherical bodies initially isolated from one another with typical dimensions < 1 µm in diameter. In more advanced alteration stages, the globular/spherical bodies coalesce to become amalgamated granular collections (Furnes et al., 2001). The *tubular* type (Fig. 1.8) consists of curving or straight tube-like structures that can reach dimensions of 1-5 µm in diameter and up to >200 µm in length. Tubular and granular structures may be hollow or infilled with crypto-crystalline or very fine-grained phyllosilicate material (smectites), and result in irregular, asymmetrical alteration fronts that protrude into fresh glass (Furnes et al., 2001, Furnes et al., 2007a; McLoughlin *et al*., 2007; Staudigel *et al*., 2008).

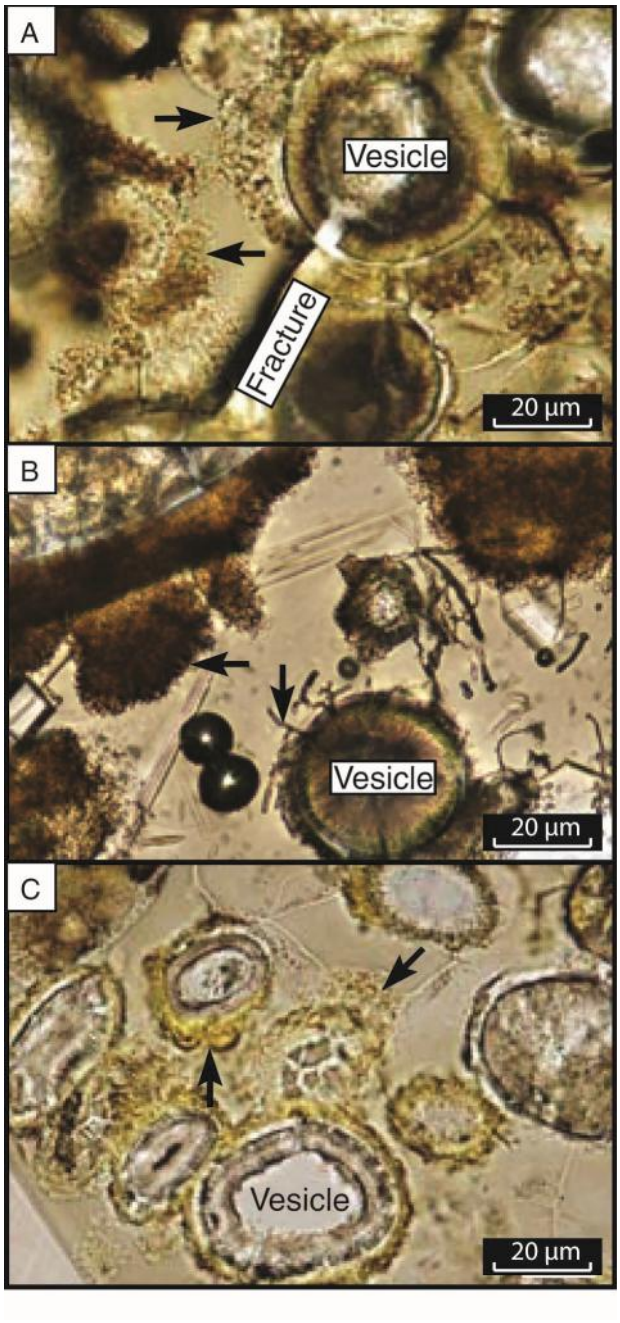

Figure 1.7. Examples of granular type alteration. (A) Wide granular incursions (arrows) are visible extending from fractures and connected vesicle surfaces in a vesicular basaltic glass pyroclast from Black Hills. (B) Wide, rounded granular incursion (left arrow) extending from the margin of a pyroclast from Black Hills. Other simple tubular micro-tunnels (right arrow) can be seen at center extending from the vesicle. (C) Irregular pitted alteration fronts extending from vesicles in a basaltic glass pyroclast from the Black Hills. Alteration fronts consist of the granular-bubble sub-type alteration (arrows).

Tubular alteration textures can show a range of morphologies including straight to curving, spiraling/corkscrew, enlargements or bud-like structures along their lengths or at termini (Fig. 1.8), bifurcations/branching, segmentation and internal filaments or ovoid bodies (Fisk et al., 1998, 2003; Furnes et al., 2001, Furnes et al., 2007a). These distinct morphological characteristics are considered indications of biological origin (Thorseth et

al., 1995, 2001, 2003; Furnes et al., 1996, 1999, 2001, 2005, 2007a, 2007b, Fisk et al., 1998a, 2003; Torsvik et al., 1998; Banerjee et al., 2003, 2011; McLoughlin *et al*., 2007; Staudigel *et al*., 2008; Walton, 2008). These features may be oriented perpendicular to alteration fronts, radially from vesicles or varioles, randomly, aligned parallel to adjacent tunnels, or growth direction may change by up to 180° in response to other tunnels, crystals, or fractures (Furnes et al., 2001, Furnes et al., 2007a). Tubes may develop from single tunnels into compact bundles of multiple elongated tunnels (Furnes et al.., 2007a). Tubular alteration is generally more commonly observed because it is more easily identified owing to its larger dimensions and higher preservation potential than the granular type. This appears to be the case in the Reed Rocks and Black Hills tuffs, and as a result, the characterization of bioalteration textures in this study is focussed more on the tubular type.

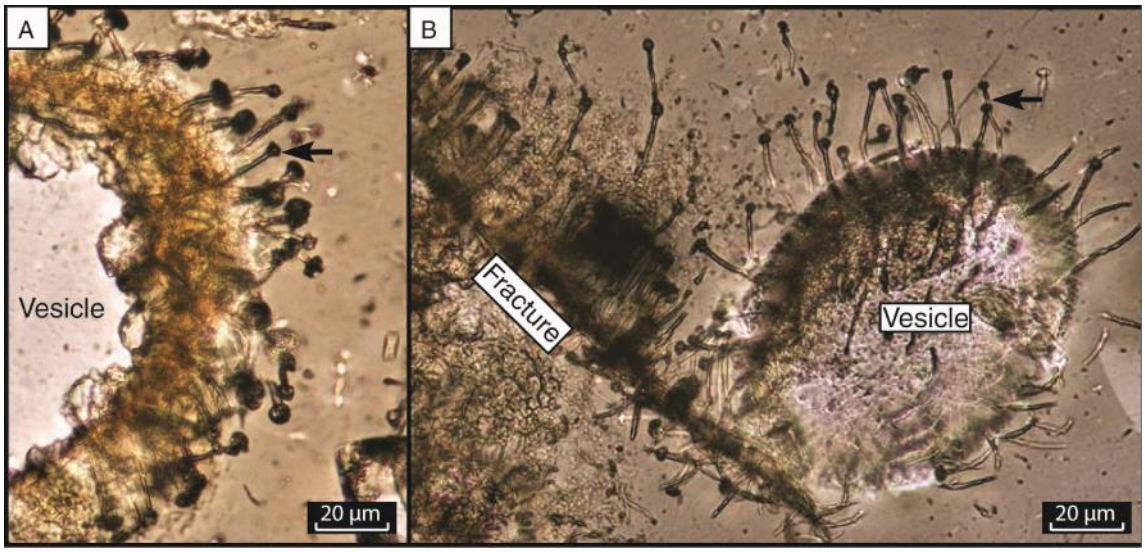

Figure 1.8. (A-B) Tubular microborings with terminal enlargements extending from vesicles and a connected fracture in basaltic glass pyroclasts from Reed Rock.

1.3.2.1. Possible Constructing Organisms

The largest reported borings found in corals (20-40 µm and 2-6 µm) are produced by algae and some larger, modern cyanobacteria, respectively (Chazottes et al., 1995). Generally bacterial and nano-bacterial borings < 1 µm wide are the smallest (c.f. Folk and Raspberry, 2002). Even with evidence indicating that these recurrent structures are the result of microbial activity, the specific organisms responsible for volcanic microborings have still not been identified. It is also likely that multiple organisms can produce structures with the same morphologies (McLoughlin et al., 2009). This is especially more likely for the simpler granular and tubular forms. It is also possible that under differing environmental conditions and with varying geochemical compositions, a single microbe may be capable of constructing microborings with multiple morphologies (McLoughlin et al., 2009). Hence a one-to-one relationship between the organisms responsible and the morphology of the structures is likely not the case.

In non-volcanic rocks, fungi, red and green algae, and cyanobacteria are the most common euendoliths (Perry, 1988; Ghirardelli, 2002). In basaltic glass, heterotrophic bacteria and chemolithoautotrophs capable of oxidizing Fe and Mn are the most likely organisms responsible for bioalteration textures (McLoughlin et al., 2007). Molecular profiling studies have revealed that microbes inhabiting submarine basalts belong to a limited set of bacteria phylogenetic groups and one group of archaea that do not match those colonizing the surrounding seawater or sea-floor sediments (Lysnes et al., 2004; Mason et al., 2007, and references therein). It is unclear how widespread bacteria are in terrestrial volcanic environments however, and some oceanic island hyaloclastites display a dominance of archaea (e.g., Fisk et al., 2003).

1.3.3. Generation of Granular and Tubular Textures

Basaltic glass is considered a high quality substrate capable of promoting microbial growth because it is essentially a chemical reservoir with nutrients and energy (Banerjee and Meuhlenbachs, 2003; Edwards *et al*., 2005; Staudigel *et al*., 2008; Cavalazzi *et al.*, 2012). Volcanic glass bio-erosion processes proposed may involve microbes that can directly alter the pH of their immediate surrounding areas and exude ligands (ions or molecules that attach to metal atoms) (Thorseth et al., 1992). It is also thought that various common groups of bacteria oxidize reduced Mn and Fe in glass (McLoughlin et al., 2008) and use oxidized compounds such as SO_2^{4-}, CO_2, Fe^{3+}, and Mn^{4+} in seawater as electron acceptors and sources of carbon (Staudigel et al., 2004). Bacterial moulds on glass resembling iron-oxidizing bacteria such as *Gallionella* and *Mariprofundus ferroxydans* that have bifurcating and entwined filaments have also been documented (e.g., Thorseth et al., 2001, 2003; Emerson et al., 2007). A significant metabolic strategy used by microbes contributing to bioalteration of basaltic glass may thus involve dissolution and oxidation of Fe and Mn (Furnes et al., 2007a).

Based on numerous observations of biotic alteration textures in basaltic glass pillow lava rims and glassy volcanic breccias (hyaloclastites), Furnes et al. (2007) proposed a model (Fig. 1.9) for the endolithic microboring process. It involves the breakdown or chemical etching and congruent dissolution of basaltic glass by microbes. This model illustrates how the distinct morphological dissimilarities between biogenic and abiotic alteration textures develop. Most notable is the irregular, non-planar alteration front produced during microbial alteration, whereas regular planar alteration fronts develop during abiotic alteration.

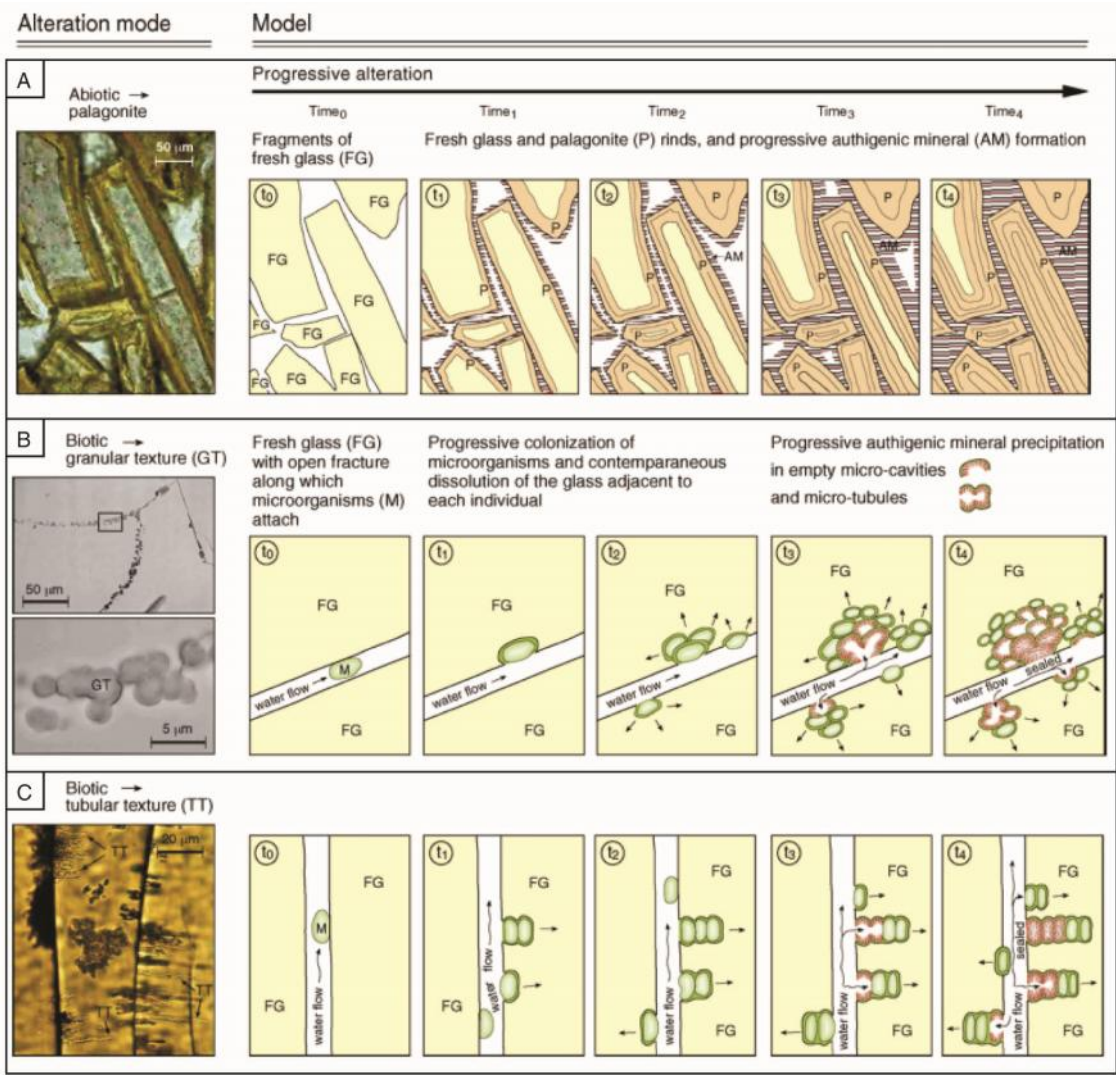

Figure 1.9. Model of alteration modes (abiotic and bioalteration) of basaltic glass. (A) Abiotic alteration in which the typically yellowish brown palagonite develops around the glass fragments with approximately equal thickness. With progressive alteration the empty spaces between the grains become filled with authigenic minerals and finally sealed, thus preventing water circulation and thus slowing down the alteration process. (B and C) Biotic alteration to granular (B) and tubular (C) types. In this model microbes attach to the glass surface where water can get access (along fractures and on the outer surface of grains) and start etching. With progressive alteration cell division occurs and the granular and/or segmented tubular structures develop as long as water is accessible. With progressive alteration there is also continuous growth of authigenic minerals in the empty micro-cavities and micro-tubules. When the authigenic minerals have sealed the structures preventing water access, the bioalteration growth eventually stops. From Staudigel et al. (2006).

1.3.4. Biogenicity Criteria

There are certain abiotic textural features that can resemble microbial bioalteration textures, therefore it is important to establish biogenicity. McLoughlin et al., (2007) proposed three lines of inquiry to test for biogenicity (Fig. 1.10). Here the following criteria are considered when evaluating the biogenicity of putative bioalteration textures in continental lacustrine hydrovolcanics of the FRVF.

1.3.4.1. Age and Syngenicity

The first criterion involves estimating the relative age of possible endolithic microborings by establishing that they are part of a depositional and diagenetic scheme. Relative ages may be deciphered by the documentation of micro-tunnel distributions and their relationship to features that likely served as pathways for fluids and microbes, such as fractures or clast margins. The relationship between microborings and infilling secondary phases and distinction from abiotic alteration are also important. For example, tunnels distributed on either side of an infilled fracture suggest that they formed prior to the fracture being infilled, because this would cut off the circulation of fluids. The growth of microbes is maintained as long as fluid is allowed to permeate the porous material (Thorseth et al., 2003, Furnes et al., 2007).

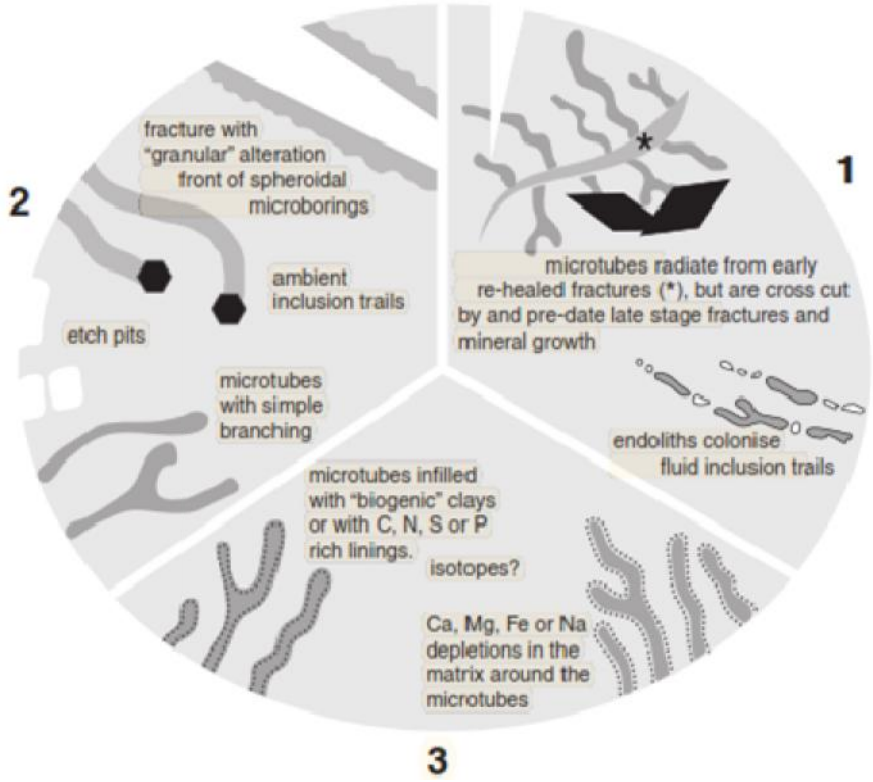

Figure 1.10. Schematic summary of the criteria required to demonstrate the biogenicity of a putative euendolithic microboring (McLoughlin et al., 2007). (1) *A geological context that demonstrates the syngenicity and antiquity of the putative biological remains.* Relative ages of candidate microborings can be determined by placing them in a diagenetic and depositional framework, or through absolute dating methods. (2) *A uniquely biogenic morphology and behaviour*. Compare with morphologies in sedimentary and other volcanic substrates and use criteria for distinguishing them from abiotic features such as ambient inclusion trails (AITs). (3) *Geochemical evidence for biological processing.* Use in situ analytical techniques, including scanning electron microscopy-energy dispersive X-ray (SEM/EDS), focused ion beam-transmission electron microscopy (FIB-TEM), and nanoSIMS to document fine scale compositional and isotopic variations within and around micro-tunnels.

1.3.4.2. Biogenic Morphology and Behaviour

Biogenicity also includes a demonstration of morphologies and behavioural characteristics that may be indicative of biology. Straight to curving, spiraling/corkscrew, enlargements or bud-like structures, bifurcations/branching, segmentation and internal filaments or ovoid bodies (Fisk et al., 1998, 2003; Furnes et al., 2001, Furnes et al., 2007a) have been considered strong indicators of biological origin. Directionality, abrupt changes in direction, and shapes and sizes similar to microbial species can indicate biological origins as well. Microborings in oceanic basalts have displayed tendencies to avoid plagioclase or to migrate toward olivine (McLoughlin et al., 2007), possibly caused by a preference of the microbe for metabolically required metals. Other characteristic distributions such as high concentrations of tunnels in areas surrounding vesicles and varioles may imply that the locations are chosen because they may have more exploitable structural defects caused by strain resulting in glass weaknesses or those locations have constrained chemical gradients (Furnes et al., 2007). Staudigel et al. (1995) demonstrated that certain areas on glass surfaces with either structural weaknesses, or submicroscopic rough regions were preferred for colonization. The terminology used to describe morphologies in this study follows Fisk and McLoughlin (2013) (Appendix 1A).

1.3.4.2.1. Ambient Inclusion Trails (AITs). Abiotic tubular structures (Fig. 1.11) produced through process involving mineral grains milling through the rock were first observed by Gruner (1923). These features were credited to metamorphic events and/or organic decomposition producing gases that force small grains through the matrices of rocks like 'millstones' resulting in hollow tubes (Tyler and Baghoorn, 1963; Knoll and Baghoorn, 1974). They are termed 'ambient inclusion trails' (AITs) and occur most

commonly in phosphorites and cherts. Morphological distinctions of AITs from endolithic microborings include metal sulfide or oxide grains present at the termini of tunnels, longitudinal striations, angular cross-sections, and microtubules cross-cutting one another. As of yet, no AITs have been reported in basaltic glass. See Appendix 1D for a summary chart of AIT and other tubular micro-cavity characteristics.

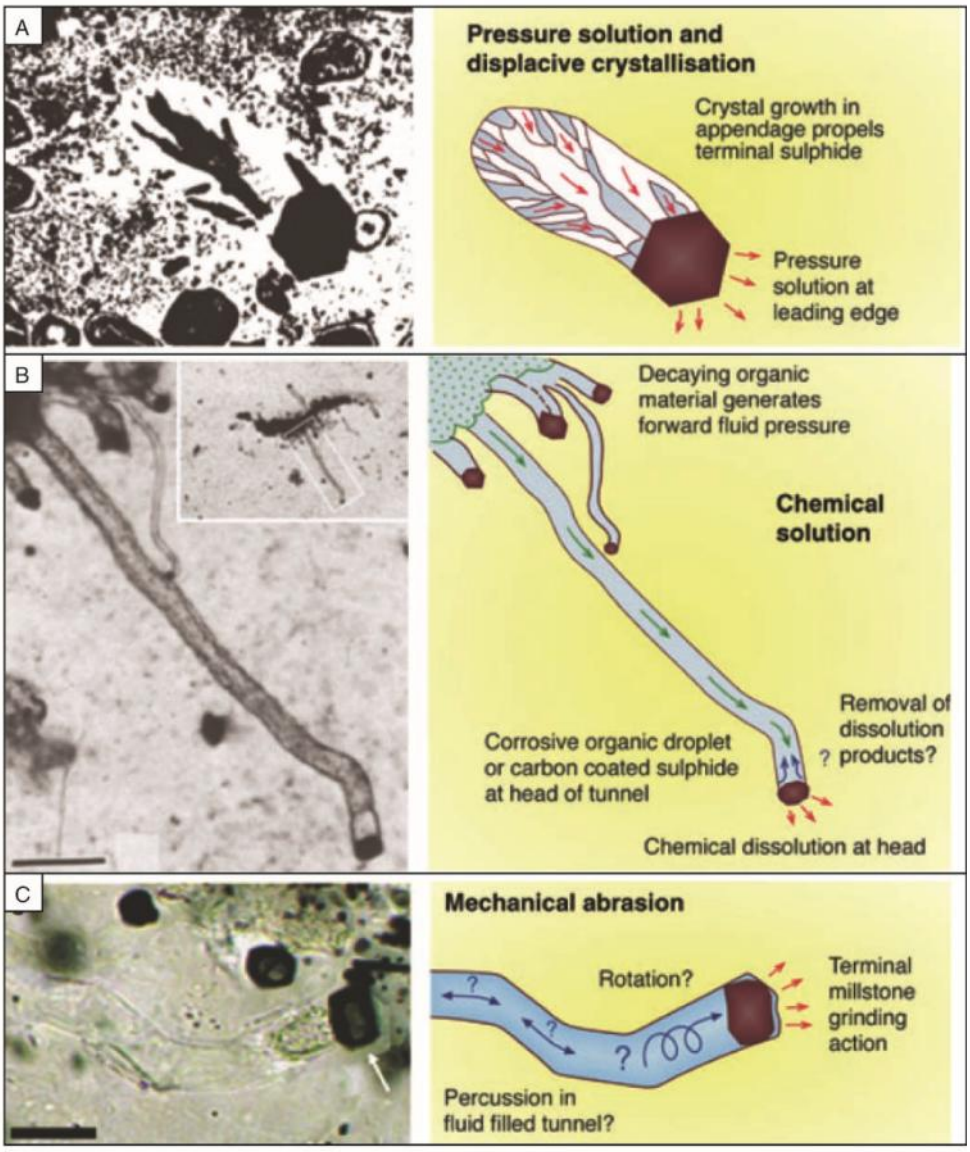

Figure 1.11. Photomicrographs of ambient inclusion trails (left-hand side) and possible mechanistic interpretations (right hand side). (A) Euhedral pyrite crystal with a quartz-filled appendage from a chert of the Gunflint Iron Formation, Ontario. (B) Cluster of pyrite and organic carbon (inset) with radiating tubular structures that show constant diameters, terminal pyrite grains, from the North Pole Chert of Western Australia. (C) Pyrite crystal with a hollow tail of constant cross-sectional geometry, from the Strelley Pool Chert, of Western Australia. (A) From plate 2 of Tyler and Baghoorn (1963), (B) from Fig. 6 of Buick (1990, and (C) from Wacey et al., (2008).

1.3.4.3. Geochemical Processing

Biological processes may leave geochemical signatures behind. Geochemical biosignatures left by the activity of endolithic microbes may be preserved if secondary infilling phases have ages related to early diagenetic processes or are synchronous with deposition (McLoughlin et al., 2007). In addition, certain elements, including Si, Mg, Ca, Na, Fe, Mn, and K, may become depleted or enriched during alteration processes.

Relative to unaltered glass, Fe and Mn can be enriched or depleted while Si, Mg, Ca, Na and Al are usually depleted (e.g., Furnes et al., 1996; Torsvik et al., 1998; Alt and Mata 2000). Alteration zones may additionally have large increases in K likely supplied by large quantities of seawater that could have also provided vital nutrients for microbes (Torsvik, et al., 1998; Alt and Mata, 2000). A common trait that living cells have is the capability of concentrating K from the environment, therefore high potassium concentrations in altered glass may be the result of microbial activity (Torsvik et al., 1998). These elemental patterns are the primary focus of micro-chemical investigations in FRVF tuffs.

Several other lines of evidence for geochemical processing, which are not examined in this study, are worth noting. Carbon isotopes from disseminated carbonate can show biological fractionation patterns because microbes acquire ^{12}C over ^{13}C. Microbes oxidize organic material and produce isotopically light CO_2 resulting in ^{12}C-enriched carbonates (Torsvik et al., 1998; Furnes et al, 1999, 2001, 2004, 2005) relative to fresh crystalline samples. While here the analysis of carbonate isotopic compositions for the purpose of paleothermometry is included, the isotopic composition of fresh

crystalline samples was not measured. Therefore identifying biological fractionation patterns was not possible.

Microbes may also concentrate C, N, P and K in interior linings < 1 µm wide within the alteration front-glass interface. N:C ratios from 0.5 to 0.35 could represent nitrogen starved cells of marine bacteria (Fagerbakke et al., 1996; Torsvik et al., 1998). No quantitative micro-chemical data was obtained in this study, so elemental ratios are not explored. Organic material left in rocks may be indicated by carbon in alteration zones not related to carbonate phases or could be preserved as inclusions within or between crystals of other enclosing secondary phases. Organics could also be preserved if they become trapped as part of a mineral's crystalline structure (Furnes et al., 2005). The presence of DNA or RNA associated with bioalteration features can indicate a microbial influence on the production of such features. These can be detected by using fluorescent dyes such as 4',6-diamidino-2-phenylindole (DAPI) that attach specifically to nucleic acids (Giovannoni et al., 1996; Torsvik et al., 1998).

1.4. STUDY SITES AND SAMPLES

Environments that in the past are known to have been or are currently inhabited possess a source of liquid water, energy and exploitable biogenic elements (Des Marais et al., 2008; Chela-Flores, 2010). The sites of this study are located in the Fort Rock Volcanic Field (FRVF), central Oregon, U.S.A (Fig. 1.12). This is the location of an ancient Pliocene-Pleistocene pluvial lake basin within an area known as the Great Basin (Heiken, 1971). The Great Basin is a region within the states of Nevada, Utah, California, and Oregon that lacks exterior surface drainage (Dworkin et al., 2005) and many modern and ancient lakes within it are confined basins. FRVF was volcanically active during the

Pliocene-Pleistocene (<2.59 Ma to 12 ka), and hydrovolcanism was the most common type of volcanism during that time. The FRVF contains over 40 hydrovolcanic edifices that include the range of forms (maars, tuffs rings, tuff cones, Heiken, et al., 1971), many of which are basaltic in composition. Hydrovolcanic basaltic eruptions in lacustrine environments result in comparable lithologies to those erupted in marine settings because upon contacting colder water, similar lava quenching processes occur mainly producing abundant basaltic glass. Basaltic glass is a known source of biogenic elements and energy (Banerjee and Meuhlenbachs, 2003; Edwards *et al*., 2005; Staudigel *et al*., 2008; Cavalazzi *et al.*, 2012), and it is clear that aqueous environments containing basaltic glass such as marine hyaloclastites and tuffs, or subglacial lavas provide habitable environments. Therefore is it very likely that the hydrovolcanic tuffs in the FRVF contain evidence of microbial activity in the form of endolithic microborings.

The samples investigated in this study were collected from two locations (Fig. 1.12) within FRVF during June of 2012 and June-July of 2013. Both sites have undergone substantial erosion so only the most indurated deposits remain. The first site located on the central northern side of the FRVF is Reed Rocks covering ~1.5 km^2 beyond the paleo-lake boundary and includes two adjacent tuff rings, one formally named Reed Rock, and a second unnamed edifice south of Reed Rock that we have named South Reed Rock. Samples from this location were collected by myself, Dr. Mariek Schmidt, and Nevena Novakovic (B.Sc.). Reed Rocks deposits consist of variable cm- to m-scale beds mainly composed of blocky, angular fine to coarse ash and lapilli basaltic glass pyroclasts. Also included are accidental lithic blocks from >64 mm up to 1 m, a central lava cap (at Reed Rock), and intrusive dike. Deposits are estimated to have

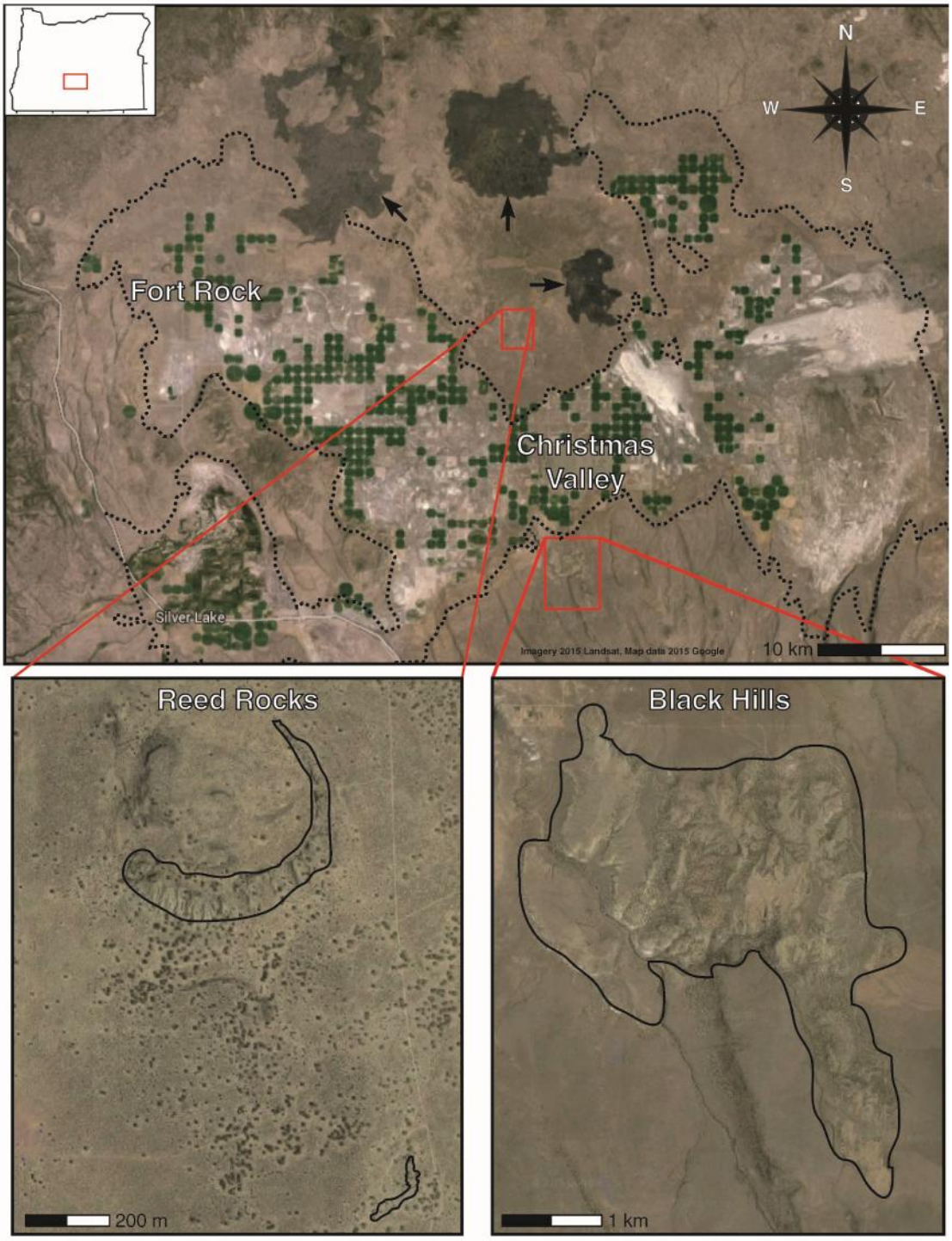

Figure 1.12. Satellite image showing the location of the Fort Rock Volcanic Field (Fort Rock-Christmas Valley basin) and the Reed Rocks and Black Hills study sites. Top left inset shows where FRVF is with respect to the state of Oregon. Upper panel displays the entire FRVF basin with the inferred paleo-lake margin represented with a dashed line. Three arrows point to large basaltic lava flows. Lower left and right panels show enlarged images of Reed Rocks and Black Hills, respectively, with the areas containing major tuff outcrops outlined in black.

erupted mainly in contact with near surface ground or shallow surface water and been saturated with ~15-20% water or vapour. They have also undergone post-depositional alteration resulting in primarily amorphous gel-palagonite and amygdaloidal/vug calcite and zeolites.

In Chapter 2 the Reed Rocks basaltic tuffs are investigated petrographically, mineralogically, and geochemically. Geochemistry of bulk unaltered lava and intrusives are obtained by X-ray fluorescence spectroscopy. Using a petrographic microscope the primary and secondary alteration textures and mineralogy are examined and point counted to estimate modal percentages. Primarily the focus is on detailing the range of bioalteration morphological types, their distribution, including petrographic relationships with secondary phases and textures, in addition to measuring their size range. Scanning electron microscopy (SEM) imaging and energy dispersive spectroscopy (EDS) are also used to detail the interiors of bioalteration textures and obtain qualitative micro-chemical data, respectively. Bioalteration textures are compared to microbial glass alteration textures that have been previously reported in oceanic basalts and placed in diagenetic sequence to support their biogenic origins. More definitive determinations of secondary phases, especially those too fine grained to be identified under the microscope, are made using micro- and powder X-ray diffraction (μXRD and pXRD, resp.). Taking into account the conditions under which they are documented to form and their relationship with bioalteration textures, the paleo-environmental conditions are estimated. Textural, mineralogical, and geochemical data are treated collectively to infer relevant environmental controls on bioalteration textures.

The second study site located on the southern edge of FRVF is formally referred to as the Black Hills (Fig. 1.12) and includes a cluster of approximately six tuff rings. Mapped as part of the Seven-Mile Ridge (Heiken, 1971; Brand and Clarke, 2009), it straddles the paleo-lake margin and is considerably larger than the Reed Rocks study site covering >20 km^2. Samples from Black Hills were collected by myself, Dr. Mariek Schmidt, Nevena Novakovic (B.Sc.), M.Sc. student Frank Popoli, Jeff Berger (M.Sc., Ph.D candidate) and Rebekka Lee (B.Sc.). These tuff deposits are also multi-layered and of variable thicknesses composed mainly of blocky, angular, basaltic glass pyroclasts. Included with accidental lithics are diatomite clasts that were not present in the Reed Rocks tuffs. Black Hills contains no lava cap, but does have at least one intrusive dike. Post depositional alteration has also resulted in the formation of a secondary phase assemblage mainly consisting of amorphous gel- and crystalline fibro-palagonite, as well as amygdaloidal and vug carbonate/zeolites.

Chapter 3 focuses on petrographic, mineralogical and geochemical characterization of the basaltic tuff from the Black Hills. This includes the same analytical techniques used for studying Reed Rocks tuffs, but with some additional areas of investigation. The purpose of Chapter 3 is also to detail bioalteration morphological types, distributions, sizes and petrographic relationships with secondary abiotic textures, and aims to compare these data with that from Reed Rocks tuffs. A comparison with Reed Rocks characteristics enables more informative conclusions to be drawn regarding the biologically important factors to microboring formation. Additional data in this study include an analysis of stable isotopes from disseminated carbonate cements and X-ray element maps of alteration textures. Using mass spectrometry and energy dispersive

spectroscopy (EDS), C- and O-isotopic and elemental (e.g., Na, Ca Mg, Fe, K) compositions are obtained, respectively, from samples of both Reed Rocks and Black Hills. The carbonate paleo-temperature scale (Leng and Marshall, 2004) is applied to estimate the temperature of carbonate precipitation and in turn paleo-environmental conditions.

In the final chapter (Chapter 4), the findings of this study are discussed in relation to previous studies of microbial bioalteration in basalts. We examine how the findings here are consistent with previous conclusions from other studies with regard to the controls on microboring formation, and possible constructing organisms. The merit of microbial alteration textures as potential biosignatures is also discussed. Finally, some of the general limitations of this study are considered and recommendations for future work to improve the quality of this work are summarized.

1.5. REFERENCES CITED

Allaby, A., and Allaby, M., 1999, A Dictionary of Earth Sciences. Retrieved July 14, 2015 from Encyclopedia.com: http://www.encyclopedia.com/doc/1O13-incongruentdissolution.html

Alt, J.C., and Mata, P., 2000, On the role of microbes in the alteration of submarine basaltic glass: a TEM study: *Earth and Planetary Science Letters*, v. 181, p. 301-313.

Banerjee, N.R., and Muehlenbachs, K., 2003, Tuff life: Bioalteration of volcaniclastic rocks from the Ontong Java Plateau. Geochemistry, Geophysics, Geosystems, v. 4, no. 4, p. 1037.

Banerjee, N.R., Furnes, H., Muehlenbachs, K., Staudigel, H., and de Wit, M., 2006, Preservation of ~3.4-3.5 Ga microbial biomarkers in pillow lavas and hyaloclastites from the Barberton Greenstone Belt, South Africa. Earth and Planetary Science Letters, v. 241, p. 707-722.

Banerjee, N.R., Simonetti, A., Furnes, H., Muehlenbachs, K., Staudigel, H., Heaman, L., and Van Kranendonk, M.J., 2007, Direct dating of Archean microbial ichnofossils: *Geology*, v. 35, p. 487-490.

Banerjee, N.R., Izawa, M.R.M., Sapers, H.M., and Whitehouse, M.J., 2011, Geochemical biosignatures preserved in microbially altered basaltic glass: *in* Proceedings, SIMS, Surface and Interface Analysis, v. 43, p. 452-457.

Bathurst, R.G.C., 1966, Boring algae, micrite envelopes and lithification of molluscan biosparites. Journal of Geology, v. 5, p. 15-32.

Canfield, D.E., Rosing, M.T., and Bjerrum, C., 2006, Early anaerobic metabolism. Philosophical Transactions of the Royal Society D, v. 361, p. 1819-1836.

Cas, R. A., and Wright, J. V., 1987,. *Volcanic successions: modern and ancient*. Springer Science & Business Media

Cockell, C.S., Olsson-Francis, K., Herrera, A., and Meunier, A., 2009, Alteration textures in terrestrial volcanic glass and the associated bacterial community: *Geobiology*, v. 7, p. 50-65.

Cole, P.D., Guest, J.E., Duncan, A.M., and Pacheco, J.-M., 2001, Capelinhos 1957–1958, Faial, Azores: deposits formed by an emergent Surtseyan eruption. *Bulletin of Volcanology*, v. 63, p. 204–220.

Cousins, C.R., Smellie, J.L., Jones, A.P., and Crawford, I.A., 2009, A comparative study of endolithic microborings in basaltic lavas from a transitional subglacial-marine environment: *International Journal of Astrobiology*, v. 8, no. 1, p. 37-49.

Crovisier, J.L., Honnorez, J., and Eberhart, J.P., 1987, Dissolution of basaltic glass in seawater: Mechanism and rate: *Geochimica et Cosmochimica Acta*, v. 51, p. 2977–2990.

De los Ríos, A., Sancho, L.G., Wierzchos, J., and Ascaso, C., 2005, Endolithic growth of two *Lecidea* lichens in granites from continental Antarctica detected by molecular and microscopy techniques. *New Phytologist*, v. 165, no. 1, p. 181-190.

Dworkin, S.I., Nordt, L., and Atchley, S., 2005, Determining terrestrial paleotemperatures using the oxygen isotopic composition of pedogenic carbonate: *Earth and Planetary Science Letters*, v. 237, p. 56-68.

Fabricius, F.H., 1977, Origin of marine ooids and grapestones. In *Contributions to sedimentology*, v. 7: Stuttgart, E. Schweizer-bart'che Verlagsbuchhandlung (Näele und Obermiller), 113 pp.

Fagerbakke, K.M., Heldal, M., and Norland, S., 1996, Content of carbon, nitrogen, oxygen, sulfur and phosphorus in native aquatic and cultured bacteria. Aquatic Microbial Ecology, v. 10, p. 15-27.

Fisk, M.R., Giovannoni, S.J., and Thorseth, I.H., 1998a, Alteration of oceanic volcanic glass: Textural evidence of microbial activity: *Science*, v. 281, p. 978-980.

Fisk, M.R., Thorseth, I.H., Giovannoni, S.J., Urbach, E., and Streck, M.J., 1998b, Endolithic Microbes from the Rattlesnake Tuff, Oregon Blue Mountain Region: *American Geophysical Union, Fall Meeting*, San Francisco, CA, Abstracts, FM98-U32A-12.

Fisk, M., and McLoughlin, N., 2013, Atlas of alteration textures in volcanic glass from the ocean basins. *Geosphere*, v. 9, no. 2, p. 317-341.

Fisher, R.V., and Schmincke, H.-U., 1984, Accretionary Lapilli. In: *Pyroclastic Rocks*. Springer-Verlag, Berlin Heidelberg New York Tokyo, pp. 238-239

Friedmann, E. I., & Koriem, A. M., 1989, Life on Mars: how it disappeared (if it was ever there). *Advances in Space Research*, v.*9, no.* 6, p. 167-172.

Furnes, H., 1984, Chemical changes during progressive subaerial palagonitization of a subglacial olivine tholeiitic hyaloclastite: A microprobe study: *Chemical Geology*, v. 43, p. 264– 271.

Furnes, H., Thorseth, I.H., Tumyr, O., Torsvik, T., and Fisk, M.R., 1996, Microbial activity in the alteration of glass from pillow lavas from Hole 896A, *Proceedings from the Ocean Drilling Program, Science Results*, v. 148, p. 191-206.

Furnes, H., and Staudigel, H., 1999, Biological mediation in ocean crust alteration: how deep is the deep biosphere? Earth and Planetary Science Letters, v. 166, no. 3-4, p. 97-103.

Furnes, H., Muehlenbachs, T., Torsvik, T., Thorseth, I.H., and Tumyr O., 2001, Microbial fractionation of carbon isotopes in altered basaltic glass from the Atlantic Ocean, Lau Basin and Costa Rica Rift: *Chemical Geology*, v. 173, no. 4, p. 313-330.

Furnes, H., Staudigel, H., Thorseth, I.H., Torsvik, T., Muehlenbachs, K., and Tumyr, and O., 2001, Bioalteration of basaltic glass in the ocean crust: *Geochemistry Geophysics Geosystems*, v. 2, Paper number 2000GC000150.

Furnes, H., Banerjee, N.R., Muehlenbachs, K., Staudigel, H., and de Wit, M., 2004, Early Life Recorded in Archean Pillow Lavas: *Science*, v. 304, p. 578-581.

Furnes, H., Banerjee, N.R., Muehlenbachs, K., and Kontinen, A., 2005, Preservation of biosignatures in metaglassy volcanic rocks from the Jormua Ophiolite complex, Finland: *Precambrian Research*, v. 136, p. 125-137.

Furnes, H., Banerjee, N.R., Staudigel, H., Muehlenbachs, K., McLoughlin, N., de Wit, M., and Van Kranendonk, M., 2007a, Comparing petrographic signatures of bioalteration in recent to Mesoarchean pillow lavas: Tracing subsurface life in oceanic igneous rocks. *Precambrian Research*, v. 158, p. 156-176.

Furnes H., Banerjee, N.R., Staudigel, H., and Muehlenbachs, K., 2007b, Pillow lavas as a habitat for microbial life: *Geology Today*, v. 23, no. 4, p. 143-145.

Furnes, H., McLoughlin, N., Muehlenbachs, K., Banerjee, N., Staudigel, H., Dilek, Y., de Wit, M., Van Kranendonk, M., and Shiffman, P., 2008, Oceanic pillow Lava and Hyaloclastites as Habitats for Microbial Life through Time - A Review. *Links Between Geological Processes, Microbial Activities and Evolution of Life*, (eds. Dilek, Y., Furnes, H., Muehlenbachs, K.) Springer, Heidelberg, pp. 1-68.

Giovannoni, S.J., Fisk, M.R., Mullins, T.D., and Furnes, H., 1996, Genetic evidence for endolithic microbial life colonizing basaltic glass/seawater interfaces. *Proceedings of the Ocean Drilling Program, Scientific Results*, v. 148, p. 207-213.

Golubic, S., 1969, Distribution, taxonomy, and boring patterns of marine endolithic algae. *American Zoologist*, v. 9, no. 747-751.

Golubic, S., Friedmann, I., and Schneider, J., 1981, The lithobiontic ecological niche, with special reference to microorganisms: *Journal of Sedimentary Petrology*, v. 51, no. 2, p. 351-361.

Grosch, E.G., and McLoughlin, N., 2014, Reassessing the biogenicity of Earth's oldest trace fossil with implications for biosignatures in the search for early life: *Proceedings of the National Academy of Sciences*, v. 111, no. 23, p. 8380-8385.

Harris, P.M., Halley, R.B., and Lukas, K.J. (1979) Endolithic microborings and their preservation in Holocene-Pleistocene (Bahama-Florida) ooids: *Geology*, v. 7, p. 216-220.

Hay, R.L., and A., Iijima, 1968, Nature and origin of palagonite tuffs of the Honolulu Group on Oahu, Hawaii, *Geological Society of America Memoirs*, v. 116, p. 338–376.

Heiken, G.H., 1971, Tuff Rings: Examples from the Fort Rock-Christmas Lake Valley Basin, South-Central Oregon: *Journal of Geophysical Research*, v. 76, no. 23, p. 5615-5626.

Hessland, I., 1949, Investigation of the Lower Ordovician of the Siljan District, Sweden, II. Lower Ordovician penetrative and enveloping algae from the Siljan District: Bulletin of the Geological Institution of the University of Uppsala, v. 33, p. 409-429.

Jackson, E. D. and Wright, T. L., 1970, Xenoliths in the Honolulu Series. Hawaiian Journal of Petrology, v. 11, p. 405-430.

Jakobsson, S.P., 1972, On the consolidation and palagonitization of the tephra of the Surtsey volcanic island, Surtsey, *Progress Reports*, VI, p.1 –8, Museum of Natural History, Department of Geology and Geoggraphy, Reykjavik.

Jones, B., and Goodbody, Q.H., 1982, The geological significance of endolithic algae in glass: *Canadian Journal of Earth Sciences*, v. 19, p. 671-678.

Konhauser, K., 2007, Introduction to Geomicrobiology. Blackwell Publishing 425 pp.

Lorenz, V., 1973, On the formation of maars. *Bulletin of Volcanology*, v. 37, p. 183-204.

Lysnes, K., Thorseth, I.H., Steinsbu, B.O., Øvreas, L., Torsvik, T., and Pedersen, R.B., 2004, Microbial community diversity in seafloor basalts from the Arctic spreading ridges: FEMS Microbiology and Ecology, v. 50, p. 213–230.

MacDonald, G.A., 1967, Forms and structures of extrusive basaltic rocks, *in* Basalts-*The Poldervaart Treatise on Rocks of Basaltic Composition*, Hess, H.H., and Poldervaart, H., eds., Interscience, New York, v.1, p. 1-61.

Madrigan, M.T., and MaReed Rocks, B.L., 1997,. Extremophiles: *Scientific American*, v. 276, p. 82-87.

Margolis, S., and Rex, R.W., 1971, Endolithic algae and micrite envelope formation in Bahamian oolites as revealed by scanning electron microscopy. *Geological Society of America Bulletin*, v. 82, p. 843-852.

McKinley, J.P., Stevens, T.O., and Westall, F., 2000, Microfossils and paleoenvironments in deep subsurface basalt samples: *Geomicrobiology Journal*, v. 17, p. 43-54.

McLoughlin, N., Brasier, M.D., Wacey, D., Green, O.R., and Perry, R.S., 2007, On the biogenicity criteria for endolithic microborings on early Earth and beyond: *Astrobiology*, v. 7, no. 1, p. 10-26.

McLoughlin, N., Furnes, H., Banerjee, N.R., Staudigel, H., Muehlenbachs, K., De Wit, M., and Van Kranendonk, M.J., 2008, Micro-bioalteration in volcanic glass: extending the ichnofossil record to Archean basaltic crust, *in* Wisshak, S., Tapanila, L., eds., *Current Developments in Bioerosion*, Springer-Verlag, Heidelberg, Germany, pp. 371-396.

McLoughlin, N., Furnes, H., Banerjee, N.R., Muehlenbachs, K., and Staudigel, H., 2009, Ichnotaxonomy of microbial trace fossils in volcanic glass: *Journal of the Geological Society*, London 166, 159-169.

Mellor, E., 1922, Les lichen vitricole et al déterioration dex vitraux d'église. PhD Thesis, Sorbonne, Paris, 128 pp.

McKay, C. P., Friedman, E. I., Wharton, R. A., and Davies, W. L., 1992, History of water on Mars: a biological perspective: *Advances in Space Research*, v. *12*, no. 4, p. 231-238.

Mojzsis, S.J., Arrhenius, G., McKeegan, K.D., Harrison, T.M., Nutman, A.P., and Friend, C.R.L., 1996, Evidence of life on Earth before 3800 million years ago: *Nature*, v. 384, p. 55-59.

Moore, J.G., 1966, Rate of palagonitization of submarine basalt adjacent to Hawaii, U. S. Geological Survey Professional Paper, no. 550-D, p. 163–171.

Muir, M.D., and Grant, P.R., 1976, Micropaleontological evidence from the Onverwacht group, South Africa. In: Windley, B.F. (Ed.), The Early History of the Earth. Wiley-Interscience, London, pp. 595-608.

Newell, N.D., Purdy, E.G., and Imbrie, J., 1960, Bahamian oolitic sand: *Journal of Geology*, v. 68, p. 481-497.

Nisbet, E.G., and Sleep, N.H., 2001, The habitat and nature of early life: *Nature*, v. 409, p. 1083-1091.

Olempska, E., 1986, Endolithic microorganisms in Ordovician ostracod valves. Acta *Paleontologica Polonica*, v. 31, no. 3-4, p. 229-236.

Peacock, M.A., 1926, The petrology of Iceland, part 1. The basic tuffs: *Royal Society of Edinburgh Transactions*, v. 55, p. 53–76.

Rittmann, A., 1960, Volcanoes and Their Activity: John Wiley and Sons, New York, 305 pp.

Reyment, R.A., 1966, Preliminary observations on gastropod predation in the Western Niger Delta: Paleogeography, Paleoclimatology, Paleoecology, v. 2, p. 81-102.

Rosing, M.T., 1999, ^{13}C-depleted carbon microparticles in >3700-Ma Sea Floor sedimentary rock from West Greenland: *Science*, v. 283, p. 674-676.

Ross, K.A., and Fisher, R.V., 1986, Biogenic grooving on glass shards: *Geology*, v. 14, p. 571-573.

Ryan, M.P., and Sammis, Ch.A., 1981, The glass transition in basalt: *Journal of Geophysical Research*, v. 86, p. 9519-9535.

Schidlowski, M., 1988, A 3800-million-year isotopic record of life from carbon in sedimentary rocks: *Nature*, v. 333, p. 313-318.

Schidlowski, M., 2001, Carbon isotopes as biochemical recorders of life over 3.8 Ga of Earth history: evolution of a concept. Precambrian Research, v. 106, p. 117-134.

Schmincke, H.-U., 1970, Base surge—Ablagerungen des Laacher See-Vulcans. *Aufschluss*, v. 21, p. 350-364.

Sheridan, M.F., Wohletz, K.H., 1983, Hydrovolcanism: basic considerations and review. *Journal of Volcanology and Geothermal Research*., v. 17, p. 1–29.

Staudigel, H., Hart, S.R., 1983, Alteration of basaltic glass: Mechanisms and significance for the oceanic crust-seawater budget: *Geochimica et Cosmochimica Acta*, v. 47, no. 3, p. 337-350.

Staudigel, H., Chastain, R.A., Yayanoe, A., and Bourcier, W., 1995, Biologically mediated dissolution of glass. *Chemical Geology*, v. 126, p. 147-154.

Staudigel, H., Furnes, H., Banerjee, N.R., Dilek, Y., and Muehlenbachs, K., 2006. Microbes and volcanoes: a tale from the oceans, ophiolites and greenstone belts. *GSA Today*, v. 16, no. 10, p. 4–11.

Staudigel, H., Furnes, H., McLoughlin, N., Banerjee, N., Connell, L.B., and Templeton, A., 2008, 3.5 billion years of glass bioalteration: Volcanic rocks as a basis for microbial life?: *Earth-Science Reviews*, v. 89, p. 156-176.

Stosch, H. G. and Seek, H. A., 1980, Geochemistry and mineralogy of two spinel peridotite suites from Dreiser Weiher, West Germany: *Geochimica et Cosmochimica Acta*, v. 44, p. 457-470.

Stroncik, N.A., and Schmincke, H.U., 2001, Evolution of palagonite: Crystallization, chemical changes, and element budget: *Geochemistry Geophysics Geosystems*, v. 2, no. 2000GC000102.

Stroncik, N.A., and Schmincke, H.U., 2002, Palagonite - a review. *International Journal of Earth Sciences (Geol. Rundsch)*, v. 91, p. 680-697, doi 10.1007/s00531-001-0238-7.

Techer, I., Advocat, T., Lancelot, J., and Liotard, J. M., 2000, Basaltic glass: alteration mechanisms and analogy with nuclear waste glasses: *Journal of nuclear materials*, v. *282*, no. 1, p. 40-46.

Thorseth, I.H., Furnes, H., and Tumyr, O., 1991, A textural and chemical study of Icelandic palagonite of varied composition and its bearing on the mechanism of the glass-palagonite transformation: *Geochimica et Cosmochimica Acta*, v. 55, p. 731–749.

Thorseth, I.H., Furnes, H., and Heldal, M., 1992, The importance of microbiological activity in the alteration of natural basaltic glass: *Geochimica et Cosmochimica Acta*, v. 56, p. 845-850.

Thorseth, I.H., Torsvik, T., Furnes, H., and Muehlenbachs, K., 1995, Microbes play an important role in the alteration of oceanic crust: *Chemical Geology*, v. 126, p. 137-146.

Thorseth, I.H., Torsvik, T., Torsvik, V., Daae, F.L., Pedersen, R.B., and Keldysh-98 Scientific Party, 2001, Diversity of life in ocean floor basalt: *Earth and Planetary Science Letters*, v. 194, p. 31-37.

Thorseth, I.H., Pedersen, R.B., and Christie, D.M., 2003, Microbial alteration of 0-30-Ma seafloor and sub-seafloor basaltic glasses from the Australian Antarctic Discordance: *Earth and Planetary Science Letters*, v. 215, p. 237-247.

Torsvik, T., Furnes, H., Muehlenbachs, K., Thorseth, I.H., and Tumyr, O., 1998, Evidence for microbial activity at the glass-alteration interface in oceanic basalts: *Earth and Planetary Science Letters*, v. 162, p. 165-176.

Van Kranendonk, M.J., Webb, G.E., and Kamber, B.S., 2003, Geological and trace element evidence for marine sedimentary environment of deposition and biogenicity of 3.45 Ga stromatolitic carbonates in the Pilbara Craton, and support for reducing Archean ocean: *Geobiology*, v. 1, no. 2, p. 91-108.

Walter, M.R., Buick, R., and Dunlop, J.S.R., 1980, Stromatolites 3400-3500 m.y. old from the North pole area, Western Australia: *Nature*, v. 284, p. 443-445.

Waters, A. C. and Fisher, R. V., 1971, Base surges and their deposits: Capelinhos and Tad volcanoes: *Journal of Geophysical Research*, v. 76, p. 5596-5614.

Wentworth, C. K., 1926, Pyroclastic geology of Oahu: *Bishop Museum Bulletin*., v. 30, p. 121.

Westhall, F., de Wit, M.J., Dann, J., van Daast, S., de Ronde, C.E.J., Gerneke, D., 2001, Early Archean fossil bacteria and biofilms in hydrothermally-influenced sediments from the Barberton Greenstone Belt, South Africa: *Precambrian Research*, v. 106, p. 93-116.

White, R. W., 1966, Ultramafic inclusions in basaltic rocks from Hawaii: *Contributions to Mineralogy and Petrology*, v. 12, p. 245-314.

Zhang, Z., and Goloubic, S., 1987, Endolithic microfossils (cyanophyta) from early Proterozoic Stromatolites, Hebel China: *Acta Micropaleontalogica Sinica*, v. 4, p. 1-12.

Zhou, Z., and Fyfe, W.S., 1989, Palagonitization of basaltic glass from DSDP site-335, LEG-37 – textures, chemical-composition, and mechanism of formation: *American Mineralogist*, v. 74, p. 1045–1053.

Chapter 2

Microbial ichnofossils in continental basaltic tuffs of central Oregon, U.S.A.: Expanding the record of endolithic microborings

Matthew P.C. Nikitczuk[1], Mariek E. Schmidt[1], and Roberta L. Flemming[2]

[1]Department of Earth Sciences, Brock University 500 Glenridge Avenue, St. Catharines, ON L2S 3A1

[2]Department of Earth Sciences, University of Western Ontario 1151 Richmond Street, London, ON N6A 3K7

This manuscript has been submitted to GSA Bulletin and generally follows the style required by the publisher of this journal.

2.1. INTRODUCTION

Over the last few decades, various studies have presented evidence that volcanic rocks, more specifically upper oceanic crust massive and pillow basalt hyaloclastites, can host endolithic microbial communities. The most widespread evidence cited are distinctive *granular* and *tubular* ichnofossils (endolithic microborings) produced during the processes of bio-erosion whereby microbes (euendoliths) etch volcanic glass surfaces and actively bore into the substrates (Thorseth et al., 1995, 2001, 2003; Furnes et al., 1996, 1999, 2001, 2005, 2007a, 2007b, Fisk et al., 1998a, 2003; Banerjee et al., 2003, 2011; Torsvik et al., 1998; Walton, 2008). The *tubular* form consists of elongate, straight, curved, spiral, or branched tunnels in fresh glass that are 1-5 μm in diameter and 10-200 μm in length (e.g., Furnes et al., 2001; Fisk et al., 2013). The *granular* form is characterized by radiating clusters of spherical-shaped cavities with diameters of ~0.4 μm (e.g., McLoughlin *et al*., 2007; Staudigel *et al*., 2008). Granular textures tend to be more common, although tubular varieties are more easily identified because they are usually larger in size and are morphologically distinct from abiotic alteration (Furnes and Staudigel, 1999). Typically the tubular and granular textures are hosted within fresh volcanic glass and originate along fractures, pillow rims or volcaniclast margins. Tubules and granules may be hollow or preserved with infillings of secondary minerals such as phyllosilicates, zeolites, iron-oxyhydroxides, or titanite (e.g., Benzerara *et al*., 2007; Staudigel *et al*., 2008; Izawa *et al*., 2010; McLoughlin *et al*., 2010).

Comparable textures have also been described in hyaloclastites erupted in subglacial environments of Iceland and Antarctica (e.g., Cockell et al., 2009; Cousins et al., 2009), as well as marine tuffs of Ontong Java (Banerjee et al., 2003). The record of

continental endoliths within volcanic rocks however, is not so extensive. Although the first description of volcanic glass etching came from a non-marine tuff layer in the Miocene John Day Formation, eastern Oregon (Ross and Fisher, 1986), they are surface features and do not penetrate far into the glass. Referred to as 'biogenic grooving', they are in the form of semi-circular and U-shaped grooves with much larger widths (4-20 µm) than tube diameters described in oceanic basalts. Evidence of endolithic microbes has also been documented in continental pyroclastic rocks such as the Rattlesnake Tuff in Oregon, a high silica rhyolite ignimbrite, (e.g., Fisk et al., 1998b) and in lava flows such as the Columbia River basalts (e.g., McKinley et al., 2000) in the form of bio-films with rod shaped microbial colonies covering glass shard surfaces, and bacteriomorphs of fossilized microbes, respectively. Likewise, no textures resembling *tubular* or *granular* bioalteration have been described is these locations.

The Fort Rock Volcanic Field (FRVF) in central Oregon, U.S.A (Fig. 2.1), also known as the Fort Rock-Christmas Valley basin, is the site of an ancient Pliocene-Pleistocence pluvial lake basin and over 40 hydrovolcanoes (Heiken, et al., 1971). These features include maars, tuff rings and tuff cones consisting of layered basaltic tuffs. Several of the deposits throughout the basin have been studied over the last few decades for various reasons (e.g., Hampton, 1964; Lorenz, 1970; Heiken, 1971; Colbath and Steele, 1982; Martin et al., 2005; Brand and Clarke, 2009) yet no tubular or granular bioalteration textures have been described in any deposit within the FRVF until now.

We here present the first account of putative endolithic microborings from continental, non-marine, non-subglacial, basaltic hydrovolcanic pyroclastic deposits (Fig. 2.1. Reed Rock and South Reed Rock) in the FRVF. Geochemical data and petrographic

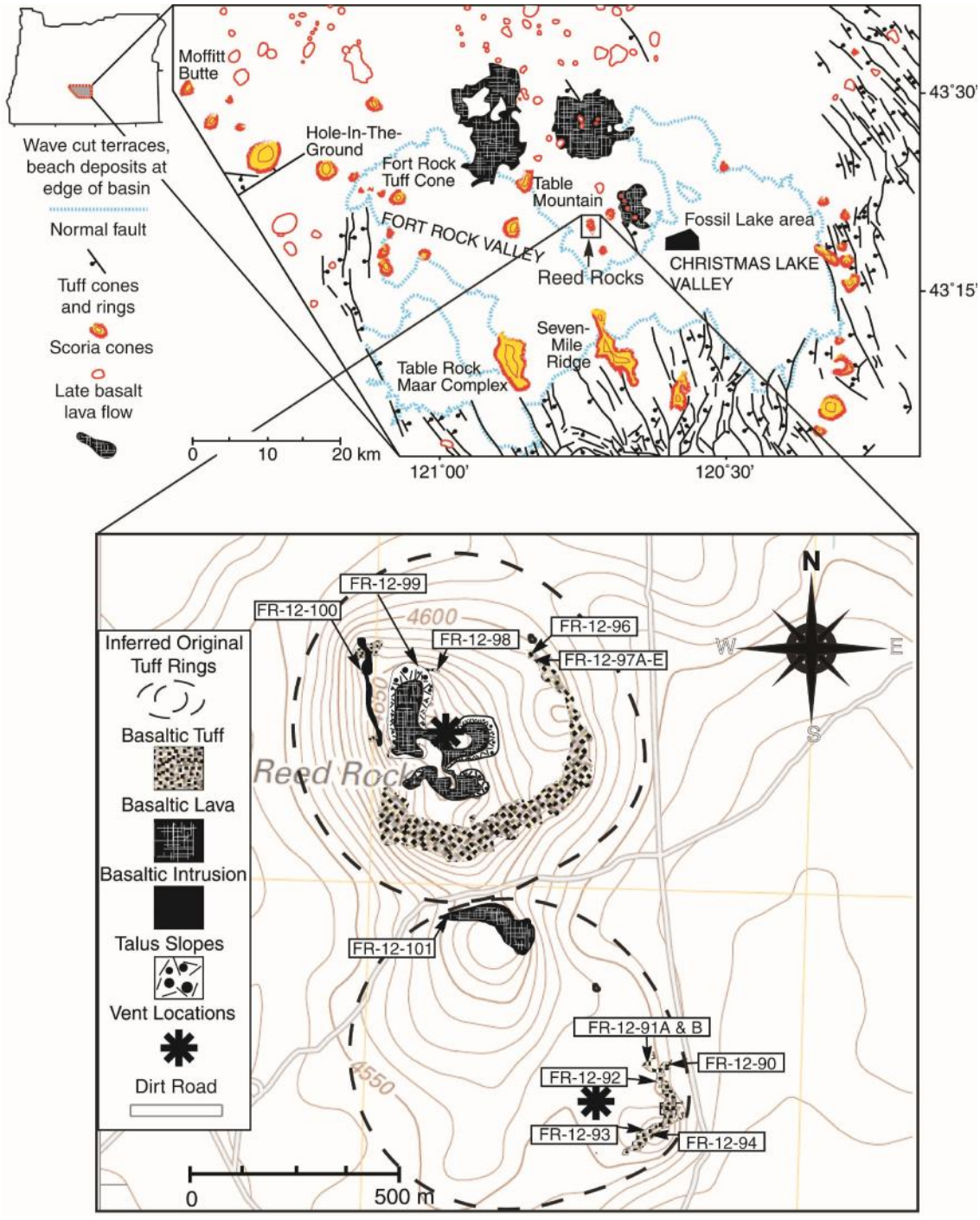
Moffitt Butte
Hole-In-The-Ground
Fort Rock Tuff Cone
Table Mountain
FORT ROCK VALLEY
Reed Rocks
Fossil Lake area
CHRISTMAS LAKE VALLEY
Seven-Mile Ridge
Table Rock Maar Complex
Wave cut terraces, beach deposits at edge of basin
Normal fault
Tuff cones and rings
Scoria cones
Late basalt lava flow
0 10 20 km
121°00'
120°30'
43°30'
43°15'
FR-12-99
FR-12-100
FR-12-98
FR-12-96
FR-12-97A-E
4600
4650
Reed Rock
FR-12-101
FR-12-91A & B
FR-12-90
FR-12-92
FR-12-93
FR-12-94
4550
Inferred Original Tuff Rings
Basaltic Tuff
Basaltic Lava
Basaltic Intrusion
Talus Slopes
Vent Locations
Dirt Road
N
W
E
S
0
500 m

Figure 2.1. Fort Rock Volcanic Field (FRVF) (modified from Heiken, 1971) and Reed Rock - South Reed Rock study area collectively referred to as Reed Rocks. Upper left inset shows the state of Oregon (U.S.A.) with the FRVF shaded gray. Shaded area is enlarged in the upper right panel showing the FRVF with the location of the Reed Rock and South Reed Rock tuff rings indicated (*outlined by box, labelled with an arrow*) relative to lava fields and other hydrovolcanic edifices and cinder cones within the basin. The high stand lake boundary is also indicated (*blue dashed line*) showing that Reed Rock and South Reed Rock are located just outside of the inferred lake margin. Lower panel shows an enlarged geologic map of the Reed Rocks study area. Larger unit in northern half of map is Reed Rock, the smaller unit in southern half of map is South Reed Rock. (Topographic base from USGS 7.5 minute series, 2011).

observations of mineralogical and textural characteristics including abiotic palagonitic alteration and fluid conditions are examined. We also describe the range in morphologies of putative bioalteration textures found within glassy pyroclasts, make a case for biogenicity and attempt to define the paleo-environmental characteristics including the temperature of formation. The term bioalteration is used to refer to both tubular and granular textures whereas the term micro-tunnel or tunnel refers only to the tubular type.

2.1.1 Geologic Setting

The FRVF (Fig. 2.1) is approximately 40 km wide and 64 km long (Heiken, 1971). A series of NW-trending faults cross cut the basin and the surrounding highlands (Heiken, 1971) and provided pathways for ascending dikes, as indicated by lineaments of vents in the same orientation. The faults also provided pathways for groundwater and allowed for hydrovolcanic eruptions to occur outside the inferred lake margin. Reed Rock and South Reed Rock tuff rings, which from hereon will be collectively referred to as Reed Rocks, unless specified, are the indurated pyroclastic remains of two adjacent Pliocene-Pleistocene (<2.59 Ma to 12 ka; Heiken, 1971) hydrovolcanoes in the central

area of the basin ~ 2.5 km beyond the inferred paleo lake margin. The phreatomagmatic-hydrovolcanic eruptions were therefore more likely driven by near-surface groundwater and/or very shallow surface water. Although no absolute ages have been determined, the majority of samples contain relatively high proportions (37-52%) of fresh glass. This may suggest a relatively younger mid to late Pleistocene age.

The Reed Rocks are composed of multiple fine to coarse ash and lapilli-rich layers ranging from ~1 cm laminated to m-scale massive quaquaversal tuffs typical of hydro-phreatovolcanism (Fig. 2.2). The blocky, angular, morphologies of fine to coarse ash and lapilli basaltic glass (sideromelane) pyroclasts (Fig. 2.3) are typical of brittle chilling fragmentation during phreatomagmatism (Fisher and Schmincke, 1984). Tuff samples are more commonly clast-supported and 3-12% vesicular, often amygdaloidal, with connecting fracture networks resulting from explosive shattering and thermal contraction upon cooling. Rapid quenching is also indicated by swallow tail, skeletal, and sieved plagioclase, hopper olivine phenocrysts, and undercooling textures of fine-grained intergrown plagioclase and pyroxene. Bomb sags (Fig. 2.2E), vesiculated matrices and scoria-cored accretionary lapilli (armored lapilli) suggest deposits saturated with up to 15-20% external water contents (Heiken, 1971). Accidental lithic blocks up to ~1 m in diameter and very coarse angular blocks of explosion breccia lensoidal interbeds are also consistent with ground water interaction. Reed Rock contains a final lava cap and dike intrusion that represent a transition to effusive volcanism that occurs when the water source is blocked from entering the vent before the eruption ceases (Heiken, 1971). Post-

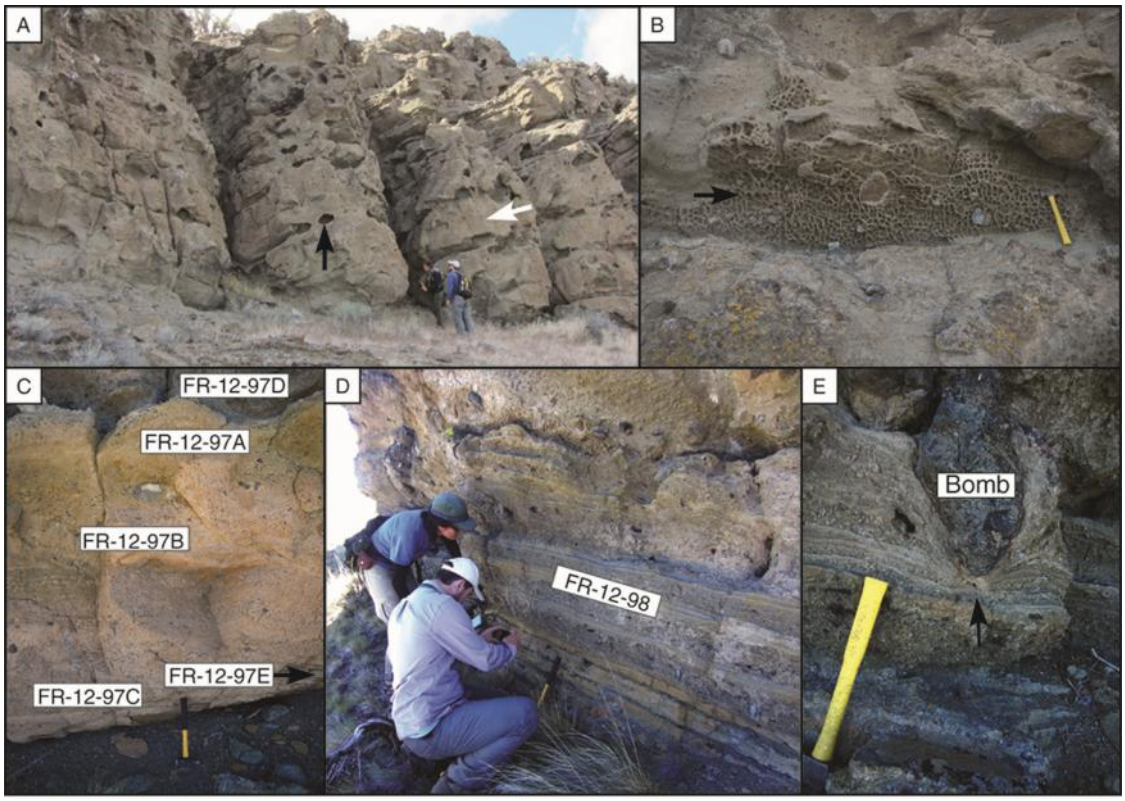

Figure 2.2. Macro-features of Reed Rock and South Reed Rock. (A) Eroded remnant of South Reed Rock showing highly cavitated (*black arrow*) edifice with beds dipping left into page (*white arrow*). Geologists for scale. (B) Cavernous tafoni weathered surface (*arrow*) with 'honey comb' like structures laterally extended along bedding plane indicated by orientation of the arrow. Hammer at right side for scale. (C) Massive pervasively altered bed at Reed Rock dipping into page. The relative locations within the sequence from which samples FR-12-97A to E were obtained are indicated with labels. The arrow beside FR-12-97E indicates the sample was obtained from a location further to the right out of the field of view. Hammer at bottom center for scale. (D) Dipping beds at Reed Rock alternating between fine undulatory ash-rich and coarser angular lapilli-rich layers. Several small bomb sags are seen as dark spots on either side of the hammer at bottom-center. Beds are dipping toward the vent. The layers from which sample FR-12-98 was obtained is indicated with a label. (E) Bomb sag: Bomb at Reed Rock has deformed layers (dipping into page to the right) beneath it (*arrow*). Hammer at left for scale.

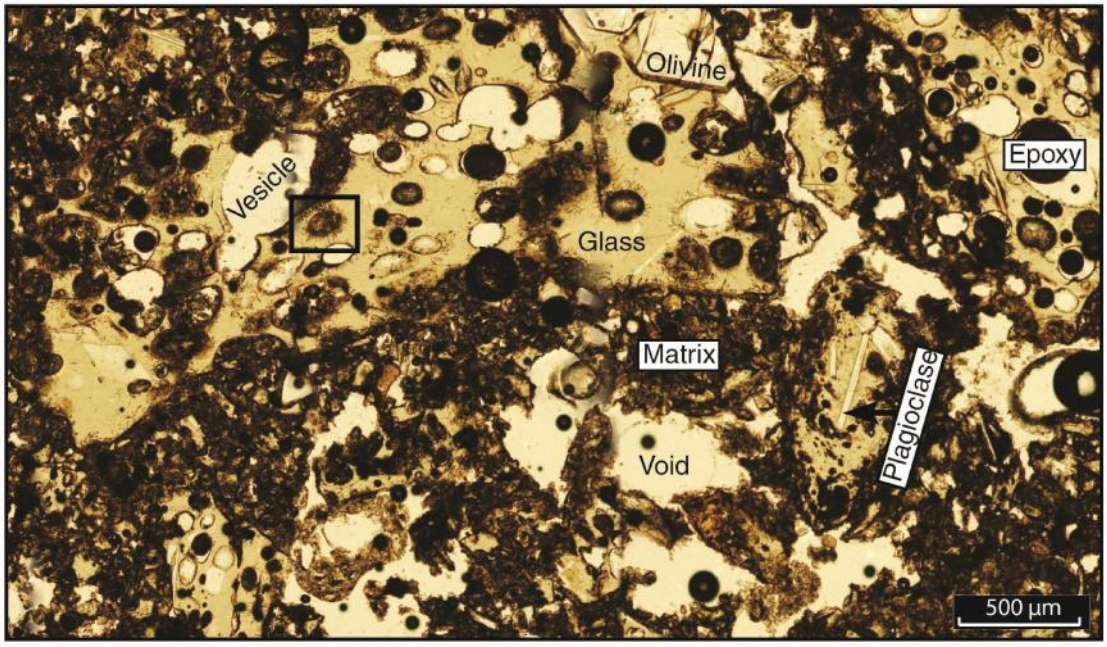

Figure 2.3. Typical fractured, vesicular, basaltic glass pyroclast (lapilli-sized) with olivine and plagioclase phenocrysts, surrounded by darker finer grained matrix with empty voids. The box in upper left outlines a vesicle with radiating micro-tunnels. See Figure 2.9A for an enlarged Enhanced Depth of Focus (EDF) image of this area. This is the first location where the tubular textures were observed in the Reed Rocks tuffs. Sample FR-12-97E.

depositional alteration, including both low temperature hydrothermal alteration of mainly juvenile basaltic glass and the precipitation of ancillary precipitates within vesicles (amygdules) and voids (vugs) produced secondary textures and an assemblage of amorphous to proto-crystalline and wholly crystalline mineral phases. Aqueous alteration resulted in the formation of palagonite. The palagonitization process involves a low to high temperature progressive aging from light yellow amorphous (isotropic) to dark yellow/orange-brown crystalline (anisotropic) material. Palagonitization proceeds by hydration, chemical exchange, and congruent and incongruent dissolution of basaltic glass, with accompanying re-precipitation of secondary phases that may include phyllosilicates, zeolites or iron-oxy-hydroxides (Peacock, 1926; Zhou and Fyfe, 1989; Thorseth et al., 1991; Stroncik and Schmincke, 2001). The distinction suggested by Peacock (1926) between the amorphous *gel-palagonite* and proto- to wholly-crystalline *fibro-palagonite* varieties is accepted. This alteration occurred where rock surfaces were exposed to circulating fluids such as fractures, vesicles and pyroclast margins.

2.1.1.1. Pluvial Fort Rock Lake

Considering the geologic and hydrologic similarities of Fort Rock Lake with modern western U.S. pluvial lakes such as Summer and Abert Lakes, it is likely that the Fort Rock lake evolved through a similar evaporitic trend (e.g., Hardie & Eugster, 1970). The Pliocene Pettus Lake Member of the Fort Rock formation, which probably underlies the majority of the Fort Rock basin, includes diatomite beds (Hampton, 1964; Allison, 1966, 1979; Heiken, 1971) with diatom associations typical of a fresh-water environment (e.g., Colbath & Steele, 1982). In addition, an abundance of centric diatom genera have been interpreted to indicate an oligotrophic or nutrient poor lake (e.g., Stockner &

Benson, 1967). In the Fossil Lake area, located in the east central part of the Fort Rock basin, rare earth element (REE) compositions of vertebrate fossils (~646 ka to 23.2 ka; mid to late Pleistocene) have suggested that lake waters evolved from neutral pH to increasingly more alkaline saline conditions (Martin et al., 2005). By analogy, Fort Rock Lake may have also evolved from a fresh water environment to more alkaline and saline. The phreatomagmatic eruptions of Reed Rocks likely involved saline and basic external ground/lake water that is more akin to marine than fresh water conditions. In order to further constrain conditions of basalt alteration (temperature, pH), we compare the Reed Rocks alteration assemblage to examples from marine environments, such as Surtsey, Iceland (e.g., Apps, 1983; Chipera and Apps, 2001).

2.2 MATERIALS AND ANALYTICAL METHODS

2.2.1 Sample Collection

As part of a regional study of the FRVF, representative samples of basaltic tuff, lava and instrusives were collected from two adjacent tuff rings. A total of 16 samples (13 tuff, 3 lava) were collected. Seven tuffs and 3 lavas/intrusive are from Reed Rocks whereas 6 tuffs are from South Reed Rock. The goal in sample collection was to obtain a suite that displays a range of textures from fresh to highly altered. Obvious color differences, bedding thickness variations from laminated to massive, grain size variations, and ancillary precipitate content were key considerations.

2.2.2 Petrographic Analysis

Petrographic analyses and scanning electron microscopy (SEM) of basaltic tuffs were performed to characterize primary and alteration textures including both aqueous (abiotic) and reputed bioalteration textures. To describe the various morphologies of bioalteration textures in comparison to those reported in oceanic basalts, we apply terminology of Fisk and McLoughlin (2013). For scanning electron microscopy and backscatter electron (SEM/BSE) observations, samples were carbon-coated and analyzed using a Hitachi SU6600 at the Zircon and Accessory Phase Laboratory (ZAPLab) at the University of Western Ontario.

Estimations of modal percentages of textural features (e.g., palagonitic alteration, fresh glass) were obtained by manual point counts of each tuff using an Olympus BX51 System microscope. The distinction between fresh glass, and abiotic or biotic glass alteration was done based on differences in textural characteristics/relationships

represented in samples containing fresh glass (Fig. 1.9; Appendices 1-4). In most cases, between 300 and 700 points were counted depending on several factors. In some cases, samples contained greater proportions of soft material so after final polishing more material may have been ground out along outer edges and softer phases may have been lost. Some sections had smaller surface areas, or only inner portions of sections that were preserved and countable. During point counting, photomicrographs of areas that contained bioalteration textures were collected using an Olympus DP72 digital camera attachment with cellSens Standard software (Olympus Life Science n.d.; http://www.olympus-lifescience.com/en/software/cellsens/). Tunnel diameters and lengths were measured from photomicrographs using the cellSens Standard and ImageJ software (Rasband n.d.; http://imagej.nih.gov.ij/) measurement tools. Photomicrographs were also visually examined and the presence or absence of each morphotype was tallied. Those values were then used to plot size distributions and calculate morphotype proportions, respectively. Photomicrographs were used for measurements and morphotype surveys instead of live microscope view to keep the focus on point counting during point counts (divide tasks) and to allow measurements to be made afterwards without the need of the microscope (e.g., using ImageJ).

In order to approximate the relative quantity of bioalteration, a two-step method was applied. During point counting, the presence or absence of microborings within the field of view was recorded for each point to assess whether bioalteration is found throughout the sample, or only in a few isolated pyroclasts. Then, a method similar to that devised by Cousins et al. (2009) was adopted whereby the proportion of bioalteration found along available alteration boundaries such as pyroclast margins, fractures and

vesicles, was visually approximated in each thin section. Each was given a 'bioalteration value' ranging from 0, representing no boundaries affected by bioalteration, to 10 for all boundaries affected by bioalteration. Other quantitative data such as modal percentages obtained by point counts were compared to the relative proportions of bioalteration to determine whether any relationships existed with other textural features. Given that this visual estimation method is subjective, the determined bioalteration values inherently have errors, likely between 5-20%.

2.2.3 Mineralogical and Geochemical Analyses

Micro X-Ray Diffraction (μXRD) was performed on cut rock slabs and polished thin sections with the Bruker D8 Discover Diffractometer at the University of Western Ontario. The diffractometer was operated with CoKα radiation (λ = 1.7889 Å) generated at 35 kV accelerating voltage and 45 mA beam current with Co Gobel mirror parallel optics system having θ-θ geometry. Use of 100 μm or 300 μm nominal beam diameters enabled *in situ* analysis at the microscopic scale and the correlation between crystal structural data and other microscopic data such as polarizing microscope observations and SEM data (Flemming, 2007). Micro XRD data were collected on a 2D General Area Detector Diffraction system (GADDS) and integrated to generate a conventional intensity versus 2theta diffraction pattern, for mineral identification using the International Center for Diffraction Data (ICDD) database. Powder X-Ray diffraction was also performed on bulk samples with a Rigaku DMAX diffractometer to verify phases identified by μXRD.

Lava samples were sent to the Washington State University (WSU) GeoAnalytical Lab to determine elemental compositions using a ThermoARLAdvant`XP+ sequential X-Ray fluorescence (XRF) spectrometer. X-ray element maps or spectra were acquired

using Energy dispersive spectrometry (EDS) of the Hitachi SU6600 scanning electron microscope (as described above).

2.3. RESULTS AND DISCUSSION

2.3.1 X-Ray Fluorescence (XRF)

Major elemental concentrations are markedly similar between the three lava/intrusive samples, ranging from 50.02 - 50.08 wt. % SiO_2, 8.36 – 8.47 wt. % total Fe as FeO*, and Mg# = 67, where Mg# is defined as molar 100MgO/(MgO+FeO). The lavas are low in K_2O (0.36 - 0.39 wt. %) consistent with a petrographic classification as low potassium tholeiitic basalts (LKT), an incompatible element-poor basalt type common in the FRVF (Jordan *et al*., 2004).

2.3.2. X-Ray Diffraction and Petrography

X-Ray diffraction patterns of the glassy tuffs are typified by a broad elevated area (or 'amorphous hump') at ~15 to 40 ° 2θ (Fig. 2.4). Igneous minerals identified include plagioclase, olivine (Fig. 2.4A), pyroxene and oxides. Secondary minerals include the zeolite chabazite with lesser phillipsite, calcite, and the smectites nontronite (Fig. 2.4B) and saponite. Chabazite infills vesicles/voids and comprises part of palagonitic alteration. A typical pattern is depicted in (Fig. 2.4B). The more common and pervasive amygdaloidal and vug calcite exhibits the most distinct diffraction pattern (Fig. 2.4C) with fine radial dendritic/bladed to granular/massive habits. Nontronitic smectite is identified in areas with yellow palagonitic alteration, and 2d spacings are consistent with some interlayered saponite. Palagonite rim coatings ranging from 5-30 μm thicknesses

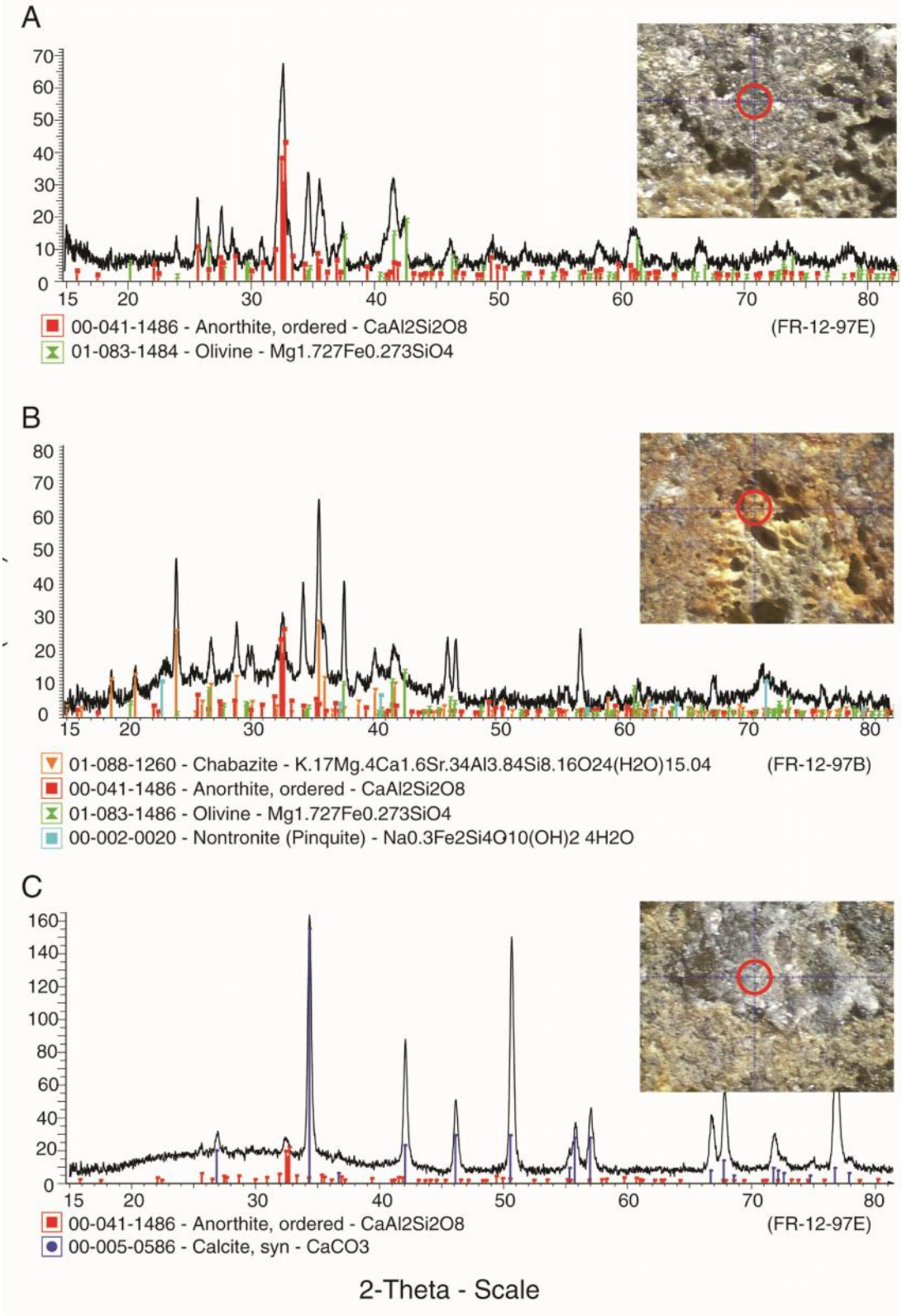
A
00-041-1486 - Anorthite, ordered - CaAl2Si2O8
01-083-1484 - Olivine - Mg1.727Fe0.273SiO4
(FR-12-97E)
B
01-088-1260 - Chabazite - K.17Mg.4Ca1.6Sr.34Al3.84Si8.16O24(H2O)15.04
00-041-1486 - Anorthite, ordered - CaAl2Si2O8
01-083-1486 - Olivine - Mg1.727Fe0.273SiO4
00-002-0020 - Nontronite (Pinquite) - Na0.3Fe2Si4O10(OH)2 4H2O
(FR-12-97B)
C
00-041-1486 - Anorthite, ordered - CaAl2Si2O8
00-005-0586 - Calcite, syn - CaCO3
(FR-12-97E)
2-Theta - Scale

Figure 2.4. Representative micro X-ray diffraction patterns showing common primary and secondary mineralogy of Reed Rocks tuffs. Images in upper right corners show the 300 µm spot (red circle) analyzed. (A) Common primary basaltic minerals olivine and plagioclase (anorthite). A background subtraction was performed on this pattern to eliminate the effects of amorphous glass in the signal which flattened the pattern out. (B) Common secondary minerals nontronite (smectite clay) and chabazite (zeolite). This pattern displays a broad elevated portion of the signal or 'amorphous hump' from 15° - 40° 2θ produced by the glass component. No background subtraction was preformed. (C) Distinct secondary pore-filling calcite diffraction pattern. This also displays a broad elevated portion of the signal from 15° - 40° 2θ produced by the amorphous glass. No background subtraction was performed. See Figure 2.1 for sample locations.

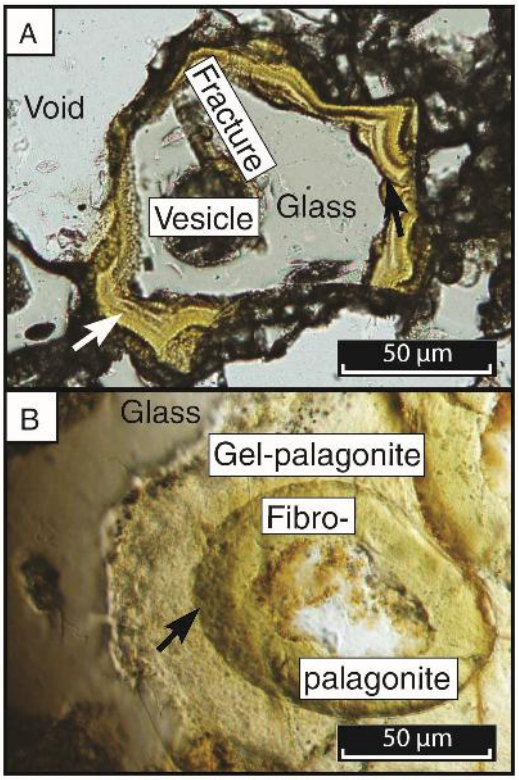

Figure 2.5. Abiotic aqueous alteration. (A) Coarse ash pyroclast with a regular banded, smooth, yellow gel-palagonitic (isotropic) alteration front along the exterior margin (*arrows*), and an unaltered glass core. From sample FR-12-91A. (B) Abiotic palagonitic alteration front originating from a vesicle surface. The smooth isopachous fibro-palagonitic (anisotropic) band (*arrow*) is a later stage proto-crystalline material formed after the amorphous gel-palagonite. The smooth regular alteration fronts of A and B differentiate this aqueous (abiotic) alteration from the irregular granular and tubular textures believed to be formed biologically. From sample FR-12-90.

propagate into the glass as alteration fronts progress toward unaltered glass, many clasts of which have unaltered cores with only exterior alteration rims (e.g., Fig. 2.5). Most completely palagonitized clasts are of fine (<0.06 mm) and coarse ash (0.06-2 mm) sizes. The amorphous gel-palagonite form is most common, but the proto-crystalline fibro-palagonite form is present in minor quantities (Table 2.1).

Table 2.1. Maximum, minimum and average values of important textural characteristics in Reed Rocks basaltic tuffs.

Variable	**Max. (%)**	**Min. (%)**	**Avg. (%)**
Total fresh glass*	52.3	6.2	34.0
Primary glass	53.8	34.2	46.0
Crystallinity[§]	19.8	5.3	10.6
Plagioclase	8.1	1.8	3.6
Olivine	2.9	0.5	1.9
Undercooling [#]	9.2	2.1	5.0
Vesicularity	12.1	2.8	8.5
Primary porosity**	30.4	16.8	23.6
Matrix	26.8	3.7	16.6
Abiotic alteration[††]	33.2	1.0	11.9
Gel-palagonite[§§]	32.9	1.0	11.7
Fibro-palagonite[##]	1.3	0.0	0.3
Total calcite	15.5	0.0	3.3
Zeolites	0.7	0.0	0.1
Bioalteration value***	8.75	0.0	2.4
	Max. (µm)	**Min. (µm)**	**Avg. (µm)**
Tunnel Diameter	4.4	0.5	0.9
Tunnel Length	47.7	6.7	22.5

All values except bioalteration and tunnel length-width measurements are modal percentages calculated from point count data.

All values are rounded to nearest 0.1.

*Total fresh glass: proportion of fresh glass currently in sample.

[†]Primary glass: total fresh glass + abiotic (palagonitic) alteration.

[§] Crystallinity: total primary igneous minerals (phenocrysts/ glomerocrysts + microlitic undercooling).

[#]Undercooling: microlitic intergrowths of plagioclase and pyroxene.

** Primary porosity: vesicularity + voids + amygdaloidal and vug calcite/zeolite.

[††]Abiotic alteration: total proportion of altered glass (palagonite).

[§§] Gel-palagonite: amorphous (isotropic) glass alteration.

[##] Fibro-palagonite: crystalline (anisotropic) glass alteration.

***Values are averages within each thin section determined using visual estimation method based on Cousins and others (2009).

Considering the secondary phase assemblage, the specific temperature and pH conditions under which they've been documented to form in, and their petrographic relationships, an approximation of hydrothermal alteration conditions within the Reed Rocks basaltic tuffs may be made. We note that the processes by which zeolites and palagonite form are complex and not fully understood, and acknowledge that these are interpretations based on observation and previous studies (Kristmannsdóttir and Tómasson, 1978; Eggleton & Keller, 1982; Apps, 1983; Staudigel & Hart, 1983; Jakobsson & Moore, 1983; Chipera & Apps, 2001; Stroncik & Schmincke, 2001. Chevrier *et al*., 2007).

2.3.2.1. Formation of Chabazite (Zeolites)

If the Fort Rock Lake waters were fresh during the late Pliocene and became more saline and alkaline during the mid to late Pleistocene, then the existence of amygdaloidal chabazite (Figs. 2.4, 2.6) is consistent with Reed Rocks having erupted in the mid to late Pleistocene into saline-alkaline waters. Chabazite forms most stably in saline-alkaline (pH 9 to 10) water in lake environments and in cavities of mafic rocks as a result of hydrothermal fluids (Kristmannsdó ttir and Tómasson, 1978; Chipera & Apps, 2001; Utada, 2001). The formation of chabazite is also most stable in the low temperature regime below 100°C (Chipera & Apps, 2001). The approximate temperature range for the formation of chabazite in Iceland geothermal deposits is for example ~10 to 80°C (Apps, 1983; Chipera & Apps, 2001). This is therefore considered to be the temperature range of zeolite formation within the Reed Rocks tuffs.

2.3.2.2. Formation of Calcite

The abundance of calcite (0-15%) is also strongly indicative of neutral to alkaline fluids (Chipera & Apps, 2001; Chevrier *et al*., 2007). Calcite forms over a much wider temperature range (0 - 270°C) than chabazite (Apps, 1983) with more variable habits. Calcite at Reed Rocks likely precipitated throughout hydrothermalism and diagenesis. Zoned amygdules in palagonitized clasts are observed where vesicle surfaces are coated by zeolites and infilled with calcite (Fig. 2.6). These amygdules suggest that calcite continued to precipitate after palagonitization was complete as well as post-zeolite formation at temperatures below 80°C (the upper temperature limit of chabazite stability; Apps, 1983).

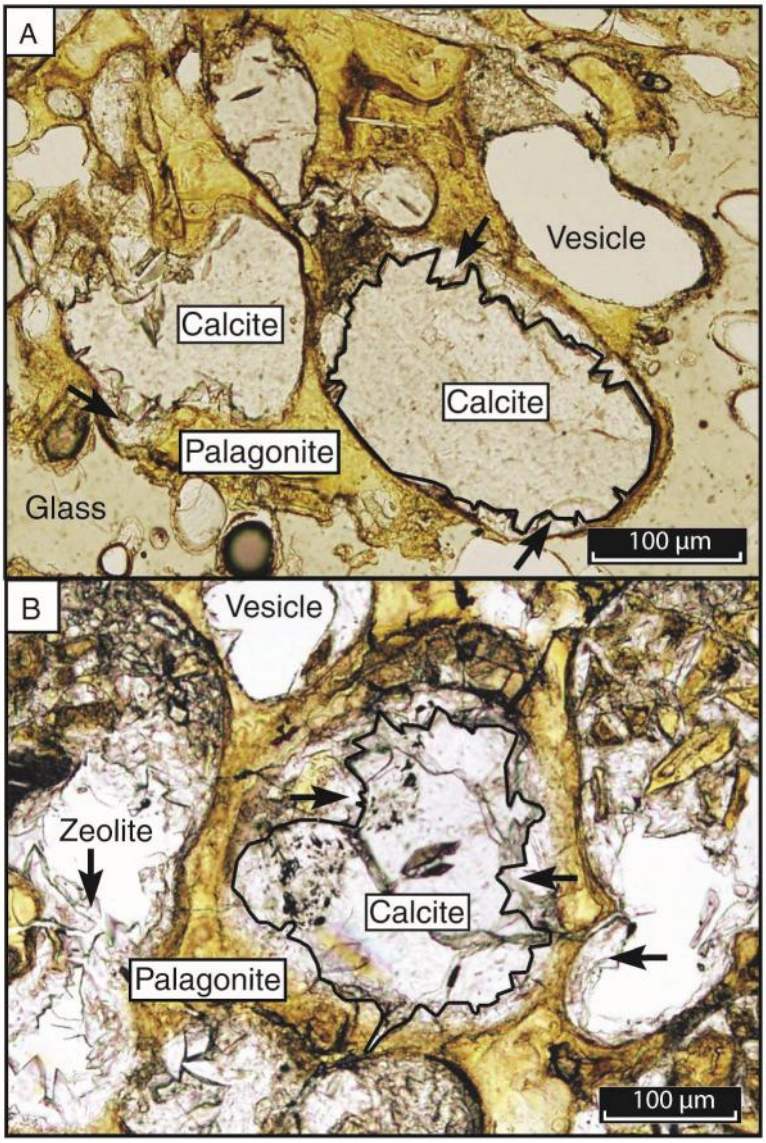

Figure 2.6. Abiotic alteration textures. (A) Partially gel-palagonitized (isotropic) vesicular pyroclast with calcite- and zeolite-filled vesicles (zoned amygdules). The black line depicts a contact between the chabazite (*arrows*) that lines the vesicle wall, and the calcite that fills the vesicle interior. (B) Wholly palagonitized vesicular pyroclast with zeolites (*arrows*) lining the vesicle walls and calcite infilling the interior of the vesicle. This relationship suggests calcite precipitating post-zeolite formation. From sample FR-12-97B. *Note:* Zeolites were only found in samples with the highest percentage of aqueous (abiotic) alteration.

2.3.2.3. Formation of Nontronite Smectite and Palagonite

Nontronite smectite is a primary component of palagonite (e.g., Eggleton & Keller, 1982; Staudigel & Hart, 1983; Stroncik & Schmincke, 2001). The lower temperature limit of smectite (nontronite) formation is interpreted to be ~25°C (Jakobsson & Moore, 1983; Chipera & Apps, 2001). Under hydrothermal conditions (>120 ± 5°C), palagonitization is complete and olivine alters to smectite (nontronite and saponite) (Jakobsson and Moore, 1986). Because olivine at Reed Rocks is unaltered, hydrothermal temperatures likely did not reach 120°C. In hydrothermally altered Icelandic basalts, Apps (1983) found palagonitization to occur over a temperature range of 50-150°C with 75-80% and >90% palagonitization occurring at temperatures of 80°C and 120°C, respectively. In the Reed Rocks, the greatest palagonitization proportion is ~66% of total primary glass or ~33% of entire sample (Table 2.1) suggesting that alteration temperatures may well have been <80°C. Higher temperatures may have been reached at Reed Rock than at South Reed Rock or higher water/rock ratios because there is a greater abundance of palagonitic alteration (Reed Rock: 1-33%, South Reed Rock: 2 - 7%).

2.3.2.4. Microbial Bioalteration

Petrographic analysis of thin sections from 13 tuff samples revealed a variety of textures that, compared to other previously-published descriptions of marine bioalteration textures and distributions, have strong similarities to the *tubular* and *granular* morphological types of microbial alteration (e.g. Fisk *et al*., 1998a; Furnes and Staudigel, 1999; McLoughlin *et al*., 2008; Staudigel *et al*., 2008; Fisk and McLoughlin, 2013).

Referring to the set of biogenicity principles proposed by McLoughlin et al. (2007), the putative microborings described here fulfill at least two of the three criteria:

2.3.2.4.1. Evidence of Biogenic Morphology and Behaviour. The Reed Rocks micro-tunnels display the following morphologies:

- wide incursions with mushroom like termini, irregular and mossy branching alteration fronts (Fig. 2.7)
- septate divisions, annulations, and spiral/helical filaments/shapes (Fig. 2.8)
- straight to curvilinear, internal divisions, and bulbous to rough terminal swells and crowns (Fig. 2.9)
- rough or disc-shaped terminal enlargements (Fig. 2.10)
- ovoid bodies or spherical buds (Figs. 2.10A, 2.11)
- simple, network and palmate branching patterns (Fig. 2.12)
- simple, thin, knotted and tangled (Fig. 2.13)
- irregular granular incursions/alteration fronts of sub-spherical pits, bubble textures (Fig. 2.14)
- directional changes upon encountering another tunnel, fracture or plagioclase crystal, migration toward olivine grains, and dark opaque contents (Fig. 2.15)

Diameters of micro-tunnels are most commonly 0.5 - 1.5 µm, but range from 0.4 µm to 5 µm (Fig. 2.16). Tunnel lengths range from 6 µm to 48 µm. Tunnels from marine environments are typically 1-5 µm in diameter with lengths of up to 100 µm (Furnes et al., 2001; Fisk et al., 2013). The size variation for micro-tunnels at Reed Rocks is log-normally distributed (Fig. 2.16). Log-normal size distributions are a common

observation in biological systems (Limpert et al., 2001; van Dover et al., 2003) and have also been observed in tunnel diameter size distributions of oceanic basalts (e.g., Furnes et al., 2007a). Tubular micro-tunnels are more highly concentrated around vesicles (Figs. 2.7B, 2.8A-C, 2.9A-D, F, 2.10B, 2.11A, D, 2.12A-C, 2.13, 2.15A-B) suggesting biological behaviour. These sites may be preferred because structural weaknesses may be exploitable or micro-environmental/chemical conditions are more favourable.

SEM imaging revealed irregular surfaces to tunnel walls. They unevenly consist of pits, possibly from incongruent dissolution, in addition to solid irregular elongate encrustation features (Fig. 2.10D-E). These may be the result of a precipitation process whereby insoluble residual and organic chemical components are deposited along the interior of tunnels or they may be secondary encrustations of smectites (Furnes et al., 2007a; Wacey et al., 2014).

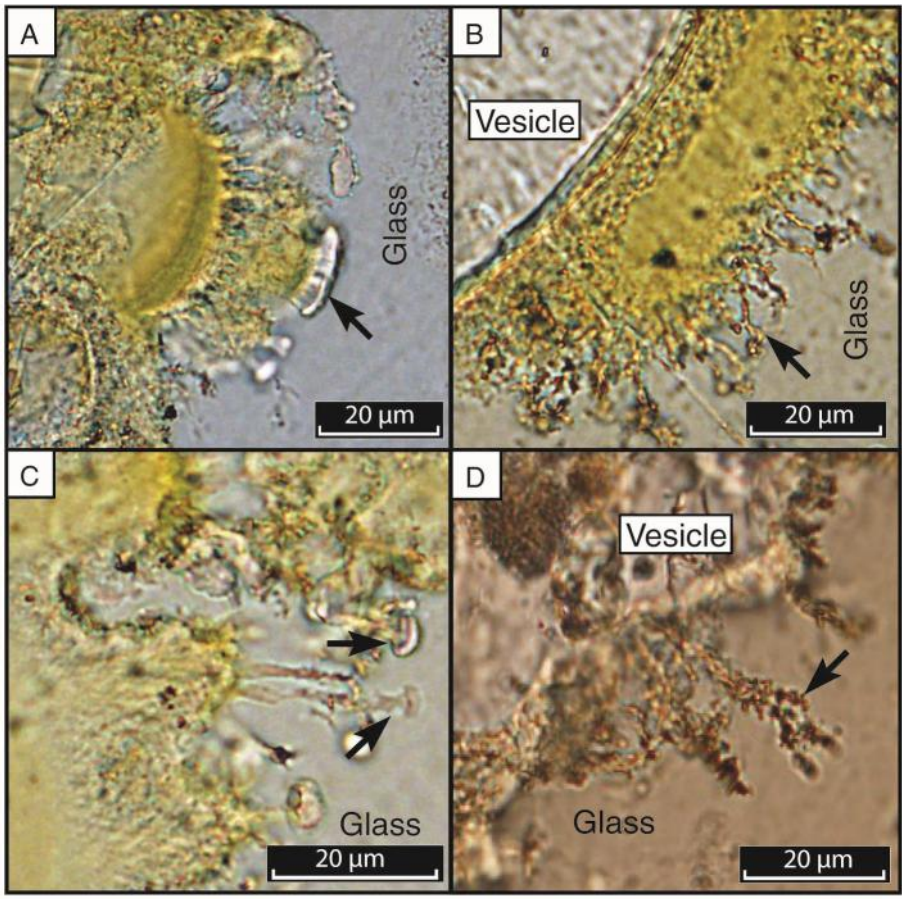

Figure 2.7. (A) Wide (>10 µm) micro-tunnel incursions with mushroom-shaped terminal cap (*arrow*) projecting beyond a yellow palagonitic alteration front in which faint concentric bands are visible. (B) Simple, short, close, mossy branching tunnels (*arrow*) extending from a yellow palagonitic alteration front along a vesicle wall. (C) Irregular tunnels that terminate with mushroom-like enlargements (*arrows*) extending from an irregular yellow palagonitic to granular alteration front. A-C are from sample FR-12-97B. (D) Rough, irregular, kinked, network branching tunnels or granular incursions (*arrow*) extending from a vesicle surface. From sample FR-12-94A.

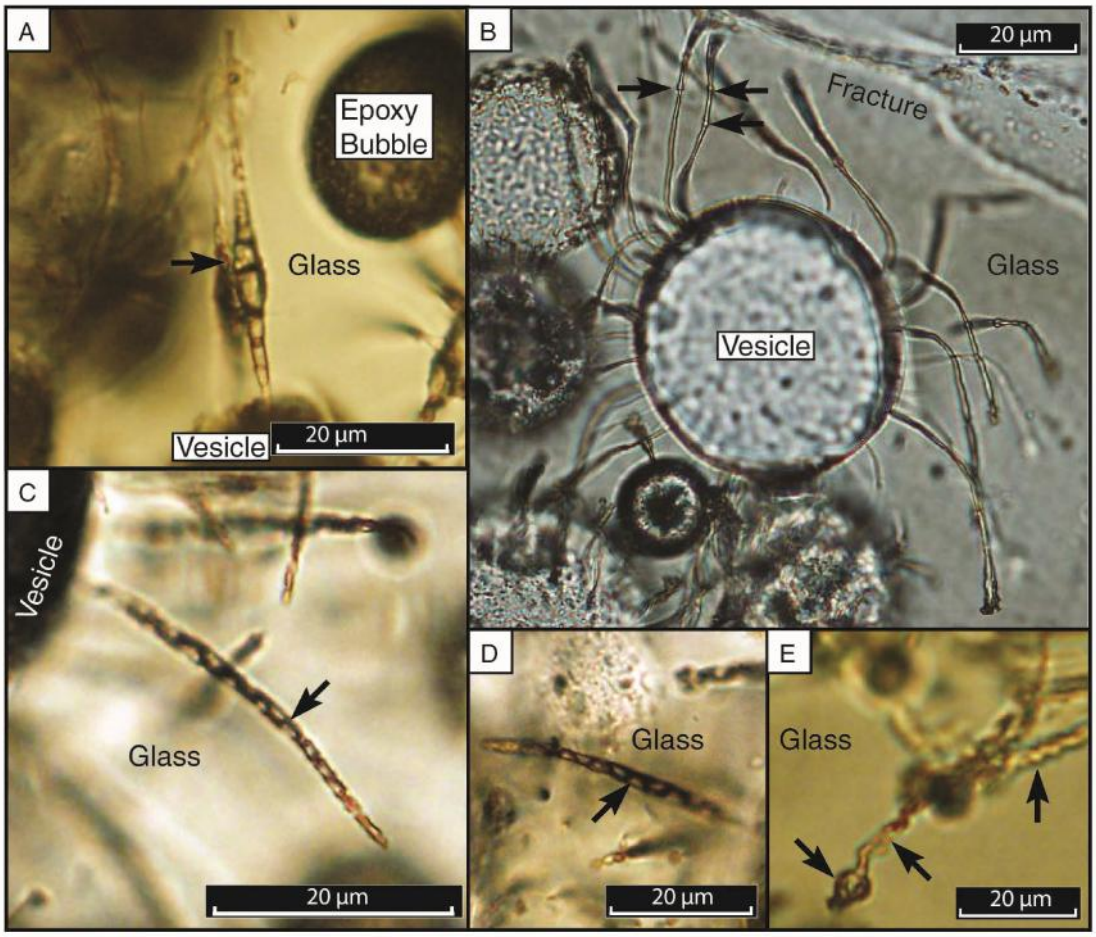

Figure 2.8. (A) Straight, engorged tunnel with septa (*arrow*), originating from a vesicle. (B) Long, curved tunnels with sparse annulations (*arrows*). These are rooted on a vesicle that has been sealed with calcite suggesting tunnel production prior to carbonate precipitation. From sample FR-12-90-1. (C-D) Curvilinear tunnels with spiral filaments or fine ornaments (*arrows*) along tunnel walls, slightly tapered toward their ends and rooted on vesicles. (E) Smooth, helical tunnels (*two right arrows*) with bulbous terminal enlargement (*left arrow*). A, C and D are from sample FR-12-94B.

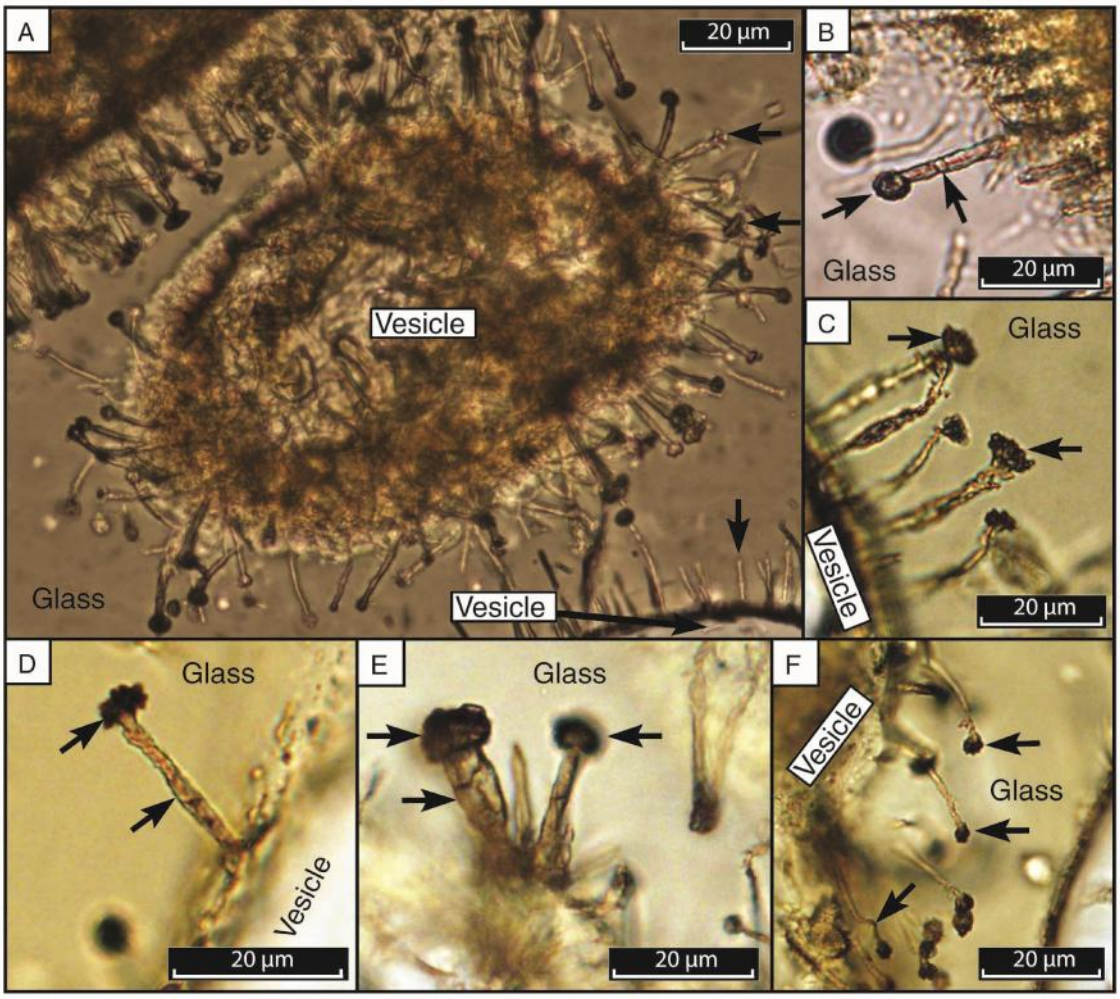

Figure 2.9. Variations of micro-tunnels with terminal enlargements. (A) Enhanced depth of focus (EDF) image showing close, smooth, thin, straight to curvilinear, constant width tunnels, with terminal bifurcating crown (*upper arrow*) and mushroom-like (*mid-arrow*) enlargements radiating from a vesicle infilled with altered matrix material. Lower arrow points to smooth, simple, thin tunnel without terminal enlargement. This is an enlarged image of the area outlined with a black box in Figure 2.3. (B) Straight, constant width tunnel with round terminal bulb (*left arrow*) and small ovoid body (*right arrow*) mid-way along its length. Tunnel emerges from a granular alteration front along a pyroclast margin at right. (C-D) Rough, irregular tunnels with rough, dark terminal crowns, rooted on vesicles. (E) Straight tunnels with round bulbous terminal enlargements (*upper arrows*) and internal divisions (*bottom-left arrow*). (F) Thin, directed tunnels curving in a similar direction, with dark terminal crowns (*upper two arrows*) and slight tapering toward terminus. Bottom arrow points to a kinked tunnel. All are rooted on vesicles. A and E are from sample FR-12-97E, B-D and F are from FR-12-97A.

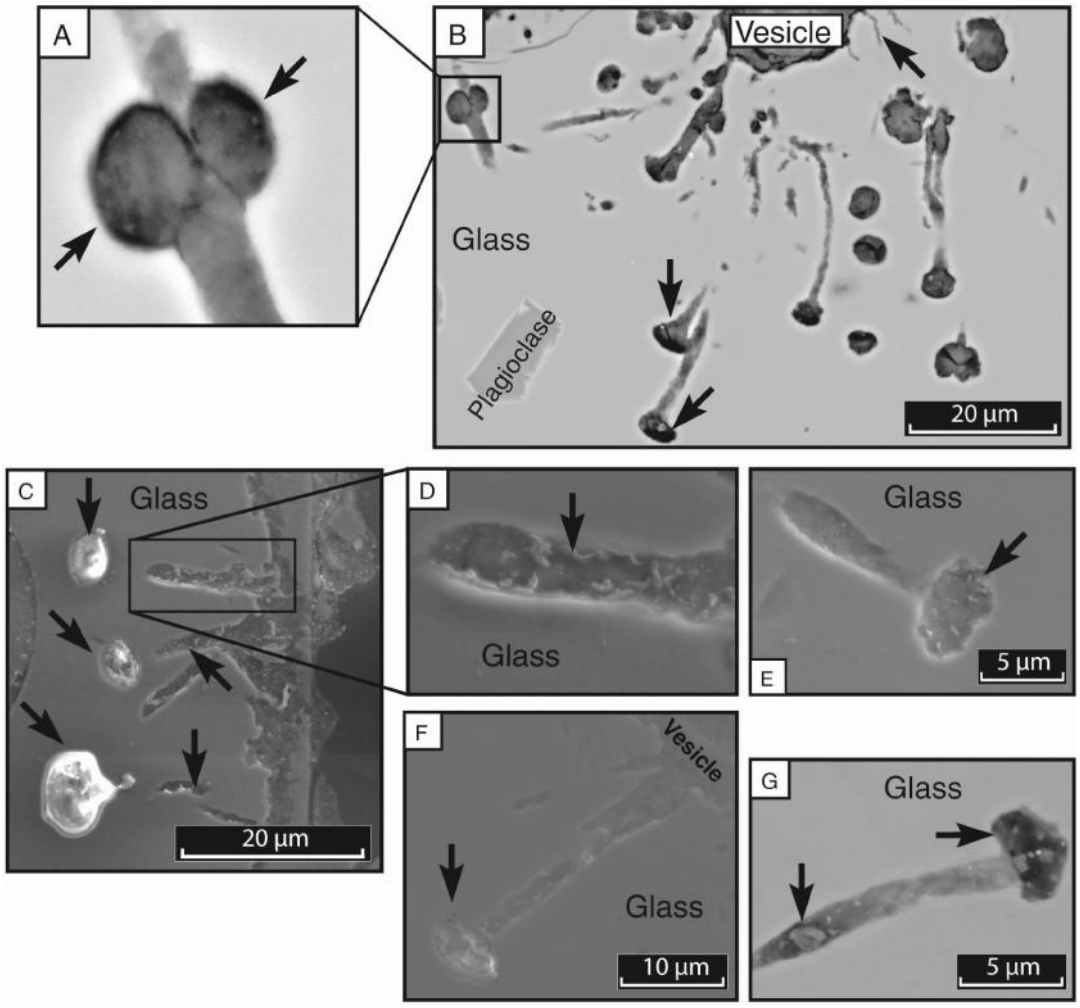

Figure 2.10. Scanning electron microscope (SEM) and back-scatter electron (BSE) images of tubular micro-tunnels. (A) BSE image of enlarged box in B displaying a smooth tunnel with ovoid cell-sized objects projecting from its margins. These are from the same sample the images in Figure 2.11D-E were taken. (B) BSE image displaying multiple straight and curved, directed tunnels with disc-like terminal enlargements (*bottom arrows*), radiating from a vesicle at top. Note that several round to irregular shaped isolated objects are located between tunnels representing normal and oblique cross sections, respectively, through only the terminal enlargements of tunnels intersecting the surface of the glass. (C) Multiple tunnels (*right arrows and box*) with associated terminal enlargements (*left three arrows*) extending from a pyroclast margin at right. Note, the three associated terminal enlargements are infilled with epoxy and appear disconnected because part of each tunnel does not intersect the glass surface. (D) Box in C enlarged displaying sinuous encrustation features (*arrow*) along the interior surface of a tunnel. (E) Straight tunnel with terminal enlargement containing small encrustation features (*arrow*). (F) Straight tunnel with a mushroom-like terminal enlargement (*arrow*), extending from a vesicle. (G) Curvilinear tunnel with terminal enlargement (*right arrow*) and small cell-sized object within tunnel (*left arrow*). From sample FR-12-97E.

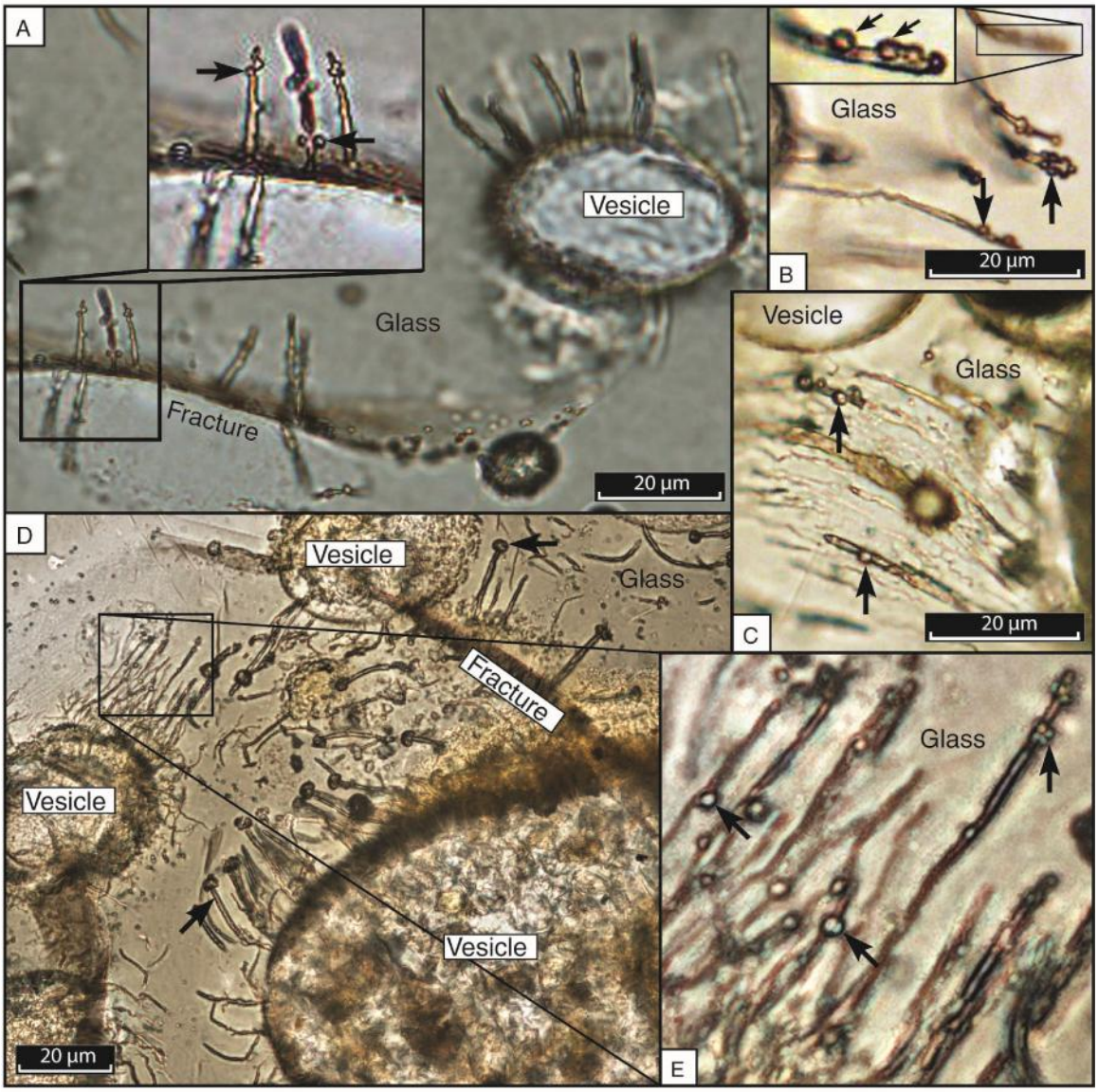
A
Vesicle
Glass
Fracture
20 µm
B
Glass
20 µm
C
Vesicle
Glass
20 µm
D
Vesicle
Glass
Fracture
Vesicle
Vesicle
20 µm
E
Glass

Figure 2.11. Micro-tunnel morphologies associated with spherical buds or ovoid bodies. (A) Asymmetrically rooted along a fracture are thin, straight to curvilinear, directed tunnels with cell-sized spherical buds projecting outward along tunnel margins (*arrows in enlarged box*). The fracture is connected to a vesicle infilled with calcite. The calcite-sealed vesicle also has simple, curvilinear tunnels radiating from it suggesting that the tunnels were produced prior to calcite precipitation. (B) Thin, curved or kinked, directed tunnels in preferred orientation with spherical buds/ovoid bodies (*arrows*) near tunnel termini. The box in upper left corner shows an enlarged focused image of the area outlined by the box in the upper right. It clearly displays spherical objects ~1-3 µm in diameter. The bottom tunnel has slight kinks mid-way along its length. All are rooted along a fracture. (C) Rooted on a vesicle are preferentially oriented straight to slightly curved, directed, close tunnels with spherical cell-sized objects (*arrows*) projecting outward along tunnel margins. (D) Enhanced depth of focus (EDF) image showing preferentially oriented close, smooth, thin, directed, straight to curvilinear, constant width tunnels, with terminal bulbs (*top arrow*), radiating asymmetrically from a fracture and connected vesicle. Note: Several micro-tunnels with terminal enlargements near the bottom of the image look as if they have longitudinal lineations (*bottom arrow*), but these are an artifact of stitching together multiple focal planes to create the EDF image. Box at left is enlarged in (E) displaying thin, directed, tunnels with ovoid bodies (*arrows*) projected outward from margins and within tunnels at various distances along their lengths. Most ovoid bodies are solitary, but arrows at bottom and right show groups of two and four clustered bodies. The ovoid bodies in the group of four are approximately one half the size of those found in the group of two. From sample FR-12-97E.

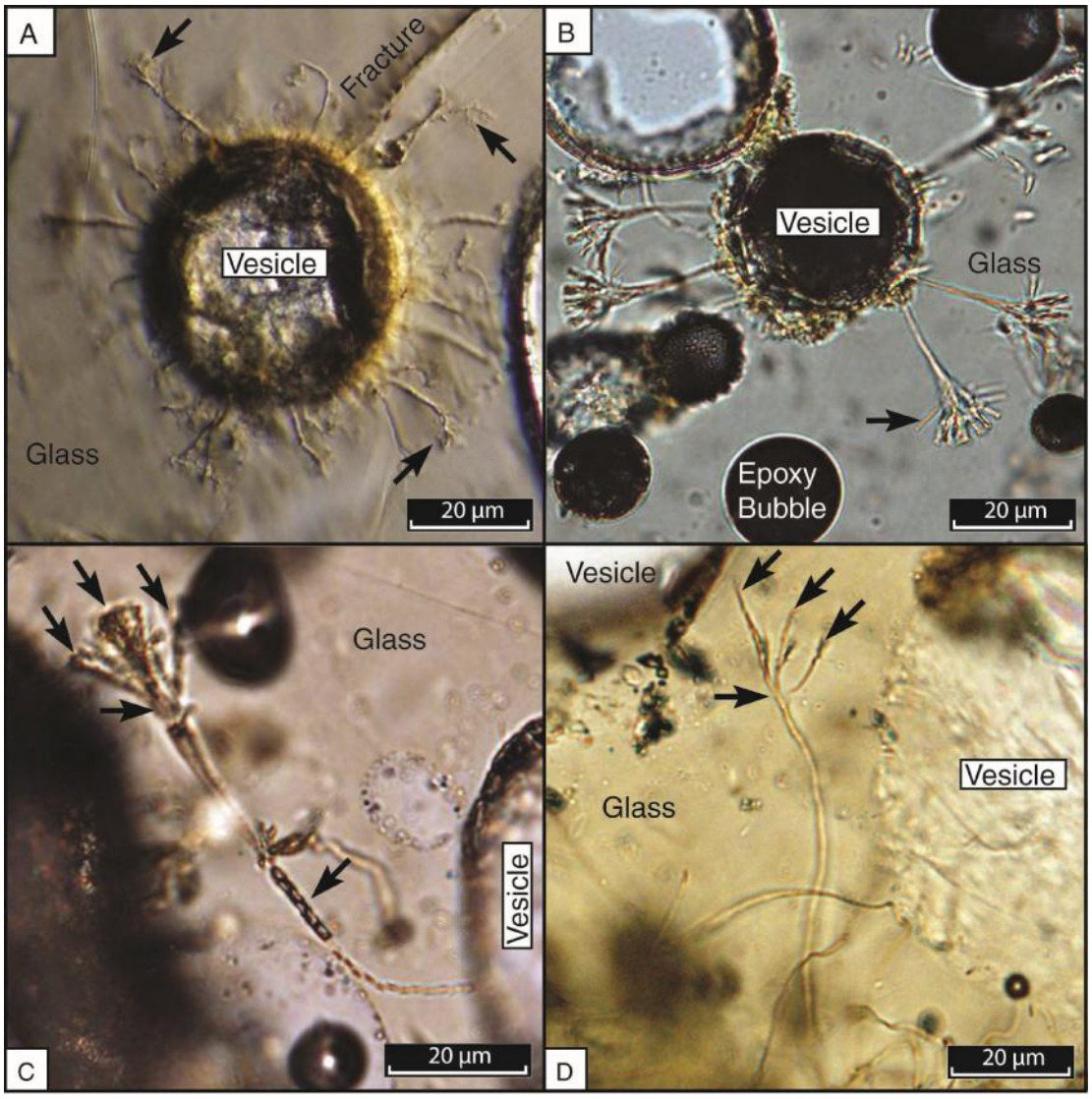

Figure 2.12. Branching micro-tunnel morphologies. (A) Thin, convoluted and bifurcating network tunnels (*arrows*) radiating from a vesicle with a yellow palagonitic alteration rim, connected to a fracture. From sample FR-12-97B. (B) Smooth tunnels with palmate bifurcating termini and nodal swelling. There are 4-6 daughter tunnels of approximately equal diameter to the main tunnel at each terminus. These are rooted on a vesicle that is connected to a fracture. (C) Long, curved tunnel with spiral filament (*bottom arrow*) and large palmate bifurcating terminus. Three daughter branches are visible (*upper three arrows*) beyond a node (*mid-arrow*). This tunnel is rooted on a vesicle, the curvature direction appears to be in avoidance of another vesicle at left. (D) Long, smooth, curved tunnel bifurcating at its terminus with three branches (*upper three arrows*) beyond a node (*lower arrow*). B-D are from sample FR-12-94B.

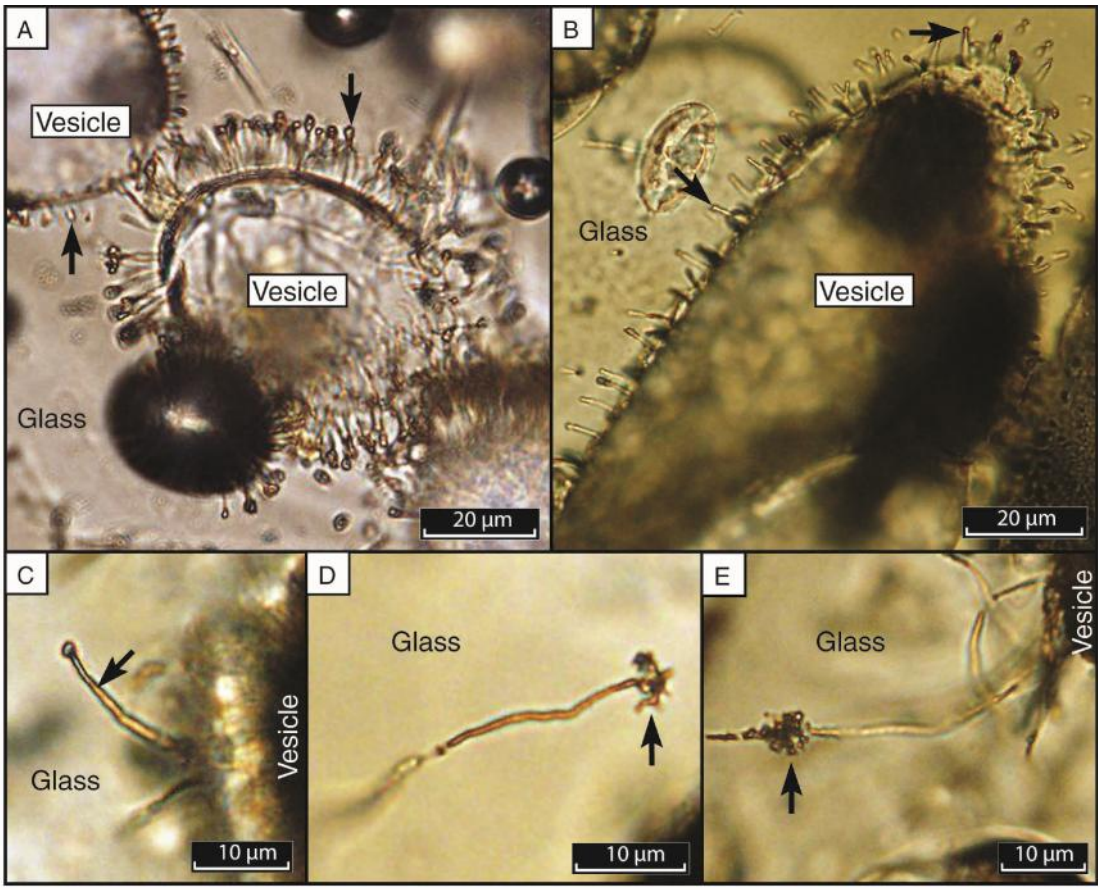

Figure 2.13. (A) Short, straight, smooth, close tunnels with slight bulbous terminal enlargements (*right arrow*), radiating from a vesicle. Left arrow points to shorter, simple, smooth tunnel without terminal enlargement, rooted on another vesicle. (B) Short, straight, simple, smooth tunnels radiating from a vesicle. (C) Smooth, curvilinear tunnel tapered toward its small terminal bulb enlargement. (D-E) Smooth, kinked tunnels with tangled regions (*arrows*) near termini, rooted on vesicles. From sample FR-12-94B.

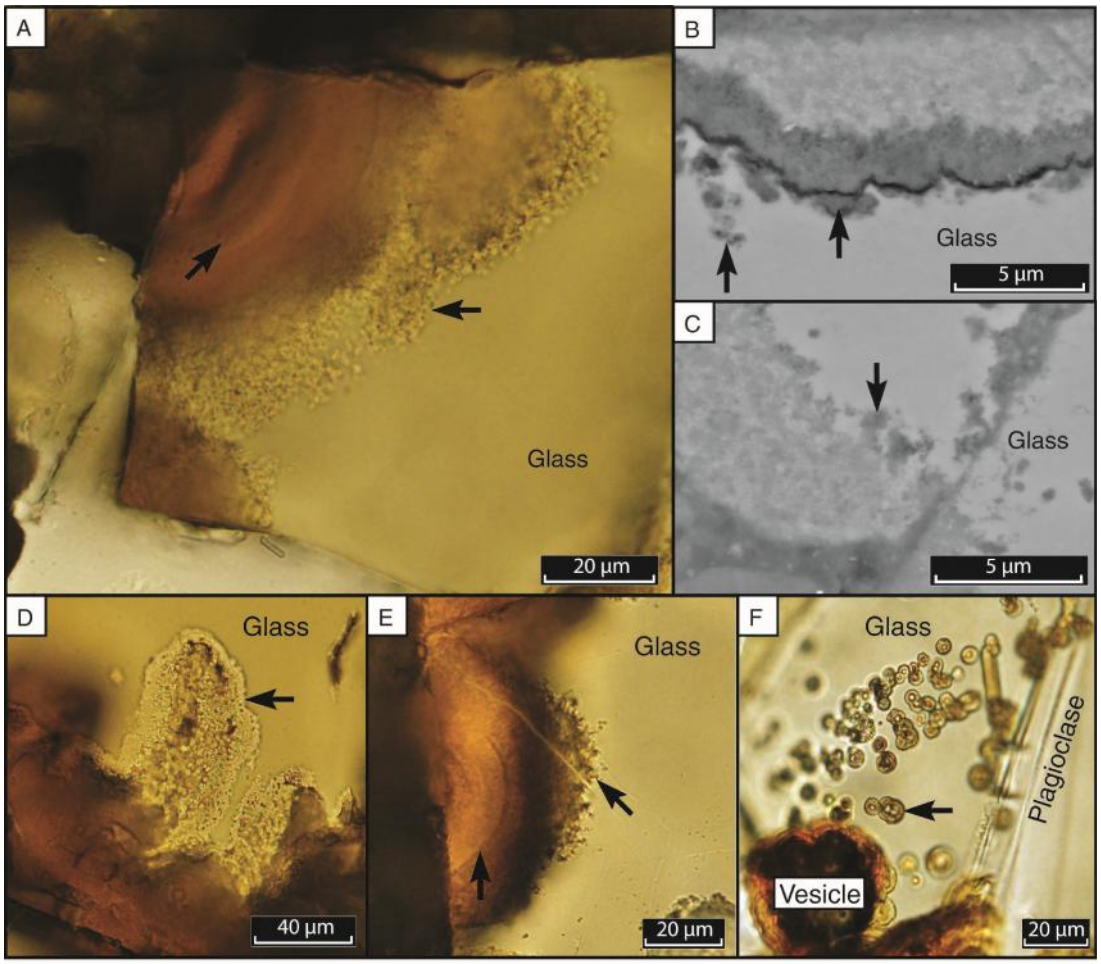

Figure 2.14. Granular bioalteration. (A) Irregular granular alteration front (*right arrow*) rooted along a blocky coarse ash pyroclast margin. Left arrow points to faint zoning. From sample FR-12-91A. (B-C) Back-scatter electron (BSE) images of granular alteration fronts rooted on pyroclast margins. Note: Image in (C) is an enlarged image of the box outlined in Figure 2.17A. From sample FR-12-97E. (D) Granular incursion (*arrow*) rooted on a pyroclast margin. From sample FR-12-90-1. (E) Irregular alteration front with granular and minute mossy branching channels (*arrow*) rooted on pyroclast margin. Left arrow points to slight palagonitic concentric bands. From sample FR-12-91B. (F) Possible less common bubble sub-morphotype texture consisting of coalesced 2-7-µm-diameter sub-spherical pits with concentric rings and central cores. Each individual sphere has a yellow to brown concentric rim. Each core is slightly anisotropic and may be composed of smectites. The vesicle at bottom left also has an irregular alteration front consisting of individual semi-circular incursions. From sample FR-12-92-1.

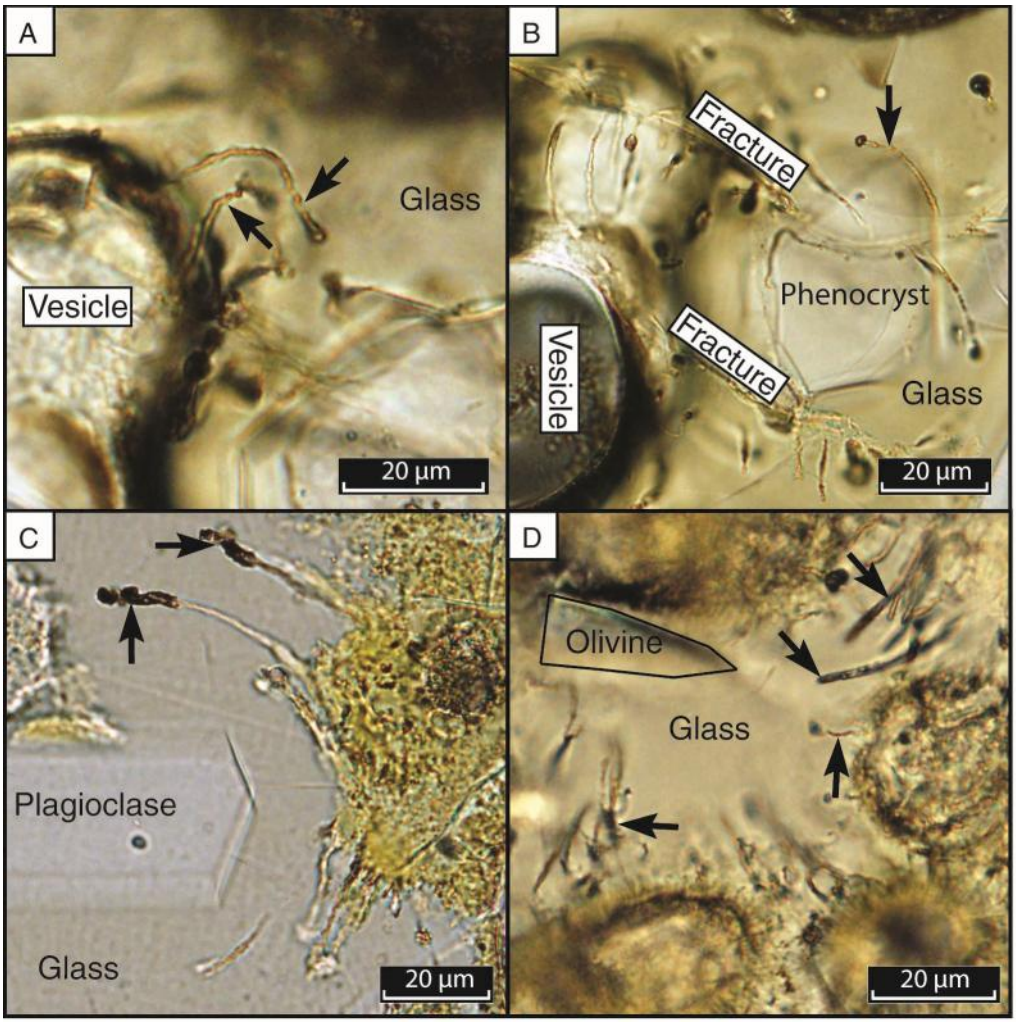

Figure 2.15. Micro-tunnels exhibiting directionality or behaviour. (A) Simple, smooth, curved tunnel (*right arrow*) curving around another simple, smooth tunnel (*left arrow*). (B) Smooth tunnel with a dark bulbous terminus (*arrow*), rooted along a fracture and curving around a phenocrysts within the glass. Both the upper and lower fractures have other simple curved tunnels extending from them. A-B are from sample FR-12-97A. (C) Smooth, curved tunnels with slight terminal enlargements of dark contents (*arrows*), extending from a granular/palagonitic alteration front and curving around a plagioclase phenocryst within the glass. This may be an example of structural weaknesses (concentric stress fractures or areas of weakness around phenocrysts) being exploited, although no concentric fractures are visible. Note that the tunnels indicated with arrows remain separated by a constant distance and that the shorter tunnels to the bottom of the image are following a similar path in the opposite direction around the crystal. From sample FR-12-97B. (D) Multiple simple curvilinear tunnels (*arrows*) originating from a pyroclast margin and migrating towards an olivine phenocryst (*outlined in black*). From sample FR-12-97E.

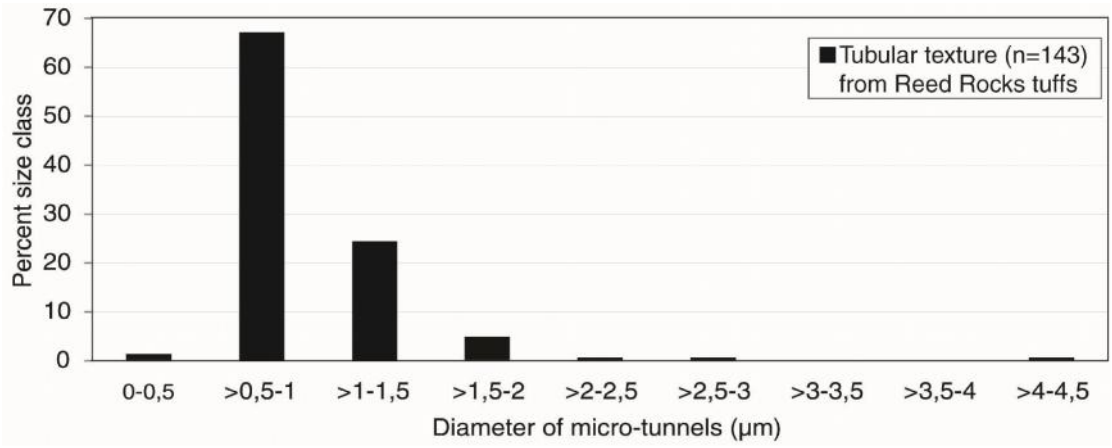

Figure 2.16. Histogram showing the relationship between the diameter of tubular micro-tunnels and percentage in size classes from Reed Rocks tuffs. No data from size classes 3-4. Values were obtained by directly measuring features in photomicrographs using cellSens Standard and ImageJ software measurement tools.

2.3.2.4.2. A Primary Geological Context that Demonstrates the Age and Syngenicity of Putative Bioalteration Textures. The Reed Rocks micro-tunnels are only found within fresh volcanic glass pyroclasts. Micro-tunnels are distributed entirely along surfaces that would have acted as pathways for external water and endoliths such as pyroclast margins, fractures, and vesicles. They are typically perpendicular or near perpendicular with respect to the surfaces from which they originate and also appear to predate infilling carbonate cement phases shown by their radiation from calcite-sealed vesicles (Figs. 2.8B, 2.11A).

2.3.2.4.3. Geochemical Evidence for Biological Processing. EDS analyses indicate that tunnel interiors are slightly depleted in Na, Mg, Al, Fe and enriched in K relative to fresh glass. In ocean basalts, similar depletions of metabolically important elements such Na, Mg, Fe and Ca, have been documented in association with bioalteration textures (e.g., Alt and Mata, 2000).

2.3.2.5. Distinguishing Biogenic from Abiotic Textures

2.3.2.5.1. Aqueous alteration (palagonite). Tubular and granular textures are distinguished from abiotic alteration fronts by their irregular rough appearance and asymmetric distribution about the fractures/surfaces from which they originate. Aqueous alteration forms planar regularly banded alteration fronts interfacing with fresh unaltered glass symmetrically along fractures and margins (Fig. 2.5).

2.3.2.5.2. Fractures. Where tunnels intersect glass surface, cross sections are generally circular/elliptical. The focal point of tunnels in thin sections is a small circle/ellipse that, when the focus level is altered, moves up or down and sideways as a one dimensional feature. Fractures however, from which many tunnels originate and are directly juxtaposed, appear as linear two-dimensional expressions of either curved or planar surfaces.

2.3.2.5.3. Ambient inclusion trails (AITs). The morphology of tubular micro-tunnels in the Reed Rocks can be distinguished from similar tubular textures known as ambient inclusion trails that are produced abiotically. They are differentiated by (1) the absence of metal sulfide or oxide grains at the ends of micro-tunnels, although unlike most oceanic pillow basalts, there is a minor source of oxide crystal inclusions within the basaltic glass, (2) the presence of annulations/ornamentations and the absence of longitudinal striations that would have been produced by the facets of a mineral grain if it were propelled through the substrate, (3) the absence of angular cross-sections, and (4) at times the presence of nodal swelling. In addition, these tunnels commonly have some preferred orientation and indication of biological behaviour, unlike AITs, which lack any preferred orientation (Wacey et al., 2008).

There is a single exception to point (1), the absence of grains at the ends of micro-tunnels, in Reed Rock. In a single tunnel, an oxide grain is found at the terminus (Fig. 2.17A-B), but in this case, it is not believed to be a result of AIT formation processes for several reasons. This tunnel originates from the margin of a pyroclast (amorphous, non-crystalline volcanic glass). It has an irregular pitted interior surface, lacks longitudinal straie, and has a variable diameter most notably shown by the tapering then terminal enlargement at its end (Fig. 2.17A-B). On the irregular boundaries, small filament structures (Fig. 2.17C) similar to those found by Banerjee and Meuhlenbachs (2003), and irregular pits (Fig. 2.17B-D) possibly indicative of biological glass etching (e.g., Thorseth et al., 1995) are present. The tunnel also emerges from what appears to be a granular alteration front at the pyroclast margin (Figs. 2.17A, 2.14C). The majority of AITs are sealed inside microcrystalline or massive layers and cut off from exterior surfaces of clasts (McLoughlin et al., 2010). There are no examples of terminal enlargements in AITs. Those that have terminal crystals possess profiles on the distal ends of the trails that are direct images of the crystal-trail interface, hence the terminus of the trail is a mould of the crystal shape. This is not the case here. Microborings have been observed to migrate toward olivine grains (e.g., McLoughlin et al., 2007) and this may be an instance of a tunnel directed toward an oxide grain in search of preferred metabolically important metals such as Fe. Fe is believed to be a key element involved in the biological dissolution of glass (Staudigel et al., 2004).

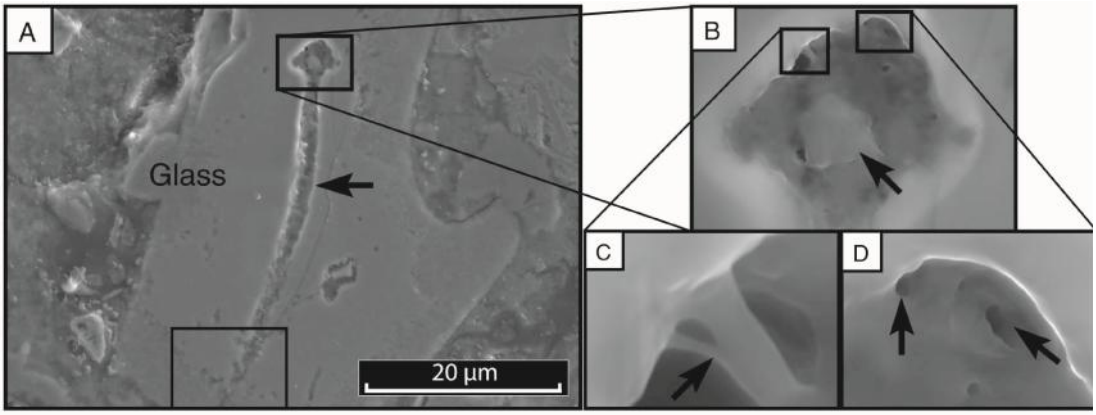

Figure 2.17. Scanning electron microscope (SEM) images of tubular micro-tunnel. (A) Smooth, curved tunnel with terminal enlargement, rooted on the margin of a coarse ash pyroclast. The lower box outlines a granular alteration front and is enlarged in Figure 2.14C. (B) Box in (A) enlarged showing the terminal enlargement with a crystal at center, interior filament structure and pits (boxes). (C-D) Boxes in B enlarged showing filament structure (*arrow*) and rounded pits (*arrows*) along the wall of the terminal enlargement. From sample FR-12-97E.

The general hydrologic regime of the Reed Rocks tuff contrasts with that believed to be necessary for AITs to form. AITs are produced by mineral grains that are driven by high fluid pressures through crypto-crystalline substrates such as cherts producing void tubular trails (Tyler and Barghoorn, 1963; Knoll and Barghoorn, 1974). In order to reach such sustained unidirectional fluid pressures required to initiate pressure solution and drive crystals, it is necessary that the surrounding material be an impermeable closed system. The systems AITs have been reported in had little or no exposure to fluid circulation (e.g., Tyler and Barghoorn, 1963; Knoll and Barghoorn, 1974; McLoughlin et al., 2010). The tunnels in the Reed Rocks occur within volcanic glass as opposed to chert or phosphorite, and in contrast to the reported occurrences of AITs, these deposits are porous and permeable open systems that were exposed to circulating fluids. This is shown by the profusion of fractures, which connect gas vesicles, the presence of ancillary precipitates, and the concentration of palagonitic- and putative bio- alteration along fluid-exposed pathways (pyroclast margins, vesicles and fractures). It is not likely that pressures could build up high enough to initiate solution, therefore the primary conditions in Reed Rocks lack a driving force necessary to propel a grain through the glass producing microtubules (McLoughlin et al., 2010).

2.3.2.5.4. Fluid inclusion trails/radiation damage trails. It is possible that tunnels can be constructed by exploiting fluid inclusion trails (e.g. Parnell et al., 2005). These may be located within solitary sedimentary quartz or other mineral grains and may be formed by the partial healing of fractures. The Reed Rocks tunnels described here do not occur in any crystalline materials and are only found in basaltic glass. We also find no fluid inclusions, as they are typically not trapped within the glass (McLoughlin et al.,

2010). Also, radiation damage trails are potential sites along which tunnels can form. These would be randomly oriented without any directionality, would not display any preference for exterior surfaces, and would likely intersect one another as fission track trails do (McLoughlin et al., 2010). In contrast, the Reed Rocks tunnels do display directionality, are strictly associated with external surfaces (margins, fractures, vesicles), and do not intersect one another.

2.3.3. Bioalteration vs. Textural Properties

To evaluate the relationships of primary and secondary textures with the intensity and type of bioalteration, we investigated key textural characteristics, including abiotic aqueous alteration, fresh glass proportions and porosity (Table 2.1). With increasing proportions of aqueous (abiotic) glass alteration, we note a general increasing intensity of bioalteration (Fig. 2.18A). This correlation is generally observed over the full suite of samples ($R^2 = 0.7$).

The most common type of tubular textures at Reed Rocks are simple, and branching forms (e.g., Figs. 2.11A, 2.12A, 2.13, 2.15). Tunnels with terminal enlargements (Figs. 2.9, 2.10) are the most abundant type in Reed Rock but they are virtually absent from South Reed Rock. The terminal enlargement type is also most abundant in samples with the highest proportions of aqueous (abiotic) alteration (Fig. 2.18B), potentially suggesting that fluid flux and composition are important controlling variables for bioalteration (c.f., Cousins et al., 2009). If the abundance of alteration phases are a gauge for aqueous alteration intensity and fluid flux, then the greater alteration proportions and precipitate abundances may suggest a greater flux of altering fluids.

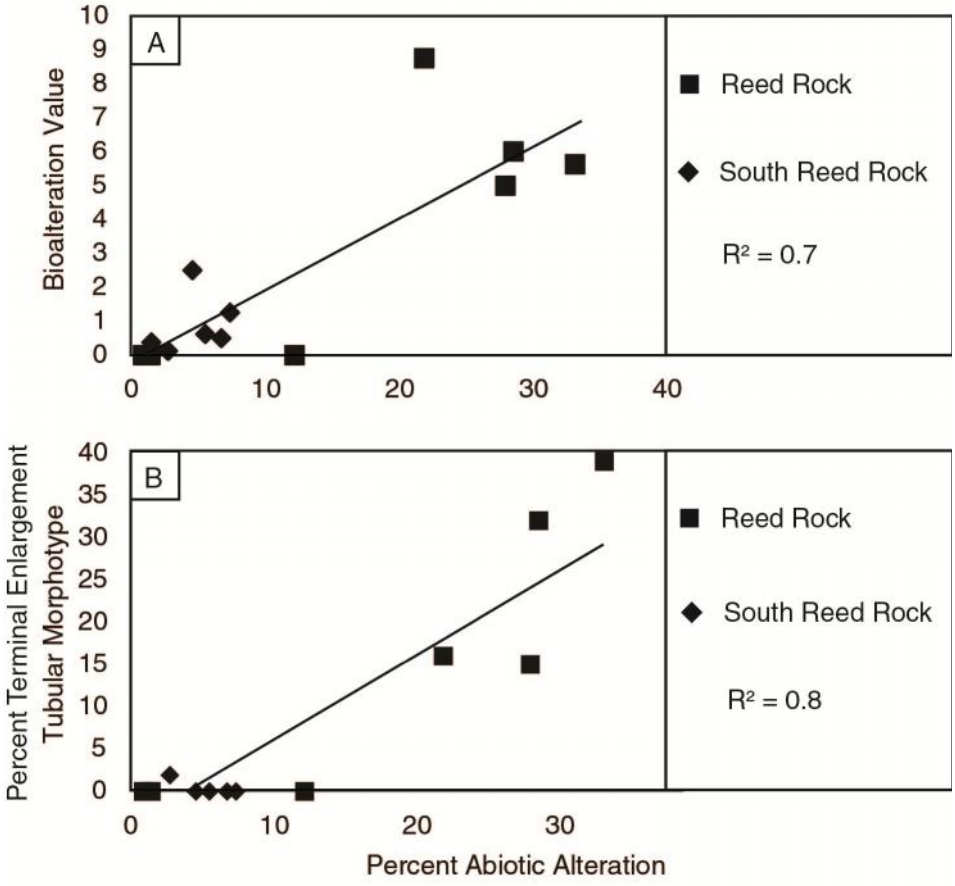

Figure 2.18. Scatter plots showing the relationship between bioalteration intensity (bioalteration value), tubular morphologies with terminal enlargements, and the percentage of total aqueous (abiotic) alteration. (A) Bioalteration intensity is positively correlated with aqueous alteration. Low and high proportions of aqueous alteration generally correspond with lower and higher bioalteration values, respectively. (B) The percentage of tubular bioalteration with terminal enlargements is positively correlated with aqueous alteration. The low and high proportions of aqueous alteration correspond to low and high percentages of the tubular morphological type with terminal enlargements.

The observed correlation between abiotic and biotic alteration degree and type suggests palagonitization leads to an environment favourable to microbes, or that the processes are linked by similar conditions of alteration. The process of palagonitization involves congruent or incongruent glass dissolution (e.g., Stroncik & Schmincke, 2002; Drief & Shiffmann, 2004), which results in the mobilization of elements such as K, or Ca (Stroncik & Schmincke, 2002). If these elements are metabolically important to the microbes, then circulating fluids may enhance or promote bioalteration. Even if metabolically important elements are relatively immobile, such as insoluble Fe, the fluid composition may change over time and the type of organisms able to construct tunnels may also change.

2.3.4. Conditions and Timing of Microbial Bioalteration

The inferred biogenic textures at Reed Rocks appear to have formed both contemporaneous with and post-low-temperature-hydrothermal alteration. Some tubular textures propagate beyond abiotic/palagonitic alteration fronts and/or contain evidence of alteration within the tunnels (e.g., Fig. 2.7) indicating formation temperatures may be bracketed by the inferred lower and upper temperatures of palagonitization (between 25 and 80°C). In only one sample are there instances of preserved microbial textures found within palagonitized glass (Fig. 2.19). This suggests that some microbial alteration may have taken place soon after emplacement while the volcanic pile was still cooling. Also, a secondary heating event, possibly caused by dike intrusion or the culminating lava lake, may have produced palagonite overprinting of those textures.

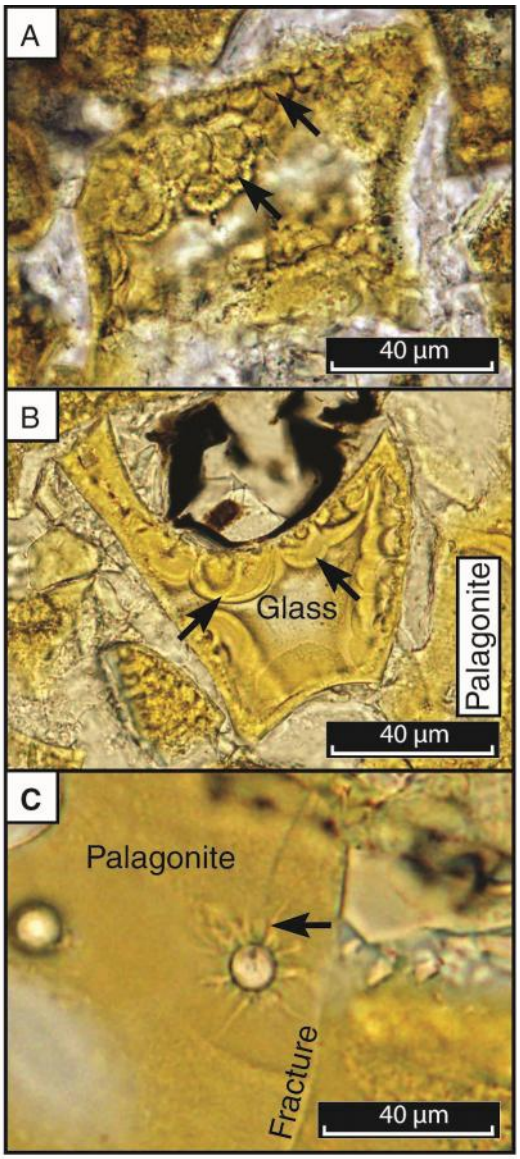

Figure 2.19. Possible bioalteration overprinted by aqueous alteration. (A) A palagonitized pyroclast with preserved semi-circular individual granular incursions rooted at margins (*arrows*). (B) Individual semi-circular granular incursions preserved along the margins of a palagonitized pyroclast. (C) Tubular structures radiating from a vesicle at centre (*arrow*), preserved in a completely palagonitized pyroclast. From sample FR-12-97B.

Microbial textures radiating from vesicles sealed by calcite, which likely precipitated at temperatures below 80°C, suggests that they were formed at temperatures above that of calcite precipitation. In open systems, fluid circulation is a sustaining factor for microbial activity and thus once circulation ceases, so too would micro-tunnel formation (McLoughlin et al., 2010). This is illustrated in Figures 2.8B and 2.11A; construction would have continued until calcite precipitation impeded fluid flow. This suggests that these tunnels were produced when fluids were still freely circulating within the rocks. Because no tunnels are found radiating from vesicles sealed with zeolites (chabazite), they likely formed at least below 80°C, the upper limit of zeolite stability.

Granular textures in ocean crust basalts have been documented as dominant in the upper crust at temperatures around 80°C, whereas tubular textures, generally constituting a smaller portion of total alteration, are most abundant at temperatures near 70°C (e.g., Furnes et al., 2007a). The inferred temperature range of the Reed Rocks fits well within the range that microbial life is known to exist (Stetter et al., 1990), although the conditions here may exclude hyperthermophiles that live above 80°C (Brock et al., 1978; Stetter et al., 1990; Stetter, 2007).

The presence of tunnels propagating from fractures/vesicles/margins not associated with abiotic/palagonitic alteration and with no evidence of alteration within them suggests microbial alteration continued at temperatures below 25°C, the lower temperature of palagonite formation. Micro-tunnels, however are more typically associated in some way with minor degrees of abiotic alteration (Fig. 2.18). In summary, mineral assemblages and textural relationships indicate that the majority of microbial

bioalteration apparently occurred at relatively low temperatures between 0 to 80°C more commonly between 25 to 80°C in neutral to alkaline (pH 9-10) saline fluids.

2.4. CONCLUSIONS

1. The Reed Rocks hydrovolcanic tuffs in the FRVF contain a suite of textures that are similar in size, morphology, and distribution to previously described bioalteration in marine and sub-glacial marine transitions zones and are characteristic of endolithic microboring biogenicity. We argue that this is the first account of endolithic microborings in a non-marine, non-subglacial continental setting and this study contributes to expanding the range of environments where endolithic microborings have been documented.

The positive correlations between abiotic aqueous alteration and the intensity of bioalteration and abundance of microborings with terminal enlargements point to a direct influence of fluid flux and composition. How intense the aqueous alteration experienced by the basaltic glass is and the flux of altering fluids, appears to promote microboring construction. The association of certain microborings morphologies with more highly altered samples suggests that the altering fluid chemical compositions was likely modified more substantially than those that experienced less aqueous alteration, and that this probably had an influence of the type of constructing organisms.

2. Based on textural relationships between secondary phases and microbial textures, the Reed Rocks microborings are inferred to have formed predominantly in neutral to alkaline, saline fluids at temperatures between 25 - 80 °C. Hydrothermal/aqueous alteration occurred in a low temperature thermal regime (≤ 80°C).

3. We note that in addition to the significant presence of endolithic microborings in the Reed and South Reed Rock tuffs, examinations of several other tuff deposits throughout the FRVF have revealed similar textures. Microbial bioalteration is not just a locally isolated phenomenon in the Reed Rocks, and is in fact a more significant component of the regional geologic history. If these features are widespread in the FRVF, then further investigation is required to compare local geology, textural and mineralogical characteristics, and possible bioalteration of other locations to those found in Reed Rocks and ocean basalts. Assessing the relationship between these qualities and the intensity and type of bioalteration textures will help in understanding the controls on their formation and habitable conditions.

2.5. REFERENCES CITED

Allison, I.S., 1966, Fossil Lake, Oregon--Its geology and fauna: Oregon State Monographs, Studies in Geology, no. 9, p. 48.

Allison, I.S., 1979, Pluvial Fort Rock Lake, Lake County, Oregon: State of Oregon, Department of Geology and Mineral Industries.

Alt, J.C., and Mata, P., 2000, On the role of microbes in the alteration of submarine basaltic glass: a TEM study: Earth and Planetary Science Letters, v. 181, p. 301-313.

Apps, J.A., 1983, Hydrothermal evolution of repository groundwaters in basalt, *in* NRC Nuclear Waste Geochemistry '83, US Nuclear Regulatory Commission Report, NUREG/CP-0052, p. 14-51.

Banerjee, N.R., and Muehlenbachs, K., 2003, Tuff life: Biolateration of volcaniclastic rocks from the Ontong Java Plateau. Geochemistry Geophysics Geosystems, v. 4, no. 4, p. 1037.

Banerjee, N.R., Izawa, M.R.M., Sapers, H.M., Whitehouse, M.J., 2011, Geochemical biosignatures preserved in microbially altered basaltic glass: *in* Proceedings, SIMS, Surface and Interface Analysis, v. 43, p. 452-457.

Benzerara, K., Menguy, N., Banerjee, N.R., Tyliszczak, T., Brown Jr., G.E., and Guyot, F., 2007, Alteration of submarine basaltic glass from the Ontong Java Plateau: A STXM and TEM study: Earth and Planetary Science Letters, v. 260, p. 187-200.

Brand, B.D., and Clarke, A.B., 2009, The architecture, eruptive history, and evolution of the Table Rock Complex, Oregon: From a Surtseyan to an energetic maar eruption: Journal of Volcanology and Geothermal Research, v. 180, p. 203-224.

Brock, T.D., 1978, Thermophilic Microorganisms and Life at High Temperatures. Springer-Verlag, Berlin, Heidelberg. New York.

Chevrier, V., Poulet, F., and Bibring, J.-P., 2007, Early geochemical environment of Mars as determined from thermodynamics of phyllosilicates: Nature, v. 448, no. 5, p. 60-63, doi:10.1038/nature05961.

Chipera, S.J., and Apps, J.A., 2001, Geochemical stability of natural zeolites: *in* Bish, D.L., Ming, D.W., eds., Reviews in Mineralogy & Geochemistry: Natural Zeolites: Occurrence, Properties, Applications, v. 45, p. 117-157.

Cockell, C.S., Olsson-Francis, K., Herrera, A., and Meunier, A., 2009, Alteration textures in terrestrial volcanic glass and the associated bacterial community: Geobiology, v. 7, p. 50-65.

Cockell, C.S., Olsson, K., Knowles, F., Kelly, L., Herrera, A., Thorsteinsson, T., and Marteinsson, V., 2012, Bacteria in weathered basaltic glass, Iceland: Geomicrobiology Journal, v. 26, no. 7, p. 491-507.

Colbath, K., and Steele, M.J., 1982, The geology of economically significant lower Pliocene diatomites in the Fort Rock basin near Christmas Valley, Lake County, Oregon: Oregon Geology, v. 44, no. 10, p. 111-118.

Cousins, C.R., Smellie, J.L., Jones, A.P., and Crawford, I.A., 2009, A comparative study of endolithic microborings in basaltic lavas from a transitional subglacial-marine environment: International Journal of Astrobiology, v. 8, no. 1, p. 37-49.

Drief, A., and Schiffman, P., 2004, Very low-temperature alteration of sideromelane in hyaloclastites and hyalotuffs from Kilauea and Mauna Kea volcanoes: Implications for the mechanism of palagonite formation: Clays and Clay Minerals, v. 52, no. 5, p. 622-634.

Eggleton, R.A., and Keller, J., 1982, The palagonitization of limburgite glass - a TEM study: Neues Jahrb Miner, v. 7, p. 321-336.

Fisk, M.R., Giovannoni, S.J., and Thorseth, I.H., 1998a, Alteration of oceanic volcanic glass: Textural evidence of microbial activity: Science, v. 281, p. 978-980.

Fisk, M.R., Thorseth, I.H., Giovannoni, S.J., Urbach, E., and Streck, M.J., 1998b, Endolithic Microbes from the Rattlesnake Tuff, Oregon Blue Mountain Region: American Geophysical Union, Fall Meeting, San Francisco, CA, Abstracts, FM98-U32A-12.

Fisk, M.R., Storrie-Lombardi, M.C., Douglas, S., Popa, R., McDonald, G., and Di Meo-Savoie, C., 2003, Evidence of biological activity in Hawaiian subsurface basalts: Geochemistry Geophysics Geosystems, v. 4, no. 12, 1103, doi:10.1029/2002GC000387.

Fisk, M., and McLoughlin, N., 2013, Atlas of alteration textures in volcanic glass from the ocean basins: Geosphere, v. 9, no. 2, p. 317-341.

Flemming, R.L., 2007, Micro X-ray diffraction (μXRD): a versatile technique for characterization of Earth and planetary materials: Canadian Journal of Earth Sciences, v.44, p. 1333-1346.

Furnes, H., Thorseth, I.H., Tumyr, O., Torsvik, T., and Fisk, M.R., 1996, Microbial activity in the alteration of glass from pillow lavas from hole 896A, *in* Proceedings, Ocean Drilling Program, Scientific Results, v.148, p. 191-206.

Furnes, H., and Staudigel, H., 1999, Biological mediation in ocean crust alteration: how deep is the deep biosphere?: Earth and Planetary Science Letters, v. 166, p. 97-103.

Furnes, H., Staudigel, H., Thorseth, I.H., Torsvik, T., Muehlenbachs, K., and Tumyr, O., 2001, Bioalteration of basaltic glass in the ocean crust: Geochemistry Geophysics Geosystems, v. 2, Paper number 2000GC000150.

Furnes, H., Banerjee, N.R., Muehlenbachs, K., and Kontinen, A., 2005, Preservation of biosignatures in metaglassy volcanic rocks from the Jormua ophiolite complex, Finland: Precambrian Research, v. 136, p. 125-137.

Furnes, H., Banerjee, N.R., Staudigel, H., Muehlenbachs, K., McLoughlin, N., de Wit, M., and Van Kranendonk, M., 2007a, Comparing petrographic signatures of bioalteration in recent to Mesoarchean pillow lavas: Tracing subsurface life in oceanic igneous rocks. Precambrian Research, v. 158, p. 156-176.

Furnes H., Banerjee, N.R., Staudigel, H., and Muehlenbachs, K., 2007b, Pillow lavas as a habitat for microbial life: Geology Today, v. 23, no. 4, p. 143-145.

Hampton, E. R., 1964, Geologic factors that control the occurrence and availability of groundwater in the Fort Rock basin, Lake County, Oregon: U.S. Geological Survey Professional Paper, no. 383B, p. B1-B29.

Hardie, L. A., and Eugster, H. P., 1970, The evolution of closed-basin brines: Mineralogical Society of America Special Paper 3, p. 273–290.

Heiken, G.H., 1971, Tuff Rings: Examples from the Fort Rock-Christmas Lake Valley Basin, South-Central Oregon: Journal of Geophysical Research, v. 76, no. 23, p. 5615-5626.

Izawa, M.R.M., Banerjee, N.R., Flemming, R.L., Bridge, N.J., and Schultz, C., 2010, Basaltic glass as a habitat for microbial life: Implications for astrobiology and planetary exploration: Planetary and Space Science, v. 58, p. 583-591.

Jakobsson, S.P., and Moore, J.G., 1986, Hydrothermal minerals and alteration rates at Surtsey volcano, Iceland: The Geological Society of America Bulletin, v. 97, no. 5, p. 648-659.

Jordan, B.T., Grunder, A.L., Duncan, R.A., and Deino, A.L., 2004, Geochronology of age-progressive volcanism of the Oregon High Lava Plains: Implications for the plume interpretation of Yellowstone: Journal of Geophysical Research, v. 109, B10202, doi:10.1029/2003JB002776.

Knoll, A.H., and Barghoorn, E.S., 1974, Ambient pyrite in Precambrian chert: New evidence and theory: *in* Proceedings, National Academy of Science USA, v.71, no. 6, p. 2329-2331.

Kristmannsdó ttir, H., and Tó masson, J., 1978, Zeolite zones in geothermal areas in Iceland, *in* Sand, L.B., Mumpton, F.A., eds., Natural Zeolites: Occurrence, Properties, Pergamon Press, NY, p. 277-284.

Limpert, E., Stahel, W.A., and Abbt, M., 2001, Log-normal distributions across the sciences: Keys and Clues: BioScience, v. 51, no. 5, p. 341-352.

Lorenz, V., 1970, Some aspects of the eruption mechanism of the Big Hole maar, Central Oregon: Geological Society of America Bulletin 81, p. 1823-1830.

Martin, J.E., Patrick, D., Kihm, A.J., Foit Jr., F.F., and Grandstaff, D.E., 2005, Lithostratigraphy, tephrochronology, and rare earth element geochemistry of fossil at the classical pleistocene Fossil Lake area, South Central Oregon: The Journal of Geology, v. 113, p. 139-155.

McKinley, J.P., Stevens, T.O., and Westall, F., 2000, Microfossils and paleoenvironments in deep subsurface basalt samples: Geomicrobiology Journal, v. 17, p. 43-54.

McLoughlin, N., Brasier, M.D., Wacey, D., Green, O.R., and Perry, R.S., 2007, On the biogenicity criteria for endolithic microborings on early Earth and beyond: Astrobiology, v. 7, no. 1, p. 10-26.

McLoughlin, N., Furnes, H., Banerjee, N.R., Staudigel, H., Muehlenbachs, K., De Wit, M., and Van Kranendonk, M.J., 2008, Micro-bioalteration in volcanic glass: extending the ichnofossil record to Archean basaltic crust, *in* Wisshak, S., Tapanila, L., eds., Current Developments in Bioerosion, Springer-Verlag, Heidelberg, Germany, pp. 371-396.

McLoughlin, N., Staudigel, H., Furnes, H., Eickmann, B., and Ivarsson, M., 2010, Mechanisms of microtunneling in rock substrates: distinguishing endolithic biosignatures from abiotic microtunnels: Geobiology, v. 8, p. 245-255.

Olympus Life Science, n.d., cellSens Software: http://www.olympus-lifescience.com/en/software/cellsens/.

Parnell, J., Baron, M., and Cockell, C.S., 2005, Endolithic colonization of fluid inclusion trails in mineral grains: Houston, Texas, Lunar and Planetary Science Conference 36, LPI Contribution No. 1234. Lunar and Planetary Institute, Abstract no. 1285.

Peacock, M.A., 1926, The petrology of Iceland, part 1. The basic tuffs: Royal Society of Edinburgh Transactions, v. 55, p. 53–76.

Rasband, W.S., n.d., ImageJ. http://imagej.nih.gov/ij/.

Ross, K.A., and Fisher, R.V., 1986, Biogenic grooving on glass shards: Geology, v. 14, p. 571-573.

Sheppard, R.A., and Hay, R.L., 2001, Formation of zeolites in open hydrologic systems: *in* Bish, D.L., Ming, D.W., eds., Reviews in Mineralogy & Geochemistry: Natural Zeolites: Occurrence, Properties, Applications, v.45, p. 117-157.

Staudigel, H., and Furnes, H., 2004, Microbial mediation of oceanic crust alteration. *in* Davis, E., Elderfield, H., eds., Hydrology of the Oceanic Lithosphere, Cambridge University Press, p. 608–626.

Staudigel, H., and Hart, S.R., 1983, Alteration of basaltic glass; mechanisms and significance for the oceanic crust-sea water budget: Geochimica Cosmochimica Acta, v. 47, p. 337-350.

Staudigel, H., Furnes, H., McLoughlin, N., Banerjee, N., Connell, L.B., and Templeton, A., 2008, 3.5 billion years of glass bioalteration: Volcanic rocks as a basis for microbial life?: Earth-Science Reviews, v. 89, p. 156-176.

Stetter, K.O., Fiala, G., Huber, G., and Segerer, A., 1990, Hyperthermophilic microorganisms: FEMS Microbiology Reviews, v. 75, p. 117-124.

Stetter, K. O., 2007, Hyperthermophiles in the History of Life, *in* Ciba Foundation Symposium 202 - Evolution of Hydrothermal Ecosystems on Earth (And Mars?), John Wiley & Sons, Ltd., (Chichester, UK), p. 169-184, doi: 10.1002/9780470514986.ch1

Stockner, J.G., and Benson, W.W., 1967, The succession of diatom assemblages in the recent sediments of Lake Washington: Limnology and Oceanography, v. 12, no.3, p. 513-532.

Stroncik, N.A., and Schmincke, H.U., 2001, Evolution of palagonite: Crystallization, chemical changes, and element budget. Geochemistry Geophysics Geosystems, v. 2, no. 2000GC000102.

Stroncik, N.A., and Schmincke, H.U., 2002, Palagonite - a review. International Journal of Earth Sciences (Geol. Rundsch), v. 91, p. 680-697, doi 10.1007/s00531-001-0238-7.

Thorseth, I.H., Furnes, H., and Tumyr, O., 1991, A textural and chemical study of Icelandic palagonite of varied composition and its bearing on the mechanism of the glass-palagonite transformation: Geochimica Cosmochimica Acta, v.55, p. 731-749.

Thorseth, I.H., Torsvik, T., Furnes, H., and Muehlenbachs, K., 1995, Microbes play an important role in the alteration of oceanic crust: Chemical Geology, v. 126, p. 137-146.

Thorseth, I.H., Torsvik, T., Torsvik, V., Daae, F.L., Pedersen, R.B., and Keldysh-98 Scientific Party, 2001, Diversity of life in ocean floor basalt: Earth and Planetary Science Letters, v. 194, p. 31-37

Thorseth, I.H., Pedersen, R.B., and Christie, D.M., 2003, Microbial alteration of 0-30-Ma seafloor and sub-seafloor basaltic glasses from the Australian Antarctic Discordance: Earth and Planetary Science Letters, v. 215, p. 237-247.

Torsvik, T., Furnes, H., Muehlenbachs, K., Thorseth, I.H., and Tumyr, O., 1998, Evidence for microbial activity at the glass-alteration interface in oceanic basalts: Earth and Planetary Science Letters, v. 162, p. 165-176.

Tyler, S.A., and Barghoorn, E.S., 1963, Ambient pyrite grains in Precambrian cherts: American Journal of Science, v. 261, p. 424-432.

Utada, M., 2001, Zeolites in hydrothermally altered rocks: *in* Bish, D.L., Ming, D.W., eds., Reviews in Mineralogy & Geochemistry: Natural Zeolites: Occurrence, Properties, Applications, v. 45, p. 305-319.

van Dover, C.L. et al., 2003, Blake Ridge methane seeps: characterization of soft-sediment, chemosynthetically based ecosystem: Deep-Sea Research. I, v. 50, p. 281-300.

Wacey, D., Kilburn, M., Stoakes, C., Aggleton, H., and Brasier, M., 2008, Ambient inclusion trails: Their recognition, age range and applicability to early life on Earth: *in* Dilek, Y., Furnes, H., Muehlenbachs, K., eds., Links Between Geological Processes, Microbial Activities & Evolution of Life, Springer Science+Business Media B.V., v. 4, p. 113-134.

Wacey, D., McLoughlin, N., Saunders, M. and Kong, C., 2014, The nano-scale anatomy of a complex carbon-lined microtube in volcanic glass from the ~92Ma Troodos Ophiolite, Cyprus: Chemical Geology, v. 363., p. 1-12.

Walton, A.W., 2008, Microtubules in basalt glass from Hawaii Scientific Drilling Project #2 phase 1 core Hilina slope, Hawaii: evidence of the occurrence and behaviour of endolithic microorganisms: Geobiology, v. 6, p. 351-364.

Zhou, Z., and Fyfe, W.S., 1989, Palagonitization of basaltic glass from DSDP site-335, LEG-37 – textures, chemical-composition, and mechanism of formation: American Mineralogist, v. 74, p. 1045–1053.

Chapter 3

Microbial ichnofossils in continental basaltic tuffs of central Oregon, U.S.A (II): The record of endolithic microborings beyond oceanic crust

Matthew P.C. Nikitczuk[1], Mariek E. Schmidt[1], and Roberta L. Flemming[2]

[1]Department of Earth Sciences, Brock University 500 Glenridge Avenue, St. Catharines, ON L2S 3A1

[2]Department of Earth Sciences, University of Western Ontario 1151 Richmond Street, London, ON N6A 3K7

3.1. INTRODUCTION

Since the early 1990's, organisms known as endoliths that dwell within rocky substrates and their apparent trace fossils have been extensively observed *in situ* in oceanic crust pillow basalts, hyaloclastite breccias, marine tuffs, terrestrial volcanic rocks and more recently in sub-glacially erupted lavas (e.g., Stevens and McKinley, 1992; Thorseth et al., 1995; Fisk et al., 1998; Banerjee et al., 2003; Furnes et al., 2001, 2007; Walton, 2008). These observations have expanded the range of environments that endolithic microbes are known to inhabit. The most commonly-cited indication of euendolithic organisms that penetrate or etch volcanic glass to extract nutrients and/or energy by dissolving it (Golubic et al., 1981; Thorseth et al., 1995; Staudigel et al., 1995), are bioalteration textures (ichnofossils) in the form of micrometer-scale tubular corrosion structures (Fisk at el., 1998; Torsvik et al., 1998; Furnes and Staudigel, 1999; Thorseth et al., 2003; Banerjee et al., 2003; Furnes et al., 2007; McLoughlin et al., 2008; Cockell et al., 2009; Cousins et al., 2009, Fisk and McLoughlin, 2013). These structures formed during microbial etching are known as endolithic microborings. While endoliths and their fossilized remains have been documented in volcanic rocks on land (e.g., Fisk et al., 1998b; Mckinley et al., 2000), the presence of tubular microborings have only recently been observed in continental basalts erupted in a lacustrine environment rather than in a marine or sub-glacial setting (Chapter 2). The characterization of bioalteration textures in volcanic rocks which have erupted in environments other than oceanic settings (Cousins et al., 2009) is vital in order to improve our understanding of the distribution and controls the formation of endolithic microborings.

Environmental controls on microboring formation are not well understood but it has been suggested that fluid flux, nutrient supply, circulating fluid composition, temperature/thermal gradients, oxygenation, fracture density, porosity and permeability may be biologically important factors (Furnes et al., 2007; McLoughlin et al., 2007; Cousins et al., 2009). Understanding how environmental factors affect endolithic microbes is important when attempting to trace subsurface microbial activity and for considering their potential as extra-terrestrial biosignatures on other planetary bodies, such as Mars (Freidmann and Koriem, 1989; McKay et al., 1992; Fisk et al., 1998; McLoughlin et al., 2007).

Recently, we documented endolithic microborings in continental lacustrine hydrovolcanic basalts with comparable sizes, distributions and morphologies to those described in oceanic and subglacial basalts (Chapter 2). Those microborings are in the deposits of two tuff rings (Reed Rocks) in the Fort Rock Volcanic Field (FRVF), Oregon, also known as the Fort Rock-Christmas Valley basin. The FRVF is the site of an ancient Pliocene-Pleistocene pluvial lake basin and contains over 40 hydrovolcanic edifices (Heiken, 1971), many of which have been the subject of various studies over the last several decades (Hampton, 1964; Lorenz, 1970; Colbath and Steele, 1982; Martin et al., 2005; Brand and Clarke, 2009, Schmidt et al., 2012). Despite the array of investigations of the area, to the author's knowledge, Chapter 2 provides the first account of putative endolithic microborings in the FRVF and within a non-marine, non-subglacial continental basalt. We herein expand our investigation to include bioalteration features at another hydrovolcanic site called Black Hills, located ~20 km away from Reed Rocks on the southern edge of the Fort Rock-Christmas Valley basin. The environmental conditions in

Black Hills tuffs may have differed from those of Reed Rocks. Black Hills is located closer to the paleo-lake margin and may have had a more substantial interaction with surface and ground water associated with Fort Rock lake. These differences may be reflected as observed differences in bioalteration textures.

The aims of the present study are to: (1) texturally, mineralogically, and geochemically characterize the alteration of the basaltic tuffs of Black Hills, (2) compare textures and environments of Black Hills to those of Reed Rocks and evaluate their similarity to previous accounts in oceanic basalts, (3) establish biogenicity of putative bioalteration features by documenting their size, distribution and range in morphologies, (4) determine if any relationships exist between bioalteration and other abiotic textures, and (5) place the formation of putative bioalteration features in a diagenetic sequence and define the environmental conditions (e.g., temperature, pH, water content) under which they formed using secondary phases and oxygen isotope paleothermometry. By characterizing bioalteration features in the Black Hills and comparing them to Reed Rocks and oceanic basalt features, we can improve our understanding of biologically-important factors affecting their formation as well as their distributions in terrestrial and potentially extra-terrestrial subsurface environments.

3.1.1. Geologic Background

The Black Hills covers an area of ~28 km^2 at the southern margin of the Fort Rock-Christmas Valley basin in central Oregon, U.S.A (Fig. 3.1). It represents a group of approximately six overlapping hydrovolcanic tuff rings that likely erupted between 2.59 Ma and 12 ka (Pliocene-Pleistocene; Heiken, 1971). Vents are aligned NW, apparently

controlled by the direction of regional normal faulting (Heiken, 1971). The close proximity of vents resulted in irregular ring shapes (Fig. 3.1B).

3.1.1.1. Pluvial Fort Rock Lake

The Fort Rock Lake basin lies within a large area that lacks exterior surface drainage within the states of Nevada, Utah, California, and Oregon known as the Great Basin (Dworkin et al., 2005). Many modern western U.S. pluvial lakes in the Great Basin, such as Summer and Abert Lakes, evolved through evaporation (Hardie and Eugster, 1970). The Fort Rock Lake shares similar geologic and hydrologic characteristics with these lakes; hence it is very likely that Fort Rock Lake also evolved through evaporation. Widespread tabular diatomite beds in the Pettus Lake member (Hampton, 1964; Allison, 1966, 1979; Heiken, 1971) of the Fort Rock Formation (Pliocene) that underlies most of the Fort Rock Basin floor, contain a diatom flora that suggests a fresh-water lacustrine environment (Colbath and Steele, 1982). Stockner and Benson (1967) also interpreted an abundance of centric diatom genera as an indication of an oligotrophic (nutrient poor) lake. So earlier in its evolutionary history, Fort Rock Lake was probably a relatively nutrient poor fresh-water environment. Later in the Fort Rock Lake history, water chemistry likely evolved to become more saline and alkaline.

In the Fossil Lake area in the east-central portion of the Fort Rock Basin heavy rare earth element (HREE) compositions of vertebrate fossils from 646 ka to 23.2 ka (mid to late Pleistocene) indicate that waters gradually evolved from low salinity with near-neutral pH to more saline, alkaline and basic (Martin et al., 2005). Analogously, the Fort Rock Lake waters likely evolved toward a more alkaline and saline chemistry from an

earlier fresh water environment. Therefore it is probable that the hydrovolcanic eruptions of the Black Hills, which probably erupted during the Pleistocene, occurred in a saline and alkaline basic lacustrine environment that likely existed in the Fort Rock Lake evolutionary history.

3.1.1.2. The Black Hills Basaltic Tuffs

Hydrovolcanic eruptions at the Black Hills deposited well bedded, fine to coarse ash tuffs, lapillistones, and agglomerate pyroclastic breccias on top of flat-lying lacustrine sediments. Variable bedding characteristics of hydrovolcanic deposits are the result of diverse deposition mechanisms, such as fallout, subaqueous debris flows, pyroclastic flows, and base surges (Fisher and Schmincke, 1984). Bedding ranges from thickly laminated (0.3-1 cm) to thickly or very thickly bedded (30-100 cm or > 1 m) fine to coarse ash and lapilli rich layers that vary from sorted to poorly sorted, graded to inversely graded, and massive.

Lava blocks and scoria bombs (> 64 mm), pumice fragments, cognate clasts (deposited earlier in eruption) and accidental lacustrine clay and diatomite lithics are dispersed throughout the deposits. Some cognate clasts contain graded scoria and diatomite layers that indicate deposition of sub-aqueous fallout tephra from sub-aerial eruptions (Chesterman, 1956; Fisher and Schmincke, 1984). Penecontemporaneous deformation features such as bedding sags and convolute bedding, occasional vesiculated matrices and deformed cognate blocks suggest external water/vapour contents of at least 15-20% (Heiken, 1971; Fisher and Schmincke, 1984). Rare cm-scale degassing pipes are

found lower in the deposit. A large intrusive dike was also found in the central area of the Black Hills.

Several other features indicate a hydrovolcanic origin. Blocky, sideromelane shards with fracture-bounded surfaces transecting breakage across vesicles, and scarce to moderate vesicularity (1-14%) are a major component. The variation from blocky vitric shards with mosaic cracks to slightly vesicular with scalloped edges indicate a combination of vesiculating magma and quenching by water or steam and are often characteristic of shallow water eruptions (Fisher and Schmincke, 1984). Additional evidence of rapid quenching include igneous undercooling textures of intergrown microlitic plagioclase and pyroxene, varioles, sieved and swallowtail plagioclase phenocrysts and hopper olivine crystals. Occasional accretionary lapilli also suggest high external water contents. The accidental fraction includes diatomite fragments that reflect eruption through the lake bed.

Post depositional aqueous alteration affected juvenile basaltic glass pyroclasts within the deposits. The main product of glass alteration is yellow-brown palagonite, which is found along clast margins, fractures and vesicles, but also appears to have occurred along the walls of voids within the matrix. Palagonite is a product of high to low temperature gradual aging from amorphous to crystalline phases. The palagonitization process involves congruent to incongruent dissolution, hydration and chemical exchange as well as the formation of secondary re-precipitates that may consist of zeolites, phyllosilicates (smectite clays), and/or iron-oxy-hydroxides (Peacock, 1926; Zhou and Fyfe, 1989; Thorseth et al., 1991; Stroncik and Schmincke, 2001).

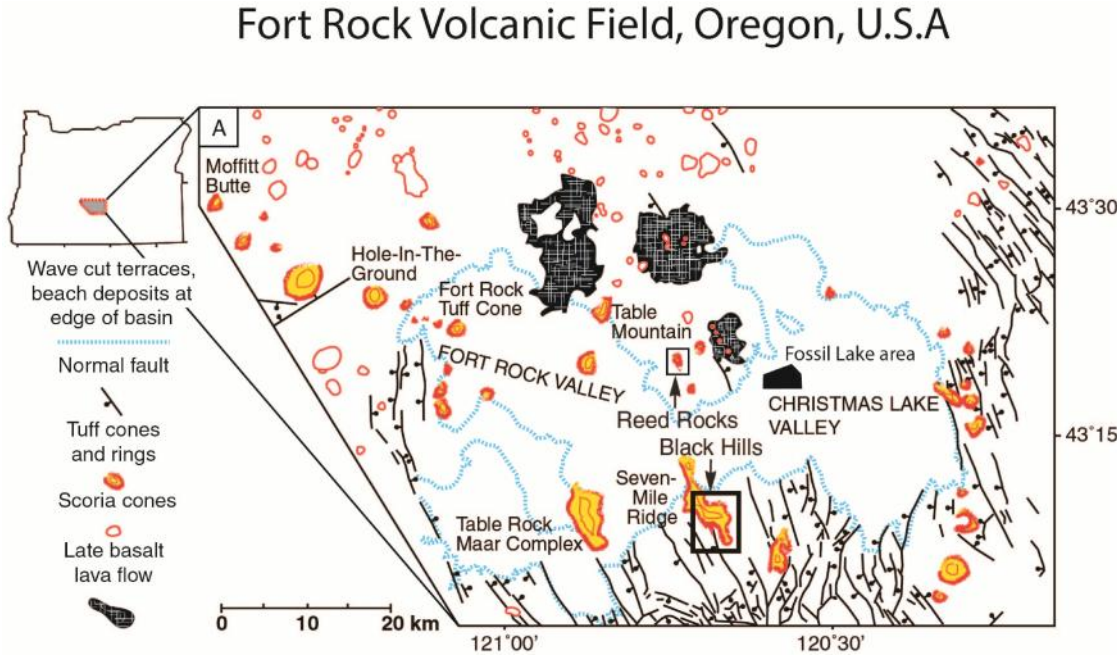

Figure 3.1. (A) Fort Rock Volcanic Field (modified from Heiken, 1971) and Black Hills study area. Upper left inset shows the state of Oregon (USA) with the FRVF shaded gray. Shaded area is enlarged in the upper right panel showing the FRVF with the location of the Black Hills vent complex, as well as Reed Rocks tuff rings (*outlined by box, labelled with an arrow*) relative to lava fields and other hydrovolcanic edifices and cinder cones within the basin. The high stand lake boundary is also indicated (*blue dashed line*) showing that Black Hills are located at the edge of the inferred lake margin. (B) Geologic map of the Black Hills study area showing the inferred locations of volcanic centers, tuff outcrops and sample locations. Note the general NW-SE alignment of vents which matches the orientation of major faulting in the region.

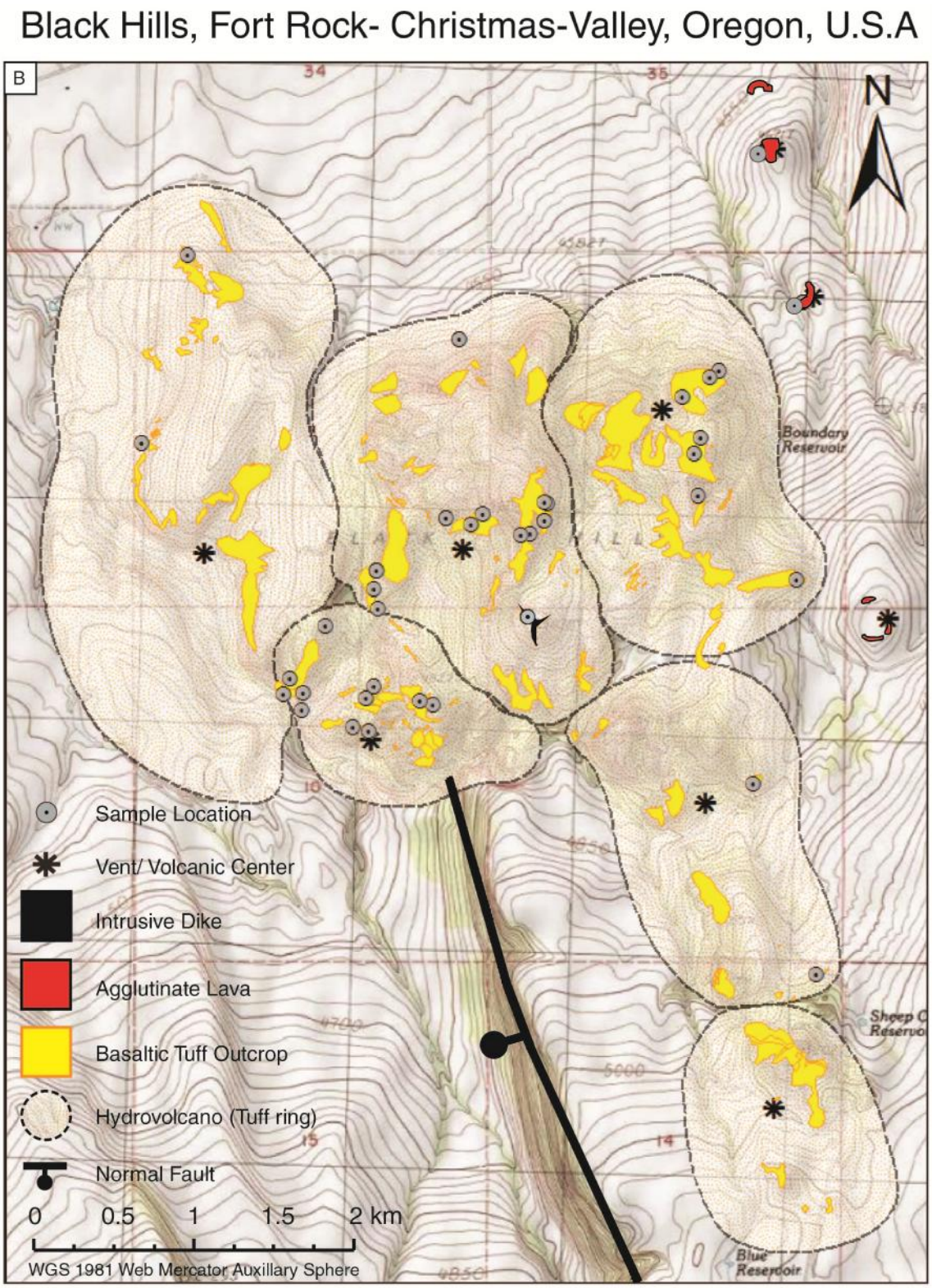
Black Hills, Fort Rock- Christmas-Valley, Oregon, U.S.A
B
N
Boundary Reservoir
Sample Location
Vent/ Volcanic Center
Intrusive Dike
Agglutinate Lava
Basaltic Tuff Outcrop
Hydrovolcano (Tuff ring)
Normal Fault
0 0.5 1 1.5 2 km
WGS 1981 Web Mercator Auxillary Sphere
Blue Reservoir

3.2. MATERIALS AND METHODS

3.2.1. Sample Collection

A suite of basaltic tuffs, scoria, agglutinated lavas and intrusive samples were collected from the Black Hills, a complex of ~6 amalgamated hydrovolcanoes (Fig. 3.1) in Fort Rock, Oregon, as part of a larger regional study. A total of 57 samples were collected (48 tuffs, 2 agglutinate lavas, 2 intrusive dike, 3 scoria bombs) that characterize the variety of textures found throughout the Black Hills. Criteria taken into account during sample collection include (1) varying degrees of alteration ranging from highly altered to fresh, often represented by distinct colour differences, (2) the presence of ancillary precipitate cements, including amygdules, (3) variations in bedding thickness from thinly laminated to thickly bedded, (4) vesicularity and (5) grain size.

3.2.2. Petrography and Mineralogy

The general methodology for textural, mineralogical and geochemical characterization of the Black Hills tuffs follows that outlined in Chapter 2. Additional methods not followed in Chapter 2 that include stable isotope geochemistry and carbonate paleothermometry are outlined below.

3.2.3. Geochemistry and Paleothermometry

Hand picked carbonates were analyzed for their C- and O-isotopic compositions by the University of Western Ontario (Western) Laboratory for Stable Isotope Science (LSIS) using a MultiPrep® system coupled to an Optima® duel-inlet isotope-ratio mass-spectrometer. In a sealed vessel, separated calcite cements from three tuff samples were

treated with 103% ortho-phosphoric acid (H_3PO_4) and reacted for 25 minutes at 90°C. This method is an adaptation of that formerly outlined by McCrea (1950). The extracted CO_2 was purified cryogenically and transferred directly into the mass spectrometer for isotopic analysis. Stable isotopic compositions of calcite are reported in the typical delta (δ) notation in units of per mil (‰) with respect to Vienna PeeDee Belemnite (VPDB) for carbon and Vienna Standard Mean Ocean Water (VSMOW) for oxygen. The $\delta^{13}C$ values were calibrated using standards NBS-19 and Suprapur. The $\delta^{18}O$ values were calibrated using standards NBS-19 and NBS-18.

Possible authigenic carbonate precipitation temperatures were calculated using the following paleotemperature equation proposed by Leng and Marshall (2004):

(Eq. 1) $$T^{o}C = 13.8 - 4.58(\delta c - \delta w) + 0.08(\delta c - \delta w)^2$$

where δc is $\delta^{18}O$ of carbonate compared to the Vienna PeeDee Belemnite (VPDB) international standard and δw is $\delta^{18}O$ of the depositing water compared to the Vienna Standard Mean Ocean Water (VSMOW) international standard. This equation is a potentially more suitable re-expression of the oxygen isotope fractionation relationship between calcite and water at low temperatures proposed by Kim and O'Neil (1997) and is based on synthetic calcite experiments. The *δc* values are those obtained from authigenic carbonate cements in Black Hills and Reed Rock basaltic tuffs. The δw are estimations of depositing water compositions based on modern meteoric and lake water data obtained from the literature (Kharaka et al., 1984; Friedmann et al., 2002; Henderson et al., 2003; Godebo, 2009; USGS, 2011; IAEO/WMO, 2015).

3.3. RESULTS

Textural, mineralogical and geochemical results of Black Hills tuffs are presented in the following section. Whole rock geochemistry of unaltered basalts is followed by a synopsis of primary igneous and secondary alteration textures and mineralogy. Included with secondary alteration textures is a detailed summary of the varieties of abiotic glass alteration (palagonite) and putative microbial bioalteration textures observed throughout the suite of samples under the petrographic microscope and scanning electron microscope. Further geochemical details of features obtained with energy dispersive spectroscopy are also summarized. The last section is a treatment of paleo environment, specifically the calculation of paleotemperatures using the carbonate paleotemperature scale.

3.3.1. Whole-Rock Geochemistry - X-ray Fluorescence (XRF)

Major whole-rock elemental concentrations of unaltered Black Hills lava and dike samples (Table 3.1) range from 48.99 - 49.76 wt. % SiO_2, 10.46 - 11.30 wt. % total Fe as FeO*. The magnesium number (Mg#) is 56 where Mg# is defined as molar 100MgO/(MgO+FeO). With 0.28 - 0.51 wt. % K_2O, the Black Hills bulk compositions are consistent with their classification as low potassium tholeiitic basalts (LKT) (Fig. 3.2), which is a common incompatible element-poor basalt type found in the FRVF (Jordan et al., 2004). Reed Rock lavas/intrusive are also classified as LKTs, but have a higher Mg# (67) and wt. % SiO_2, and lower wt. % Fe as FeO* (Table 3.1).

Table 3.1. Normalized whole-rock oxide concentrations of unaltered rocks from the Black Hills and Reed Rocks.

	FR-12-108B (BH)	FR-13-147 (BH)	FR-13-157 (BH)	FR-13-178A (BH)	FR-13-178B (BH)	FR-12-99 (RR)	FR-12-100 (RR)	FR-12-101 (RR)
SiO_2	49.76	48.93	49.33	49.03	48.99	50.05	50.02	50.08
TiO_2	1.536	1.451	1.467	1.481	1.481	1.029	1.049	1.030
Al_2O_3	17.77	17.89	18.01	17.81	17.74	17.55	17.43	17.56
FeO*	10.84	10.46	10.82	11.10	11.30	8.43	8.47	8.36
MnO	0.177	0.167	0.174	0.179	0.179	0.159	0.160	0.158
MgO	6.20	6.65	6.53	6.64	6.70	8.22	8.27	8.37
CaO	9.63	10.17	9.70	9.56	9.51	11.17	11.21	11.13
Na_2O	3.33	3.29	3.34	3.56	3.44	2.80	2.84	2.79
K_2O	0.51	0.31	0.28	0.43	0.43	0.39	0.37	0.36
P_2O_5	0.259	0.686	0.347	0.209	0.219	0.205	0.183	0.174
Mg#	*54.5*	*57.1*	*55.8*	*55.7*	*55.4*	*67.2*	*67.2*	*67.7*

Samples: Black Hills - BH, Reed Rock - RR

Whole-rock geochemistry of lavas and intrusives from Black Hills and Reed Rock study areas obtained by X-ray fluorescence analyses. Black Hills samples FR-12-108, FR-13-157 and FR-13-147 are lava bombs/scoria, FR-13-178A-B are from an intrusive dike. Reed Rock samples FR-12-99 and FR-12-101 are from lava flows and FR-12-100 is from intrusive dike.

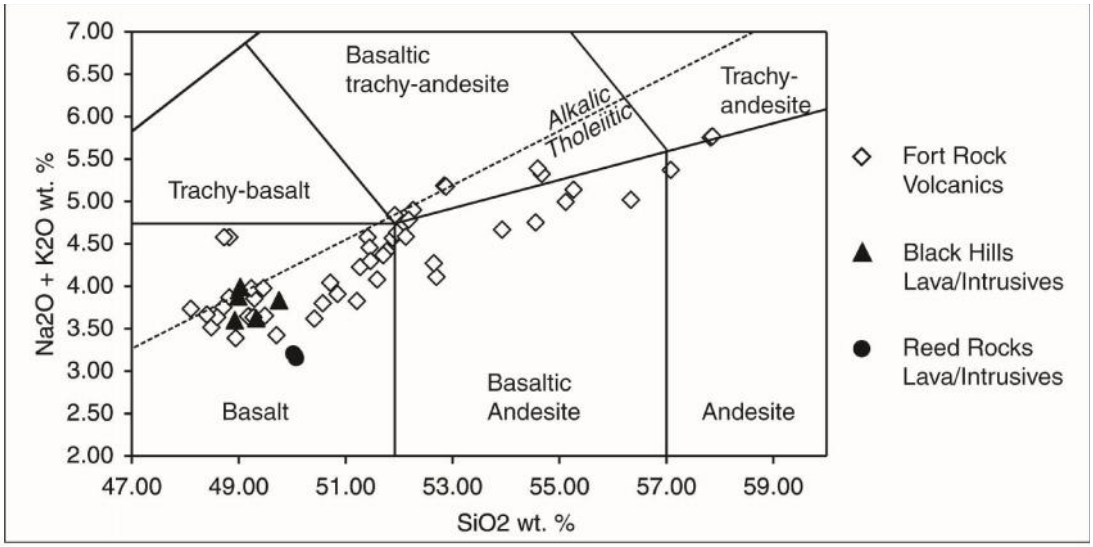

Figure 3.2. Total alkali versus silica diagram showing where the Black Hills geochemistry plots with respect to other volcanic rocks, including Reed Rocks in the Fort Rock Volcanic Field. The Black Hills samples may be classified as low potassium tholeiites (LKT). The Reed Rocks samples are also classified as low potassium tholeiites (LKT).

3.3.2. Transmitted Light Petrography and Mineralogy

Black Hills tuffs are primarily vitric, composed of ~16-53% fine to coarse ash and lapilli basaltic glass (sideromelane) pyroclasts ranging from <0.01 - 21 mm. Pyroclasts are low to moderately vesicular (1-14%) with blocky, angular to sub-angular shapes supported in fine ash and clayey matrix with occasional disseminated diatomite. Primary igneous crystal content ranges from 7 - 29%, primarily consisting of euhedral to subhedral olivine and plagioclase (anorthite) (Fig. 3.3) phenocrysts/glomerocrysts and broken subhedral to anhedral solitary olivine and plagioclase grains scattered throughout the matrix ± opaques. XRD analysis indicates plagioclase (anorthite) and pyroxene (diopside) are found within mafic glass (vitrophyric) as microlitic intergrowths and opaques consist of Ti-magnetite/magnetite (Fig. 3.3). Rarer trachyitic and intersertal textures in pyroclasts and lithics are also observed. Refer to Table 3.2 for a summary of the modal percent ranges of petrographic features determined by point counts.

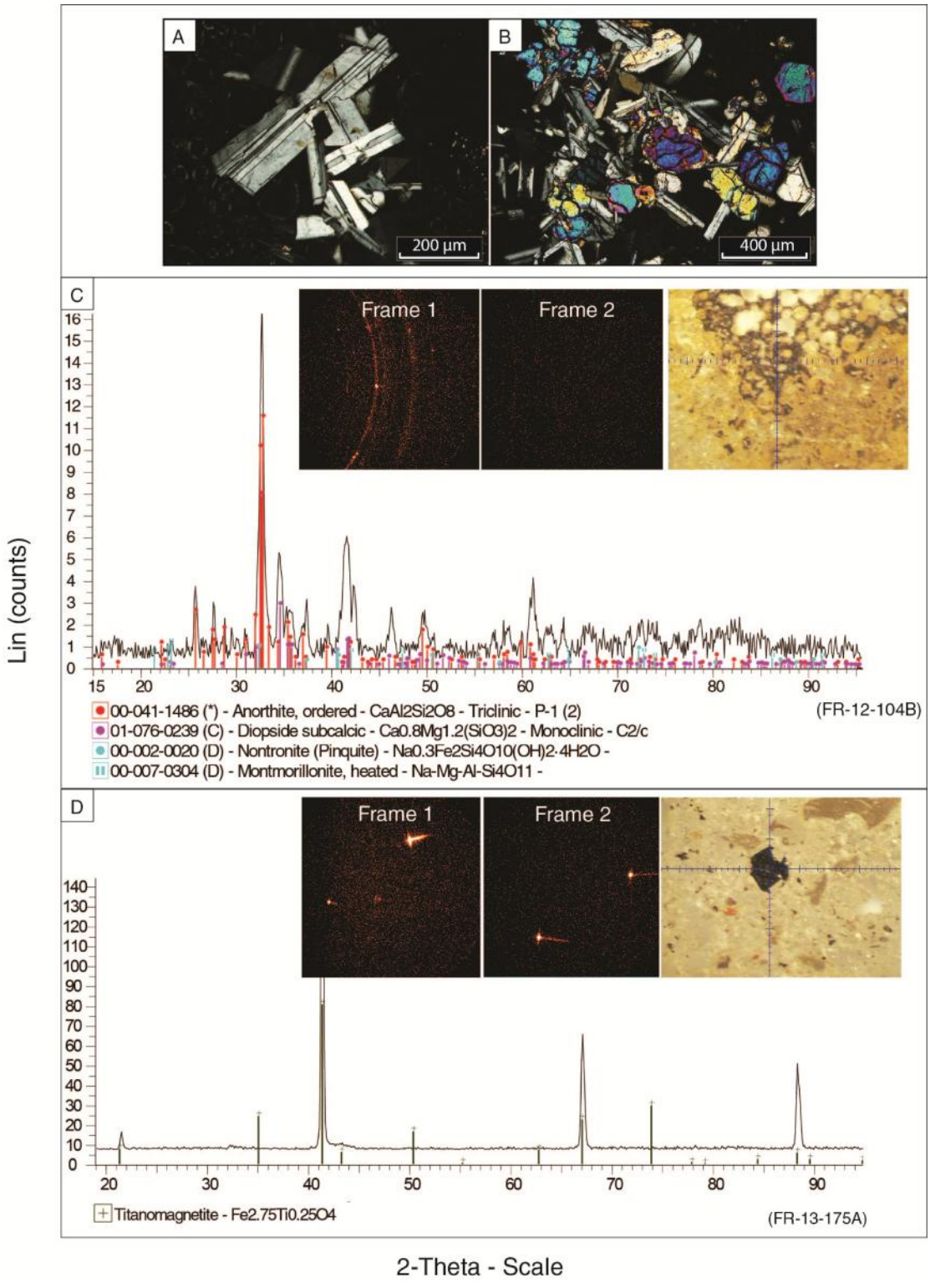
A
200 µm
B
400 µm
C
Frame 1
Frame 2
Lin (counts)
00-041-1486 (*) - Anorthite, ordered - CaAl2Si2O8 - Triclinic - P-1 (2)
01-076-0239 (C) - Diopside subcalcic - Ca0.8Mg1.2(SiO3)2 - Monoclinic - C2/c
00-002-0020 (D) - Nontronite (Pinquite) - Na0.3Fe2Si4O10(OH)2·4H2O -
00-007-0304 (D) - Montmorillonite, heated - Na-Mg-Al-Si4O11 -
(FR-12-104B)
D
Frame 1
Frame 2
Titanomagnetite - Fe2.75Ti0.25O4
(FR-13-175A)
2-Theta - Scale

Figure 3.3. Photomicrographs and micro X-ray diffraction patterns of common minerals in Black Hills basalts. (A) Cross-polarized image of a plagioclase glomerocryst. (B) Cross-polarized image of plagioclase-olivine glomerocryst. (C-D) Images at top of each pattern in C and D display the General Area Detector Diffraction system (GADDS) image (left) and photomicrograph (right) of the 100 µm spot analyzed. (C) Igneous minerals plagioclase (anorthite) and pyroxene (diopside) comprising microlitic intergrowths (undercooling) in glass and indications of phyllosilicates (smectites) nontronite-montmorillonite. A sample composed of crystallites in many orientations will display cones of diffraction that are visible as a uniform powder ring on the GADDS detector screen. Therefore the rings visible in the GADDS image indicate fine grains in multiple orientations. (D) Solitary Ti-magnetite (opaque-oxide) grain within the matrix. A solitary crystal grain will display distinct diffraction spots each corresponding to a stack of lattice planes in diffraction condition. Therefore the spots in the GADDS images indicate a single large crystal in one orientation.

Table 3.2. Maximum, minimum and average modal percentages of key textural characteristics, bioalteration values and tubular/granular alteration dimensions in the Black Hills and Reed Rocks tuffs.

Variable	Max. (%)		Min. (%)		Avg. (%)	
	RR	**BH**	**RR**	**BH**	**RR**	**BH**
Total fresh glass*	52.3	45.5	6.2	0.0	34.0	25.7
Primary glass[†]	53.8	53.2	34.2	15.9	46.0	37.4
Crystallinity[§]	19.8	28.9	5.3	7.5	10.6	14.3
Plagioclase	8.1	14.2	1.8	2.8	3.6	6.9
Olivine	2.9	4.5	0.5	0.4	1.9	2.4
Undercooling[#]	9.2	14.7	2.1	0.0	5.0	4.8
Vesicularity	12.1	14.0	2.8	1.3	8.5	6.2
Primary porosity**	30.4	26.0	16.8	11.0	23.6	19.0
Matrix	26.8	63.0	3.7	15.1	16.6	39.0
Abiotic alteration[††]	33.2	26.6	1.0	0.0	11.9	11.7
Gel-palagonite[§§]	32.9	19.6	1.0	0.0	11.7	7.4
Fibro-palagonite[##]	1.3	18.5	0.0	0.0	0.3	4.3
Total calcite	15.5	32.0	0.0	0.0	3.3	2.6
Zeolites***	0.7	3.5	0.0	0.0	0.1	0.1
Bioalteration value[†††]	8.75	10.0	0.0	0.0	2.4	3.7
	Max. (µm)		**Min. (µm)**		**Avg. (µm)**	
	RR	**BH**	**RR**	**BH**	**RR**	**BH**
Tunnel Diameter	4.4	4.5	0.5	0.1	0.9	0.8
Tunnel Length	47.7	139.7	6.7	1.2	22.5	31.9
Bubble Diameter	-	9.8	-	0.4	-	2.8

Note: Reed Rock: RR; Black Hills: BH

All values except bioalteration, tunnel length-width measurements and Black Hills porosity are proportions determined by point counting. All values are rounded to nearest 0.1.

*Total fresh glass: proportion of fresh glass currently in sample.

[†]Primary glass: total fresh glass + abiotic alteration.

[§] Crystallinity: total primary igneous minerals (phenocrysts/glomerocrysts + microlitic undercooling. Values are for samples FR-12-97A and FR-12-91B

[#]Undercooling: microlitic intergrowths of plagioclase and pyroxene.

** Primary porosity: vesicularity + voids + amygdaloidal and vug calcite/zeolite.

Black Hills porosity values were determined with digital image analysis (ImageJ).

[††]Abiotic alteration: total proportion of altered glass (palagonite).

[§§] Gel-palagonite: amorphous (isotropic) glass alteration.

[##] Fibro-palagonite: crystalline (anisotropic) glass alteration.

***Zeolites likely consist of mainly chabazite and possibly phillipsite, although they were not identified in XRD analysis.

[†††]Values are averages within each thin section determined using visual estimation method by Cousins et al. (2009).

3.3.2.1. Aqueous (Abiotic) Alteration

Most of the Black Hills samples studied display textures characteristic of relatively low temperature (<100 ºC) aqueous alteration of basaltic glass including palagonite (Figs. 3.4, 3.5), and intergranular/amygdaloidal authigenic calcite and zeolite cements (Fig. 3.4G-H). In all Black Hills samples with palagonite, its formation was initiated at locations on glass surfaces that would have been exposed to circulating fluids such as pyroclast margins, fractures and vesicles in addition to the walls of matrix voids. The intensity of palagonitic alteration and properties of palagonite (e.g., crystallinity, anisotropism, zonation/banding) vary between and within samples (Figs. 3.4, 3.5). Darker, more-intensely coloured and crystalline alteration may represent more advanced alteration stages (Stroncik and Schmincke, 2001). Several varieties, listed in interpreted order of increasing alteration progress based on colour, crystallinity and elemental composition, were identified: a golden yellow, clear to translucent, amorphous (isotropic) material with a relatively smooth structure (Fig. 3.4G) ; dull yellow orange amorphous to grainy crystalline massive matrix alteration (Fig. 3.5A-B); bright clear yellow to dark yellow-orange, fibrously/lath-like crystalline (anisotropic) matrix alteration with distinct isopachous zonation and fine laminations (Fig. 3.5C-H); a yellow to orange-brown, translucent, spherically or grainy crystalline material on glass with smooth concentric isopachous zonation/banding (Fig. 3.4A-C); a dull gold-yellow to dark brown, lath-like or fibrously crystalline (anisotropic) material on glass with zoned bands/laminations (Fig. 3.4D-F); a bright golden yellow, fractured, highly lath-like/fibrously crystalline (anisotropic) material in glass formed on the surface of the amorphous variety and rimming zeolite-filled vesicles (Fig. 3.4G-H). Alteration fronts form from exposed

surfaces inward and alteration intensity decreases moving from palagonite toward fresh sideromelane or unaltered matrix. Matrix-altered zones are consolidated appearing as cohesive masses. Late-stage fractures, possibly formed by contraction caused by desiccation or non-isovolumetric alteration, may cross-cut both consolidated matrix and vug calcite and are occasionally infilled with calcite. Indications of nontronite and possibly montmorillonite were also detected with µXRD analysis (Fig. 3.3C).

Total thicknesses of isotropic gel- and crystalline grainy to fibrous/lath-like palagonite bands directly on glass have a range of 10 to 50 µm with individual banded zones/laminations ranging from 10 to 30 µm. Thicknesses between adjacent individual bands may differ by ~20 µm. Where the crystalline types are present, boundaries between either fibrous/lath-like or grainy crystalline rinds and the amorphous type or glass are very smooth and distinct (Fig. 3.4A-C, G-H) whereas boundaries between individual bands within the grainy crystalline type are moderately diffuse (Fig. 3.4B-C). Grainy and fibrous/lath-like crystalline palagonite bands resulting from matrix alteration (very fine ash) range from 20 µm to >100 µm thick as measured from the central void to the edge of the altered zone. Individual banded zones/laminations in this type are more variable in thickness (2 to 50 µm). Thicknesses between adjacent individual bands in these alteration zones may differ by >45 µm. Boundaries separating individual bands are very sharp and distinct (Fig. 3.5C-H).

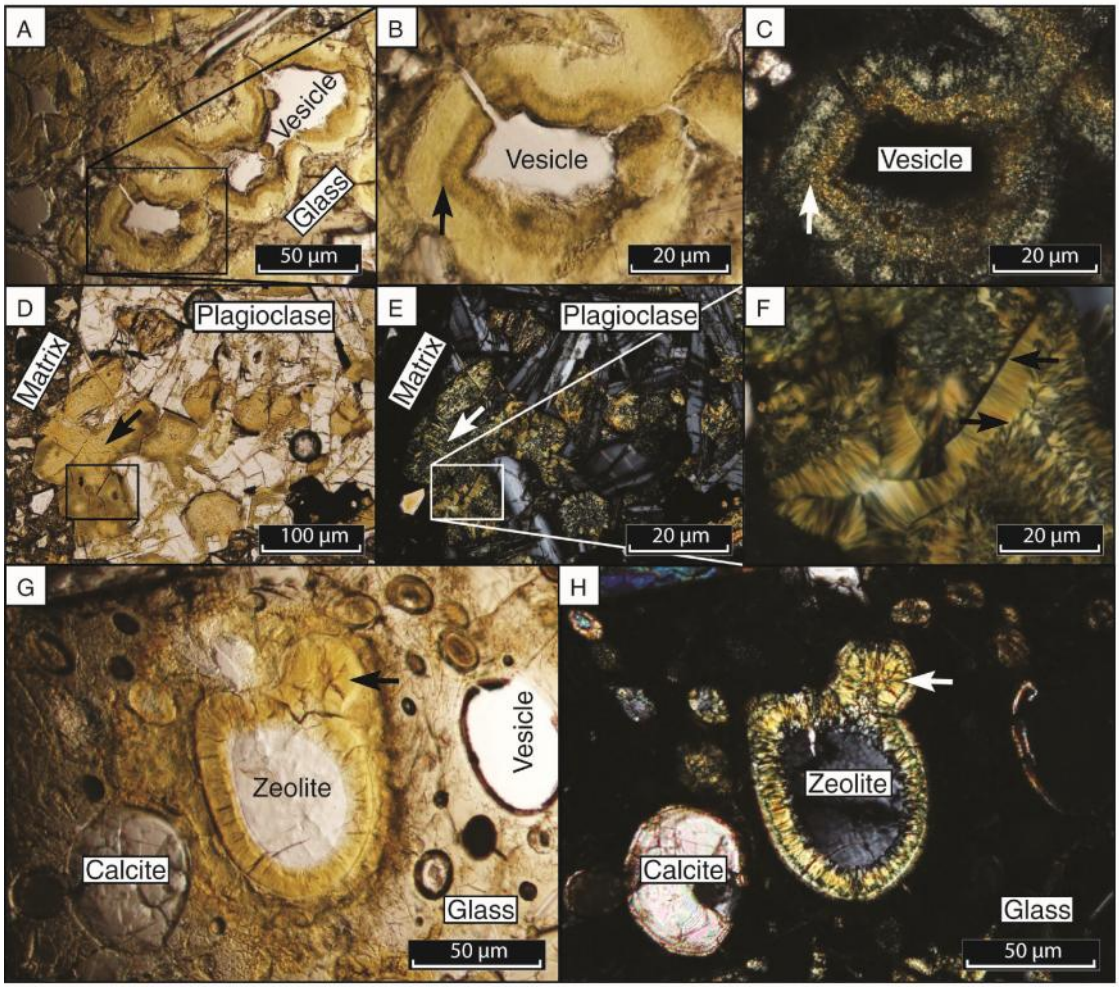
A
Vesicle
Glass
50 µm
B
Vesicle
20 µm
C
Vesicle
20 µm
D
Plagioclase
Matrix
100 µm
E
Plagioclase
Matrix
20 µm
F
20 µm
G
Zeolite
Vesicle
Calcite
Glass
50 µm
H
Zeolite
Calcite
Glass
50 µm

Figure 3.4. Abiotic alteration of sideromelane pyroclasts. (A) Isopachous proto-crystalline fibro-palagonite bands rimming several vesicles within a pyroclast. The box in A is enlarged in B-C. (B-C) Plane and cross-polarized images, respectively, of isopachous fibro-palagonite bands. The different coloured bands (*arrow*) represent differences in chemical composition and crystallinity, but overall appear to be composed of grainy crystallites < 1µm. A-C from sample FR-12-111B. (D-E) Plane and cross-polarized images, respectively, of a highly crystalline lithic clast that has been altered to proto-crystalline (anisotropic) fibro-palagonite (*arrow*) between plagioclase phenocrysts. Darker bands are observed along either fractures or the interfaces between plagioclase crystals and what would have previously been glass. Box in D-E is enlarged in F. (F) Cross-polarized image. Darker palagonite bands (*top arrow*) appear to be composed of elongated fibrous crystallites in a preferred orientation (perpendicular to surface of initiation) whereas the lighter cores (*bottom arrow*) are composed of smaller less oriented fibrous crystallites. D-F from sample FR-12-113. (G-H) Plane- and cross-polarized images, respectively, of a yellow fibro-palagonite (anisotropic) rim around a zeolite-filled vesicle. It appears to be composed of elongated fibrous crystallites oriented perpendicular to the vesicle surface. Between the fibro-palagonite rim and unaltered glass is amorphous (isotropic) gel-palagonite more prominently visible along the left side of the vesicle. The unaltered glass along the right side of the vesicle has several very fine tubular features extending beyond the palagonitic alteration margin, and also from the smaller adjacent vesicles at top right. A smaller calcite-filled vesicle is located at lower left and is separated from the crystalline fibro-palagonite by isotropic gel-palagonite, which partially rims the calcite-filled vesicle. G-H from sample FR-12-107.

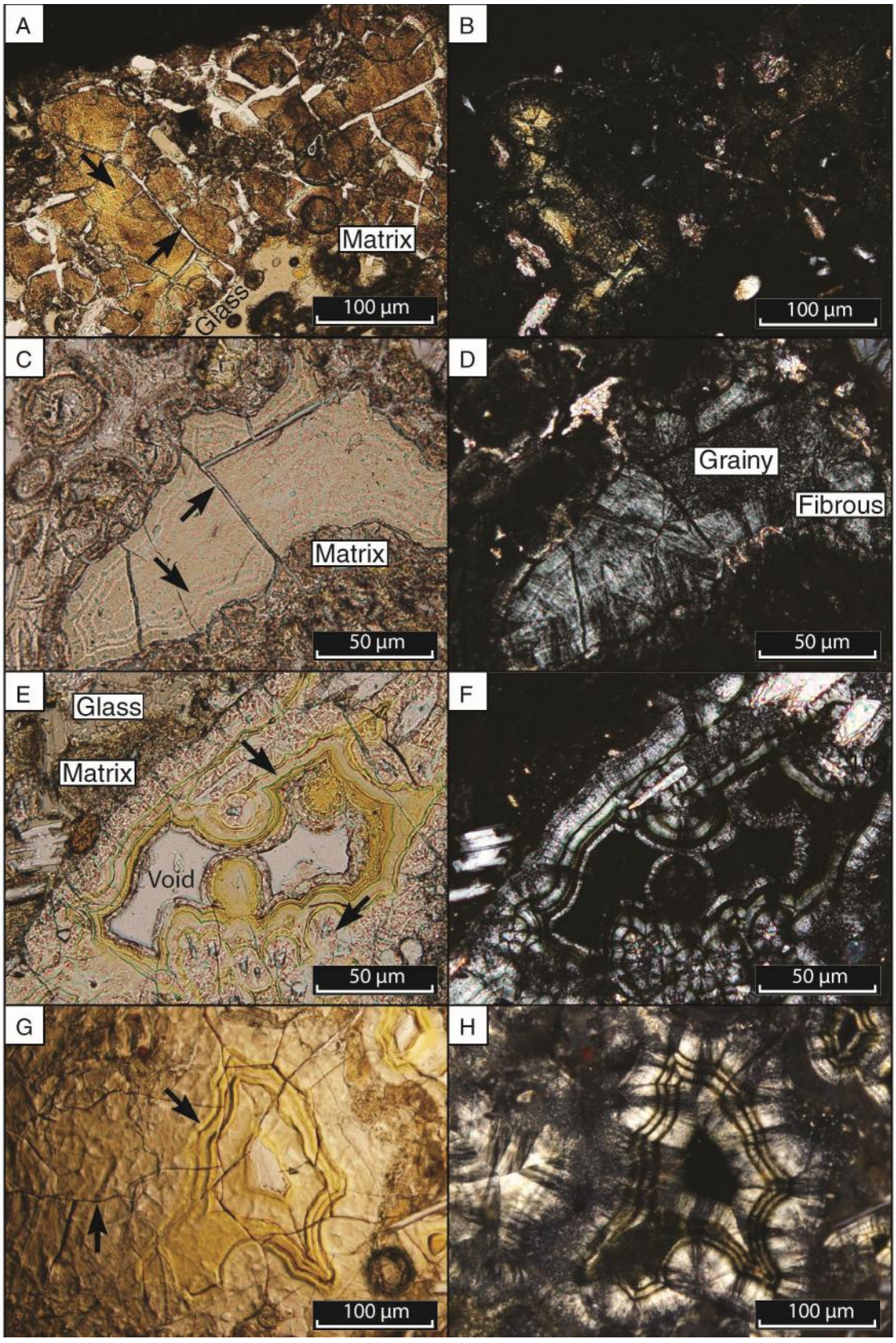
A
Matrix
Glass
100 µm
B
100 µm
C
Matrix
50 µm
D
Grainy
Fibrous
50 µm
E
Glass
Matrix
Void
50 µm
F
50 µm
G
100 µm
H
100 µm

Figure 3.5. Abiotic alteration of ash and matrix material. (A-B) Plane and crossed-polarized images of consolidated and partially palagonitized portion of matrix (*top arrow*) with obvious later stage mosaic fractures (*bottom arrow*). In crossed-polarized light, the proto-crystalline material appears to be composed of grainy crystallites. A calcite-filled vesicle is visible in the bottom of the image (at top left corner of the scale bar). Sample FR-13-177. (C-D) Completely altered portion of matrix between the remnants of pyroclasts also completely altered and partially replaced with calcite. Isopachous concentric 5-10 µm thick bands (*bottom arrow*) are observed along the outer edge of the proto-crystalline fibro-palagonitic material, through which later stage fractures can be seen (*top arrow*), possibly crystallographically controlled. In D, the fibrous character of the material can be observed. Sample FR-12-116-1x. (E-F and G-H) Plane and cross polarized images of completely altered matrix material initiated at central voids outward. Later fractures are visible (*bottom arrow in G*) that crosscut bands. The smooth concentric bands (*top arrows in E and G*) are distinct, especially in cross-polarized light where very dark thin bands separate thicker, lighter ones. The darker bands may contain more Fe-oxides. Proto-crystalline material appears to have radial elongate fibrous character. Some calcite inclusions are visible in F at ~center. Sample FR-13-145A.

Altered olivine grains are observed within three tuff samples. Olivine grains are altered to a reddish-brown fine grained intergrowth of secondary phases. Olivine alteration is only observed in solitary grains within matrix and occurs both along exterior crystal surfaces and fractures or follows parting surfaces.

3.3.2.2. Secondary Precipitates

Authigenic calcite is observed in 33 tuff samples. Amygdaloidal calcite (Fig. 3.4G-H) is common in most samples as anhedral intergrown grains or as single optically continuous crystals. Calcite vugs with anhedrally intergrown crystals ranging from 10 - 600 µm are most common. In 8 tuffs, angular, vesicular pyroclasts 200 µm to > 1 cm completely preserved by extensive replacement with calcite are observed. Calcite amygdules optically continuous with the replaced pyroclast are also observed (Fig. 3.6A). The samples that have calcite replaced pyroclasts are generally associated with moderate

to high degrees of palagonitization (9 - 19%). Rarely, calcite replaced pyroclasts have palagonite cores where calcite separates palagonitic alteration from vesicle surfaces or margins (Fig.3.6B). Rare zeolite amygdules and vugs are also observed in 2 tuffs usually bound within highly birefringent fibro-palagonite lined vesicles or voids (Fig. 3.4G-H). The zeolites are optically identical to those identified in Reed Rock as chabazite that exhibit typical low first order gray interference colours and radial extinction. The pore-filling zeolites in Black Hills is also likely chabazite, and minor phillipsite, although no signals identifying these minerals were produced during XRD analysis.

3.3.2.3. Microbial Bioalteration

Petrographic analysis of 48 basaltic tuff samples containing fresh glass from the Black Hills reveals a diverse suite of possible microbial alteration textures that resemble the morphology and distribution of those reported in oceanic and sub-glacial lavas (Fisk et al., 1998, 2003; Furnes and Staudigel 1999; Furnes et al., 2001, 2007a). At least some traces of putative bioalteration are observed in all tuffs with 17 samples having average bioalteration values greater than 5 (50% of available surfaces affected). The textures are also similar to those described from Reed Rocks tuffs (Chapter 2). Tubular and granular bioalteration textural types (Furnes and Staudigel, 1999) are observed at glass surfaces (margins, fractures, glass-crystal boundaries, vesicles) and glass alteration interfaces.

Tubular alteration is predominant and is characterized by tunnel-like features with vermicular or tubular and bifurcating forms that project into fresh glass most commonly from vesicles, clast margins, fractures and occasionally glass alteration fronts (Figs. 3.7, 3.8, 3.9, 3.10). Individual tubular tunnel diameters range from 0.1 to 4.5 µm, are most

frequently 0.5 - 1 µm (Fig. 3.11) with an average of 0.8 µm. Tunnel lengths range from 1.2 µm to 140 µm (Fig. 3.12) with an average of 31.9 µm. In order of decreasing abundance and commonality (Fig. 3.13) tubular alteration shows the following morphological varieties: *simple* unornamented, straight to curving, convoluted or kinked (Fig. 3.7); simple and network *branching*, nodal swells (Fig. 3.8); engorged, annulated (Fig. 3.9); ovoid bodies, septa bearing, terminal enlargements (Fig. 3.10). Simple and branching tunnels usually occur in groups of several close parallel tunnels with common directionality or irregular convoluted paths that appear to be caused by the avoidance of adjacent tunnels, vesicles, plagioclase crystals (Fig. 3.7C, 3.14), or rarely the seeking of olivine crystals. Branching types have daughter tunnels slightly smaller in diameter than parent tunnels or are the same diameter as the parent tunnel (Fig. 3.8C) and may taper toward their ends (Fig. 3.8B). We observed several examples of tunnels rooted on amygdaloidal vesicles (Fig. 3.8C), indicating their formation prior to calcite precipitation. Engorged or annulated tunnels are typically long (up to 50 times their width) and have periodic increases and decreases in diameter that are regularly spaced along tunnel lengths (Fig. 3.9). Some occasionally terminate in very fine branches or appear to be rooted on a wide base that may actually be branches bifurcating near the point of origin (Fig. 3.9A-B). Others are shorter and have annulations near their termini (Fig. 3.9C). Elongate ovoid bodies 1-3 µm are sometimes visible within kinked and tapered tunnels (Fig. 3.10A). Only rare (1 tuff) examples of tunnels with bulbous terminal enlargements

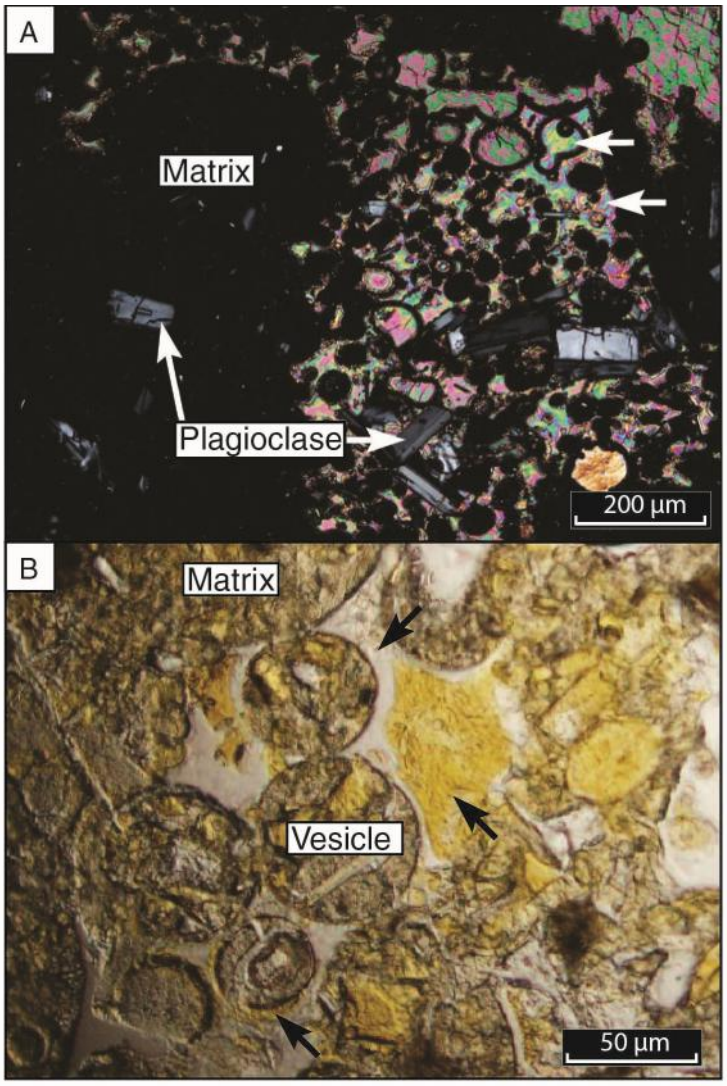

Figure 3.6. (A) Cross-polarized image of pyroclast completely replaced by calcite (*bottom right arrow).* The primary pyroclast shape, including vesicles are preserved. Top arrow indicates a preserved vesicle that is also infilled with calcite. Calcite in top right corner is an irregular void infilled with calcite with some visible rhombohedral cleavage planes. Sample FR-12-104B. (B) Plane polarized image of a pyroclast that has been partially replaced by calcite (*top arrow*) preserving clast shape and vesicles. Part of the pyroclast appears to have a palagonite core (*mid-arrow)* with calcite separating the palagonite from the vesicle or margin (fluid exposed) surface. In other locations there appear to be palagonite rims that separate the calcite from the vesicle surface (*bottom arrow*). Sample FR-12-105B.

are observed, which are long, curved and have large tangles or rough engorgements near their termini (Fig. 3.10B). In thin section, most tunnels appear light and hollow, but many show darker yellow to brown interiors, with dark margins that could be due to partial infilling.

Granular alteration typically forms globular rounded/ irregular 5-20 µm wide incursions into fresh glass consisting of amalgamated spherical bodies < 1 µm in diameter (Fig. 3.15). Included with the granular type are the bud-bubble sub-type. Bud-bubbles are composed of individual sub-spherical pits 0.4 - 9.8 µm in diameter (Fig. 3.16) with an average of 2.8 µm, usually with central proto-crystalline cores and ringed/zoned interiors that project into fresh glass in irregular coalesced groups or individual semi-circular pits (Fig. 3.17).

Tubular and granular textures typically occur in the same samples (27 of 48 tuffs). Rarely (1 tuff) various tubular morphologies extending beyond granular or bubble-type alteration fronts (Fig. 3.17B) or granular alteration apparently extending from bubble structures is observed (Fig. 3.15D). In sample FR-13-149, small vertical pipe-like structures, enriched in coarse and dense particles and depleted in fines (elutriation pipes; Druitt, 1995) were observed. These are typically caused by the fluidization or elutriation of fine particles by degassing through deposits (Druitt, 1995). Where such pipes were observed, only the granular-bubble type alteration was present.

3.3.2.3.1. Biogenicity. The putative microborings described in the Black Hills tuffs fulfill at least two of the three biogenicity criteria proposed by McLoughlin et al. (2007):

1. '*A primary geological setting that demonstrates a syn-genetic origin for the euendolithic microborings*'. The occurrence of Black Hills microborings is restricted to pyroclast margins, fractures and vesicles that may have provided pathways for circulating fluids and endolithic organisms. In addition, microborings are distinct from symmetric abiotic alteration fronts (Figs. 3.7, 3.8, 3.9, 3.10, 3.15, 3.17 vs. Figs. 3.4, 3.5). Overall microborings appear to have a greater affinity for vesicle walls. Some microborings predate carbonate cement phases and late-stage fractures, and post-date abiotic glass alteration, indicating the relative timing of biotic alteration.

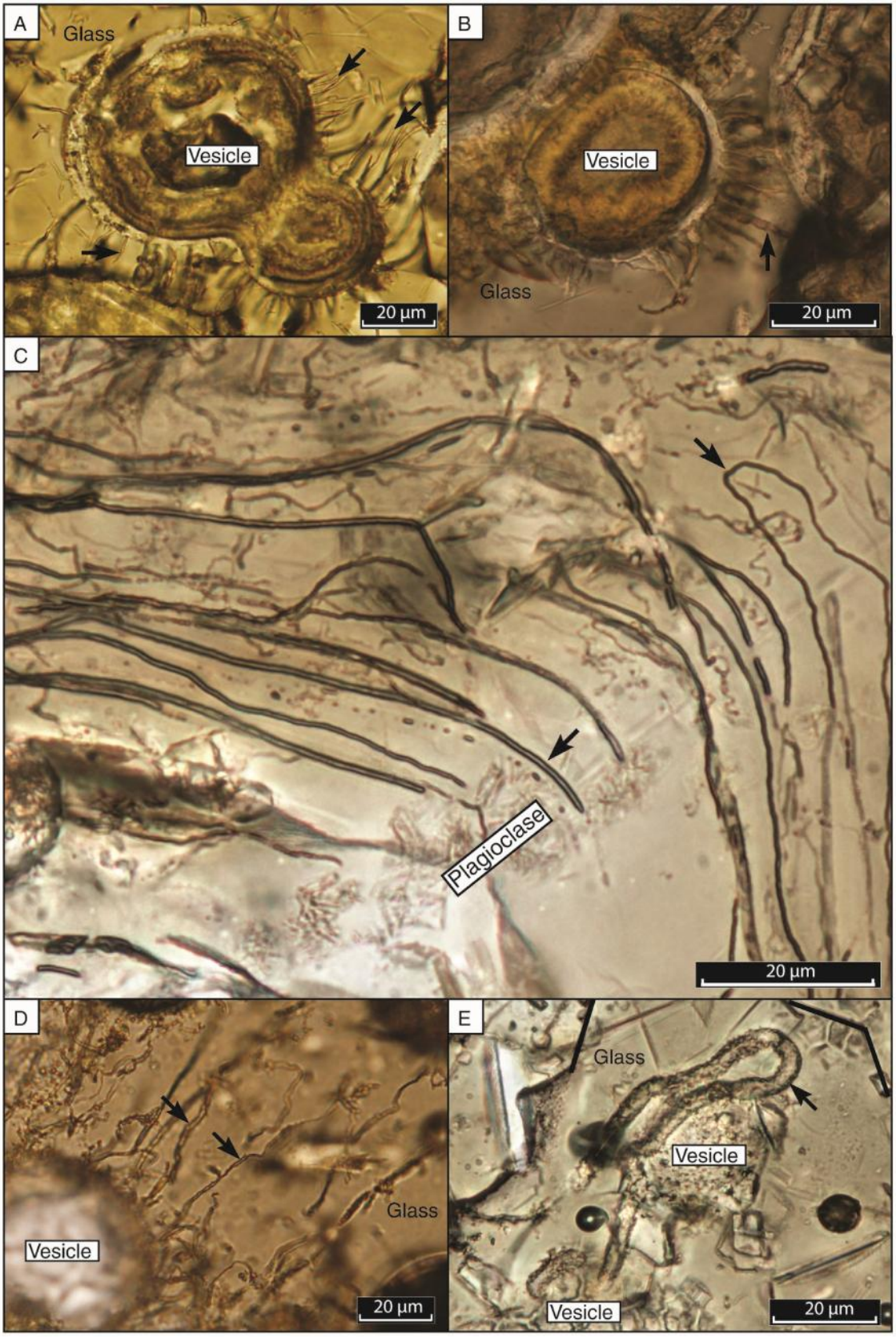
A
Glass
Vesicle
20 µm
B
Vesicle
Glass
20 µm
C
Plagioclase
20 µm
D
Glass
Vesicle
20 µm
E
Glass
Vesicle
Vesicle
20 µm

Figure 3.7. (A) Close, smooth, simple, parallel, curvilinear tunnels *(top arrow)* and simple branching tunnels (*right arrow*) rooted on a vesicle. From FR-12-116-1x. (B) Straight to curved simple and annulated, tapered, tunnels *(arrow)* rooted on a vesicle. From FR-12-104B. (C) Long, smooth, simple, parallel, curved tunnels (*bottom arrow*) directed around a plagioclase phenocryst below. Top arrow indicates a thin, long convoluted tunnel that changes direction 180°. From FR-12-107. (D) Thin, parallel, kinked tunnel (*arrows*) rooted on a vesicle. (E) Long, rough, ~90 µm long, convoluted tunnel (*arrow*) originating from a vesicle. The curvature and directionality appear to be in response to the vesicle at center, and plagioclase phenocryst at top.

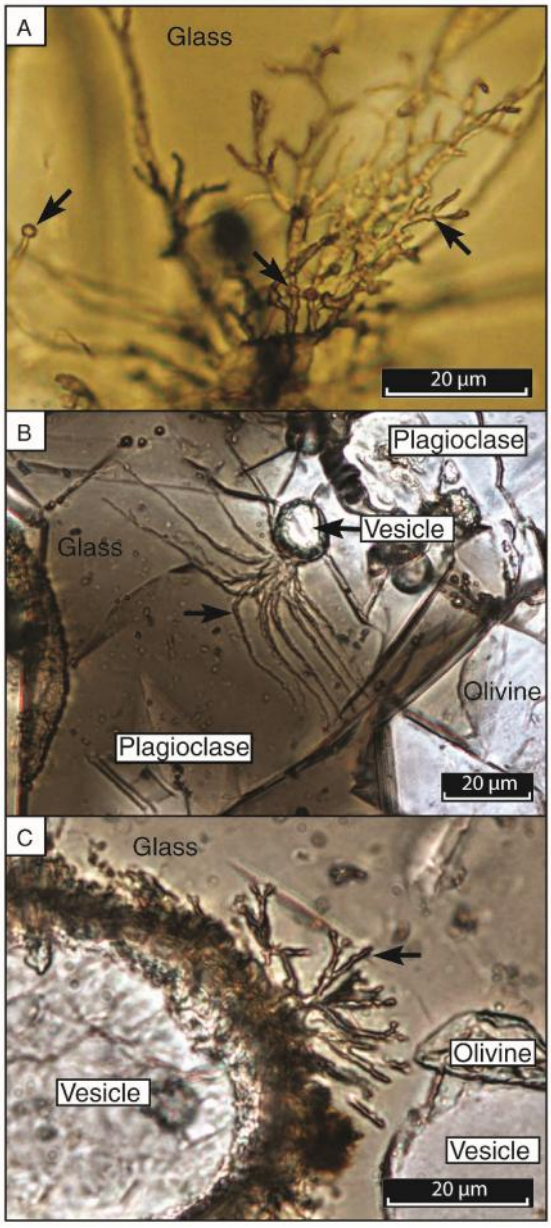

Figure 3.8. (A) Network branching, engorged tunnels originating from a vesicle located just beyond the lower boundary of the frame. Several nodes and enlargements are visible along the tunnel lengths *(right arrow)* and the diameters of daughter tunnels mostly smaller than the parent tunnels. A single tunnel *(left arrow)* appears to have a bulbous terminal enlargement. From sample FR-12-106. (B) Multiple parallel, simple branching and tapered tunnels *(left arrow)* originating from a wide root on a vesicle. Tunnels are changing direction in avoidance of a clast margin at left and small plagioclase crystal at bottom left and are directed toward larger olivine crystal at right. From sample FR-13-146. (C) Short, smooth, network branching tunnels rooted on a calcite-sealed vesicle (amygdule) indicating tunnel formation prior to calcite precipitation. Daughter tunnels are the same diameter as parent tunnels, several of which appear to be directed toward a small olivine phenocryst at right. From sample FR-13-177.

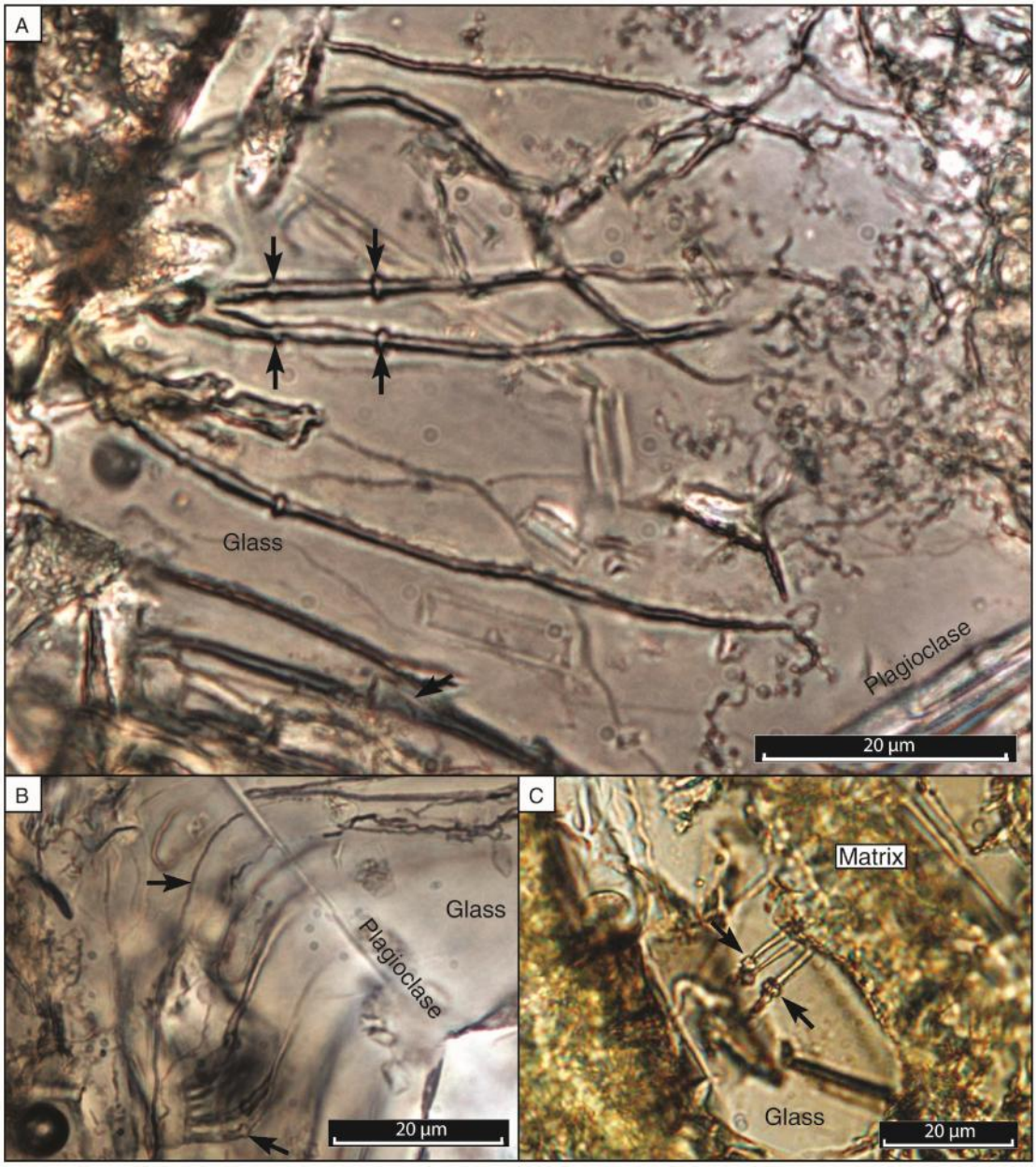

Figure 3.9. (A) Long, annulated *(four left arrows)* tunnels terminating in thin branches and originating from a fracture at left. Note that the annulations on individual tunnels are equally spaced. From sample FR-12-106. (B) Multiple, close, long, curvilinear and annulated or engorged tunnels *(bottom arrow)* rooted on a vesicle (not visible) and directed around a plagioclase crystal beneath. The small enlargements indicated with the bottom arrow occur at approximately equal distances from the point of origination. Upper arrow indicates an long, simple, curvilinear tunnel also curving around the plagioclase crystal. From sample FR-12-107. (C) Close, engorged tunnels (arrows) originating from a pyroclast margin at right. From sample FR-12-107.

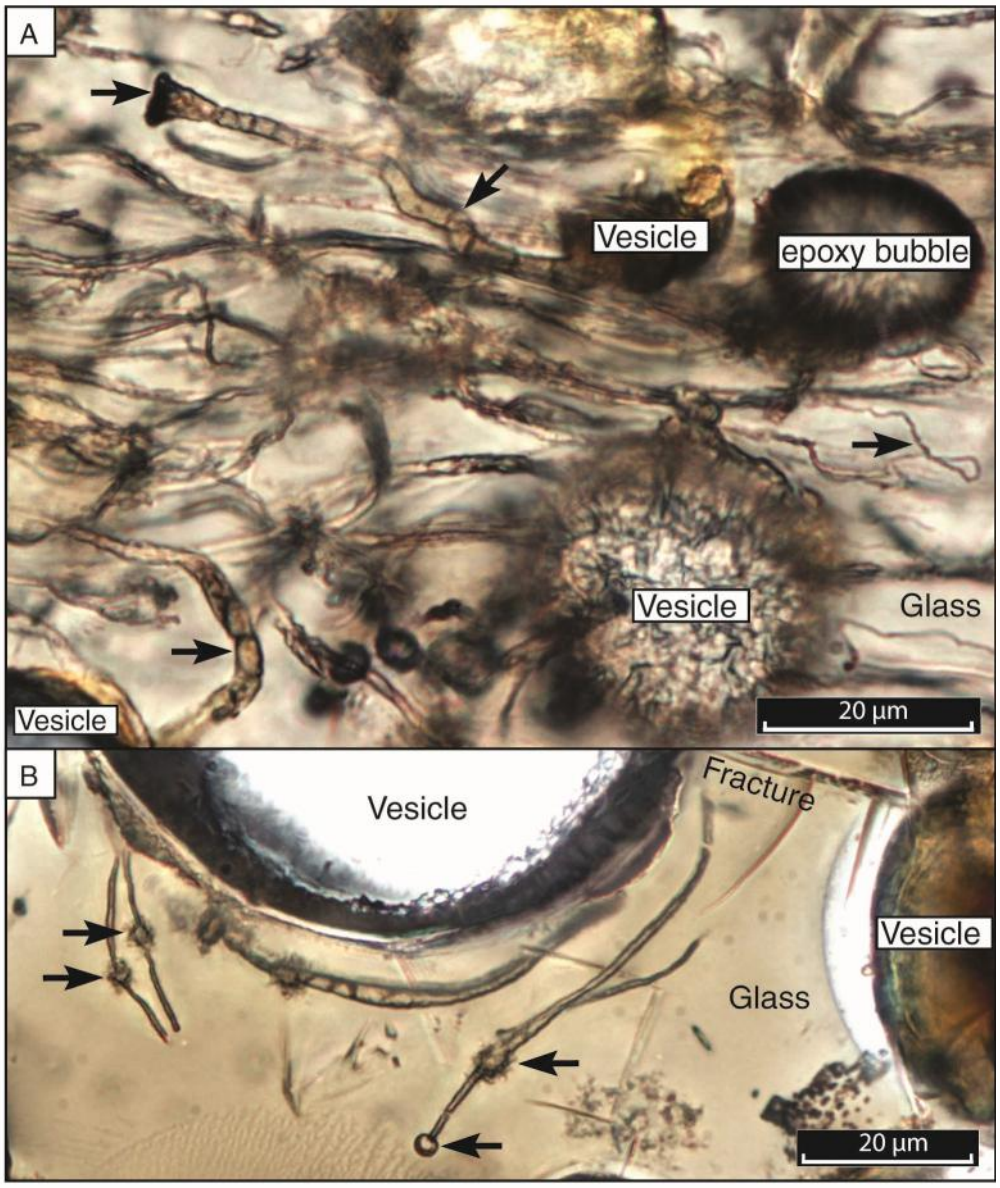

Figure 3.10. (A) Kinked tunnel *(upper center arrow)* with a dark mushroom-like terminal enlargement (upper-left arrow) and septa along its length originating from a vesicle. Bottom left arrow indicates a curved and tapered tunnel with septa or ovoid bodies along its length, originating from a vesicle. Right arrow indicates a thin, kinked and convoluted tunnel that changes overall direction by 180°. From FR-12-106. (B) Curvilinear tunnels with tangled regions near tunnel termini (*upper three arrows*). Bottom arrow indicates a round bulb terminal enlargement and is one of the only instances of this in the Black Hills. From FR-13-146.

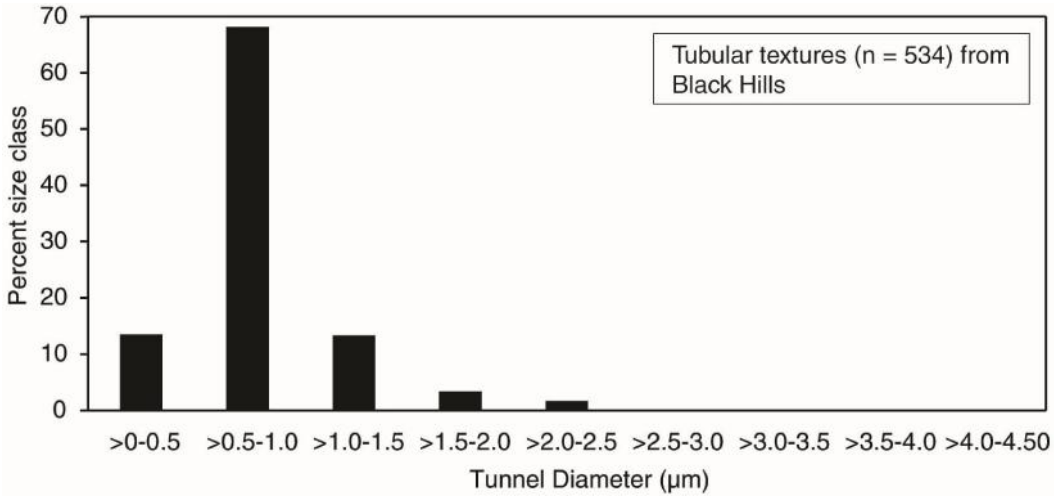

Figure 3.11. Relationship between diameter of tubular structures, ranging from >0-4.5 µm, and the percentage in size classes from the Black Hills basaltic tuffs. The greatest percentage falls within the 0.5-1 µm diameter size class and sizes are log-normally distributed (left skewed). No data points from 2.5-4.5 µm. Values were obtained by directly measuring features in photomicrographs using cellSens Standard and ImageJ software measurement tools.

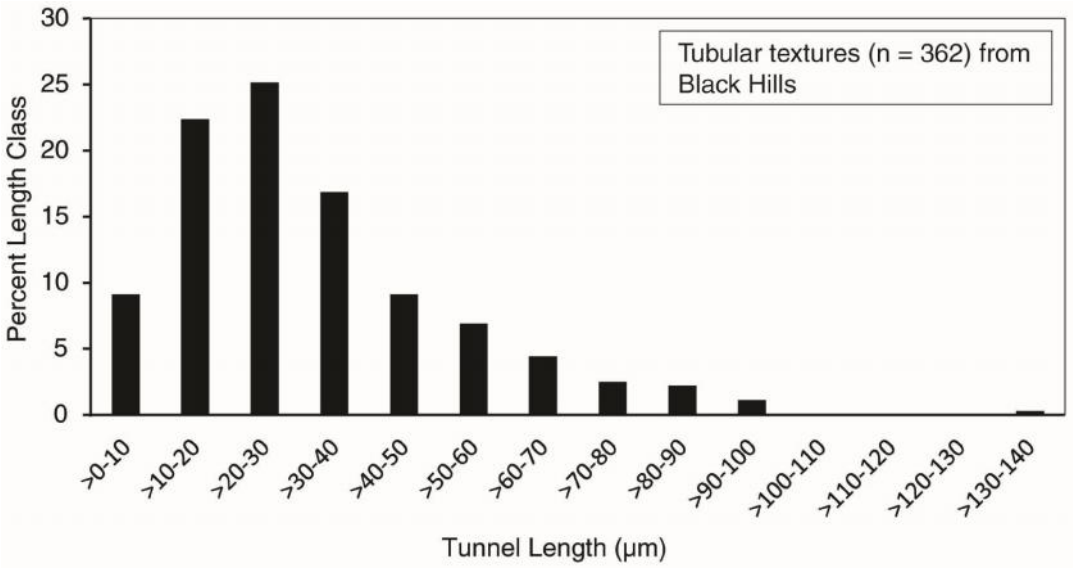

Figure 3.12. Relationship between the length of tubular structures, ranging from 0-140 µm, and the percentage in size classes from the Black Hills basaltic tuffs. The greatest percentage falls in the 20-30 µm size class and sizes are log-normally distributed (left skewed). No data points from 100-130 µm. Values were obtained by directly measuring features in photomicrographs using cellSens Standard and ImageJ software measurement tools.

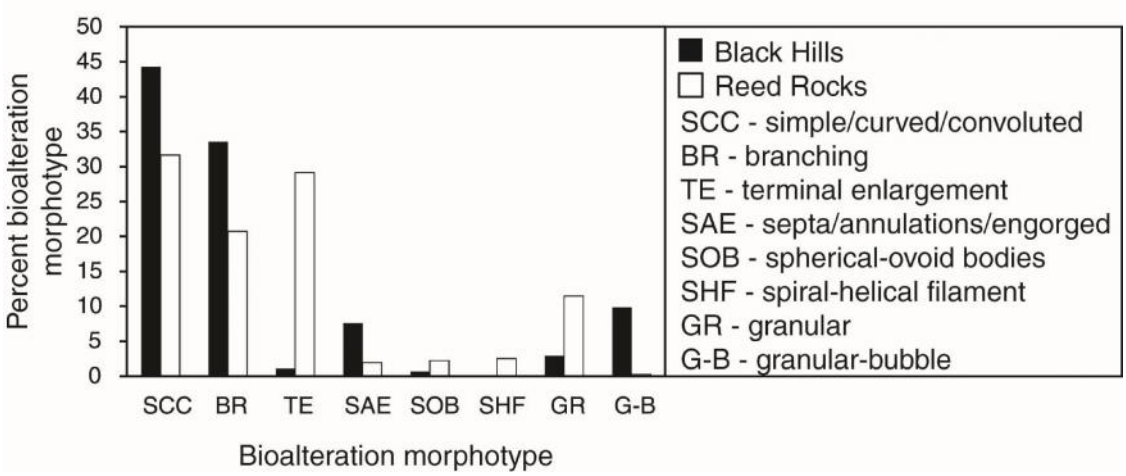

Figure 3.13. Relative differences in bioalteration morphotypes within and between Black Hills and Reed Rocks tuffs. Proportions were determined by surveying a suite of photomicrographs and recording each morphotype occurrence with a tally.

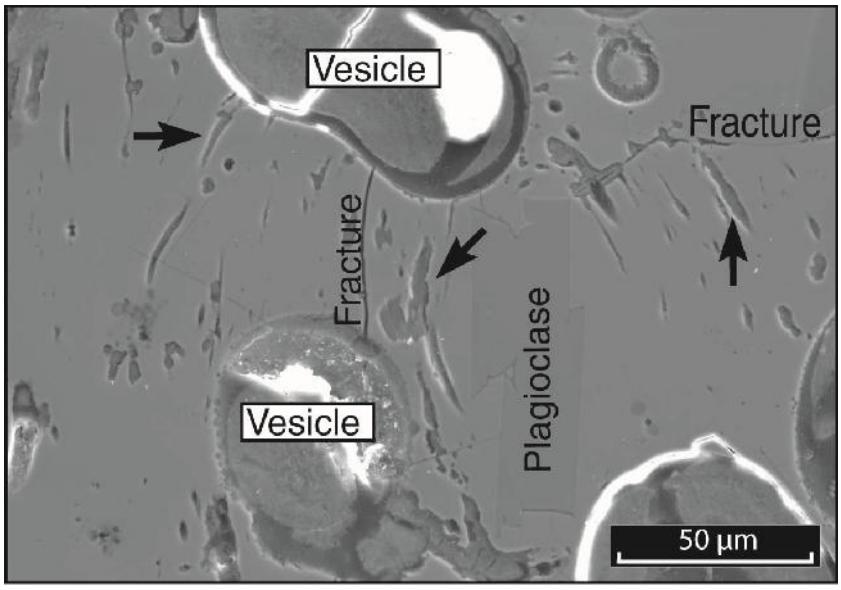

Figure 3.14. Scanning electron microscope (SEM) image displaying tubular bioalteration glass 'etching' textures. At right, features are clearly extending asymmetrically from a fracture into adjacent glass and are curving in parallel around a plagioclase crystal. At center and right, features are extending from a vesicle, the center textures are also curving around a plagioclase crystal and away from the lower vesicle. From FR-13-177.

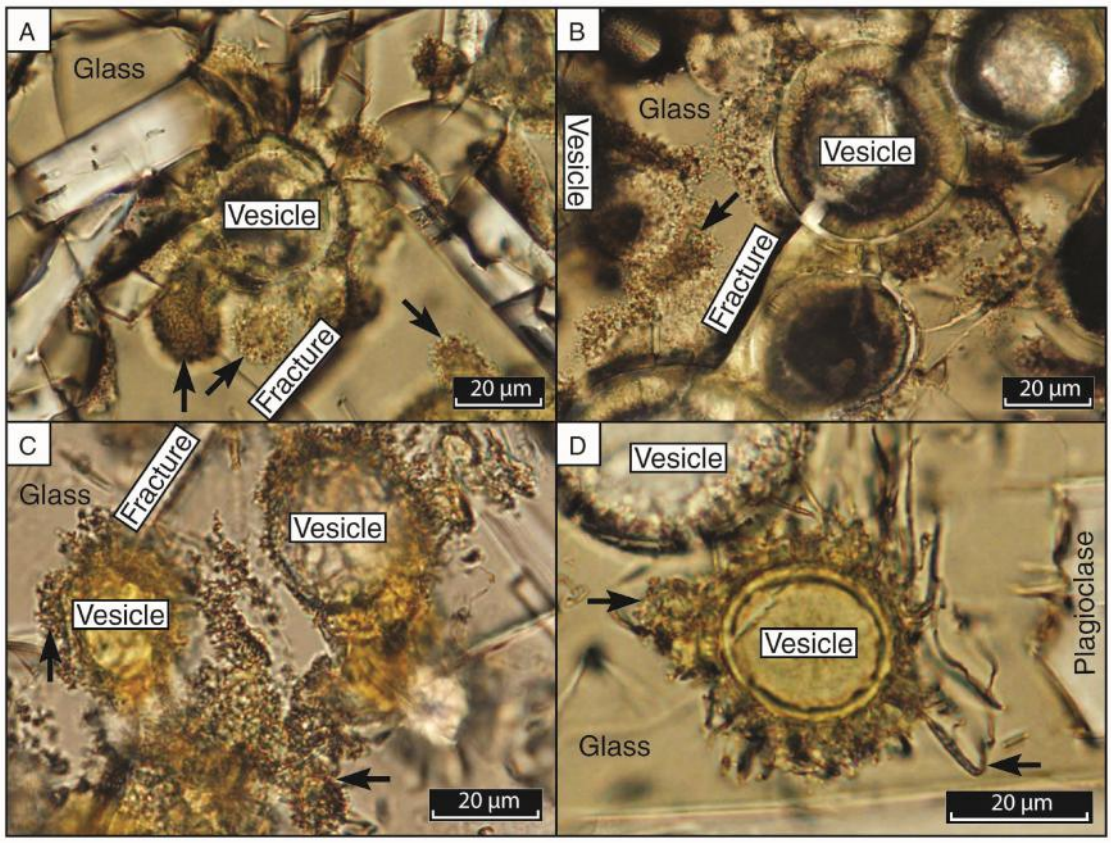

Figure 3.15. (A-C) Wide granular incursions *(arrows)* originating from vesicles and along fractures. From samples FR-12-108 (A and B) and FR-12-111 (C). (D) Granular alteration *(left arrow)* surrounding a vesicle with emerging curvilinear tunnels. The tunnel emerging from bottom *(right arrow)* is convoluted; it curves back toward the starting point and avoids the plagioclase crystal at right. From FR-13-177.

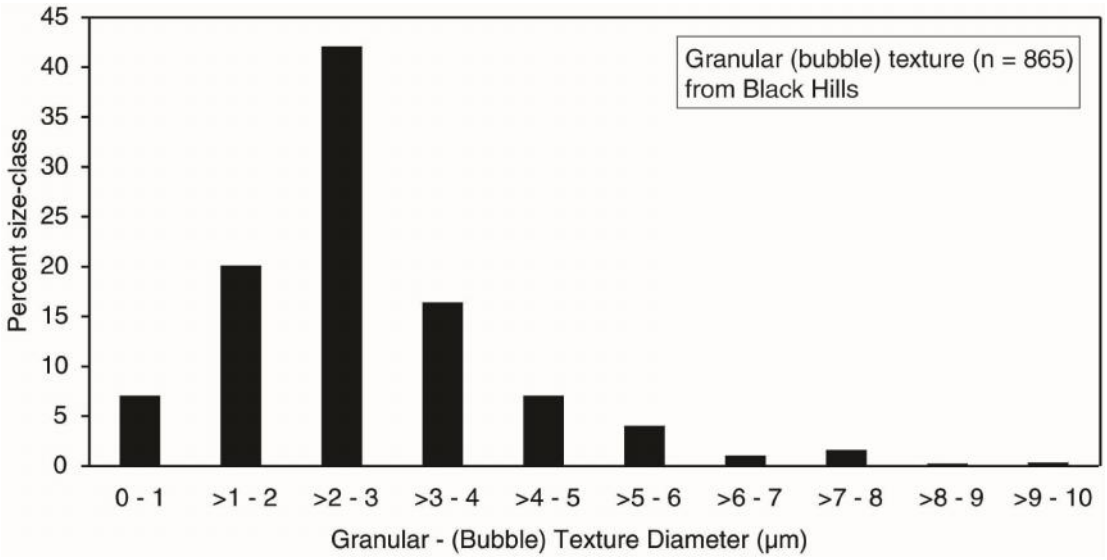

Figure 3.16. Relationship between diameter of granular-bubble structures, ranging from 0-10 µm, and the percentage in size classes from the Black Hills basaltic tuffs. The greatest percentage falls within the 2-3 µm diameter size class and sizes are log-normally distributed (left skewed). Only 2 and 3 data points for >8-9 and >9-10 µm ranges, respectively. Values were obtained by directly measuring features in photomicrographs using cellSens Standard and ImageJ software measurement tools.

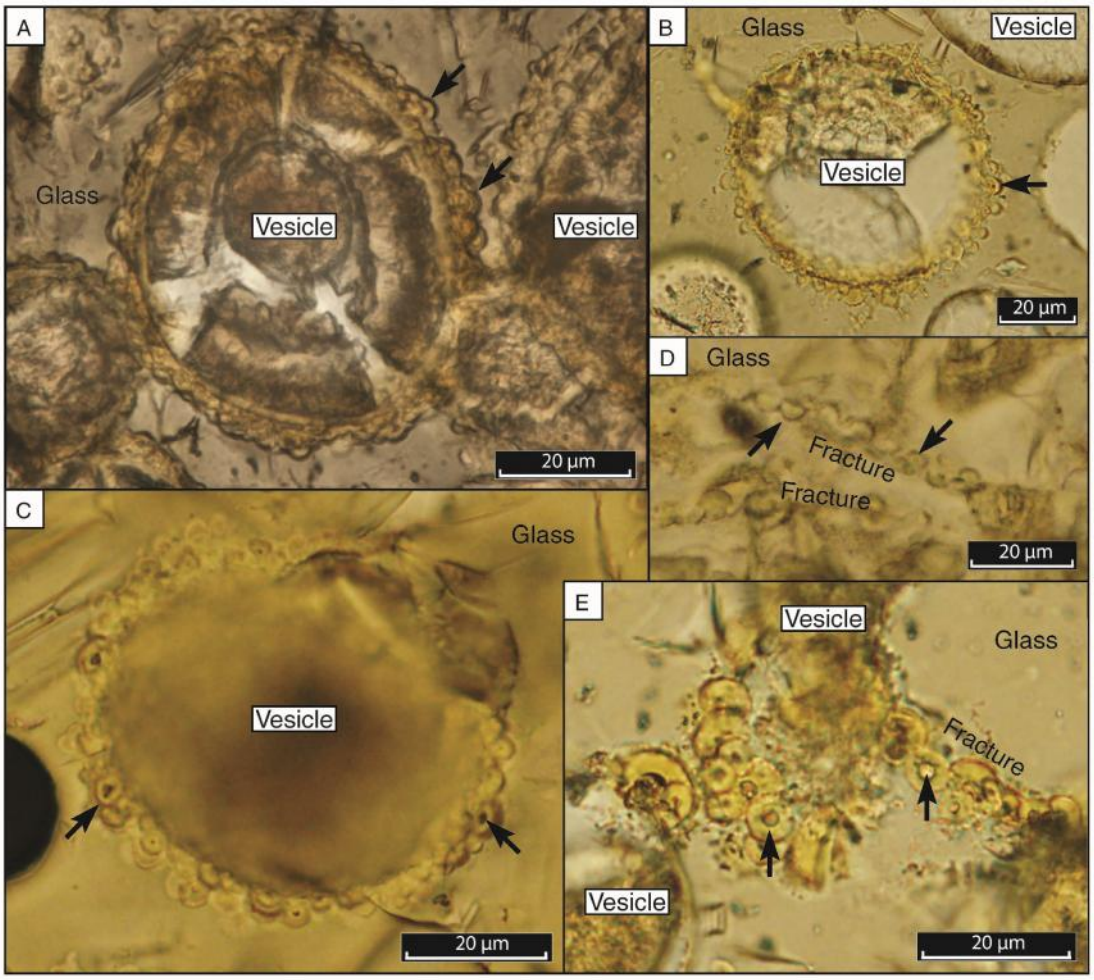

Figure 3.17. (A-C) Semi-spherical pits *(arrows)* comprising the bubble sub-type of granular alteration. Irregular alteration front composed of individual amalgamated spherical pits with dark cores (possibly smectite clay) and slight concentric rings in some, all originating from vesicles. From FR-12-104 (A and C), FR-13-77 (B). A is an enhanced depth of focus (EDF) image. (D) Semi-spherical bubble pits asymmetrically distributed along a fracture. From FR-12-111B. (E) Semi-spherical bubble pits with circular cores *(arrows)* originating from a fracture at right and vesicle at left and top. From FR-13-177.

2. *'Microboring morphologies and distributions that are suggestive of biogenic behaviour and distinct from ambient inclusion trails'***.** Black Hills microborings appear as the two main types previously described in volcanic glass: tubular and granular (e.g., Furnes et al., 2001). There is evidence of simple and complex branching, irregular pathways, segmentation/septa, annulations and directionality among the tubular types in response to mineral crystals, vesicles or other tunnels. The tubular and granular types also have log-normal size distributions (length, diameter) that are within the ranges described in other volcanic rocks (Fig. 3.11, 3.12, 3.16). Log-normal distributions are commonly observed in biological systems (Limpert et al., 2001; van Dover et al., 2003). Their distinction from ambient inclusion trails is demonstrated by (1) the lack of metal oxide or sulfide grains within the termini of micro-tunnels, (2) the absence of longitudinal striations formed by metal sulfide or oxide grain facets upon propulsion through the substrate, and the existence of morphologies suggestive of biogenicity, (3) non-angular cross-sections, (4) nodal swelling in branching tunnels, and (5) common preferred orientations, distributions and directionality indicative of biological behaviour (Tyler and Barghoorn, 1963; Knoll and Barghoorn, 1974; Wacey et al., 2008; McLoughlin et al., 2010). Possible abiotically produced features such as fluid inclusion trails, radiation damage trails, skeletal crystals, healed fractures can also be refuted as alternative to the putative bioalteration textures in Black Hills tuffs (Walton, 2008; McLoughlin et al., 2010).

3.3.2.3.2. Bioalteration and Textural Properties. Assessment of relationships between major primary igneous and secondary alteration textures with bioalteration intensity and morphological type revealed no strong correlations within Black Hills tuffs.

General comparison with Reed Rock textures indicates some fundamental differences (Table 3.2). Although the overall average proportions of abiotic glass alteration are approximately equal, Black Hills has a greater proportion and wider range of aqueous alteration as crystalline fibro-palagonite (0 - 18.5 % vs. 0 - 1.3 %), secondary calcite (0 - 32 % vs. 0 - 15.5 %) and zeolites (0 - 3.5 % vs. 0 - 0.7 %). The Black Hills bioalteration intensity (Average: 3.7 vs. 2.4; Max: 10 vs. 8.75) and the tunnel lengths (1.2 - 139.7 µm vs. 6.7 - 47.7 µm) are also higher and wider ranging, respectively.

We also observed differences in bioalteration morphological type between the two deposits (Fig. 3.13). Here, the granular and granular-bubble sub-type are considered as separate types because they are morphologically distinguishable. In Reed Rock, the granular morphotype is more abundant than in Black Hills, whereas the bubble sub-morphotype (Fig. 3.17) is more abundant in Black Hills. In Reed Rock, the tubular morphotype with terminal enlargements (Fig. 2.9) were very common whereas in Black Hills they are almost absent. The tubular morphotype with spherical-ovoid bodies projecting from tunnel margins (Fig. 2.11), or with spiral filaments/ornaments (Fig. 2.8) were observed in Reed Rock but not in Black Hills tuffs. Common to both Reed Rocks and Black Hills as the most abundant type are simple, unornamented, straight to curving and branching tunnels (Figs. 3.7, 3.8, 3.13, 2.12, 2.13).

3.3.3. SEM/BSE Imaging and Element Mapping

In addition to transmitted light petrography, we performed SEM imaging of putative microborings in carbon coated polished sections. In several cases, tunnels identified in transmitted light intersect the upper surface of the thin section and interior

tunnel features such as possible cellular structures or encrusted material were imaged (Figs. 3.14, 3.18, 3.19). We note however, that the polishing process may have affected or destroyed certain delicate structures.

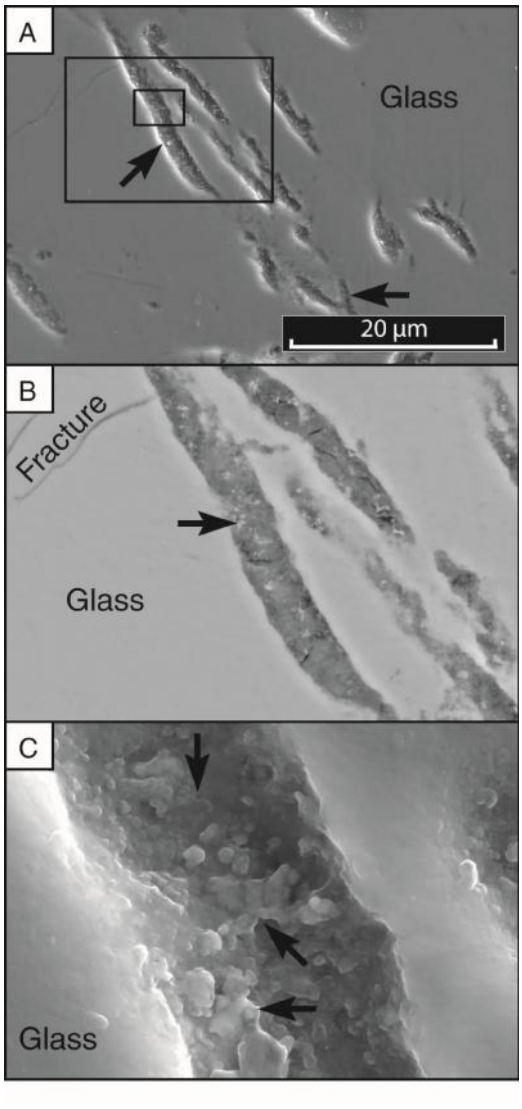

Figure 3.18. (A) Scanning electron microscope (SEM) image displaying tubular textures (*arrows)* oriented in the same direction. The bottom arrow indicates a branching tunnel. The larger black box is enlarged in (B) and the smaller box is enlarged in (C). (B) Back-scattered electron (BSE) image showing the mottled interior with lighter, possibly surface encrusted, spots (*arrow*). (C) SEM image showing irregular, rough, internal tunnel surface consisting of pits <0.5 µm (*top arrows*) and what appear to be surficial encrustations (possibly smectites). Sample FR-12-106.

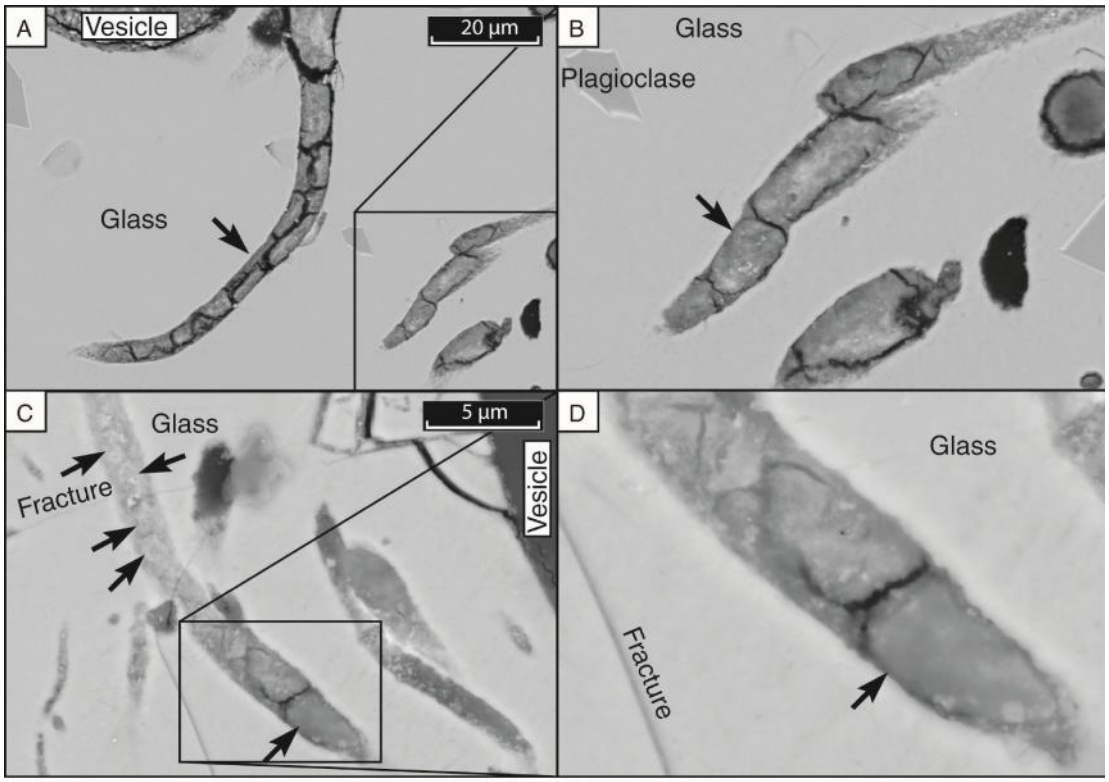

Figure 3.19. BSE images of tubular alteration textures. (A) Tubular texture extending from a vesicle with internal divisions and an infilling of Mg, Fe, Ti, Ba-bearing material. The box at bottom right is enlarged in (B). (B) Tubular textures with ovoid bodies/internal divisions. (C) Tubular texture with faint round objects along its length (*top arrows*) and larger ovoid bodies at the termini (*bottom arrow*) similar to those in (A-B). A portion of another tunnel at right is seen parallel to the one indicated with arrows. A later stage fracture cross-cuts the tunnel and intersects the vesicle at right. Box is enlarged in (D) showing the ovoid internal object/division and lighter surficial mottles. Sample FR-12-112.

Individual tunnels are elongated channel-like, ovular, to irregularly round or equant, depending of the angle of intersection. They commonly display smooth, curved, or slightly rough irregular edges (Figs. 3.14, 3.18, 3.19). Consistent with observations in transmitted light, we observed some tunnels connected to exposed glass surfaces, occasionally at glass-palagonite interfaces. They display clear asymmetrical and near perpendicular extensions from those surfaces, common directionality, and avoidance of plagioclase phenocrysts (Fig. 3.14). The surfaces of tunnel walls may appear rough and consist of small < 0.5 µm pits and positive irregularly shaped (possibly smectite) encrustation features (Fig. 3.18). In BSE images, ovoid bodies can be more clearly observed (Fig. 3.19) and other smaller faint round objects 1-2 µm in diameter are also observed along tunnel lengths (Fig. 3.19C). Qualitative EDS analysis of tunnel interiors indicate similar compositions relative to fresh glass, but with decreased abundances of Mg, Na, Fe, and Ca. In 6 out of 20 EDS analyses of tunnel interiors, elevated K was detected. Elemental maps of areas with exposed tunnels display similar depletions within tunnels, but no N, P, K or C spikes were detected.

The distinct zoned/banded character of palagonitic alteration is a result of differing degrees or habits of crystallinity (grainy-spherical vs. fibrous/lath-like), crystallite grain size and orientation (Fig. 3.4F), colour differences (Fig. 3.4A-B, D) and variations in elemental concentrations (Figs. 3.20, 3.21, 3.22, 3.23, 3.24). In the sample containing highly-crystalline palagonite rimming zeolite amygdules (Fig. 3.20), Fe and Mg are concentrated with respect to glass and zoned Mg variation is observed in the BSE images and Mg X-ray element map. Where matrix alteration has been identified, palagonite bands display higher Fe and K levels with respect to glass, where banding is

mainly a result of Fe variations (Fig. 3.21). In other examples of altered matrix where banding is observed under the petrographic microscope, variations in Fe, Mg, Na, K and Al have resulted in elemental zoning/banding (Fig. 3.5 G-H) and is emphasized in BSE images (Fig. 3.22). Massive zones of altered matrix with slightly grainy crystalline characters typically have higher Fe concentrations (Fig. 3.24). Amygdaloidal zeolites have the highest concentrations of Na, Al and K (Fig. 3.20). The differences in concentrations of Na, and K within the zeolite produce a distinct radial appearance (Fig. 3.20) that is commonly seen in cross polarized light as radial extinction.

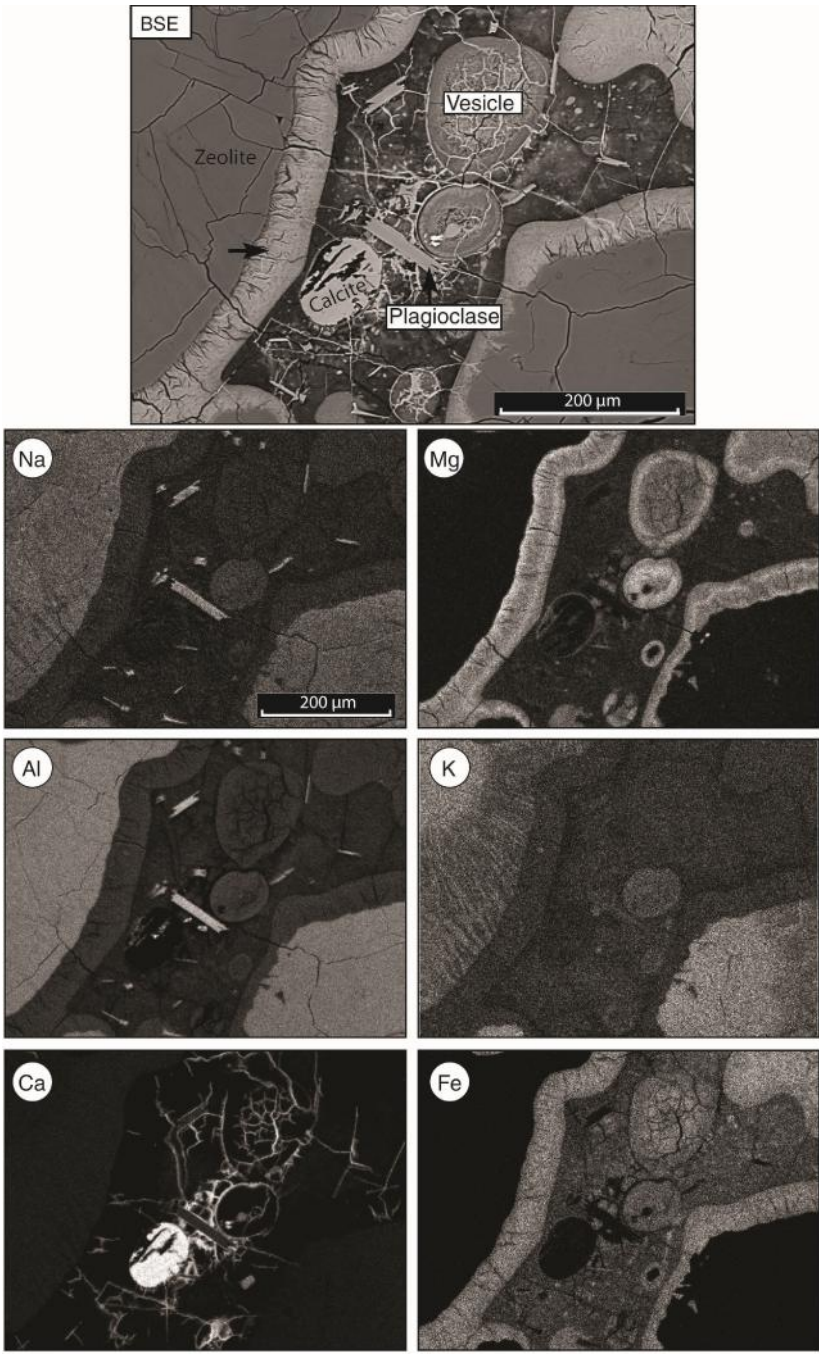

Figure 3.20. Backscattered electron image (BSE) and X-ray maps (Na, Mg, Al, K, Ca, and Fe) of abiotically altered basaltic tuff from Black Hills sample FR-12-107. Increasing tone from dark to light indicates an increase in elemental abundance. Highly altered pyroclast with fibrous-lath-like crystalline fibro-palagonite rim around vesicles infilled with zeolites. Fibro-palagonite rims have high concentrations of Mg and Fe. Amygdaloidal zeolites have high concentrations of Na, Al, and K. The highest Ca concentrations are in calcite cements. Plane and crossed polarized images of this alteration are shown in (Figure 3.4 G-H).

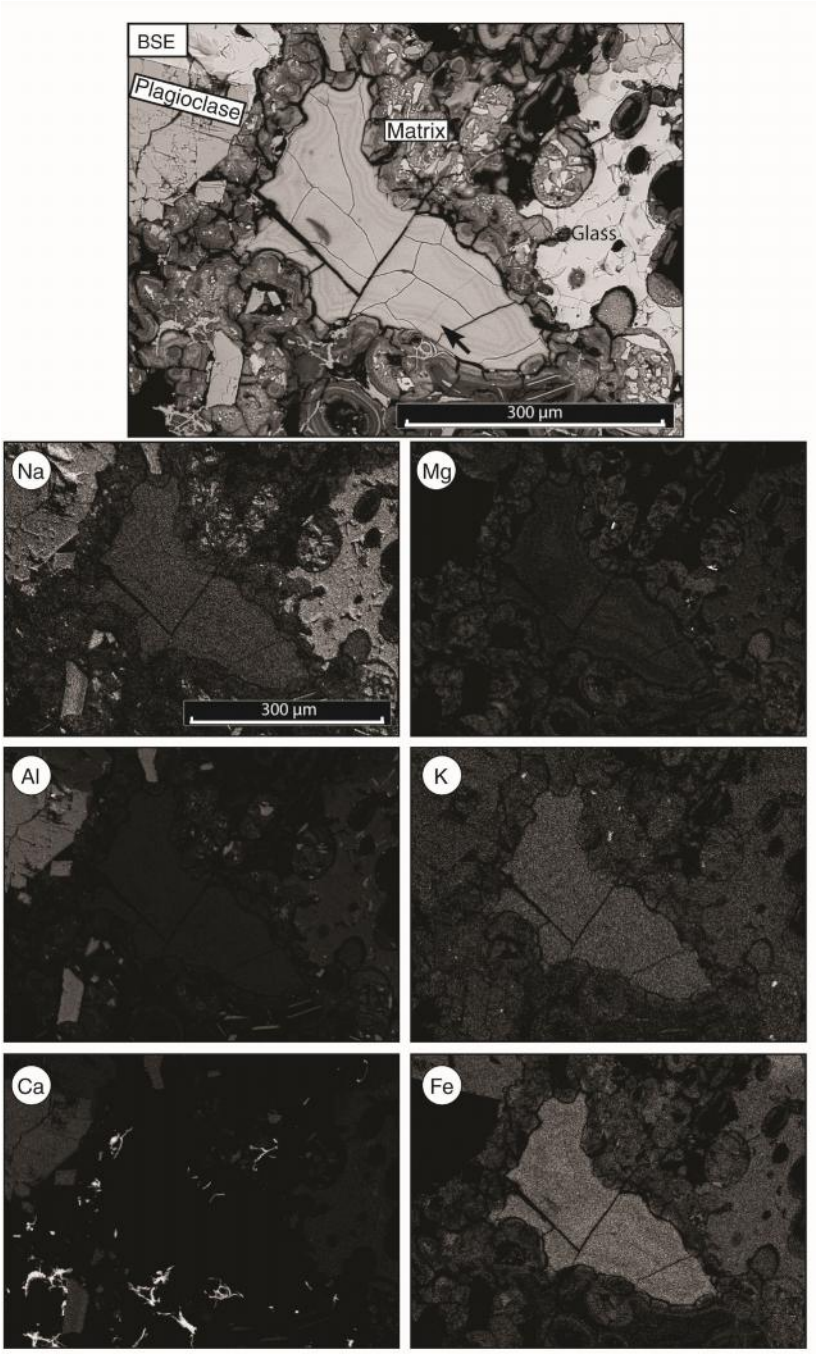

Figure 3.21. Backscattered electron image (BSE) and X-ray maps (Na, Mg, Al, K, Ca, and Fe) of abiotically altered basaltic tuff from Black Hills sample FR-12-116.1x. Increasing tone from dark to light indicates an increase in elemental abundance. Matrix (fine ash) that has been altered to a fibrous palagonitic material with high concentration of Fe and K. Plane and cross-polarized images of this alteration are shown in (Figure 3.5C-D).

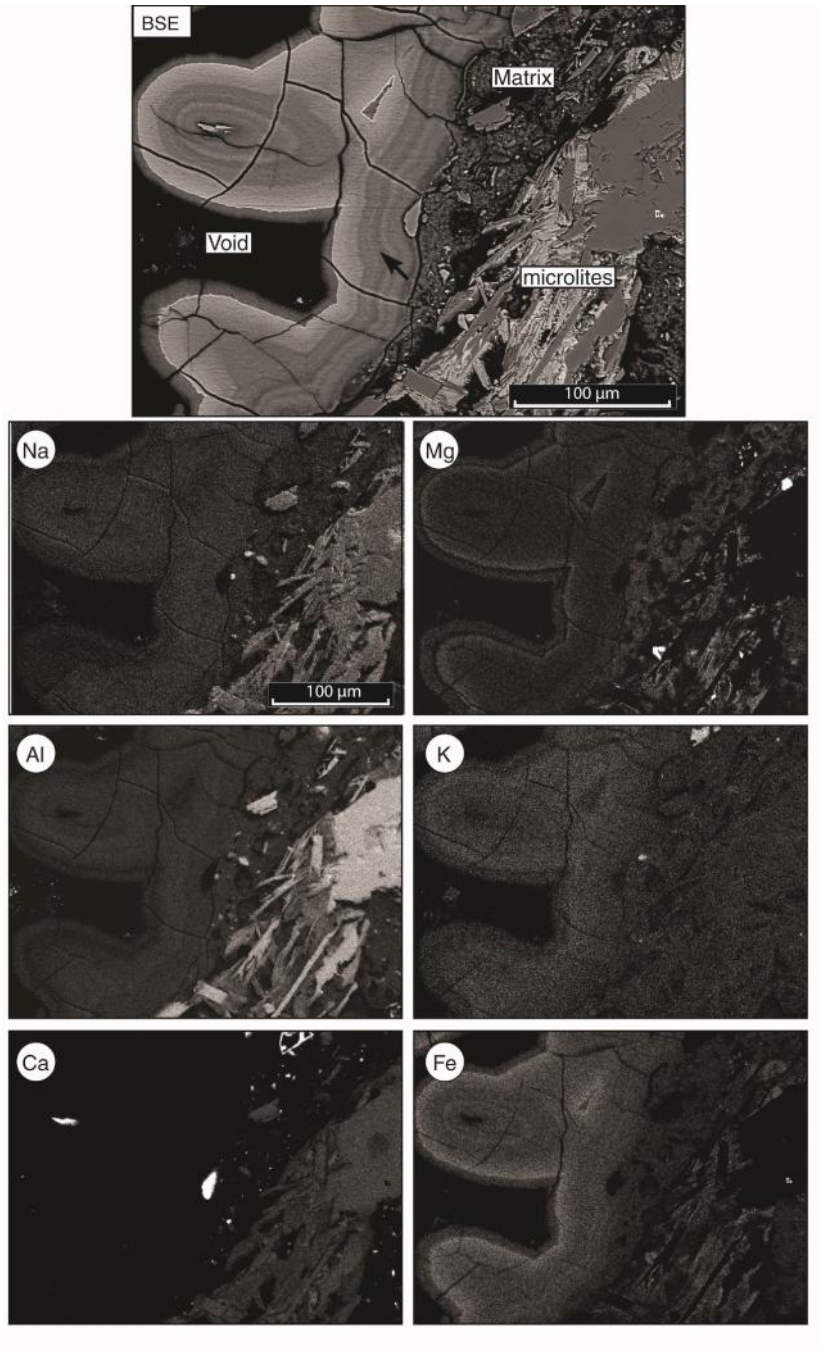

Figure 3.22. Backscattered electron image (BSE) and X-ray maps (Na, Mg, Al, K, Ca, and Fe) of abiotically altered basaltic tuff from Black Hills sample FR-13-145. Increasing tone from dark to light indicates an increase in elemental abundance. Variable concentrations of Na, Mg, Al, K as well as the highest concentrations of Fe in altered matrix. Plane and cross-polarized images of this alteration are shown in Figure 3.5G-H.

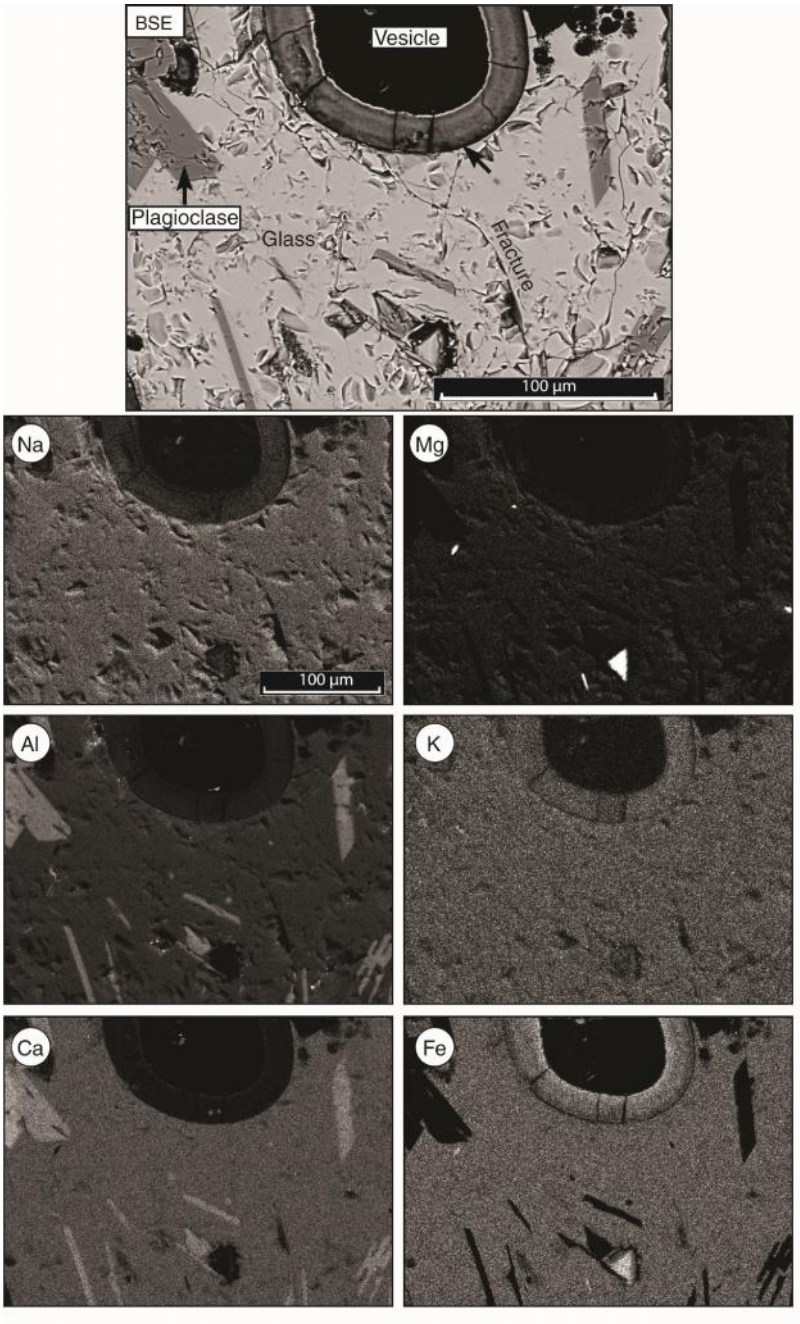

Figure 3.23. Backscattered electron images (BSE) and X-ray maps (Na, Mg, Al, K, Ca, and Fe) of abiotically altered basaltic tuff from Black Hills sample FR-13-145. Increasing tone from dark to light indicates an increase in elemental abundance. Fibro-palagonite alteration rim around pyroclast vesicle with high Fe concentrations. Rectangular laths are high-Ca-plagioclase. Triangular grain having high Mg and Fe is consistent with magnesioferrite spinel.

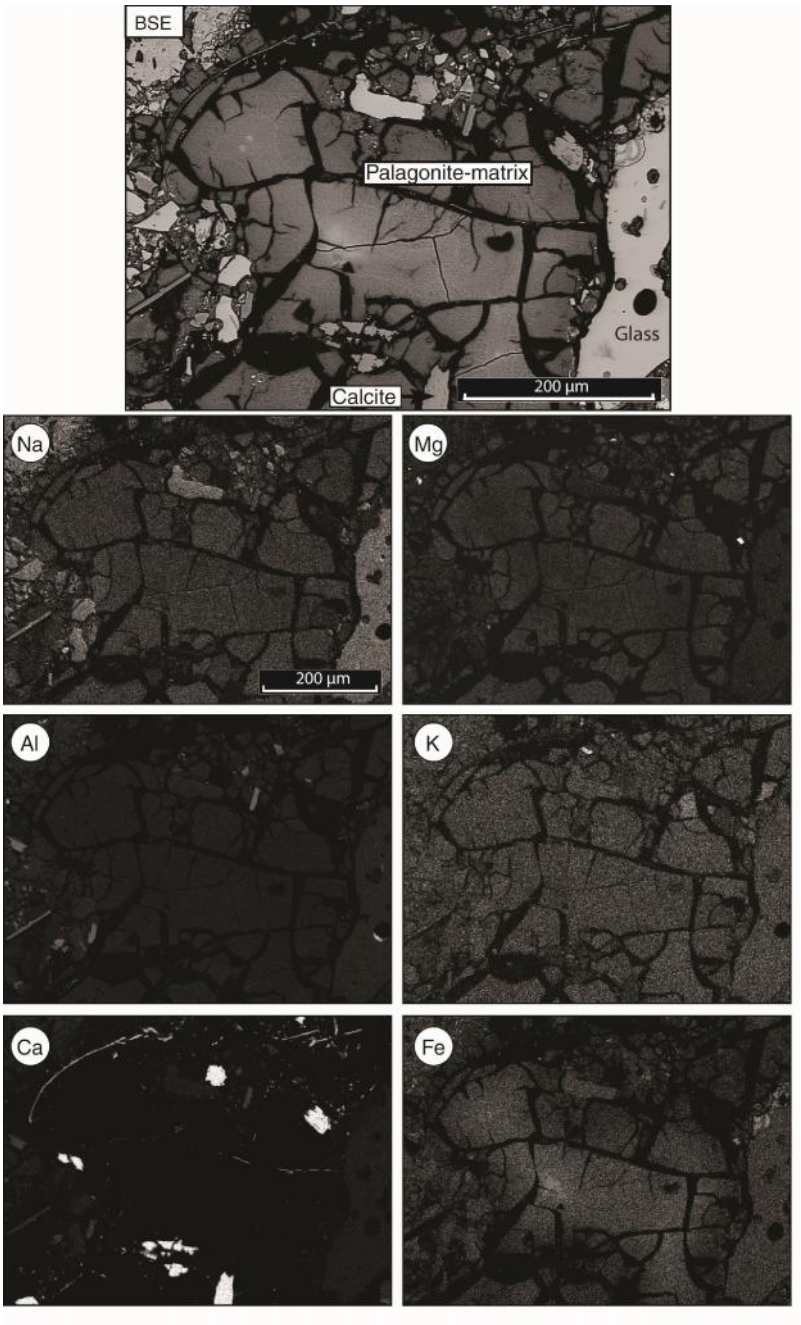

Figure 3.24. Backscattered electron image (BSE) and X-ray maps (Na, Mg, Al, K, Ca, and Fe) of abiotically altered basaltic tuff from Black Hills sample FR-13-177. Increasing tone from dark to light indicates an increase in elemental abundance. (E) Altered and consolidated matrix with grainy crystalline character and concentrations of Fe from sample FR-13-177. Plane and cross-polarized images of this alteration are shown in Figure 3.5A-B.

3.3.4. Isotope Geochemistry

The mean $\delta^{13}C$ values of NBS-18 (carbonatite, −5.05 ± 0.05) and WS-1 (internal laboratory standard calcite, +0.73 ± 0.03) were in good agreement with their accepted values (−5.0 and +0.76, respectively). The mean $\delta^{18}O$ values of Suprapur (internal laboratory standard synthetic calcite, +13.08 ± 0.22) and WS-1 (internal laboratory standard calcite, +26.25 ± 0.02) were in good agreement with their accepted values (+13.30 and +26.23, respectively). $\delta^{13}C$ and $\delta^{18}O$ (VPDB) compositions of calcite cements from three basaltic tuff samples (Black Hills: 1, Reed Rock: 2) reveal Black Hills carbonates to be slightly depleted and enriched, respectively, compared to the Reed Rock carbonates (Table 3.3). Both of the $\delta^{18}O$ values of Reed Rock carbonates are negative whereas the Black Hills carbonate is positive with respect to VPDB.

Table 3.3. Isotopic compositions for Black Hills and Reed Rocks authigenic carbonate cements.

Sample	$\delta^{13}C$ (VPDB)	$\delta^{18}O$ (VSMOW)	$\delta^{18}O$ (VPDB)
FR-13-159 (Black Hills)	4.86	32.02	1.08
FR-12-97E (Reed Rock)	6.52	27.76	-3.06
FR-12-92 (South Reed Rock)	7.71	25.71	-5.04

Samples: BH - Black Hills, Reed Rock - Reed Rocks

$\delta^{18}O$ (VPDB): Oxygen 18 isotopic composition with respect to Vienna PeeDee Belemnite. These values are used in calculation of paleotemperatures using the equation by Leng and Marshall (2004).

$\delta^{18}O$ (VSMOW): Oxygen 18 isotopic composition with respect to Vienna Standard Mean Ocean Water.

3.3.3.1. Paleothermometry

Paleotemperatures were calculated using the carbonate paleotemperature scale equation (Eq. 1) proposed by Leng and Marshall (2004). No modern Fort Rock lake water exists so the isotopic composition of the carbonate-depositing waters were estimated based on values of modern meteoric and similar lake environment water.

Calculations of paleotemperatures based on $\delta^{18}O$ values obtained from Black Hills and Reed Rock authigenic carbonates produced a wide range in temperatures (Table 3.4). When negative potential depositing water isotopic compositions <1 ‰ like modern meteoric water compositions was used, unrealistic temperatures (<0°C) were calculated, ranging from -50.7 to -5.0ºC. However, calculations that used potential depositing water compositions of lakes with similar closed alkaline and saline basin environments resulted in more realistic positive temperature values, ranging from 6.8 to 86.6ºC. Each potential depositing water isotopic composition used resulted in Black Hills calculated temperatures that were lower than those of Reed Rock. The overall range in Black Hills temperature calculations is lower than the Reed Rock ranges, but the ranges from both locations overlap. Black Hills calculations using lake water compositions resulted in a temperature range of 6.8 to 48.9 ºC whereas Reed Rock calculations resulted in a temperature range of 26.1 to 86.6 ºC.

Table 3.4. Estimated isotopic compositions of depositing water and calculated paleotemperatures for Black Hills and Reed Rocks authigenic carbonates.

Estimated $\delta^{18}O$ Value of Depositing Waters		FR-13-159 (Black Hills)	FR-12-97E (Reed Rock)	FR-12-92 (S. Reed Rock)
$\delta^{18}O$ (VSMOW)	Reference	Paleotemperature (^oC)	Paleotemperature (^oC)	Paleotemperature (^oC)
-24	USGS (2011)	-50.7	-47.0	-44.3
-17.9	Friedmann et al. (2002)	-44.3	-36.5	-31.9
-16.4	USGS (2011)	-41.8	-33.1	-27.9
-13.76	IAEO/WMO (2015)	-36.5	-26.0	-20.1
-12.1	Friedmann et al. (2002)	-32.7	-21.1	-14.5
-12	USGS (2011)	-32.4	-20.8	-14.2
-9.43	IAEO/WMO (2015)	-25.5	-12.1	-4.8
-7.52	IAEO/WMO (2015)	-19.7	-5.0	2.9
-0.49	Kharaka et al. (1984)	6.8	26.1	36.3
0.01	Kharaka et al. (1984)	9.0	28.6	39.0
2.64	Henderson et al. (2003)	21.1	42.5	53.7
2.85	Henderson et al. (2003)	22.2	43.7	54.9
3.98	Godebo (2009)	27.8	50.0	61.6
4.88	Godebo (2009)	32.4	55.2	67.1
6.99	Godebo (2009)	43.7	67.9	80.5
7.03	Godebo (2009)	43.9	68.2	80.7
7.92	Godebo (2009)	48.9	73.7	86.6

Samples: Black Hills, Reed Rock, South Reed Rock

The paleotemperature equation used is from Leng and Marshall (2004):

(Eq. 1) $$T^oC = 13.8 - 4.58(\delta c - \delta w) + 0.08(\delta c - \delta w)^2$$

where here the δc used is the $\delta^{18}O$ of CO_2 obtained from the carbonate by reaction with 103% ortho-phosphoric acid for 25 minutes at 90°C and δw is the estimated $\delta^{18}O$ of the water from which the carbonate was deposited. The above equation uses the SMOW and PDB protocol but for practical purposes they are equivalent to the 'VSMOW' and 'VPDB' values that have been implemented by several laboratories to denote that the data has been standardized in line with international protocols (Coplen, 1994). Isotopic values for calcite used in paleotemperature calculations for each sample are $\delta^{18}O$ (VPDB) values found in Table 3. Estimated isotopic values used for depositing water are data obtained from water sources that include mainly hydrologically closed alkaline and saline lakes and modern meteoric water (precipitation).

3.4. DISCUSSION

Geologic and textural evidence suggest that microbes were involved in the alteration of Black Hills hydrovolcanic tuffs. The diverse morphology and distributions of textures described by this study are similar to tubular and granular structures that have been recognized as the remnants of endolithic microbial alteration in glassy pillow rims and tuffs in modern oceanic crust and subglacial lavas (Thorseth et al., 1992, 1995, 2001, 2003; Fisk et al., 1998, 2013; Torsvik et al., 1998; Furnes and Staudigel, 1999; Furnes et al., 2001, 2007a, b; McLoughlin et al., 2007, 2008, 2010; Cousins et al., 2009; Cockell et al., 2009). These textures, which we consider to be endolithic microborings, are also distinct from the range of observed abiotic aqueous alteration styles and we believe that possible abiotic processes that may account for these features have been plausibly excluded. These findings are important because (1) FRVF is the first terrestrial lacustrine setting where putative endolithic microborings have been described; (2) unlike many oceanic crust basalts, these rocks are geological and environmentally relatively well constrained and (3) they help improve our understanding of important environmental factors that may influence the formation of microbial alteration textures.

In the following sections, the Black Hills textures and inferred conditions of alteration are examined in the context of a comparison with another site in the FRVF known as Reed Rocks (Chapter 2). The microboring morphotype assemblage within Black Hills tuffs differs from Reed Rocks tuffs (e.g., lack tubular microborings with terminal enlargements/spiral filaments, greater proportion of granular-bubble sub-type). Mineralogical, textural, and isotopic data from the two sites support the hypothesis that observed differences are linked to contrasting water/rock ratios and related environmental

factors (e.g., abiotic aqueous alteration intensity, fluid composition and flux, and temperature) that in turn affected the type of constructing organisms or the processes by which they obtain nutrients and energy from glass.

3.4.1. Water/Rock Ratio

Observations in Black Hills indicate that eruption was likely through shallow surface water and point toward a relatively higher water-rock ratio than at Reed Rock. Closer proximity of Black Hills to the inferred paleo-lake margin (Fig. 3.1), and the presence of diatomite, altered olivine, highly crystalline palagonite, calcite replaced pyroclasts and plastic deformation in the form of load structures suggest high water-rock ratios with at least 15-20% external water in the primary volcanic deposit (Heiken, 1971). Accidental diatomite clasts and disaggregated diatomite mixed with glass shards in tuff breccias indicate the eruption directly through lake sediment and entrainment of lake sediment blocks during deposition in turbulent debris flows that may have moved across the lake bed (Heiken, 1971). Iddingsitized olivine crystals indicates formation in a oxidizing and fluid-rich environment (Kuebler et al., 2003). Although the exact mineralogy and composition of this alteration product has not been defined, it likely consists of iron hydroxide (red colour), and phyllosilicate (smectites) intergrowths that have been documented to form where drainage is poor and water/rock ratios are high (Delvigne et al., 1979). In contrast, Reed Rock deposits located farther from the paleo lake margin, contained no highly crystalline glass alteration products, load structures, diatomite, altered olivine or calcite-replaced pyroclasts.

3.4.1.1. Abiotic Aqueous Alteration (Palagonite)

3.4.1.1.1. Palagonite alteration stage. Compared to Reed Rocks, the glass shards in the Black Hills tuffs appear to have proceeded to a more advanced stage of alteration. Gel- and fibro-palagonite are not entirely separate palagonite species, but correspond to different periods in the evolution of glass from the amorphous gel- type to the more crystalline fibro- type (Stroncik and Schmincke, 2002). Fibro-palagonite is thought to be a combination of amorphous gel-palagonite and crystallizing smectite clay minerals that develop on the exterior surfaces of aging gel-palagonite (Peacock, 1926; Zhou and Fyfe, 1989). Therefore palagonitization reaction progress may be inferred on the basis of crystallinity (i.e., gel- to fibro-palagonite; Stroncik and Schmincke, 2001, 2002). Mg accumulation may also be taken as a measure of how advanced the alteration process is, where those that have experienced high enrichments in Mg appear to indicate greater crystallization and more advanced palagonitization (Stroncik and Schmincke, 2001).

In the crystalline glass alteration products (palagonite) in Black Hills and Reed Rocks Mg is enriched (Figs. 3.20, 3.25), but crystalline palagonite in Black Hills (Figs. 3.4, 3.5) is more abundant (Table 3.2). A greater abundance of other secondary crystalline phases such as zeolites and calcite that accompany palagonitic alteration are also indications of more advanced alteration (Stroncik and Schmincke, 2002). Black Hills has a higher maximum proportion of crystalline pore-filling zeolite than Reed Rock (3.5% vs. 0.7 %) as well as a greater maximum proportion of ancillary carbonates (32% vs. 15.5%). Furthermore, the presence of clasts that are partially palagonitized and replaced by calcite suggests that calcite replacement occurred subsequent to palagonitization and that calcite replaces palagonite (Fig. 3.6). This has been observed in

other basaltic palagonite tuffs and metabasaltic volcanic ash beds (e.g., Nayudu, 1963; Lepot et al., 2011) and may also indicate that Black Hills is at a more advanced stage of alteration. Therefore Black Hills tuffs containing fibro-palagonite may be more 'aged' than those of Reed Rock that lack it, whereby the term 'aging' is synonymous with the palagonitization processes of crystal growth and overall crystallization (Stroncik and Schmincke, 2001). The more crystallized material may have proceeded to a more advanced stage of alteration as a result of differing alteration conditions.

3.4.1.1.2. Fluid Composition. The assemblage of microbial textures may reflect either differing methods of construction by differing organisms or differing micro-chemical environments and/or pH changes. The accepted mechanism of palagonitization is a dissolution/micro-solution-precipitation process (Crovisier et al., 1987; Daux et al., 1984; Thorseth et al., 1995; Stroncik and Schmincke, 2002) with hydration and elemental exchange controlled by diffusion (Moore, 1966). For dissolution and hydration to occur, water must be present, the relative abundance of which would have significant influence. The water/rock ratio is significant to alteration product formation and composition because water-rock systems have intricate feedback mechanisms between the alteration fluid and the primary constituents of the parental materials (Berner 1983; Crovisier et al., 1992; Gislason et al., 1993; Steefel and Lasaga 1994; Stumm and Morgan 1996).

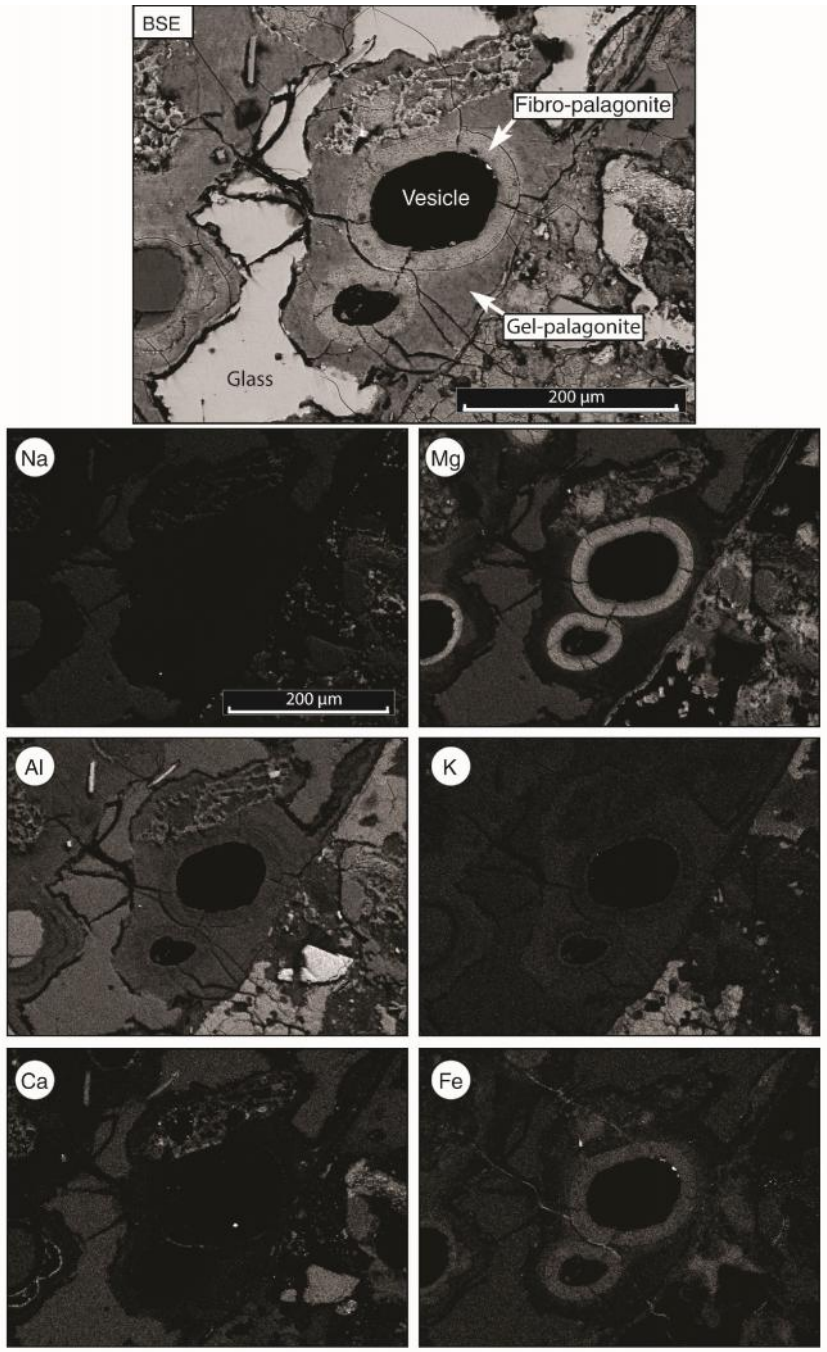

Figure 3.25. Backscattered electron image (BSE) and X-ray maps (Na, Mg, Al, K, Ca, and Fe) of abiotically altered basaltic tuff from Reed Rocks sample FR-12-90-1. Increasing tone from dark to light indicates an increase in elemental abundance. A partially altered pyroclast displaying a transition from unaltered glass to amorphous gel-palagonite to slight grainy proto-crystalline fibro-palagonite. The most crystalline portion rimming the vesicle at center has the highest concentration of Mg whereas the surrounding gel-palagonite is depleted. This is the most advanced alteration in Reed Rocks, though compared to Black Hills alteration is less crystalline.

In Black Hills samples, single chemical characteristics of glass alteration (fibro-palagonite) including the distinct zonation/banding (Figs. 3.4, 3.5) and the contrast in elemental enrichments/depletions (Figs. 3.20-3.24) are possible evidence of the control that evolving fluid composition has on their formation (Hay and Iijima, 1968; Furnes 1975; Fisher and Schmincke, 1984; Jercinovic et al., 1989; Thorseth et al., 1991). Palagonitization and palagonite chemical composition is partially controlled by altering fluid composition. Its evolution reflects how the material being altered is in continuous re-equilibration with the evolving fluids (Crovisier et al., 1987, 1992). Surficial reactions control the dissolution process and the dissolved species that reach their solubility limits are re-precipitated in thermodynamic equilibrium with the dissolving fluids (Crovisier et al., 1987, 1992). Hence differences in water/rock ratios have large influences on the activities of chemical components such as SiO_2, MgO, Al_2O_3, TiO_2, K_2O, Na_2O and CaO that are either trapped as secondary products or lost to solution (Crovisier et al., 1987, 1992).

During rock weathering processes, the consumption of protons can produce micro-environmental increases in pH (Bland and Rolls, 2005). Palagonite formation has been found to be associated with pH changes in hyaloclastites (Thorseth et al., 1991). The metabolic activity of the active bacteria/microbes may also affect weathering rates and pH fluctuations (Thorseth et al., 1992; 1995; Staudigel et al., 1995) potentially creating a feedback loop that controls which microbes are or are not metabolically active (Cockell et al., 2009). The microbes actively altering basalts may therefore depend on temporal and micron-scale spatial variations of certain secondary phases such as varieties of palagonite that form from the alteration of basaltic glass (Cockell et al., 2009). Darker toned, more-

intensely coloured palagonite (Figs. 3.4, 3.5) is more common in Black Hills tuffs and suggests high pH (>9; Thorseth et al., 1991). In both Reed Rock and Black Hills though, distinctive physical contacts between glass and palagonite are frequent and indicate formation by congruent dissolution, which is usually favoured at high fluid-pH (Bunker et al., 1983; Sholze, 1988; Stoncik and Schmincke, 2001, 2002). In basic pH conditions, congruent dissolution occurs resulting in the production of large pits on glass surfaces (Thorseth et al, 1992, 1995; Staudigel et al., 1995) such as those that comprise granular-bubble textures. These characteristics, indicating relatively high fluid pH, are consistent with the presence of zeolites and carbonate in both deposits, but bioalteration-related textural differences and relative abundances of secondary phases may reflect temporal and spatial variations in fluid pH as well as chemical composition.

3.4.2. Temperature

3.4.2.1. Aqueous (Abiotic) Alteration

The palagonitization process and reaction rate depend on temperature (Jakobsson and Moore, 1986; Crovisier et al., 1987). As temperatures increase, the rate of glass dissolution is enhanced as well as the rate of secondary phase precipitation. The overall means by which alteration proceeds may also change (Crovisier et al., 1987). The temperature dependence of textures could indicate that samples containing fibro-palagonite (Black Hills) may have been altered under higher temperatures than those lacking it. We note however that evidence indicating a greater water-rock ratio is consistent with lower temperatures of alteration at Black Hills than at Reed Rocks.

The observed alteration phase assemblage is consistent with low temperature (<100°C) conditions. In Reed Rock tuffs, the major secondary phases identified were calcite, chabazite-phillipsite, and nontronite-saponite. The overlapping formation temperature ranges of these phases indicate alteration temperatures between ~25 - 80°C. No evidence of higher temperature phases (> 100°C) such as chlorite (175-240°C) was observed. In Black Hills tuffs, indications of calcite, possible phillipsite and nontronite were also observed. Comparing amygdaloidal/vug zeolite in Black Hills optically to those in Reed Rock, they display the same characteristics as those identified as chabazite as well. These phases are also consistent with low temperature alteration conditions at the Black Hills. Inferred temperature ranges based on secondary mineralogy are further supported by calculated carbonate precipitation temperatures that are presented in the following section.

3.4.2.2. $\delta^{18}O$ Paleothermometry

We here quantify paleotemperatures of carbonate formation using $\delta^{18}O$. It is not possible to infer temperature variations using measured isotopic compositions of carbonates without making assumptions. Previous methods of quantifying terrestrial paleotemperatures have been restricted because the constraints on the isotopic composition of meteoric/terrestrial waters are more lacking than that of oceanic waters (Dworkin et al., 2005). This study involves an ancient lake environment and assumptions must consider lake hydrology and possible hydrologic changes that may have occurred.

The Black Hills and Reed Rock carbonates are believed to have precipitated from fluids of the Fort Rock Lake. Therefore the isotopic composition of the depositing fluids

is assumed to be approximately that of the lake water. Micro-chemical changes associated with basalt alteration, including bioalteration are not considered by paleotemperature calculations. Paleoclimate investigations involving ancient lacustrine environments should include detailed analyses of contemporary lake water and related precipitates that demonstrate a systematic relationship between their isotopic composition and temperature (Leng and Marshall, 2004). Since no modern Fort Rock lake water and associated precipitates exist, the Black Hills and Reed Rocks carbonates are assumed to have precipitated in isotopic equilibrium with ancient lake waters. We therefore assume that the isotopic composition of the carbonates only depends on the temperature of precipitation and $^{18}O/^{16}O$ of the depositing water.

In many lake environments the modern or ancient isotopic composition of lake water cannot be assumed to reflect the meteoric composition because factors such as water residence time, and catchment and lake processes such as evaporation modify water compositions (Leng and Marshall, 2004).). Fort Rock Lake is one of many hydrologically closed lake basins within the Great Basin, an area that has no exterior surface drainage (Friedman et al., 2002). In hydrologically closed lakes, especially those in arid regions such as ancient Fort Rock Lake, evaporation is the primary means of water loss (Hardie and Eugster, 1970: Leng and Marshall, 2004; Dworkin et al., 2005; Martin et al., 2005). This means $\delta^{18}O$ values are always higher than precipitation and lie along a local evaporation line (LEL), determined by local climate (Clark and Fritz, 1997), rather than along the local meteoric water line (LMWL) (Leng and Marshall, 2004). Therefore we also assume that the isotopic composition of Fort Rock Lake waters does not reflect the isotopic composition of meteoric water. Given that no exact age dates have been

obtained for either the Black Hills or Reed Rock deposits and the exact age difference is unknown, we also assume that the isotopic composition of the depositing waters at Black Hills and Reed Rock were approximately the same.

Paleotemperature calculations for Black Hills and Reed Rocks using modern day $\delta^{18}O$ compositions of meteoric water from -7.52‰ to -24‰ did not produce realistic temperatures (-5.0 to -50.7°C). Paleotemperature calculations using $\delta^{18}O$ compositions of similar modern day closed lakes ranging from -0.49 ‰ to +7.92 ‰ yielded positive temperatures (26.1 - 86.6 ºC) consistent with the inferred temperature range based on alteration mineralogy (25 - 80°C). In many large closed lake basins, both $\delta^{18}O$ and $\delta^{13}C$ are also commonly positive and show covariance that may be a useful indicator for how hydrologically closed the basin is (Talbot, 1999; Leng and Marshall, 2004). The $\delta^{18}O$ (VSMOW) and $\delta^{13}C$ (VPDB) of carbonates in Black Hills and Reed Rock are positive and co-vary (Fig. 3.26), consistent with a closed basin environment, although it is a negative correlation. Since the isotopic composition of hydrologically closed lake basins is determined by local climate, it is possible that the isotopic composition of Fort Rock Lake was very similar to the modern day examples. Even if the isotopic composition of precipitation was changing due to Pleistocene glacial fluctuations, the local climate may have had a greater influence of the composition of lake waters in Fort Rock. Therefore, the calculated paleotemperatures using positive $\delta^{18}O$ values obtained from modern confined basin lake waters are likely more representative of Fort Rock carbonate precipitation temperatures.

It appears that the Black Hills tuffs likely experienced lower temperatures of alteration than the Reed Rocks tuffs (Table 3.4). This is consistent with the calculated

paleotemperatures, indications of greater external water contents (higher water/rock ratio) at Black Hills as well as the presence of large hoodoo chimney-like structures observed in the SRR tuff. Such structures can form as a result of fumarolic gas escape (Fisher and Schmincke, 1984).

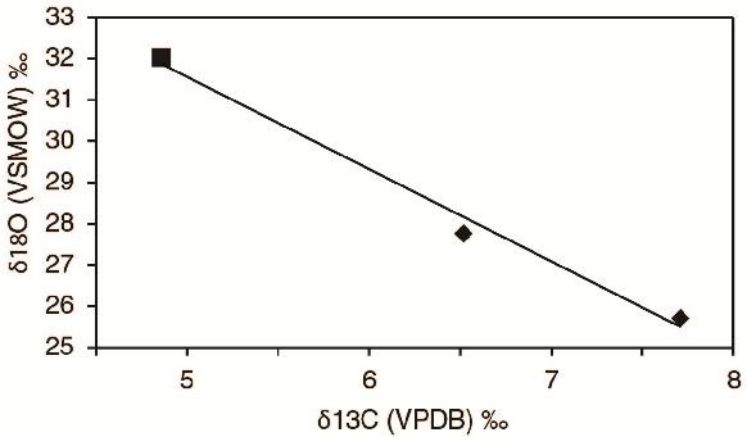

Figure 3.26. Positive stable isotope compositions of Black Hills and Reed Rocks authigenic carbonates displaying covariance. This may be taken as an indication of the degree of hydrologic closure of the Fort Rock lake basin.

3.4.3. Bioalteration Morphotypes and Timing

In contrast to studies of oceanic basalts, the Black Hills and Reed Rock bio-alteration textures are predominantly tubular (Furnes and Staudigel, 1999; Furnes et al, 2001; Staudigel et al., 2006) with an estimated tubular/granular alteration ratio of ~5:1. A higher proportion of tubular alteration is consistent with relatively low temperature alteration conditions (Torsvik et al., 1998; Furnes et al., 2001; 2007; Stroncik and Schmincke, 2002).

In several of the Black Hills samples, micro-tunnels appear to originate at the primary margins of glass shards, not the interface between palagonite and glass and some show yellow-palagonite/smectite appearing interiors. Most are simple tubular types and this suggests that they began to form earlier than most pore lining palagonite rims. There are however, examples of simple tunnels propagating beyond palagonite-glass interfaces, suggesting that simple tunnels formed throughout the alteration sequence. Instances of simple and branching tunnels extending beyond granular alteration fronts also suggests they formed after granular alteration and that all bioalteration post-dates burial and fracturing.

Microbial bioalteration may be constrained by the temperature of calcite formation and petrographic relationships with calcite. Calculated paleotemperatures for carbonates in sample FR-13-159 range from 6.9 to 48.9 ºC. Although no tunnels were found radiating from sealed pores in this sample, several examples of this are observed in Black Hills. This demonstrates that microborings were constructed when fluid was freely circulating and construction would have occurred above the temperature of calcite precipitation. A factor important in maintaining microboring formation is fluid circulation. Microbial activity can only continue as long as fluid is still flowing, but upon sealing of pores by precipitation of secondary phases, fluid flow would be impeded and microbial alteration would cease (McLoughlin et al., 2010). Black Hills covers a larger area than Reed Rocks. It is possible that the thermal conditions may have been more variable than at Reed Rocks. An indication of localized higher temperatures for example (cm-scale gas pipes where only granular-bubble and no tubular textures are observed) were observed in Black Hills. Despite this variance, higher water rock ratios and overall

lower paleotemperatures are indicated at Black Hills. Taking into account the close match between temperatures estimated in Reed Rocks based on secondary phases and those calculated using the oxygen isotopes with the carbonate paleotemperature scale, we are confident in the estimated carbonate precipitation temperatures. Microbial bioalteration overall appears to have occurred in neutral to alkaline waters at temperature between 6.9 and >49 ºC.

We consider the evidence presented here as a strong indicator of microbial activity. We recognize that isotopic and strong elemental evidence in the regions around and within putative microborings, which are required to support the textural evidence, are lacking here (McLoughlin et al., 2007). Therefore the biogenic origins of these reported textures can only be tentatively inferred.

3.5. CONCLUSIONS

Studies of bioalteration textures in basaltic glass have been mostly focussed on lava erupted in a marine setting. Basaltic glass from Pliocene-Pleistocene continental-lacustrine hydrovolcanic tuffs display alteration textures that provide evidence of microbial activity. The results of this study suggest the following:

1. The Black Hills-FRVF basaltic tuffs contain several examples of bioalteration textures, predominantly as micro-tunnels forming the tubular type, with characteristic sizes, morphologies and distributions of endolithic microboring biogenicity (c.f. McLoughlin et. el., 2007). The similarities of Black Hills textures with examples recognized in Reed Rocks-FRVF basaltic tuffs denotes that this is the second account of endolithic microborings in a continental lacustrine (non-subglacial) setting. Therefore endolithic microborings are not an isolated occurrence at Reed Rocks. This supports the addition of this type of environment to the range known to contain endolithic microborings and suggests that microbial bioalteration is likely a more significant part of the regional geologic history of the Fort Rock Volcanic Field and possibly of other continental volcanic rocks.

2. Black Hills and Reed Rock tuffs both exhibit the same most common tubular bioalteration morphological type (simple straight to curved, branching) but display differences in other types (granular-bubble, tubular types with terminal enlargements/spiral-helical filaments). This indicates that certain constructing organisms may be more tolerant of a wider range in environmental conditions than others.

3. The water-rock ratios in Black Hills-Reed Rock tuffs were less than in ocean crust basalts but the water-rock ratio in Black Hills tuffs was greater than in the Reed Rocks tuffs. Black Hills tuffs have progressed to a more advanced stage of abiotic aqueous alteration. If more intense glass alteration occurred in Black Hills, than the micro-chemical changes that occurred in the altering fluid were likely greater or more variable. In addition to eruptive setting, water-rock ratio, which may be related to fluid composition and temperature, may also have contributed to the observed differences in bioalteration morphotype assemblage (lack of tubular microborings with terminal enlargements/spiral-helical filaments, more abundant granular-bubble types).

4. Black Hills microborings are inferred to have formed primarily in neutral to alkaline fluids at temperatures between ~6 - >49 °C. Hydrothermal/aqueous alteration occurred in the low-temperature thermal regime (≤ 80°C). Reed Rock microborings are inferred to have formed in neutral to alkaline, saline fluids predominantly between 26 - 87 °C. The conditions of abiotic and microbial alteration in Reed Rock tuffs were therefore likely at slightly higher temperatures than Black Hills tuffs.

5. This study demonstrates the importance of fully characterizing bioalteration textures in volcanic rocks erupted in settings other than marine and subglacial basalts to define the full range of environments and conditions under which such textures are able to form. This is particularly important for tracing subsurface microbial activity, accurately reconstructing Earth history and regional geologic histories and if such morphologically distinct features are to serve as potential biosignatures on other planetary bodies such as Mars. For example, if the water rock/ratio influences the type of microbes responsible for bioalteration and certain morphological types are more common or better

preserved than others, the probability of detecting such features may depend on how wet the basalt alteration conditions were.

3.6. REFERENCES CITED

Allison, I.S., 1966, Fossil Lake, Oregon--Its geology and fauna: Oregon State Monographs, Studies in Geology, no. 9, p. 48.

Allison, I.S., 1979, Pluvial Fort Rock Lake, Lake County, Oregon: State of Oregon, Department of Geology and Mineral Industries.

Banerjee, N.R., and Muehlenbachs, K., 2003, Tuff life: Bioalteration of volcaniclastic rocks from the Ontong Java Plateau. Geochemistry Geophysics Geosystems, v. 4, no. 4, p. 1037.

Bergfeld, D., Lowenstern, J.B., Hunt, A.G., Pat Shanks III, W.C., and Evans, W.C., 2011, Gas and isotope geochemistry of thermal features in Yellowstone National Park, Wyoming: U.S. Geological Survey Scientific Investigations Report 2011-5012.

Berner, R.A., 1983, Kinetics of weathering and diagenesis. In: Lasage AC, Kirkpatrick, R.J. (eds) Kinetics of geochemical processes. Mineral Society of America, Washington, DC, p. 111–134.

Bland, W., and Rolls, D., 2005, Weathering: An Introduction to the Scientific Principles. Arnold, London.

Brand, B.D., and Clarke, A.B., 2009, The architecture, eruptive history, and evolution of the Table Rock Complex, Oregon: From a Surtseyan to an energetic maar eruption: Journal of Volcanology and Geothermal Research, v. 180, p. 203-224.

Bunker, B.C., Arnold, G.W., Beauchamp, E.K., and Day, D.E., 1983, Mechanism for alkali leaching in mixed Na–K silicate glasses: Journal of Non-Crystalline Solids, v. 58, p. 295–322.

Chesterman, C.W., 1956, Pumice, pumicite and volcanic cinders in California: Calif. Div. Mines Bull., v. 174, p. 3-97.

Clark, I., and Fritz, I., 1997, Environmental Isotopes in Hydrogeology. Boca Raton, Lewis.

Cockell, C.S., Olsson-Francis, K., Herrera, A., and Meunier, A., 2009, Alteration textures in terrestrial volcanic glass and the associated bacterial community: Geobiology, v. 7, p. 50-65.

Cockell, C.S., Olsson, K., Knowles, F., Kelly, L., Herrera, A., Thorsteinsson, T., and Marteinsson, V., 2012, Bacteria in weathered basaltic glass, Iceland: Geomicrobiology Journal, v. 26, no. 7, p. 491-507.

Colbath, K., and Steele, M.J., 1982, The geology of economically significant lower Pliocene diatomites in the Fort Rock basin near Christmas Valley, Lake County, Oregon: Oregon Geology, v. 44, no. 10, p. 111-118.

Cousins, C.R., Smellie, J.L., Jones, A.P., and Crawford, I.A., 2009, A comparative study of endolithic microborings in basaltic lavas from a transitional subglacial-marine environment: International Journal of Astrobiology, v. 8, no. 1, p. 37-49

Crovisier, J.L., Honnorez, J., Eberhart, J.P., 1987, Dissolution of basaltic glass in sea water: mechanism and rate: Geochimica et Cosmochimica Acta, v. 51, p. 2977–2990.

Crovisier, J.L., Honnorez, J., Fritz, B., Petit, J.C., 1992, Dissolution of subglacial volcanic glasses from Iceland – laboratory study and modelling: Applied Geochemistry, v. 7, p. 55–81.

Daux, V., Crovisier, J.L., Hemond, C., Petit, J.C., 1994, Geochemical evolution of basaltic rocks subjected to weathering: fate of the major elements, rare earth elements, and thorium. Geochimica et Cosmochimica Acta, v. 58, p. 4941–4954.

Delvigne, J., Bisdom, E. B. A., Sleeman, J., and Stoops, G., 1979, Olivines, their pseudomorphs and secondary products: Pedologie, v. 29, no. 3, p. 247–309.

Druitt, T.H., 1995, Settling behaviour of concentrated dispersions and some volcanological applications: *Journal of Volcanology and Geothermal Research*, v. 65, p. 27-39.

Dworkin, S.I., Nordt, L., and Atchley, S., 2005, Determining terrestrial paleotemperatures using the oxygen isotopic composition of pedogenic carbonate: Earth and Planetary Science Letters, v. 237, p. 56-68.

Fisher, R.V., and Schmincke, H.-U. (1984) Accretionary Lapilli. In: *Pyroclastic Rocks*. Springer-Verlag, Berlin Heidelberg New York Tokyo, pp. 238-239

Fisk, M.R., Giovannoni, S.J., and Thorseth, I.H., 1998a, Alteration of oceanic volcanic glass: Textural evidence of microbial activity: Science, v. 281, p. 978-980.

Fisk, M.R., Thorseth, I.H., Giovannoni, S.J., Urbach, E., and Streck, M.J., 1998b, Endolithic Microbes from the Rattlesnake Tuff, Oregon Blue Mountain Region: American Geophysical Union, Fall Meeting, San Francisco, CA, Abstracts, FM98-U32A-12.

Fisk, M., and McLoughlin, N., 2013, Atlas of alteration textures in volcanic glass from the ocean basins: Geosphere, v. 9, no. 2, p. 317-341.

Flemming, R.L., 2007, Micro X-ray diffraction (μXRD): a versatile technique for characterization of Earth and planetary materials: Canadian Journal of Earth Sciences, v.44, p. 1333-1346.

Friedmann, E.I., Koriem, A.M., 1989. Life on Mars: how it disappeared

(if it was ever there): Adv. Space Res., v. 9, p. 167–172.

Friedman, I., Smith, G.I., Johnson, C.A., and Moscati, R.J., 2002, Stable isotope compositions of waters in the Great Basin, United States 2. Modern precipitation: Journal of Geophysical Research, v. 107, no. D19, 4401, doi:10.1029/2001JD000566.

Furnes, H., 1975, Experimental palagonitization of basaltic glasses of varied composition: Contributions in Mineral Petrology, v. 50, p. 105–113.

Furnes, H., and Staudigel, H., 1999, Biological mediation in ocean crust alteration: how deep is the deep biosphere?: Earth and Planetary Science Letters, v. 166, p. 97-103.

Furnes, H., Staudigel, H., Thorseth, I.H., Torsvik, T., Muehlenbachs, K., and Tumyr, O., 2001, Bioalteration of basaltic glass in the ocean crust: Geochemistry Geophysics Geosystems, v. 2, Paper number 2000GC000150.

Furnes, H., Banerjee, N.R., Staudigel, H., Muehlenbachs, K., McLoughlin, N., de Wit, M., and Van Kranendonk, M., 2007a, Comparing petrographic signatures of bioalteration in recent to Mesoarchean pillow lavas: Tracing subsurface life in oceanic igneous rocks. Precambrian Research, v. 158, p. 156-176.

Furnes H., Banerjee, N.R., Staudigel, H., and Muehlenbachs, K., 2007b, Pillow lavas as a habitat for microbial life: Geology Today, v. 23, no. 4, p. 143-145.

Gislason, S.R., Veblen, D.R., Livi, K.J.T., 1993, Experimental meteoric water–basalt interactions: characterisation and interpretation of alteration products. Geochimica et Cosmochimica Acta, v. 57, p. 1459-1471.

Godebo, T.R., 2009, Geochemical and isotopic compositions of natural waters in the Central Main Ethiopian Rift: emphasis on the study of source and genesis of fluoride [Ph.D. thesis]: University of Ferrara, Ethiopia, 136 p.

Golubic, S., Friedmann, I., and Schneider, J. (1981) The lithobiontic ecological niche, with special reference to microorganisms. J. Sediment. Petrol. 51 (2), 351-361.

Hampton, E. R., 1964, Geologic factors that control the occurrence and availability of groundwater in the Fort Rock basin, Lake County, Oregon: U.S. Geological Survey Professional Paper, no. 383B, p. B1-B29.

Hardie, L. A., and Eugster, H. P., 1970, The evolution of closed-basin brines: Mineralogical Society of America Special Paper 3, p. 273–290.

Hay, R.L., Iijima, A., 1968, Nature and origin of palagonite tuffs of the Honolulu Group on Oahu, Hawaii. In: Studies in volcanology – a memoir in honor of Howel Williams. Geological Society of America, Boulder, pp. 331–376.

Heiken, G.H., 1971, Tuff Rings: Examples from the Fort Rock-Christmas Lake Valley Basin, South-Central Oregon: Journal of Geophysical Research, v. 76, no. 23, p. 5615-5626.

Henderson, A.C.G., Holmes, J.A., Jiawu, Z., Leng, M.J., Carvalho, L.R., 2003, A carbon- and oxygen-isotope record of recent environmental change from Qinghai Lake, NE Tibetan Plateau: Chinese Science Bulletin, v. 48, no. 14, p. 1463-1468.

IAEA/WMO (2015). Global Network of Isotopes in Precipitation. The GNIP Database. Accessible at: http://www.iaea.org/water

Jakobsson, S.P., and Moore, J.G., 1986, Hydrothermal minerals and alteration rates at Surtsey volcano, Iceland: The Geological Society of America Bulletin, v. 97, no. 5, p. 648-659.

Jercinovic, M.J., Murakami, T., Ewing, R.C., 1989, Palagonitization of deep sea dredge sample glasses. In: Miles, D.L. (ed.) 6th International Symposium on Water–Rock Interaction WRI-6. AA Balkema, Rotterdam, pp. 337–340.

Jordan, B.T., Grunder, A.L., Duncan, R.A., and Deino, A.L., 2004, Geochronology of age-progressive volcanism of the Oregon High Lava Plains: Implications for the

plume interpretation of Yellowstone: Journal of Geophysical Research, v. 109, B10202, doi:10.1029/2003JB002776.

Kharaka, Y.K., Robinson, W.S., Law, L.M., and Carothers, W.W., 1984, Hydrogeochemistry of Big Soda Lake, Nevada: an alkaline meromictic desert lake. Geochimica et Cosmochimica Acta, v. 48, p. 823-835.

Kharaka, Y.K., Thordsen, J.J., and White, L.D., 2002, Isotope and chemical compositions of meteoric and thermal waters and snow from the greater Yellowstone National Park Region: U.S. Geological Survey Open-File Report 02-194, 75 p.

Kim, S.T., and O'Neil, J.R., 1997, Equilibrium and nonequilibrium oxygen isotope effects in synthetic carbonates: Geochimica et Cosmochimica Acta, v. 61, p. 3461–3475.

Kuebler, K., Wang, A., Haskin, L. A., and Jolliff, B. L., 2003, A study of olivine alteration to iddingsite using Raman spectroscopy: In *Lunar and Planetary Science Conference*, v. 34, p. 1953.

Leng, M.J., and Marshall, J.D., 2004, Paleoclimate interpretation of stable isotope data from lake sediment archives: Quaternary Science Reviews, v. 23, p. 811-831.

Lepot, K., Benzerara, K., Philippot, P., 2011, Biogenic versus metamorphic origins of diverse microtubes in 2.7 Gyr old volcanic ashes: Multi-scale investigations. Earth and Planetary Science Letters, v. 312, p. 37-47.

Limpert, E., Stahel, W.A., and Abbt, M., 2001, Log-normal distributions across the sciences: Keys and Clues: BioScience, v. 51, no. 5, p. 341-352.

Lorenz, V., 1970, Some aspects of the eruption mechanism of the Big Hole maar, Central Oregon: Geological Society of America Bulletin 81, p. 1823-1830.

Martin, J.E., Patrick, D., Kihm, A.J., Foit Jr., F.F., and Grandstaff, D.E., 2005, Lithostratigraphy, tephrochronology, and rare earth element geochemistry of fossil at the classical pleistocene Fossil Lake area, South Central Oregon: The Journal of Geology, v. 113, p. 139-155.

McCrea, J.M., 1950, On the isotopic chemistry of carbonates and a paleotemperature scale*: The Journal of Chemical Physics, v. 18, no. 6., p. 849-857.

McLoughlin, N., Staudigel, H., Furnes, H., Eickmann, B., and Ivarsson, M., 2010, Mechanisms of microtunneling in rock substrates: distinguishing endolithic biosignatures from abiotic microtunnels: Geobiology, v. 8, p. 245-255.

McKay, C.P., Friedman, E.I., Wharton, R.A., Davies, W.L., 1992, History of water on Mars: a biological perspective: Adv. Space. Res., v. 12, p. 231–238.

McKinley, J.P., Stevens, T.O., and Westall, F., 2000, Microfossils and paleoenvironments in deep subsurface basalt samples: Geomicrobiology Journal, v. 17, p. 43-54.

McLoughlin, N., Brasier, M.D., Wacey, D., Green, O.R., and Perry, R.S., 2007, On the biogenicity criteria for endolithic microborings on early Earth and beyond: Astrobiology, v. 7, no. 1, p. 10-26.

McLoughlin, N., Furnes, H., Banerjee, N.R., Staudigel, H., Muehlenbachs, K., De Wit, M., and Van Kranendonk, M.J., 2008, Micro-bioalteration in volcanic glass:

extending the ichnofossil record to Archean basaltic crust, *in* Wisshak, S., Tapanila, L., eds., Current Developments in Bioerosion, Springer-Verlag, Heidelberg, Germany, pp. 371-396.

McLoughlin, N., Staudigel, H., Furnes, H., Eickmann, B., and Ivarsson, M., 2010, Mechanisms of microtunneling in rock substrates: distinguishing endolithic biosignatures from abiotic microtunnels: Geobiology, v. 8, p. 245-255.

Moore, J.G., 1966, Rate of palagonitization of submarine basalt adjacent to Hawaii: U.S. Geological Survey Professional Paper 550-D, p. D163–D171.

Nayudu, Y.R., 1963, Palagonite tuffs (hyaloclastites) and the products of post-eruptive processes. Bulletin Volcanologique, v. 27, no. 1, p. 391 - 410.

Peacock, M.A., 1926, The petrology of Iceland, part 1. The basic tuffs: Royal Society of Edinburgh Transactions, v. 55, p. 53–76.

Schmidt, M.E., Flemming, R.L., Stickles, J., and Morena, J. (2012). Hydraulic properties control phyllosilicate and zeolite formation in basaltic tuffs: Implications for detection of alteration processes on Mars: *43rd Lunar and Planetary Science Conference*, abstract 1226.

Scholze, H., 1988, Glass–water interactions. Journal of Non-Crystalline Solids, v. 102, p. 1–10.

Staudigel, H., Chastain, R.A., Yayanoe, A., Bourcier, W. (1995) Biologically mediated dissolution of glass. Chemical Geology 126, 147-154.

Staudigel, H., Yayanos, A., Chastain, R., Davies, G., Verdurmen, E.A.Th., Schiffman, P., Bourcier, R., De Baar, H., 1998, Biologically mediated dissolution of volcanic glass in seawater: *Earth and Planetary Science Letters*, v. 164, p. 233–244.

Steefel, C.I., Lasaga, A.C., 1994, A coupled model for transport of multiple chemical species and kinetic precipitation/dissolution reactions with application to reactive flow in single phase hydrothermal systems: American Journal of Science, v. 294, p. 529–592.

Stevens, T.O., and McKinley, J.P., 1995, Lithoautotrophic microbial ecosystems in deep basalt aquifers: Science, v. 270, p. 450.

Stockner, J.G., and Benson, W.W., 1967, The succession of diatom assemblages in the recent sediments of Lake Washington: Limnology and Oceanography, v. 12, no.3, p. 513-532.

Stroncik, N.A., and Schmincke, H.U., 2001, Evolution of palagonite: Crystallization, chemical changes, and element budget. Geochemistry Geophysics Geosystems, v. 2, no. 2000GC000102.

Stroncik, N.A., and Schmincke, H.U., 2002, Palagonite - a review. International Journal of Earth Sciences (Geol. Rundsch), v. 91, p. 680-697, doi 10.1007/s00531-001-0238-7.

Stumm, W., Morgan, J.J., 1996, Aquatic chemistry. Wiley, New York.

Talbot, M.R., 1990, A review of the palaeohydrological interpretation of carbon and oxygen isotopic ratios in primary lacustrine carbonates: Chemical Geology (Isotopes Geoscience Section), v. 80, p. 261–279.

Thorseth, I.H., Furnes, H., and Tumyr, O., 1991, A textural and chemical study of Icelandic palagonite of varied composition and its bearing on the mechanism of the glass-palagonite transformation: Geochimica Cosmochimica Acta, v.55, p. 731-749.

Thorseth, I.H., Furnes, H., Heldal, M., 1992, The importance of microbiological activity in the alteration of natural basaltic glass: Geochimica et Cosmochimica Acta, v. 56, p. 845-850.

Thorseth, I.H., Torsvik, T., Furnes, H., and Muehlenbachs, K., 1995, Microbes play an important role in the alteration of oceanic crust: Chemical Geology, v. 126, p. 137-146.

Thorseth, I.H., Torsvik, T., Torsvik, V., Daae, F.L., Pedersen, R.B., and Keldysh-98 Scientific Party, 2001, Diversity of life in ocean floor basalt: Earth and Planetary Science Letters, v. 194, p. 31-37

Thorseth, I.H., Pedersen, R.B., and Christie, D.M., 2003, Microbial alteration of 0-30-Ma seafloor and sub-seafloor basaltic glasses from the Australian Antarctic Discordance: Earth and Planetary Science Letters, v. 215, p. 237-247.

Torsvik, T., Furnes, H., Muehlenbachs, K., Thorseth, I.H., and Tumyr, O., 1998, Evidence for microbial activity at the glass-alteration interface in oceanic basalts: Earth and Planetary Science Letters, v. 162, p. 165-176.

van Dover, C.L. et al., 2003, Blake Ridge methane seeps: characterization of soft-sediment, chemosynthetically based ecosystem: Deep-Sea Research. I, v. 50, p. 281-300.

Walton, A.W., 2008, Microtubules in basalt glass from Hawaii Scientific Drilling Project #2 phase 1 core Hilina slope, Hawaii: evidence of the occurrence and behaviour of endolithic microorganisms: Geobiology, v. 6, p. 351-364.

Zhou, Z., and Fyfe, W.S., 1989, Palagonitization of basaltic glass from DSDP site-335, LEG-37 – textures, chemical-composition, and mechanism of formation: American Mineralogist, v. 74, p. 1045–1053.

Chapter 4

General Discussion and Conclusions

Microbial borings in volcanic glass have been an undervalued part of the ichnofossil record. Until relatively recently, volcanic rocks were mostly not considered as being able to provide habitats for microbes and only sediments were explored by biogeoscience research (Furnes et al., 2007a). Convincing evidence collected from oceanic crust over the last ~20 years, has demonstrated that glassy basaltic rocks can provide habitable environments for microbes (Thorseth et al., 1992, 1995; Furnes et al., 1996, 2001, 2004, 2005, 2007a, b, 2008; Fisk at el., 1998, 2003; Torsvik et al., 1998; Furnes and Staudigel, 1999; Thorseth et al., 2003; Banerjee et al., 2003; Benzerara et al., 2007; McLoughlin et al., 2007, 2008; Izawa et al., 2010; Fisk and McLoughlin, 2013). Now the validity of endolithic microborings as microbial trace fossils is strongly supported and their presence in continental volcanic settings is apparent. This study of the Reed Rocks and Black Hills tuffs in the Fort Rock Volcanic Field is unique from previous work because these rocks contain well preserved examples of putative endolithic microborings from an environment that has not been influenced by marine or glacial melt water sources.

The specific organisms and metabolic strategies responsible for generating microborings remain uncertain. Relatively little is currently known about the environmental controls on their production. To understand the important controlling variables on microbial alteration, data sets from various independent studies of bioalteration in volcanic rocks must be mutually consistent. Using preserved fluid

inclusions or secondary (alteration) minerals for instance can allow alteration fluid temperatures to be determined. If separate studies find relationships between the morphology and distribution of microborings and abiotic controls such as temperature, then arguments for biogenicity would be more reliable (McLoughlin et al., 2007).

In Chapter 2, microboring abundance and certain morphotypes in Reed Rocks tuffs (e.g., tubular types with terminal enlargements) displayed a positive correlation with abiotic alteration phases (palagonite). In Chapter 3, a comparison between Reed Rocks and Black Hills tuffs revealed distinct differences in bioalteration morphotype assemblage and abiotic alteration. These findings appear to support those of other oceanic and sub-glacial basalt studies that suggest that water-rock ratio, fluid composition and flux, secondary phase formation, and temperature may be important factors controlling the formation of endolithic microborings (Furnes and Staudigel, 1999; Furnes et al., 2001; 2007b; Banerjee et al., 2003; Cousins et al. 2009; Cockell et al., 2009). Taking into account these findings, we can also consider possible constructing organisms in addition to the potential merit of microbial alteration textures in astrobiological investigations.

4.1. CONSISTENCY WITH PREVIOUS STUDIES

4.1.1. Controls on Microbial Bioalteration

Marine tuffs of the Ontong Java Plateau have densities and varieties of bioalteration textures that are higher and more diverse, compared to ocean crust pillow basalts (Banerjee et al., 2003). Marine tuffs are thought to have experienced higher water-rock ratios than pillow basalts and so the circulation of both seawater and nutrients, controlled by porosity and permeability are possible limiting factors in microbial

alteration of oceanic basalts (Banerjee et al., 2003). In sub-glacially erupted lavas, those thought to have experienced only freshwater (glacial melt-water) alteration contain substantially less bioalteration textures than those affected by marine water (Cousins et al., 2009). Greater microbial biomass and nutrient supply as well as differences in aqueous geochemistry produce a bias toward marine-affected samples. Hence other than eruptive setting, the altering fluid composition plays an important role in controlling the formation of endolithic microborings (Cousins et al., 2009).

Active microbes isolated from weathered terrestrial sub-glacial hyaloclastites in Iceland comprise only a small fraction of the overall microbial diversity identified by Cockell et al. (2009). Those basalts contain intensely coloured palagonite varieties and Fe, Ti and Al deposition in pores suggesting high pH (>9) conditions (Thorseth et al., 1991). The palagonite types and secondary phases that form by alteration of basaltic glass and vary in space and time can thus influence the activity of microbes that are likely sensitive to such variations (Cockell et al., 2009).

Bioalteration in oceanic crust is associated with depth within the crust, where microbial glass alteration occurs in the shallow upper 250 m and is less at greater depths (Furnes and Staudigel, 1999). In upper oceanic crust, porosity and permeability are higher and temperatures are more optimal (60 - 90 ºC). With increasing depth into the crust, fracture widths and porosity decrease, while compaction, fracture density and surficial clay adsorption increase reducing porosity and permeability (Furnes et al., 2001). Temperature also increases with depth into crust; the most favourable growth conditions in oceanic crust appear to be 60-70 ºC; no microbial activity occurs above 110ºC (Furnes et al.,2007). Therefore changes in the flux of circulating fluids, nutrient supply and

temperature associated with ocean depth and depth into the crust are likely controlling factors on the distribution of microbial alteration (Furnes et al., 2007b).

4.1.2. Ichnotaxonomy of Microbial Trace Fossils

While the patterns produced by endoliths can be used to identify the organisms responsible, they are regarded as trace fossils and so identifications should use ichnological classification. A reliable way of comparing recent reports of bioalteration textures with previous accounts in oceanic crust is to assign ichnotaxa to trace-fossils that possess similar distinguishing features. The guide to morphological characterization by Fisk and McLoughlin (2013) used in this study expands on the systematic ichnotaxonomic classification scheme for trace-fossils in volcanic rocks proposed by McLoughlin et al. (2009). The primary criterion for establishing the ichnogenera is that they occur only in volcanic glass materials. In Reed Rocks and Black Hills tuffs we have identified the two major ichnogenera *Granulohyalichnus* igen. nov. and *Tubulohyalichnus* igen. nov. that correspond to the granular and tubular alteration types, respectively. These ichnogenera are subdivided into five ichnospecies based on more specific morphological variation between forms: " *Tubulohyalichnus simplus* isp. nov., an unornamented tubular form; *Tubulohyalichnus annularis* isp. nov., an annulated tubular form; *Tubulohyalichnus spiralis* isp. nov., a helicoidal tubular form; *Tubulohyalichnus stipes* isp. nov., a branched tubular form." We have identified at least one example of each of the five ichnotaxa within the Reed Rocks and Black Hills basaltic tuffs (Fig. 4.1).

Figure 4.1

Line drawings of bioalteration ichnotaxa proposed by McLoughlin et al., 2009, related schematic diagrams from the guide to morphological characterization by Fisk and McLoughlin (2013) and corresponding examples identified in basaltic glass pyroclasts from Reed Rocks (RR) and Black Hills (BH) tuffs.

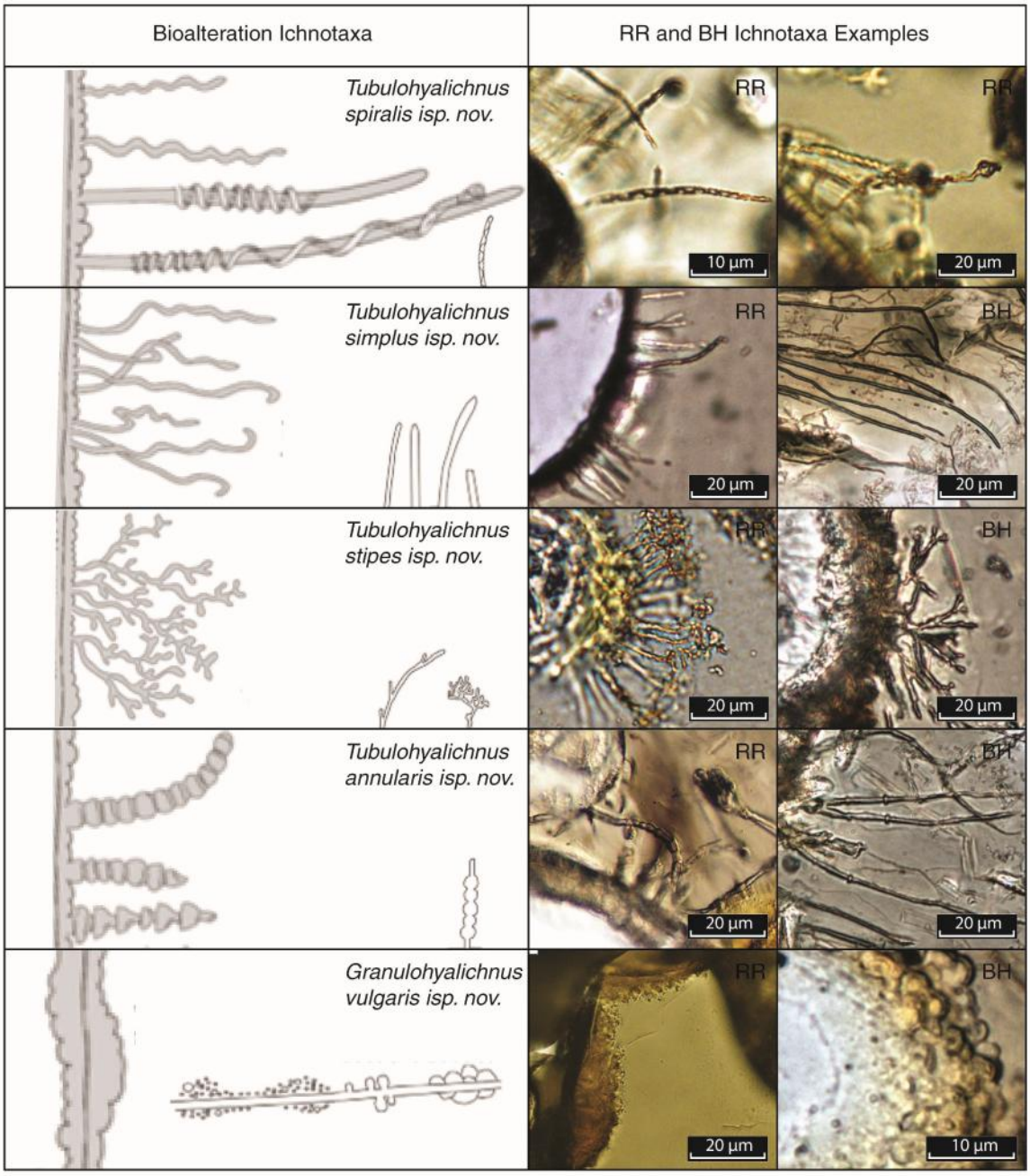

4.1.3. Possible Constructing Organisms

Considering the small size range of Reed Rock and Black Hills tubular microborings, including several examples < 1 µm in diameter, algae likely did not play a role in their construction. It is more likely that bacteria are responsible for the features reported in this study. Although oceanic and terrestrial basalts are mineralogically similar and provide nutrients and energy for microbes, their environments are different. The terrestrial volcanics at the Reed Rocks and Black Hills sites are exposed to UV radiation, fresh water from snowmelt or acidic rain, lower atmospheric/hydrostatic pressures, large changes in temperature, and extreme aridity. Terrestrial basalt environments, especially those that undergo pervasive physical and chemical weathering or contain clay-like secondary phases such as palagonite, may therefore host microbial populations resembling those found in soils (Cockell et al., 2009).

In weathered Icelandic sub-glacial basaltic glass/palagonite (hyaloclastite) for example, a diverse microbial community exists predominantly consisting of phylotypes in Actinobacteria, Proteobacteria, Bacteroidetes and Acidobacteria groups (Cockell et al., 2009). Actinobacteria and Proteobacteria are significant in soils and an abundance of them in other endolithic environments has been documented (de la Torre et al., 2003; Walker and Pace, 2007), including in pyroclastic deposits from the Mount St Helens 1980 eruption (Ibekwe et al., 2007) and Hawaiian lava flows (Gomez-Alvarez et al., 2007). Active actinobacteria isolates in Icelandic basalts have filaments capable of branching and growing directionally in vesicles and along surfaces (Cockell et al., 2009) in a similar way to fungal hyphae invasion of rocks (Buford et al., 2003; Cockell et al., 2008). Icelandic Actinobacteria also have an observed resistance to desiccation possibly related

to their filamentous growth habit (Cockell et al., 2009). Actinobacteria may thus be significant colonizers and an important influence on the weathering of vesiculated terrestrial volcanic rocks and ash such as those of Reed Rocks or Black Hills (Cockell et al., 2009).

It is worth noting however, that in some sea-floor basalts, possible marine fungi, which typically generate long filaments that can create tubular structures in silicate minerals (Smits, 2006), have been reported in carbonate amygdules (Schumann et al., 2004). Many of the tunnels produced by fungi exhibit swellings related to reproductive sporangia (Golubic et al., 2005; Cockell and Herrera 2008). Their association with swellings differentiates them from the similar uniform tunnels produced by cyanobacteria such as *Plectonema terebrans* (Golubic et al., 2005). Also, in soils and non-marine and saline water environments, fungi dominate euendolithic communities (Radtke, 1993; Smits, 2006). Fungal microborings have only been reported in silicate minerals and not from glass.

4.2. PALEOENVIRONMENT AND MARS

The textural characteristics of rocks and mineralogical and geochemical composition of secondary minerals formed within them during diagenetic or metasomatic processes (e.g., low temperature aqueous or hydrothermal alteration) can be potentially robust proxies of paleoenvironmental conditions. Many authigenic minerals (e.g., zeolites, phyllosilicates) form under restricted ranges in temperature and/or fluid-pH. Smectite clays for example, require an appreciable water source and neutral to alkaline pH conditions to form (Velde et al., 2013). Other hydrated minerals such as sulfates

require more acidic pH conditions (pH 3-5) to form (Bigham et al., 1996). At Reed Rocks and Black Hills, macro- and micro- volcanic textural features and the secondary phase assemblages that include carbonates, zeolites, smectite clays, and palagonite point toward an environment that contained a significant water reservoir and alkaline pH conditions. Furthermore, the range in formation temperatures inferred from mineralogy are consistent with carbonate paleothermometry calculations suggesting temperatures between 6.8 - 86.6°C. These relationships are important when searching for habitable environments on other planetary bodies. Identifying mineral types on Mars for example can help constrain the presence of habitable environments (Mustard et al., 2008; Murchie et al., 2009).

The search for extraterrestrial life requires the identification of potential habitable environments therefore an understanding of habitable environments on Earth is essential. Certain conditions are shared by known inhabited environments, including the existence of liquid water, a sufficient source of energy that allows basic metabolic processes to be maintained, and a source of biogenic elements that may be exploited in the photo- or chemosynthesis of bio-molecules (Des Marais *et al*., 2008; Chela-Flores, 2010). By understanding the full distribution and processes governing the formation of biosignatures, attempts to trace subsurface life and seek evidence of extraterrestrial habitable environments or life will be better served (Freidmann and Koriem, 1989; McKay et al., 1992; Fisk et al., 1998; McLoughlin et al., 2007).

Microbes are the most widespread form of life on Earth found in environments ranging from hydrothermal vents on the ocean floor (Takai *et al*., 2004; Nakagawa and Takai 2008), to cold Antarctic dry valleys (Cowan *et al*., 2002). Evidence indicating that endolithic microbes have an influence on the basaltic glass weathering process on Earth

(e.g., Torsvik et al., 1998; Thorseth et al., 1995; Fisk et al., 1998; Staudigel et al.,; 2008; Furnes et al., 2001, 2007a, 2007b) has expanded the ichnofossil record and what has been thought of as the "habitable zone" (Fisk et al., 1998; Edwards et al., 2005; Staudigel et al, 2008; Izawa et al., 2010). Basaltic rocks are an extensive component of the silicate crusts of Earth, therefore the biosignatures we find in basaltic rocks here on Earth may be present but unknown in other environments on Earth as well as other bodies in our solar system. It is possible that growing and metabolizing organisms could have adapted to the inhospitable, dry, far below freezing, intensely ultraviolet radiated and low organic carbon bearing Martian surface conditions (Klein et al., 1992; Klein, 1998; Clark, 1998). It is more likely that any life, if present, would be restricted to the subsurface environment (Boston et al;., 1992; Carr, 1996; Nealson, 1997; Shock, 1997). It appears that Mars was volcanically active (Greeley and Spudis, 1981; Mustard *et al*., 2005; Schmidt *et al*., 2009; McEwen *et al*., 2010), had water in its past (Mustard et al., 2008), and possibly water at present (Malin and Edgett, 2000). Therefore endolithic microborings seem to be extremely good morphological biosignatures for exploring potential Martian exobiology.

Volcanism is a geologic process known to occur on terrestrial bodies in our solar system and there is clear evidence indicating volcanic activity, on Mercury, Venus, Mars, our Moon, the satellite Io of the Jovian planet Jupiter, and a widely studied asteroid called 4 Vesta (Head and Wilson, 1992; Spencer *et al*., 2007; Brož and Hauber 2012; Head *et al*.,1992). Volcanism is also one of the most significant geologic processes occurring on Mars over the course of its history (Greeley and Spudis, 1981) and basaltic volcanism has been indicated by both orbital and rover based studies (i.e. Mustard *et al*., 2005; Schmidt

et al., 2009; McEwen *et al*., 2010). The older Noachian or Hesperian aged southern highlands of Mars are predominantly basaltic in composition (Bandfield *et al*., 2000) and pyroclastic rocks forming hydrovolcanic land forms such as tuff cones or tuff rings are indicated in multiple regions (Brož and Hauber, 2012). Extensive layered deposits such as the Medusae Fossae Formation may be pyroclastic (Chapman, 2002), which has been identified in the vicinity of Gale Crater, the Mars Science Laboratory (MSL) site (Zimbleman and Scheidt, 2012). Some of the regularly layered upper units within the interior layered mound (Aeolis Mons/Mount Sharp) of Gale Crater may be composed of pyroclastics that originated as part of the Medusae Fossae Formation (Zimbelman and Scheidt, 2012).

In addition to the existence of basaltic volcanism on Mars, there is also evidence of aqueous (abiotic) alteration. Devitrification products including hydrated phyllosilicates, a major constituent of palagonite, and amorphous nano phase Fe-oxides have been identified (Poulet *et al*., 2005; Squyres *et al*., 2007; Ehlmann *et al*., 2008; Mustard *et al*., 2008; Schmidt *et al*., 2009) and may be the products of aqueous alteration, chemical weathering or low temperature hydrothermal processes (Ming *et al*., 2008; Schmidt *et al*., 2009). Compact Reconnaissance Imaging Spectrometer for Mars (CRISM) data suggested that there are phyllosilicate minerals present in the lower sequences found in Gale Crater (Milliken *et al*., 2010). The Mars Science Laboratory Curiosity rover confirmed the presence of phyllosilicate minerals (smectites) in Gale crater by CheMin X-Ray diffraction analysis of rocks that appear to be fine-grained mudstones deposited at the terminus of an ancient fluctuating river system (Morrison, 2013). The presence of basalts combined with evidence of aqueous alteration suggest that

ancient Martian environments may have been wetter and more Earth-like therefore the potential for endolithic microbes to alter subaqueous basalts and form biosignatures was likely high (e.g. Fisk and Giovannoni, 1999; Banerjee et al., 2004a, b, 2006; Joliff *et al*., 2006; Baker, 2006).

4.3. LIMITATIONS OF STUDY

If putative microborings are found to have a geological context and morphologies suggesting they are biogenic, then examination of isotopic and elemental variations in areas surrounding and within micro-tunnels that may suggest biological processing is necessary for further support. Similarly, morphological and contextual information is needed to distinguish chemical biosignatures from isotopic and elemental variations that can be produced by abiotic weathering processes (McLoughlin et al., 2007). If geochemical variations associated with putative microborings that are needed to support morphological and contextual information are lacking, then establishing their biogenicity is more complicated. In such cases, biogenicity can only be assumed by comparing their morphology with either existing euendolithic organisms or other fossils (McLoughlin et al., 2007). Despite the Reed Rock and Black Hills displaying a biogenically suggestive geologic context and diverse examples of alteration textures resembling microboring morphologies reported in ocean basalts, no strong geochemical data indicative of biological processing has been obtained. Therefore even though the Reed Rocks and Black Hills are convincing examples of bioalteration, they can ultimately only be tentatively inferred as biogenic. Future work should be focused on gaining biogeochemical information to support the biogenicity of the putative Reed Rock-Black Hills-FRVF microborings.

Even though basalts are generally pervaded by abiotic aqueous alteration, no abiotic mechanisms capable of producing these textures have been identified (Fisk et al., 2006; Walton, 2008). The diverse variety of morphologies and their distributions are also quite distinctive. They show features indicative of biological activity such as segmentation, bifurcations, septa, directionality and affinities for certain locations that may be structurally weak or provide favourable micro-chemical conditions (McLoughlin et al., 2007). In addition, the interior surfaces of microborings in fresh basalts have been found to contain identifiable DNA linings in some cases giving support the argument for their biogenic origins (Giovannoni et al., 1996; Torsvik et al., 1998; Furnes et al., 2001) in volcanic rocks.

Interpreting our results to identify the controls on the formation of bioalteration textures, quantifying bioalteration and deducing these data makes biases and uncertainties that create limitations. Some uncertainties may be the result of sample choice, underlying assumptions or erroneous measurements and subjective estimations.

Bioalteration in volcanic rocks is generally only observed in fresh glass fragments and so the effect on other materials are either completely absent or are not easily identified. Since bioalteration textures are apparently confined to fresh glass, although rare overprinting of textures may be identified, the data collected and the conclusions drawn from the results may be limited. This is because glass is readily affected by abiotic alteration processes, including dissolution that can potentially damage or completely destroy fine microbial bioalteration textures. Because abiotic alteration can potentially overprint biological alteration, it is possible that some points counted during point counting as abiotic alteration/palagonite may have originally been biological alteration.

Palagonitization may therefore have erased the evidence of microbial influence. This could have resulted in an excessive estimation of abiotic alteration and an underestimation of bioalteration. Several of the samples examined experienced intense aqueous alteration many of which were also highly bioaltered reflecting a high fluid flux through the deposits. Our estimates of abiotic and biotic alteration are thus considered to be maximum and minimum approximations, respectively. Furthermore, because the tubular type of bioalteration is more easily identified and better preserved than the granular type, a slight bias in relative proportions of tubular and granular bioalteration may exist. It is possible that the granular type may be more common than determined here, the percentage of which could consist of up to several times more.

For all thin sections that had bioalteration values determined, only one set of results were obtained. If a random selection of sections were analyzed a second time, the results could be compared to the initial estimation and verified. Also, thin section analysis was done on samples in order, non-randomly, and not blind, therefore this may have also produced a bias in results.

In order to detect certain depletions indicative of biological processing in rock matrix surrounding putative microborings, areas that may only be a few tens of nanometers wide likely need to be examined (Alt and Mata, 2000). During EDS point analysis and elemental mapping, analyses were done on a moderate scale. As a result the elemental data for areas believed to have experience bioalteration were not spatially resolved at a useful enough scale to test for biological processing across areas that may only be 200 to 400 nm wide.

4.4. SUMMARY OF CONCLUSIONS

The Reed Rocks and Black Hills hydrovolcanic tuffs contain a suite of basaltic glass alteration textures that closely match descriptions of microbial bioalteration (endolithic microborings) from oceanic and sub-glacial basalts. Their geologic contextual and textural characteristics suggest they have biological origins. We posit that the Fort Rock Volcanic Field is the first location where well preserved microborings have been documented in basaltic glass that has not been affected by marine or glacial melt water conditions. Also, new data suggests that micro-tunnels appear to be present in other locations throughout the FRVF that were clearly well within the Fort Rock Lake basin rather that at the lake margin. At Reed Rocks, the abundance and morphology of microborings appear to be related to secondary alteration phases (palagonite). The discrete dissimilarities in abiotic alteration and microboring abundance and morphotype assemblage between Reed Rocks and Black Hills are consistent with other basalt studies that indicate water/rock ratio, fluid composition and flux, temperature and secondary phase formation are important influences on microborings formation. Although the organisms responsible for the textures have not been identified, it is likely that bacteria/cyanobacteria and possibly fungi played a role in constructing these bioalteration textures. Furthermore, considering the geologic similarities to certain areas on Mars, (e.g., hydrovolcanism, basaltic composition, aqueous basalt alteration), the findings at Reed Rocks and Black Hills further support the potential of volcanic microborings as astrobiological biosignatures.

4.5. FUTURE WORK

The main purpose of this study has been to document the variety of bioalteration textures and relate those to abiotic controls. Several areas of investigation that were not included in this study could greatly improve the quality. These are as follows:

- *Compare percent abiotic vs. biotic alteration in continental basalts from the Fort Rock Volcanic Field (FRVF) to values determined in samples obtained during the Deep Sea Drilling Program/Ocean Drilling Program (DSDP/ODP).* Relative proportions of biotic and abiotic alteration in ocean basalts have been determined by point counting and display a dependence on depth in crust, fracture density, and temperature (Furnes and Staudigel, 1999; Furnes et al., 2001).
- *Relate the density of endolithic microborings to mechanical weaknesses*. The density of bioalteration textures (microborings) in volcanic glass have been reported to positively correlate with mechanical weaknesses such as micro-fractures (Furnes et al., 2001).
- *Relate density/abundance of endolithic microborings to elemental composition of individual pyroclast fragments*. Endolithic organisms have shown a preference for colonizing Fe and P rich silicate fragments (Roberts-Rogers and Bennett, 2004).
- *Relate microborings density/morphology to pyroclast grain size distributions.* Qualitatively, this study has suggested that microborings density/abundance may be related to grain size. The larger grains appear to have more bioalteration whereas in small ash grains they are generally absent.
- *Quantify and visualize density, porosity and permeability.* In many basalt studies, porosity is determined by point counting (2 dimensional) and permeability is

inferred relative to other rocks based on textural features. Another way of characterizing these properties in natural materials to understand the nature and variability of pore structures can be done by applying helium pycnometry (density), mercury intrusion porosimetry (MIP) and 3D X-ray tomography (e.g., Ketcham and Carlson, 2001; Dekayir et al., 2003; Chalmers et al., 2012).

- *Obtain geochemical data that support the biogenic origin of alteration textures: (1) Map elemental abundance distributions to reveal biological processing.* Elemental distribution in this study only used qualitative energy dispersive spectroscopy (EDS). Elements across alteration fronts on nano-scales can be mapped using electron microprobe analysis (e.g., Storrie-Lombardi and Fisk, 2004); *(2) Fluorescent DNA staining.* Fluorescent dyes such as 4'6-diamidino-2-phenylindole (DAPI), PO-PRO-3, Hoechst 33342, and Styo 11, specifically bind to nucleic acids and can show the presence of DNA in altered basalts (e.g., Giovannoni et al., 1996; Torsvik et al., 1998). This method was attempted on 3 thin sections and one cut rock slab from Reed Rocks-Black Hills tuffs, but was unsuccessful. Improper sample preparation and the absence of a unaltered reference standard likely contributed to this fault; (3) *Search for organic carbon along bioalteration margins, and analyze for $\delta^{13}C$ isotopic fractionation patterns in carbonates.* Organic carbon and isotopically light carbonates with respect to unaltered portions are indicative of biological processing (e.g., Furnes et al., 2001; Banerjee et al., 2006). During elemental mapping using EDS, this may entail using a coating other than carbon if organic carbon is to be detected and obtaining isotopic data from unaltered samples.

- *SEM/BSE and TEM imaging of whole separated pyroclasts.* All SEM imaging in this study was done on thin sections. Delicate features may have been destroyed in the thin sectioning process so imaging of exterior surfaces of pyroclasts may reveal additional features not seen in thin section (e.g., Banerjee et al, 2003; Cockell et al., 2009).
- *Radiometric age dating.* The Reed Rocks and Black Hills deposits have not yet been dated so it is still unclear whether the deposits are relatively similar in age or if one is much older than the other. Such information could have important implications for all interpretations of data including the differences in abiotic and biogenic alteration textures.

4.6. REFERENCED CITED

Alt, J.C., and Mata, P., 2000, On the role of microbes in the alteration of submarine basaltic glass: a TEM study: Earth and Planetary Science Letters, v. 181, p. 301-313.

Baker, V.R., 2006, Geomorphological evidence for water on Mars: *Elements*, v. 2, no. 3, p. 139–143.

Bandfield, J.L., Hamilton, V.E., and Christensen, P.R., 2000, A Global View of Martian Surface Compositions from MGS-TES. *Science* 287:1626; DOI: 10.1126/science.287.5458.1626.

Brock, T.D., 1978, Thermophilic Microorganisms and Life at High Temperatures. Springer-Verlag, Berlin, Heidelberg. New York.

Banerjee, N.R., and Muehlenbachs, K., 2003, Tuff life: Bioalteration of volcaniclastic rocks from the Ontong Java Plateau. Geochemistry Geophysics Geosystems, v. 4, no. 4, p. 1037.

Banerjee, N.R., Furnes, H., Muehlenbachs, K., and Staudigel, H., 2004a, Microbial alteration of volcanic glass in modern and ancient oceanic crust as a proxy for studies of extraterrestrial material: In Proc. Lunar and Planetary Science Conf., XXXV (LPI Contribution No. 1197, abstract 1248). Lunar and Planetary Institute, Houston.

Banerjee, N.R., Muehlenbachs, K., Furnes, H., Staudigel, H., and de Wit, M., 2004b, Potential for early life hosted in basaltic glass on a wet Mars. In Proc. Second Conf. on Early Mars, Jackson Hole, WY, 11–15 October (Abstract 8048). Lunar Planetary Institute, Houston.

Banerjee, N.R., Furnes, H., Simonetti, A., Muehlenbachs, K., Staudigel, H., deWit, M. & Van Kranendonk, M., 2006, Ancient microbial alteration of oceanic crust on two early Archean Cratons and the search for extraterrestrial life: In Proc. Lunar and Planetary Science Conf., XXXVII (Abstract 2156). Lunar and Planetary Institute, Houston.

Benzerara, K., Menguy, N., Banerjee, N.R., Tyliszczak, T., Brown Jr., G.E., and Guyot, F., 2007, Alteration of submarine basaltic glass from the Ontong Java Plateau: A STXM and TEM study: Earth and Planetary Science Letters, v. 260, p. 187-200.

Bigham, J. M., U. Schwertmann, S. J. Traina, R. L. Winland, and M. Wolf, 1996, Schwertmannite and the chemical modeling of iron in acid sulfate waters: Geochimica et Cosmochimica Acta, v. 60, p. 2111 –2121, doi:10.1016/0016-7037(96)00091-9.

Boston, P. J., Ivanov, M. V. and McKay, C. P., 1992, On the possibility of chemosynthetic ecosystems in subsurface habitats on Mars, Icarus, v. 95, p. 300-308.

Brand, B.D., and Clarke, A.B., 2009, The architecture, eruptive history, and evolution of the Table Rock Complex, Oregon: From a Surtseyan to an energetic maar eruption: Journal of Volcanology and Geothermal Research, v. 180, p. 203-224.

Brož, P., and Hauber, E., 2012, A unique volcanic field in Tharsis, Mars: Pyroclastic cones as evidence for volcanic explosive eruptions. *Icarus, v.* 218, p. 88-99.

Burford, E.P., Kierans, M., and Gadd, G.M., 2003, Geomycology: Fungi in mineral substrata: Mycologist, v. 17, p. 98–107.

Carr, M. H., 1996, Water on Mars, Oxford Univ. Press, New York.

Chalmers, G.R., Bustin, R.M., and Power, I.M., 2012, Characterization of gas pore systems by porosimetry, pycnometry, surface area, and field emission scanning electron microscopy/transmission electron microscopy image analysis: Examples from the Barnett, Woodford, Haynesville, Marcellus, and Doig units: AAPG Bulletin, v. 96, no. 6, p. 1099-1119.

Chapman, M.G., 2002, Layered, massive and thin sediments on Mars: possible Late Noachian to Late Amazonian tephra? *Geological Society, London, Special Publications, v*. 202, p. 273-293.

Chazottes, V., Le Campion-Alsumard, T., and Peyrot-Clausade, T., 1995, Bioerosion rates on coral reefs: interactions between macroborers, microborers and grazers (Moorea, French Polynesia).: Palaeogeography, Paleoclimatology and Paleoecology, v. 113, no. 2, p. 189-198.

Chela-Flores, J., 2010, Instrumentation for the search for habitable ecosystems in the future exploration of Europa and Ganymede: *International Journal of Astrobiology, v.* 9, no. 2, p. 101-108.

Clark, B. D., 1998, Surviving the limits to life at the surface of Mars: Journal of Geophysical Research, v. 103, p. 28545-28555.

Cockell, C. S., & Herrera, A., 2008, Why are some microorganisms boring?: *Trends in microbiology*, v. *16, no.* 3, p. 101-106.

Cockell, C.S., Olsson-Francis, K., Herrera, A., and Meunier, A., 2009, Alteration textures in terrestrial volcanic glass and the associated bacterial community: Geobiology, v. 7, p. 50-65.

Colbath, K., and Steele, M.J., 1982, The geology of economically significant lower Pliocene diatomites in the Fort Rock basin near Christmas Valley, Lake County, Oregon: Oregon Geology, v. 44, no. 10, p. 111-118.

Cowan, D.A., Russel, N.J., Mamais, A., and Sheppard, D.M., 2002, Antarctic Dry Valley mineral soils contain unexpectedly high level of microbial biomass: *Extremophiles, v.* 6, p. 431-436.

Dekayir, A., Roouai, M., and Moustier, S., 2003, Basalt pore fractal dimensions from image analysis and mercury porosimetry: Arabian Journal for Science and Engineering, v. 28, no. 1:Part C, p. 223-232.

de la Torre, J.R., Goebel, B.M., Friedmann, E.I., and Pace, N.R., 2003, Microbial diversity of cryptoendolithic communities from the McMurdo Dry Valleys, Antarctica: Applied Environmental Microbiology, v. 69, p. 3858–3867.

Des Marais, D.J., Nuth III, J.S.A., Allamandola, L.J., Boss, A.P., Farmer, J.D., Hoehler, T.M., Jakosky, B.M., Meadows, V.S., Pohorille, A., Runnegar, B., and Spormann,

A.M., 2008, The NASA Astrobiology Roadmap: *Astrobiology, v.* 8, no. 4, p. 715-730.

Edwards, K.J., Bach, W., and McCollom, T.M., 2005, Geomicrobiology in oceanography: microbe mineral interactions at and below the sea floor. *Trends in Microbiology*, *v.* 13, p. 449–456.

Ehlmann, B.D.L., Mustard, J.F., Fassett, C.I., Schon, S.C., Head III, J.W., Des Marais, D.J., Grant, J.A., and Murchie, L., 2008, Clay minerals in delta deposits and organic preservation potential on Mars: *Nature Geoscience* v. 1, p. 355-358.

Emerson, D., Rentz, J.A., Lilburn, T.G. , et al., 2007, A novel lineage of Proteobacteria involved in formation of marine Fe-oxidizing microbial mat communities: PLoS ONE, v. 2, e667.

Fisk, M.R., Giovannoni, J., and Thorseth, H., 1998, Alteration of Oceanic Volcanic Glass: Textural Evidence of Microbial Activity: *Science, v.* 281, p. 978-980.

Fisk M.R., and Giovannoni, S.J., 1999, Sources of nutrients and energy for a deep biosphere on Mars: Journal of Geophysical Research Letters, v. 104, no. E5, p. 11805-11815.

Fisk, M.R., Storrie-Lombardi, M.C., Douglas, S., Popa, R., McDonald, G., and Di Meo-Savoie, C., 2003, Evidence of biological activity in Hawaiian subsurface basalts: Geochemistry Geophysics Geosystems, v. 4, no. 12, 1103, doi: 10.1029/2002GC000387.

Fisk, M.R., Popa, R., Mason, O.U., Storrie-Lombardi, M.C., and Vicenzi, E.P., 2006, Iron-magnesium silicate bioweathering on earth (and Mars?): Astrobiology, v. 6, no. 1, p. 48–68.

Fisk, M., and McLoughlin, N., 2013, Atlas of alteration textures in volcanic glass from the ocean basins: Geosphere, v. 9, no. 2, p. 317-341.

Friedmann, E.I., Koriem, A.M., 1989. Life on Mars: how it disappeared (if it was ever there): Advances in Space Research, v. 9, p. 167–172.

Furnes, H., Thorseth, I.H., Tumyr, O., Torsvik, T., and Fisk, M.R., 1996, Microbial activity in the alteration of glass from pillow lavas from hole 896A, *in* Proceedings, Ocean Drilling Program, Scientific Results, v.148, p. 191-206.

Furnes, H., and Staudigel, H., 1999, Biological mediation in ocean crust alteration: how deep is the deep biosphere?: Earth and Planetary Science Letters, v. 166, p. 97-103.

Furnes, H., Staudigel, H., Thorseth, I.H., Torsvik, T., Muehlenbachs, K., and Tumyr, O., 2001, Bioalteration of basaltic glass in the ocean crust: Geochemistry Geophysics Geosystems, v. 2, Paper number 2000GC000150

Furnes, H., Banerjee, N.R., Muehlenbachs, K., Staudigel, H., and de Wit, M., 2004, Early life recorded in Archean pillow lavas: Science, v. 304, p. 578-581.

Furnes, H., Banerjee, N.R., Muehlenbachs, K., and Kontinen, A., 2005, Preservation of biosignatures in metaglassy volcanic rocks from the Jormua ophiolite complex, Finland: Precambrian Research, v. 136, p. 125-137.

Furnes, H., Banerjee, N.R., Staudigel, H., Muehlenbachs, K., McLoughlin, N., de Wit, M., and Van Kranendonk, M., 2007a, Comparing petrographic signatures of bioalteration in recent to Mesoarchean pillow lavas: Tracing subsurface life in oceanic igneous rocks. Precambrian Research, v. 158, p. 156-176.

Furnes H., Banerjee, N.R., Staudigel, H., and Muehlenbachs, K., 2007b, Pillow lavas as a habitat for microbial life: Geology Today, v. 23, no. 4, p. 143-145.

Furnes, H., McLoughlin, N., Muehlenbachs, K., Banerjee, N., Staudigel, H., Dilek, Y., de Wit, M., Van Kranendonk, M., Shiffman, P., 2008, Oceanic pillow lavas and hyaloclastites as habitats for microbial life through time - a review: In: Y. Dilek et al. (eds.), Links Between Geological Processes, Microbial Activities & Evolution of Life, Springer Science+Business Media, B.V.

Ghirardelli, L.A., 2002, Endolithic microorganisms in live and dead thalli of coralline red algae (Corallinales, Rhodophyta) in the Northern Adriatic Sea: Acta Geologica Hispanica, v. 37, p. 53–60.

Giovannoni, S.J., Fisk, M.R., Mullins, T.D. & Furnes, H., 1996, Genetic evidence for endolithic microbial life colonizing basaltic glass/seawater interfaces. In Proceedings of the Ocean Drilling Program, Science Results 148, eds Alt, J.C., Kinoshita, H., Stokking, L.B. & Michael, P.J., pp. 207–214. Ocean Drilling Program, College Station, TX.

Golubic, S., Radtke, G., and Le Campion-Alsumard, T., 2005, Endolithic fungi in marine ecosystems: Trends in Microbiology, v. 13, no. 5., p. 229-235.

Gomez-Alvarez, V., King, G.M., Nüsslein, K., 2006, Comparative bacterial in recent Hawaiian volcanic deposits of different ages: FEMS Microbiology Ecology, v. 60, p. 60–73.

Greeley, R., and Spudis, P.D. (1981) Volcanism on Mars. *Reviews of Geophysics*, *v.* 19, no. 1, p. 13-41.

Hampton, E. R., 1964, Geologic factors that control the occurrence and availability of groundwater in the Fort Rock basin, Lake County, Oregon: U.S. Geological Survey Professional Paper, no. 383B, p. B1-B29

Head, J.W., and Wilson, L., 1992, Lunar are volcanism: Stratigraphy, eruption conditions, and evolution of secondary crust: *Geochimica et Cosmochimica Acta v.* 56, p. 2155-2175.

Head, J. W., Crumpler, L. S., Aubele, J. C., Guest, J. E., & Saunders, R. S., 1992, Venus volcanism: Classification of volcanic features and structures, associations, and global distribution from Magellan data: *Journal of Geophysical Research: Planets (1991–2012)*, v. *97*, no. E8, p. 13153-13197.

Heiken, G.H., 1971, Tuff Rings: Examples from the Fort Rock-Christmas Lake Valley Basin, South-Central Oregon: Journal of Geophysical Research, v. 76, no. 23, p. 5615-5626.

Ibekwe, A.M., Kennedy, A.C., Halvorson, J.J., and Yang, C.H., 2007, Characterization of developing microbial communities in Mount St. Helens pyroclastic substrate: Soil Biology Biochemistry, v. 39, p. 2496–2507.

Izawa, M.R.M., Banerjee, N.R., Flemming, R.L., and Bridge, N.J., 2010, Preservation of Microbial Ichnofossils in Basaltic Glass by Titanite Mineralization: *The Canadian Mineralogists, v.* 48, p. 1255-1265.

Joliff, B.L., McLennan, S.M., and Athena Science Team, 2006, Evidence for water at Meridiani: *Elements,* v. 2, p. 163–167.

Ketcham, R.A., and Carlson, W.D., 2001, Acquisition and interpretation of X-ray computed tomographic imagery: applications to the geosciences: Computers & Geosciences, v. 27, no. 4, p. 381-400.

Klein, H. P., Horowitz, N.H., and Biemann, K., 1992, The search for extant life on Mars, in Mars, edited by H. H. Kieffer, B. M. Jakosky, C. W. Snyder, and M. S. Matthews, pp. 1221-1233, Univ. of Ariz. Press, Tucson.

Klein, H. P., 1998, The search for life on Mars: What we learned from Viking: Journal of Geophysical Research, v. 103, p. 28463-28466.

Lorenz, V., 1970, Some aspects of the eruption mechanism of the Big Hole maar, Central Oregon: Geological Society of America Bulletin, v. 81, p. 1823-1830.

Lysnes, K., Thorseth, I.H., Steinsbu, B.O., Øvreas, L., Torsvik, T., and Pedersen, R.B., 2004, Microbial community diversity in seafloor basalts from the Arctic spreading ridges: FEMS Microbiology and Ecology, v. 50, p. 213–230.

Malin, M.C., and Edgett, K.S., 2000, Evidence for recent groundwater seepage and surface runoff on Mars: *Science*, v. 288, no. 5475, p. 2330-2335.

Martin, J.E., Patrick, D., Kihm, A.J., Foit Jr., F.F., and Grandstaff, D.E., 2005, Lithostratigraphy, tephrochronology, and rare earth element geochemistry of fossil at the classical pleistocene Fossil Lake area, South Central Oregon: The Journal of Geology, v. 113, p. 139-155.

Mason, O.U., Stingl, U., Wilhelm, L.J., Moeseneder, M.M., Di Meo-Savoie, C.A., Fisk, M.R., and Giovannoni, S.J., 2007, The phylogeny of endolithic microbes associated with marine basalts: Environmental Microbiology, v. 9, p. 2539–2550.

McEwen et al., 2010, The high resolution imaging science experiment (HiRISE) during MRO's primary science phase (PSP): Icarus, v. 205, p. 2-37.

McLoughlin, N., Brasier, M.D., Wacey, D., Green, O.R., and Perry, R.S., 2007, On the biogenicity criteria for endolithic microborings on early Earth and beyond: Astrobiology, v. 7, no. 1, p. 10-26.

McLoughlin, N., Furnes, H., Banerjee, N.R., Staudigel, H., Muehlenbachs, K., De Wit, M., and Van Kranendonk, M.J., 2008, Micro-bioalteration in volcanic glass: extending the ichnofossil record to Archean basaltic crust, *in* Wisshak, S., Tapanila, L., eds., Current Developments in Bioerosion, Springer-Verlag, Heidelberg, Germany, pp. 371-396.

McLoughlin, N., Furnes, H., Banerjee, N.R., Muehlenbachs, K., and Staudigel, H., 2009, Ichnotaxonomy of microbial trace fossils in volcanic glass: Journal of the Geological Society, London, v. 166, p. 159-169.

McKay, C.P., Friedman, E.I., Wharton, R.A., Davies, W.L., 1992. History of water on Mars: a biological perspective: Advances in Space Research, v. 12, p. 231–238.

Milliken, R.E., Grotzinger, J.P., and Thomson, B.J., 2010, Paleoclimate of Mars as captured by the stratigraphic record in Gale Crater: *Geophysical Research Letters, v.* 37, L04201, doi:10.1029/2009GL041870.

Ming et al., 2008, Geochemical properties of rocks and soils in Gusev crater, Mars: Results of the Alpha Particle X-ray Spectrometer from Cumberland Ridge to Home Plate: *Journal of Geophysical Research: Planets (1991–2012)*, v. *113* no. E12, doi: 10.1 029/2008JE003195.

Morrison, S.M., 2013, Crystal-chemistry of Mars Minerals at Rocknest, John Klein and Cumberland: *Geological Society of America Annual Meeting* 125: no.6-7.

Murchie et al., 2009, A synthesis of Martian aqueous mineralogy after 1 Mars year of observations from the Mars Reconnaissance Orbiter: *Journal of Geophysical Research, v.* 114, no. E00D06, doi:10.1029/2009JE003342.

Mustard, J. et al., 2008, Hydrated silicate minerals on Mars observed by the Mars Reconnaissance Orbiter CRISM instrument: *Nature*, v. *454*, no. 7202, p. 305-309.

Mustard, J. F., Poulet, F., Gendrin, A., Bibring, J. P., Langevin, Y., Gondet, B., Mangold, N., Bellucci, G., and Altieri, F., 2005, Olivine and pyroxene diversity in the crust of Mars: *Science*, v. *307*, no. 5715, p. 1594-1597.

Nakagawa, S., and Takai, K., 2008, Deep-sea vent chemoautotrophs: diversity, biochemistry and ecological significance: *FEMS Microbial Ecology*, v. 65, p. 1-14.

Nealson, K. H., 1997, The limits of life on Earth and searching for life on Mars: Journal of Geophysical Research, v. 102, p. 23675-23686.

Perry, C.T., 1988, Grain susceptibility to the effects of microboring: implications for the preservation of skeletal carbonates: Sedimentology, v. 45, p. 39–51.

Poulet, F., Bibring, J.-P., Mustard, J.F., Gendrin, A., Mangold, N., Langevin, Y., Arvidson, R.E., Gondet, B., Gomez, C., and the OMEGA team, 2005, Phyllosilicates on Mars and implications for early Martian climate: *Nature*, v. 438, p. 623–627.

Radtke, G., 1993, The distribution of microborings in molluscan shells from recent reef environments at Lee Stocking Island. Bahamas: Facies, v. 29, p. 81–92.

Roberts-Rogers, J., and Bennett, P.C., 2004, Mineral stimulation of sub surface microorganisms: release of limiting nutrients from silicates: *Chemical Geology*, *v.* 203, no. 1–2, p. 91–108.

Schmidt et al., 2009, Spectral, mineralogical, and geochemical variations across Home Plate, Gusev Crater, Mars indicate high and low temperature alteration. *Earth and Planetary Science Letters*, v. *281*, no. 3, p. 258-266.

Shock, E. L., 1997, High-temperature life without photosynthesis as a model for Mars: Journal of Geophysical Research, v. 102, p. 23687-23694.

Schumann, G., Manz, W., Reitner, J., and Lustrino, M., 2004, Ancient fungal life in North Pacific Eocene oceanic crust: Geomicrobiology Journal, v. 21, p. 241–246.

Smits, M.M., 2006, Mineral tunneling by fungi. In: Gadd, G.M. (ed.) Fungi in Biogeochemical Cycles, Cambridge, Cambridge University Press, p. 681–717.

Spencer et al., 2007, Io volcanism seen by New Horizons: A major eruption of the Tvashtar volcano: *Science*, v. *318*, no. 5848, p. 240-243.

Squyres et al., 2007, Pyroclastic activity at Home Plate in Gusev Crater, Mars: Science, v. 316, no. 738, doi: 10.1126/science.1139045.

Staudigel, H., Furnes, H., Banerjee, N.R., Dilek, Y., and Muehlenbachs, K., 2006, Microbes and volcanoes: a tale fromthe oceans, ophiolites and greenstone belts: GSA Today, v. 16, no. 10, doi:10.1130/GSAT01610A.1.

Staudigel, H., Furnes, H., McLoughlin, N., Banerjee, N., Connell, L.B., and Templeton, A., 2008, 3.5 billion years of glass bioalteration: Volcanic rocks as a basis for microbial life?: Earth-Science Reviews, v. 89, p. 156-176.

Stetter, K.O., Fiala, G., Huber, G., and Segerer, A., 1990, Hyperthermophilic microorganisms: FEMS Microbiology Reviews, v. 75, p. 117-124.

Stetter, K. O., 2007, Hyperthermophiles in the History of Life, *in* Ciba Foundation Symposium 202 - Evolution of Hydrothermal Ecosystems on Earth (And Mars?), John Wiley & Sons, Ltd., (Chichester, UK), p. 169-184, doi: 10.1002/9780470514986.ch1

Takai, K., Gamo, T., Tsunogai, U., Nakayama, N., Hirayama, H., Nealson, K.H., and Horikoshi, K., 2004, Geochemical and microbiological evidence for hydrogen-based, hyperthermophilic subsurface lithoautotrophic microbial ecosystem (HyperSLiME) beneath an active deep-sea hydrothermal field: *Extremophiles,* v. 8, p. 269-282.

Thorseth, I.H., Furnes, H., and Tumyr, O., 1991, A textural and chemical study of Icelandic palagonite of varied composition and its bearing on the mechanism of the glass-palagonite transformation: Geochimica et Cosmochimica Acta, v. 55, p. 731–749.

Thorseth, I.H., Furnes, H., and Heldal, M., 1992, The importance of microbiological activity in the alteration of natural basaltic glass. Geochimica et Cosmochimica Acta, v. 56, p. 845-850.

Thorseth, I.H., Torsvik, T., Furnes, H., and Muehlenbachs, K., 1995, Microbes play an important role in the alteration of oceanic crust: Chemical Geology, v. 126, p. 137-146.

Thorseth, I.H., Pedersen, R.B., and Christie, D.M., 2003, Microbial alteration of 0-30-Ma seafloor and sub-seafloor basaltic glasses from the Australian Antarctic Discordance: Earth and Planetary Science Letters, v. 215, p. 237-247.

Torsvik, T., Furnes, H., Muehlenbachs, K., Thorseth, I.H., and Tumyr, O., 1998, Evidence for microbial activity at the glass-alteration interface in oceanic basalts: Earth and Planetary Science Letters, v. 162, p. 165-176.

Velde, B., 2013, Origin and mineralogy of clays: clays and the environment. Springer Science & Business Media

Walker, J.J., Pace, N.R., 2007, Phylogenetic composition of rocky mountain endolithic microbial ecosystems: Applied Environmental Microbiology, v. 73, p. 3497–3504.

Walton, A.W., 2008, Microtubules in basalt glass from Hawaii Scientific Drilling Project #2 phase 1 core Hilina slope, Hawaii: evidence of the occurrence and behavior of endolithic microorganisms: Geobiology, v. 6, p. 351-364.

Zimbelman, J.R., Scheidt, S.P., 2012, Hesperian Age for the Western Medusae Fossae Formation, Mars: *Science, v.* 336, no. 6089, p.1683, DOI: 10.1126/science.1221094.

APPENDIX 1A

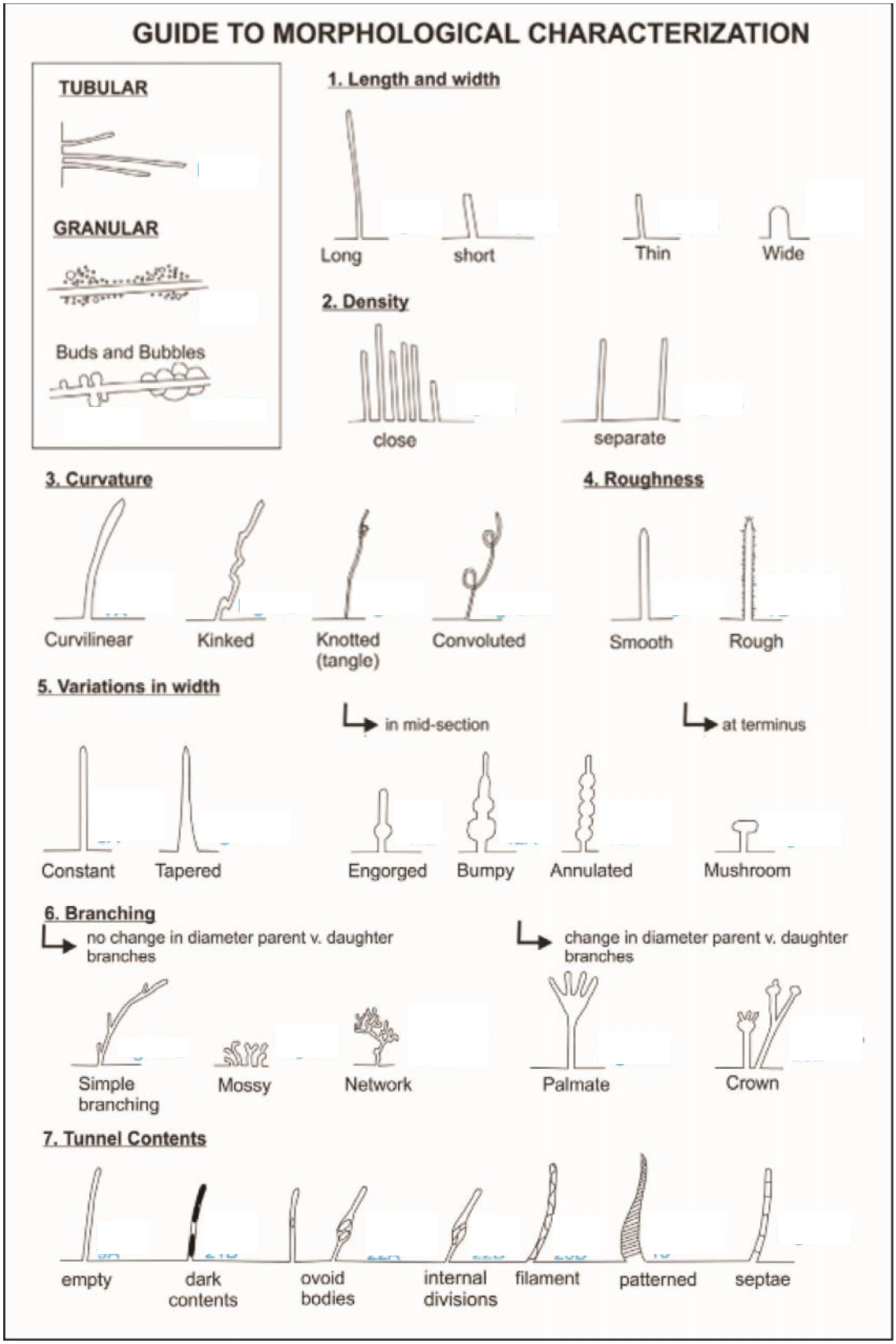
GUIDE TO MORPHOLOGICAL CHARACTERIZATION
TUBULAR
GRANULAR
Buds and Bubbles
1. Length and width
Long
short
Thin
Wide
2. Density
close
separate
3. Curvature
Curvilinear
Kinked
Knotted (tangle)
Convoluted
4. Roughness
Smooth
Rough
5. Variations in width
in mid-section
at terminus
Constant
Tapered
Engorged
Bumpy
Annulated
Mushroom
6. Branching
no change in diameter parent v. daughter branches
change in diameter parent v. daughter branches
Simple branching
Mossy
Network
Palmate
Crown
7. Tunnel Contents
empty
dark contents
ovoid bodies
internal divisions
filament
patterned
septae

APPENDIX 1A

GLOSSARY OF TERMS, DESCRIPTIONS, AND ILLUSTRATIVE FIGURES FROM FISK AND McLOUGHLIN (2013) USED TO DESCRIBE ALTERATION TEXTURES

Term	R	Description	Figure*
Annulated	f	Periodic increases and decreases in tunnel width	13A
Branch	f	Bifurcation of a tunnel	17B
Bulb	f	Round enlarged end of a tunnel	20A
Close	o	Distance between tunnels is <10 times the width of the tunnels, as measured on the surface of the thin section along the feature from which tunnels emerge	7A
Concentric rings	ts	Laminations that form semicircles around a point on a fracture	8B
Constant width	f	Tunnel diameter changes less than 20%	21B
Convoluted	f	Tunnel direction turns back toward starting point	24A
Crack	ts	Break in the material of the thin section that is interpreted to have been produced during or after the collection of the sample	9A
Crown	f	Enlarged end of a tunnel giving rise to multiple tunnels or other alteration features	20B
Dark border	f	Thin opaque granular/glass boundary	3A
Dark zone	f	Broad opaque granular region between a fracture and glass	4B
Directed	o	Multiple tunnels are parallel or nearly parallel to each other and trend in the same direction	5A
Empty	c	No visible contents	9A
Engorged	c	Tunnel with enlargement between its origin and end	11B
Fracture	ts	A break in the material of the thin section that is interpreted to have been produced in situ	16A
Glass	ts	Quenched silicate magma (sideromelane)	All
Granular	f	Micron- and submicron-size spherical and subspherical pits in glass or replacing glass	3B
Granular incursion	f	Granular alteration extending from fracture into glass without tunnels	8B
Hair tunnel	f	Thin (typically <1 μm), linear , colored or dark feature without separate margins	8A
Helical (form of tunnel)	f	Coiled tunnel	21A
High angle	o	Tunnels emerge nearly perpendicular to a glass/alteration border or fracture	22A
Honeycomb	c	Dark or opaque hexagonal pattern	15A
Intermediate enlargement	f	Single enlargement (annular bulge) between the origin and tip of a tunnel	11
Kinked	f	Multiple sharp angular bends in a tunnel	5A
Laminations	ts	Alternating thin, dark lines and broader, lighter areas in an area of alteration	29B
Light border	f	A thin granular/glass boundary with some darkening but not opaque	3A
Long	f	A tunnel whose length is >50 times its width	6A
Microphenocryst	ts	Mineral <300 microns long in glass or fine-grained matrix	28B
Mossy	f	Mass of dark, branched, short tunnels along the glass/alteration border	4B
Mushroom	f	Terminal enlargement that tapers	14A
Network	f	Multiple, branching, directed tunnels	19B
Node	f	Point of branching (bifurcation)	17B
Ovoid bodies	c	Cell-like features	22A
Palagonite	ts	Aqueous alteration of silicate glass	3A
Palmate	f	Branches that radiate from a point	20A
Parallel	o	Tunnels originate at high angle to a fracture and then turn parallel to the fracture	31
Pattern	c	Intricate filigree of dark or opaque material	15A
Petal	f	Flat tunnel form	14B
Preserved texture	ts	Alteration texture that remains visible after a second phase of alteration has occurred	29A
Quench crystal	ts	Crystal that formed as the magma was rapidly cooling	10B
Radiating	o	Tunnels originate and diverge from a point, microphenocryst, or other feature	25A
Random	o	Tunnels have many changes in direction and are not directed, and the length of the tunnel between changes of direction is not uniform	5A
Rough	f	Walls of the tunnel are irregular on a scale of 1 micron or less	10B
Separated	o	The distance between tunnels is >10 times the width of the tunnel, as measured on the surface of the thin section along the feature from which tunnels emerge	7B
Septa	c	Evenly spaced, dark divisions in a tunnel	23A
Short	f	Length of tunnel is <10 times its width	6B
Simple	f	Tunnel without branches, enlargements, or sharp changes in direction	9A
Smooth	f	The walls of the tunnel have no irregularities >0.5 microns	10A
Spiral	c	Linear filament wrapped inside a tunnel	13A
Tangle	f	Region of knotted appearance between origin and tip of a tunnel	8A
Tapered	f	Tunnel tapers to a point	13B
Terminal enlargement	f	Broadening of the tunnel at its terminus	11A
Thin	f	Alteration feature <3 microns from edge to edge	8A
Tunnel	f	Linear cavity with identifiable margins	22A
Variable width	f	Tunnel diameter changes more than 20% over its length	23A
Variole	ts	Cluster of quench crystals often nucleated on and radiating from a microphenocryst	24A
Wide	f	Alteration feature >10 microns from edge to edge	11A

Note: The second column (R) indicates if the term refers to an alteration feature (f), tunnel contents (c), organization of alteration features (o), or characteristics of thin sections (ts).

*Many terms are illustrated in more than one figure, but usually only one figure number is listed.

APPENDIX 1B

Example bioalteration values used to determine the extent of bioalteration within the Reed Rocks and Black Hills basaltic hydrovolcanic tuffs. A bioalteration value represents the visually estimated fraction of all alteration boundaries within a sideromelane clast that show textural exidence of bioalteration. Bioalteration values range from 0 to 10, and examples of values 0, 6, and 10 are shown. This is based on a method developed by Cousins and other (2009).

Bioalteration value	Description	Example thin section image
0	Any textural evidence of bioalteration is entirely absent from the sideromelane clast. Aqueous alteration is purely abiotic, producing a typical palagonite alteration boundary.	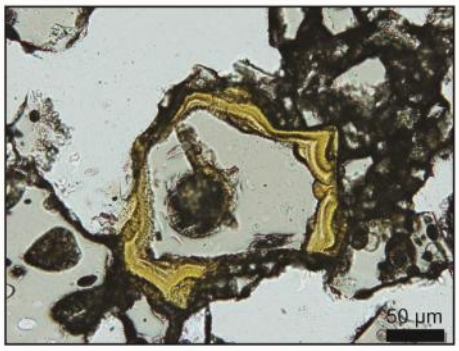
6	Textural evidence of bioalteration is present in 60% of the available sideromelane boundaries within a clast. This image shows a fracture and vesicle (bottom left) within a sideromelane clast, partially affected by bioalteration.	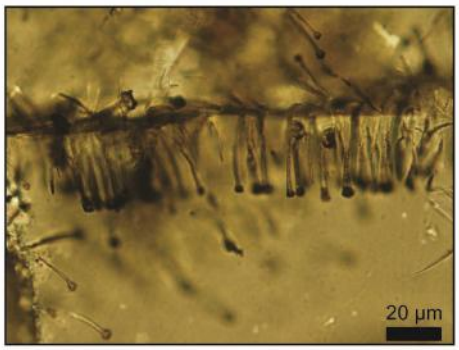
10	All boundaries (cracks, fissures, vesicles) within and around the sideromelane clast have undergone bioalteration. This image shows numerous microborings extending along the entire boundary of vesicles within a sideromelane clast.	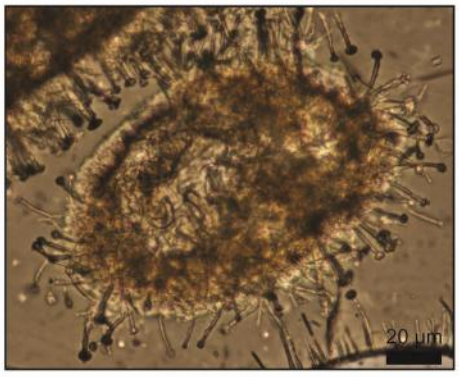

APPENDIX 1C

A summary of the morphological and petrological characteristics of tubular micro-cavities (TMCs) showing hypothesized mechanism of formation (McLoughlin et al., 2010).

	Euendolithic microborings	Ambient inclusion trails	Dissolution of Heterogeneities	Cryptoendolithic filaments	Chasmoendolithic filaments
Timing of Formation	Pre-metamorphic, dissolution of glass	Diagenetic to syn-metamorphic, form by migration in a solid substrate	Diagenetic	Pre-metamorphic growth into a fluid-filled cavity	Pre-metamorphic growth into a fluid-filled vein or fracture
Morphology	*Tubes with circular cross-section and variable diameters.* Maybe curvilinear, branched, annulated, helical, or show terminal swellings. Also granular clusters	*Tubes with polygonal cross-section and constant diameters. Show longitudinal straie*, are curvilinear, may be branched, helical, and some retain *terminal crystals*	*Show irregular diameters, may intersect*	Filaments with circular cross-section, of a non-uniform diameter are curvilinear, or branched, and may show swellings along their lengths	Filaments with circular cross-section, of non-uniform diameter, may be curvilinear, branched, show internal septae or terminal swellings
Infilling mineralogy	Clays, iron-oxyhydroxide, titanite with or without traces of carbon	Silica, carbonate, sulfide, chlorite, garnet, sometimes traces of carbon	Hollow, fluid-filled, or secondary minerals	Clays with or without organics	*Iron-oxides* or clays
Host matrix	*Volcanic glass or* meta-volcanic glass assemblage of: chlorite, quartz, epidote, and/or carbonate	Chert, i.e. microcrystalline silica, or phosphorite, fish scales, or chlorite	Sedimentary quartz grains or crystalline silicate minerals	Carbonate-filled vesicles	Carbonate or zeolite-filled veins
Distribution	Grow into glass are *rooted at external surfaces* such as pillow rims or the surface of volcanic glass fragment 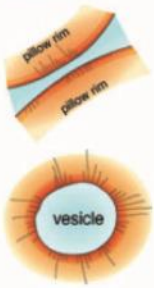	*Radial 'starburst' propagate outwards*, concentrated in the vicinity of organic material and/or pyrite grains. Or isolated examples 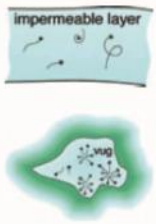	Show no preference for external surfaces and may intersect one another 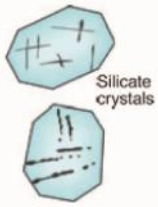	*Grow into cavities* 	Grow into fluid-filled vein or fracture, nucleate on walls 
Mechanical Abrasion	No	Very unlikely	No	No	No
Dissolution	Biologically mediated	Chemical and/or pressure dissolution	Chemical and/or pressure solution	Possibility of secondary chemical dissolution	Possibility of secondary chemical dissolution

The columns compare endolithic microborings (column 1) in volcanic glass; with ambient inclusion trails (AITs) (column 2) in sedimentary rocks and authigenic minerals; with the dissolution of pre-existing heterogeneities (column 3); with the remains of cryptoendolithic filaments (column 4) and chasmoendolithic filaments (column 5). The distinguishing criteria are gathered from a review of the literature, and diagnostic criteria are given in *italics*. In the sketches: fresh glass (brown); meta-volcanic glass (green); carbonate minerals or quartz (blue); microtubular cavities (black). Scale: vesicle approximately 500 μm across.

APPENDIX 2A

REED ROCKS SAMPLE LOCATIONS, ELEVATIONS AND THIN SECTION DESCRIPTIONS

Sample	Latitude	Longitude	Elevation (m)	Description	Abiotic (aqueous) Alteration	Bioalteration	Analyses
FR-12-90-1	N 43°20.125'	W 120°44.026'	1383	Matrix supported, aphyric hydrovolcanic coarse ash-lapilli tuff from resistant hydro-tuff ledge, angular to sub-angular blocky sideromelane shards (MGS 5.9 mm), ~40% fresh glass, low vesicularity (size range 30 µm to 6.5 mm), pl + ol phenocrysts/ fragmented crystals/glomerocrysts, pl microlites in glass, minor pl+px microlitic undercooling (varioles), ~23% porous	Low alteration (~5% gel-palagonitized) as ~0.1 mm rims along clast margins and vesicles, minor isopachous banding, very rare amygdaloidal/vug calcite (< 1%)	Rare granular alteration along clast margins (ABV 2.5)	pXRD, µXRD, SEM/BSE/EDS
FR-12-91A	N 43°20.135'	W 120°44.050'	1388	Very fine grained, clast supported hydrovolcanic tuff, occasional accretionary lapilli, angular to sub-angular blocky sideromelane shards with some scalloped edges (MGS 4 mm), ~ 38% fresh glass, fractures transecting vesicles, very low vesicularity (size range < 60 µm to 0.5 mm), euhedral pl+ol	Low to moderately altered (~7% gel-palagonitized along clast margins and vesicles), alteration rims ~0.05 mm), infrequent calcite vugs, rare red-brown oxides	Very low, rare granular and simple tubular types along clast margins/vesicles (ABV 1.3)	

Sample	Latitude	Longitude	Elevation (m)	Description	Abiotic Alteration	Bioalteration	Analyses
				phenocrysts and subhedral to anhedral fragmented crystals (0.1 - 1.5 mm), scattered pl+px varioles (undercooled microlitic intergrowths), ~22% porous			
FR-12-91B	N43°20.135'	W 120°44.050'	1388	Coarse grained, clast supported hydrovolcanic lapilli tuff, blocky angular to sub-angular to sub-rounded sideromelane shards (MGS 4 mm), ~38% fresh glass, lower fraction of coarse ash and fine ash more frequently cuspate angular shards, moderately vesicular (~8%, size range < 0.1 to 0.3 mm), euhedral pl+ol phenocrysts (0.1 - 1 mm) and glomerocrysts, sieved and twinned pl, ~22% porous	Low alteration (~5% gel-palagonitized), concentrated along clast margins ~0.05 mm thick, smaller grains are completely altered, rare sparry matrix calcite and red oxides	Low, branching and simple tubular type, granular alteration (ABV < 1)	
FR-12-92	N43°20.097'	W 120°44.035'	1389	Coarse grained, clast supported hydrovolcanic lapilli-tuff, blocky angular to sub-angular sideromelane shards with some cuspate to curved and flat margins (0.05 to > 12 mm), (MGS 12	Low to moderate (~7% palagonitized, ~1% fibro-palagonite), palagonitized along margins and vesicles, abundant vug and amygdaloidal calcite most frequently with	Minor branching and simple tubular and granular microborings (ABV <1)	pXRD, µXRD, SEM/BSE/EDS, $\delta^{18}O$, $\delta^{13}C$

Sample	Latitude	Longitude	Elevation (m)	Description	Abiotic Alteration	Bioalteration	Analyses
				mm), moderately vesicular (~11%, size range < 0.1 - 1.5 mm), euhedral to subhedral and anhedral broken pl+ol phenocrysts, and crystal fragments (0.05-1.2 mm), hopper ol, microlitic pl+px undercooled intergrowths/variolitic, minor opaques, ~20% porous	dendritic habit or radial concentric layering,		
FR-12-93	N43°20.061'	W 120°44.032'	1389	Coarse grained, clast supported hydrovolcanic coarse ash-lapilli-tuff from top of near vent outcrop, angular to sub-rounded sideromelane shards (~52% fresh glass) and lithics (<0.06 - 5.5 mm), (MGS 5.5 mm), moderately vesicular (~7%, size range < 0.2 - 1 mm), euhedral to subhedral pl+ol phenocrysts/glomerocrysts and crystal fragments (0.04-0.8 mm), sparsely variolitic pl+px microlites, ~20% porous	Low (< 2% palagonitized)	Very rare granular alteration (ABV 1.6)	pXRD, µXRD

Sample	Latitude	Longitude	Elevation (m)	Description	Abiotic Alteration	Bioalteration	Analyses
FR-12-94	N43°20.034'	W 120°44.047'	1388	Coarse grained, clast supported hydrovolcanic lapilli-tuff from vent proximal tafoni weathered outcrop, possibly vapour phase altered, angular blocky sideromelane shards (<0.06 - 11.8 mm), ~40% fresh glass, (MGS 11.8 mm), moderately vesicular (~12%), many vesicles has fluidized elongated and deformed shapes (size range <0.1 - 0.5 mm), lapilli are most vesicular, euhedral and anhedral pl+ol phenocrysts and crystal fragments (0.03-0.9 mm), sieved plagioclase, ~17% porous	Very low (~3% palagonitized along clast margins, highly calcite cemented-vugs, amygdules, sparry to matrix disseminated, highest calcite content (~13%), minor oxides	Low to moderate and diverse, all tubular types-spiral/branching, septae, terminal swells, ovoid bodies, and granular type (ABV < 1)	pXRD, µXRD
FR-12-96	N43°20.654'	W 120°44.262'	1406	Coarse grained, clast supported hydrovolcanic coarse ash-lapilli-tuff, angular to sub-rounded equant to sub-equant sideromelane clasts (~45% fresh glass) with flat/curvilinear to cuspate margins, (MGS 3.2 mm), rare lithics, moderately vesicular (~9%), some clasts have fluidized and stretched vesicles, circular to ovular	Low alteration (<2% palagonitized mainly at clast margins and along some vesicles, red oxides within matrix, rare amygdaloidal calcite	Little to none, possible rare granular alteration, (ABV 0)	

Sample	Latitude	Longitude	Elevation (m)	Description	Abiotic Alteration	Bioalteration	Analyses
				vesicles most frequent (<0.1 - 0.4 mm), euhedral to subhedral pl+ol phenocrysts and crystal fragments (0.03 - 1 mm), sieved/swallowtail and zoned pl phenocrysts, undercooled microlitic pl+px (brown), glass is pl microlite-rich (mottled appearance), ~22% porous			
FR-12-97A	N43°20.638'	W 120°44.242'	1408	Coarse grained, matrix supported hydrovolcanic lapilli-rich coarse ash tuff from tope of massive altered layer at RR, sub-angular to sub-rounded blocky lapilli to fine ash (<0.06 - 9.9 mm), most clasts have flat to curvilinear fracture surface margins, finer ash fraction have cuspate angular bubble junctions to blocky shapes, ~50% fresh glass, (MGS 9.9 mm), low to moderately vesicular (~7%) ranging from <0.2 to 1 mm, highly crystalline (~20%) - euhedral to subhedral (0.2 - 1 mm) pl+px phenocrysts and crystal fragments, zoned	Highly altered (~28% gel-palagonitized, minor fibro-palagonite ~1%), alteration fronts along clast margins, rare amygdaloidal and vug calcite (~1%), no zeolites	Moderately to highly bioaltered, mainly tubular microborings with terminal enlargements, lesser spiral filaments/simple/branching tubular types and rare granular alteration, concentrated mainly along vesicles and less along fractures and margins, (ABV 6)	

Sample	Latitude	Longitude	Elevation (m)	Description	Abiotic Alteration	Bioalteration	Analyses
				and sieved pl, brown microlitic pl+px undercooled clasts, ~16% porous			
FR-12-97B	N43°20.638'	W 120°44.242'	1408	Fine-ash-rich, matrix supported hydrovolcanic lapilli tuff from middle of massive altered layer at RR below FR-12-97A, angular to sub-angular blocky and vesicular sideromelane shards (6% fresh glass, MGS 8 mm), moderately to highly vesicular (~12%) mainly circular rounded-ovular shapes with some fluidized and stretched (size range <0.1 - 0.7 mm), moderately crystalline (~8% pl+ol phenocrysts and crystal fragments, hopper ol, ranging from 0.04 - 1.3 mm, ~ 2% undercooled microlitic pl+px), ~29% porous	Pervasively altered (~28% gel-palagonitized along vesicles, fractures, margins), frequent completely palagonitized clasts retaining primary shapes, amygdaloidal and vug calcite and zeolite, zoned amygdule with zeolites enclosing calcite	Moderately to highly bioaltered, mainly simple/branching/terminal enlargement bearing tubular types, lesser granular alteration, mainly along vesicles and clast margins, rare bioalteration (tubular and granular) overprinted by palagonitization, (ABV 5)	pXRD, µXRD
FR-12-97C	N43°20.638'	W 120°44.242'	1408	Fine grained, matrix supported hydrovolcanic ash-tuff from bottom of massive altered layer at RR below FR-1297B, angular to sub-angular blocky vesicular sideromelane shards	Highly/pervasively altered (~33% gel-palagonitized), the highest proportion of alteration at RRs, alteration front propagating from margins and vesicles,	Tubular types with terminal enlargements and engorgements/simple/branching, granular types, several extending beyond palagonitic alteration	pXRD, µXRD

Sample	Latitude	Longitude	Elevation (m)	Description	Abiotic Alteration	Bioalteration	Analyses
				(~17% fresh glass), clasts from <0.06 to 4.6 mm, (MGS 4.6 mm), low vesicularity (~6%, mainly circular to ocular shapes from 0.05 to 1.7 mm), euhedral to anhedral pl+ol phenocrysts/ glomerocrysts (0.03 - 1.7 mm), ~4% undercooled/ variolitic pl+px microlites (brown), melt inclusions in ol/pl, hopper ol crystals, ~16% porous	amygdaloidal and vug calcite-visible rhombohedral cleavage frequent	fronts, mainly along clast margins and vesicles, several tubular types appearing altered within tunnels, irregularity of alteration fronts distinct, tubules with 1-3 µm diameters/ 5-20 µm lengths, (ABV 5.6)	
FR-12-97D	N43°20.638'	W 120°44.242'	1409	Coarse grained, clast supported hydrovolcanic lapilli tuff from tafoni weathered layer at RR above FR-12-97A, possibly vapour phase altered, angular blocky to sub-rounded vesicular sideromelane pyroclasts (~50% fresh glass), occasional highly rounded clast, moderately vesicular (~12%, rounded circular to oblong and globular vesicles 0.1-1 mm), ~13% crystalline - euhedral to anhedral pl+ol phenocrysts/ glomerocrysts and	Low alteration (<1% palagonitized, possible disseminated f.gr. calcite in matrix	Low to none, possible rare simple and branching type on vesicles and margins, (ABV 0)	pXRD, µXRD

Sample	Latitude	Longitude	Elevation (m)	Description	Abiotic Alteration	Bioalteration	Analyses
				crystal fragments (0.1 - >1 mm), undercooled pl+px microlites/varioles (~6%), ~9% porous			
FR-12-97E	N43°20.638'	W 120°44.242'	1408	Coarse grained, matrix to clast supported hydrovolcanic lapilli-tuff from bottom of massive altered layer at RR-south of FR-12-97C, blocky angular to sub-angular sideromelane pyroclast shards (~21% fresh glass, from <0.05 to 7.9 mm), (MGS 7.9 mm), moderately vesicular (~10%, circular, oblong to globular shapes <0.05 - >1 mm), larger 1.5-2 mm vesicles indicates by partial vesicle walls along clast margins, highly crystalline (~14% euhedral to anhedral pl+ol phenocrysts, microlitic undercooled pl+px, sieved pl, <0.1 mm to 1.5 mm), ~28% porous	Highly altered (~22% gel-palagonitized from clast margins and vesicles, fine ash fragments are completely altered, amygdaloidal and vug calcite cements	Most highly bioaltered, mainly tubular types with terminal enlargements/ spherical ovoid bodies/ simple branching and septa bearing/annulated morphologies rooted on vesicles/fractures/margins, examples of tubule along fractures and connected vesicles infilled with calcite indicating formation prior to cementation, (ABV 8.8)	pXRD, µXRD, SEM/BSE/EDS, $\delta^{18}O$, $\delta^{13}C$
FR-12-98	N43°20.644'	W 120°44.430'	1418	Very fine grained laminated matrix to clast supported hydrovolcanic ash-tuff, alternation between coarse and fine ash 1-3 mm layers,	Moderate (~12% gel-palagonitized along clast margins and vesicles, 1-5 µm rims, no completely altered clasts, red oxides in	None, (ABV 0)	pXRD, µXRD

Sample	Latitude	Longitude	Elevation (m)	Description	Abiotic Alteration	Bioalteration	Analyses
				blocky angular to sub-angular sideromelane pyroclasts (~40% fresh glass), (MGS 12 mm), rare accidental lithics, moderately vesicular (~10%, 0.05 - 1 mm, circular to oblong and less frequent fluidized stretched shapes), ~11% euhedral to anhedral pl+ol phenocrysts (0.3-1.1 mm)/ glomerocrysts/~3% undercooled microlitic pl+px, infrequent opaques, ~28% porous	matrix, amygdaloidal and vug calcite		
FR-12-99	N43°20.628'	W 120°44.453'	1432	Hypidiomorphic, holocrystalline, poikilitic, porphyritic olivine basalt from RR lava cap, pl+ol anhedral to subhedral phenocrysts (0.1-2.2 mm)/ glomerocrysts (0.5-2 mm), magnetite (magnetic), dyktitaxitic, pl zonation, albite/Carlsbad/pericline twinning, sieved pl, ~65.9% groundmass of pl+ol+op, 19.9% vesicular, 10.7% pl phenocrysts, 3.5% ol phenocrysts	-	-	pXRD, µXRD, XRF

Sample	Latitude	Longitude	Elevation (m)	Description	Abiotic Alteration	Bioalteration	Analyses
FR-12-100	N43°20.636'	W 120°44.541'	1418	Hypidiomorphic, holocrystalline, poikilitic, porphyritic olivine basalt from RR intrusive dike, " "		-	XRF
FR-12-101	N43°20.317'	W 120°44.425'	1400	Hypidiomorphic, holocrystalline, poikilitic, porphyritic olivine basalt from lava flow, " "	-	-	XRF

MGS: Maximum grain size in thin section; ABV: Average bioalteration value; pl: plagioclase; ol: olivine; px: pyroxene; op: opaques; crystallinity = pl + ol + op + px; pXRD: powder X-ray diffraction; µXRD: micro X-ray diffraction; SEM/BSE/EDS: scanning electron microscope imaging/backscatter electron imaging/energy dispersive spectroscopy; XRF: X-ray fluorescence spectroscopy; $\delta^{18}O$, $\delta^{13}C$: oxygen-18 and carbon-13 isotope geochemistry of carbonate cements (mass spectrometry)

APPENDIX 2B

BLACK HILLS SAMPLE LOCATIONS, ELEVATIONS AND THIN SECTION DESCRIPTIONS

Sample	Latitude	Longitude	Elevation (m)	Description	Abiotic (aqueous) Alteration	Bioalteration	Analyses
FR-12-104A	N 43°10.155'	W 120°40.670'	1506	Matrix supported hydrovolcanic ash tuff, angular to sub-angular sideromelane shards (maximum grain size (MGS) 6 mm), ~24% fresh glass, low vesicularity, pl + ol phenocrysts/fragmented crystals, undercooling	Highly gel-palagonitized (~20%), carbonate cements (vugs + amygdales)	Granular and tubular branching types concentrated along vesicles/margins, average bioalteration value (ABV 10)	
FR-12-104B	N 43°10.155'	W 120°40.670'	1506	Matrix supported hydrovolcanic ash tuff, angular to sub-angular sideromelane shards (MGS 5 mm), ~18% fresh glass, moderate vesicularity/ rare matrix vesicles, pl + ol phenocrysts/ fragmented crystals, undercooling	Highly palagonitized (~19%), more crystalline isopachous fibro - palagonite (`6%) rims (margins and vesicles), completely palagonitized clasts altered matrix, calcite cements (vugs/amygdales) and replaced clasts (shapes preserved)	Granular, granular-bubble, tubular simple-complex branching, engorged, simple-convoluted, along margins/ vesicles/fractures (ABV 9.3)	µXRD
FR-12-104C	N 43°10.155'	W 120°40.670'	1506	Matrix supported fine-coarse ash hydrovolcanic tuff, blocky angular to sub-angular and highly fractured vitro-phyric sideromelane shards (MGS 10 mm), ~23% fresh glass, moderate vesicularity, pl + ol. phenocrysts/fragmented	Highly palagonitized (~23%), crystalline fibro-palagonite (~11%)-fibrous isopachous rims on vesicles/margins, crystalline altered matrix with fractures or contraction/desiccation features in consolidated matrix, brown smectite	Mostly granular type, (ABV 5)	

Sample	Latitude	Longitude	Elevation (m)	Description	Abiotic Alteration	Bioalteration	Analyses
				crystals, undercooling			
FR-12-105A	N 43°10.112'	W 120°40.680'	1518	Matrix supported hydrovolcanic lapilli-tuff, angular to sub-angular vitro-phyric sideromelane shards (MGS 7 mm), ~ 24% fresh glass, moderate vesicularity, pl + ol. phenocrysts/fragmented crystals, undercooling, lithics clasts	Highly crystalline fibro-palagonite (~10%), some calcite cements	Granular and simple-network branching/simple curved or convoluted tubular types mainly along margins and vesicles, (ABV 6.8)	
FR-12-105B	N 43°10.112'	W 120°40.680'	1518	Matrix supported coarse ash hydrovolcanic tuff, angular to sub-angular vitro-phyric to aphyric sideromelane shards, (MGS 10 mm), ~33% fresh glass, moderate vesicularity, pl + ol. phenocrysts/fragmented crystals	Low alteration- (~7%) palagonitized, fibrous and granularly crystalline fibro-palagonite, consolidated-palagonitized matrix with fractures infilled with calcite cements, calcite replaced clasts-some retaining palagonite cores-preserving primary textures	Granular, granular-bubble and simple curved tubular types, (ABV 7), some tubules originate from calcite-sealed vesicles	
FR-12-106	N 43°10.081'	W 120°40.728'	1540	Matrix supported ash tuff from tafoni weathered portion, angular to sub-angular phyric fine to coarse ash and lapilli sideromelane shards, (MGS 3.5 mm), ~34% fresh glass, moderate to high vesicularity (0.01-0.4 mm), pl + ol	Low alteration- (~7%) palagonitized along margins and vesicles/fractures, mostly amorphous gel-palagonite, calcite vugs/amygdales and calcite replaced clasts-preserving primary clast textures	Tubular types simple and complex branching/some annulated, engorged, or septae/rare terminal enlargements/ mainly simple curved or convoluted (1-2 µm diameter/10-50 µm lengths), pl avoidance,	SEM/BSE/ EDS

Sample	Latitude	Longitude	Elevation (m)	Description	Abiotic Alteration	Bioalteration	Analyses
				phenocrysts and crystal fragments, 0.4-1.3 mm glomerocrysts		margins/fractures/vesicles, radiate from some calcite sealed vesicles, (ABV 8.5)	
FR-12-107	N 43°10.076'	W 120°40.761'	1538	Matrix supported hydrovolcanic ash-tuff from radial fracture complex in outcrop, angular to sub-angular vitro-phyric to aphyric coarse to fine ash and lapilli sideromelane shards, poorly sorted, (MGS 2 mm), ~24% fresh glass, very low vesicularity (0.05-0.5 mm), pl + ol phenocrysts and crystal fragments, undercooling, rare ~ 2 mm lithics w/ opaques	Highly altered, (~19%) fibrous crystalline palagonite-rimming vesicles mainly-in areas adjacent to large transecting fractures-rims enclose amygdaloidal (calcite and zeolite), some zeolite vugs, granularly crystalline altered matrix	Pervasive tubular alteration-simple and complex branching/annulated/mainly simple curving to convoluted, (ABV 9.3), some 50 µm long w/ annular nodes (~1 µm width), most 60-90 µm long	µXRD, SEM/BSE/EDS
FR-12-108A	N 43°10.119'	W 120°41.014'	1467	Matrix supported hydrovolcanic ash tuff, angular to sub-angular vitro-phyric to aphyric fine to coarse ash and some lapilli sideromelane clasts, ~38% fresh glass, poorly sorted, (MGS 17 mm) clayey f.gr. consolidated and fractured matrix with disseminated diatomite, moderate vesicularity, pl + ol phenocrysts and glomerocrysts, some	Moderately altered, (~10%) palagonite-mainly amorphous gel-, no zeolite or carbonate cements	Mainly granular incursions and granular-bubbles from vesicles and margins, minor tubular - network branching and simple curvilinear, (ABV 1.7),	

Sample	Latitude	Longitude	Elevation (m)	Description	Abiotic Alteration	Bioalteration	Analyses
				rounded grains, undercooling (pl + px)			
FR-12-108B	N 43°10.119'	W 120°41.014'	1467	Scoria bomb	-	N/A	XRF
FR-12-110	N 43°10.157'	W 120°40.681'	1512	Matrix supported hydrovolcanic lapilli-tuff, angular to sub-angular vitro-phyric sideromelane fine to coarse ash and mainly lapilli clasts, ~26% fresh glass, moderate-high vesicularity, (MGS 6 mm), consolidated fractured and partially crystalline altered matrix, undercooling, pl + ol phenocrysts and glomerocrysts, undercooling (pl + px)	Low alteration, mostly gel-palagonite (~10%), matrix and vesicles/margins/fractures, fibrous vesicle rims and matrix alterations, negligible calcite (<1%), rare infilled fractures, red-brown oxide patches,	Tubular-mainly simple to complex branching and simple curving or convoluted, minor granular bubble, rooted on vesicles and less commonly margins, some granular bubble, (ABV 8.2)	
FR-12-111A	N 43°10.479'	W 120°40.091'	1459	Fine grained, clast supported, hydrovolcanic ash-tuff from above 111C, angular to sub-angular vitro-phyric sideromelane fine and coarse ash clasts, some lapilli, ~36% fresh glass, moderate vesicularity, (MGS 6mm), mainly pl phenocrysts and crystal fragments, minor ol and undercooling (pl + px)	Very low alteration (<2% palagonitized) vesicle rims, no calcite, rare zeolite vugs, rare diatomite accidentals	Granular textures surrounding vesicles and along some fractures-incursions and irregular front in glass, minor simple curved/convoluted tubular types avoiding pl crystals, (ABV 3.3)	

Sample	Latitude	Longitude	Elevation (m)	Description	Abiotic Alteration	Bioalteration	Analyses
FR-12-111B	N 43°10.479'	W 120°40.090'	1459	Medium grained, matrix supported, hydrovolcanic ash tuff from beside 111A, angular to sub-angular vitro-phyric sideromelane fine to coarse ash and lapilli clasts, ~29% fresh glass, low vesicularity, (MGS 10 mm), mainly pl phenocrysts, minor ol and undercooling, highly fractured glass shards, disseminated diatomite, rare obsidian clasts	Low alteration (~7%) fibro palagonite-fibrous and granularly crystalline vesicle and clast margins rims with isopachous bands, fibrous type shows radial extinction and finer layering, granularly crystalline type more common	Very low, granular, mostly granular-bubble/bubs, and tubular - network branching types mostly rooted on vesicles and fractures, (ABV 0.3)	
FR-12-111C	N 43°10.479'	W 120°40.091'	1458	Coarse grained, matrix supported, hydrovolcanic ash-lapilli-tuff from below 111A, angular to sub-angular sideromelane shards, ~35% fresh glass, (MGS 14 mm), moderate to high vesicularity, pl > ol, undercooling, disseminated diatomite, rounded obsidian clasts	Very low alteration (<2% palagonite),	Low, granular-bubble and tubular network branching/simple curved along fractures and vesicles (ABV 0.7)	
FR-12-112	N 43°10.463'	W 120°40.125'	1483	Medium grained, matrix supported, hydrovolcanic ash-tuff, angular to sub-angular fine and mostly coarse ash and some scalloped margin lapilli sideromelane shards, ~24% fresh glass, (MGS	Highly palagonitized (~12% crystalline fibro-palagonite), completely altered clasts showing fibrous bands around vesicles in granularly crystalline altered clasts, consolidated and	Pervasive, mainly simple curved and convoluted/simple and complex branching/ minor septae tubular types rooted on vesicles and margins and showing	SEM/BSE/ EDS

Sample	Latitude	Longitude	Elevation (m)	Description	Abiotic Alteration	Bioalteration	Analyses
				4 mm), as low as <0.01 mm, low vesicularity (0.01-0.9 mm), pl>>ol, undercooling (pl + px), highly crystalline lithic accidentals, melt inclusions in ol, 0.5-1.1 mm glomerocrysts, opaques mostly in accidental lithics	palagonitic matrix optically identical to altered clasts, altered at crystal-glass interfaces, glassy lithics with intense fibrous altered glass, larger lapilli and coarse ash are most altered	plagioclase/vesicle avoidance, up to 100 µm long/ 1µm wide, minor granular-bubble, (ABV 8)	
FR-12-113	N 43°10.415'	W 120°40.218'	1500	Medium to coarse grained matrix supported hydrovolcanic ash-tuff, blocky, angular to sub-angular to sub-rounded/ some scalloped margin-sideromelane shards, accretionary lapilli surrounded by opaque oxides, ~23% fresh glass, (MGS 11 mm), low vesicularity, pl>ol, undercooling (pl + px), pl-phyric accidental lithics,	Moderate (~10% gel-palagonitic), only crystalline accidentals have intense fibrous palagonitized portions between crystals-banding, altered solitary olivine grains (iddingsite)	Granular along margins, (ABV 7.3)	
FR-12-114	N 43°10.653'	W 120°39.800'	1432	Agglutinate lava	-	N/A	
FR-12-115	N 43°10.332'	W 120°39.878'	1453	Agglutinate lava	-	N/A	
FR-12-116-1x and x2	N 43°10.315'	W 120°40.152'	1510	Matrix supported, fine to coarse ash-tuff with moderate lapilli, blocky, angular to sub-angular, equant to inequant fractured sideromelane	Intensely altered (~14% fibro-palagonite)-includes clasts and altered matrix, very fibrous oriented banding (~5-10 µm thick) and	Low, mainly simple curved and convoluted tubular types, some simple branching, rare terminal enlargements or engorged/annulated	SEM/BSE/ EDS

Sample	Latitude	Longitude	Elevation (m)	Description	Abiotic Alteration	Bioalteration	Analyses
				shards, ~23% fresh glass, (MGS 10 mm), fine ash (<0.01 mm), largest fresh glass clast (5 mm), low vesicularity (0.01-0.3 mm), moderate undercooling, pl + px phenocrysts and minor glomerocrysts (0.3-1.5 mm), swallowtail and skeletal pl (0.05-0.4 mm), rare trachyitic textures, irregular ~4 mm voids, fractured/contracted matrix	randomly oriented, radial extinction, crystalline rims in vesicular undercooled lithics-fibrous to granularly crystalline	and granular-bubble, tubule from 10 to > 100 µm long/ 2-3 µm diameters, (ABV 0.3 and 1)	
FR-12-117A and B	N 43°10.277'	W 120°40.177'	1515	Laminated hydrovolcanic ash-tuff with alternating fine to med. gr. matrix supported and coarse ash clast supported layers, angular blocky to sub-angular sideromelane shards, ~28% fresh glass, (MGS 5 mm), low vesicularity and undercooling, pl>ol, rare ~1 mm pl glomerocrysts, clast supported layers with frequent intergranular voids, matrix with frequent mosaic fractures	Moderate (~14% palagonitized), completely altered clasts along transecting fractures showing isopachous bands (2-4 µm) around vesicles	Low to moderate, minor tubular simple branching/simple curved-convoluted/annulated and distinct engorged branching, rare granular bubble, mainly rooted on fractures and margins in partially palagonitized clasts, (ABV 3.7 and 5)	

Sample	Latitude	Longitude	Elevation (m)	Description	Abiotic Alteration	Bioalteration	Analyses
FR-12-118	N 43°10.173'	W 120°40.161'	1526	Matrix supported hydrovolcanic lapilli-tuff, angular fracture bound vesicle transecting sideromelane shards, ~27% fresh glass, (MGS 8 mm), moderate to high vesicularity-frequent irregular globular >100 µm vesicles, pl>ol vitro-phyric, moderately fractured clasts	Moderate (~9% fibro-palagonite)- fibrous banded vesicle rims/completely palagonitized clasts, calcite replaced clasts with primary textures preserved, fine grained bladed calcite rimming vesicles, amygdaloidal calcite	Low, minor simple curved/engorged-annulated/complex branching tubular types, minor granular, (ABV 3.3)	
FR-12-119	N 43°09.468'	W 120°39.977'	1512	Very fine grained matrix supported hydrovolcanic ash-tuff, angular to sub-angular or sub-rounded vitro-phyric to aphyric sideromelane shards, ~20% fresh glass, (MGS 1.1 mm for fresh glass, 7.7 mm pumice) low vesicularity and crystallinity, pl~ol, minor undercooling pl + px	Low (~6% palagonitized)-amorphous gel- mainly, rare calcite	Very low, rare complex branching/simple curved tubular types, minor granular-bubble along ol phenocrysts-glass interfaces, (ABV 0).	
FR-13-143	N 43°10.767'	W 120°41.906'	1385	Clast supported medium grained hydrovolcanic coarse ash-tuff, angular/sub-angular to sub-rounded with some scalloped margin sideromelane shards, mostly pl vitro-phyric, ~28% fresh glass, (MGS 2 mm), moderate	Moderately altered (~13 % gel-palagonite) initiated at margins and vesicles, rarer granularly crystalline fibro-palagonite, sparse amygdaloidal calcite	Very low, occasional granular and granular-bubble around vesicles, (ABV 1.3)	

Sample	Latitude	Longitude	Elevation (m)	Description	Abiotic Alteration	Bioalteration	Analyses
				vesicularity, highly crystalline (pl >> ol + undercooling pl + px), trachyitic (sub-parallel pl laths), very rare solitary px crystals, >300 µm pl glomerocrysts			
FR-13-144	N 43°10.764'	W 120°41.883'	1515	Clast supported hydrovolcanic lapilli-tuff, angular to sub-angular vitro-phyric sideromelane shards, ~27% fresh glass, (MGS 14 mm), moderately vesicular, highly crystalline (pl + ol phenocrysts)/undercooling pl + px microlites), solidified clayey matrix with transecting fractures, contraction spaces between vesicles and infilling matrix	Moderate alteration (~6% gel-palagonite, minor fibro-palagonite, granularly crystalline fibro- rims around vesicles, amorphous completely altered clasts with unaltered phenocrysts, rare red oxides	Rare granular alteration, (ABV 2.3)	
FR-13-145A	N 43°09.685'	W 120°41.560'	1526	Matrix supported hydrovolcanic lapilli-tuff, sub-angular to sub-rounded blocky elongate to equant vitro-phyric sideromelane shards (0.01 - 12 mm), ~22% fresh glass, (MGS 12 mm), very low vesicularity (0.3-2 mm), ~12% pl>>ol 0.05-4 mm phenocrysts and crystal	Moderate altered (~6% fibro-palagonite), distinct variable 5-10 µm thick band/lamination-alteration of fine matrix material and glass initiated at from void walls, most radial fibrous or lath like internal structure, partially calcite replaced pyroclasts from vesicles inward with	Very low, rare granular, (ABV 0.3)	µXRD, SEM/BSE/ EDS

Sample	Latitude	Longitude	Elevation (m)	Description	Abiotic Alteration	Bioalteration	Analyses
				fragments, poikilitic inclusions of pl in ol grains, accidental diatomite clasts and disseminated diatomite in matrix	some phenocrysts inclusions, amygdaloidal calcite		
FR-13-145 B-1 and 2	N 43°09.685'	W 120°41.560'	1526	Fine grained matrix supported hydrovolcanic ash-tuff, angular to sub-angular to sub-rounded with some scalloped margin vitro-phyric sideromelane shards, ~33% fresh glass, (MGS 1 mm), low vesicularity, pl>ol, sieved and zoned plagioclase phenocrysts, melt inclusions in ol grains, vesicular lithics and undercooled microlitic glass (pl + px)	Very low (<2% palagonitized), fine grained bladed calcite lining vesicles/voids	Low, sparse simple curved and branching tubular alteration, rare granular, (ABV 0.7)	
FR-13-145B-2	N 43°09.685'	W 120°41.560'	1526	Fine grained matrix supported hydrovolcanic ash-tuff, angular to sub-angular/sub-rounded vitro-phyric sideromelane shards-fracture bound-transect vesicles, ~22% fresh glass, (MGS 5 mm), low vesicularity, moderately crystalline (pl + ol) phenocrysts, swallowtail pl microlites, angular and rounded accidental	Moderately altered (~8% granularly crystalline fibro-palagonite) along margins and mainly vesicles-slight diffuse isopachous banding	Low, rare granular and simple tubular types rooted on vesicles, (ABV 2.7)	

Sample	Latitude	Longitude	Elevation (m)	Description	Abiotic Alteration	Bioalteration	Analyses
				diatomite lithics			
FR-13-146	N 43°09.725'	W 120°41.539'	1512	Matrix supported hydrovolcanic ash-tuff, angular to sub-angular vitro-phyric fine to coarse ash and lapilli sideromelane shards, low to moderate vesicularity, (MGS 9 mm), pl + ol phenocrysts, undercooling pl + px microlites	Moderately altered, gel- and granularly crystalline fibro-palagonite from margins and isopachous vesicles rims-single banded	Low, sparse simple curved-convoluted/annulated/rare terminal enlargement/septae/ mainly simple and network branching, (ABV 4.7)	
FR-13-148	N 43°09.854'	W 120°41.421'	1421	Coarse grained matrix supported hydrovolcanic lapilli-tuff from near vent agglomerate pyroclastic breccia, angular to sub-angular vitro-phyric coarse ash and lapilli sideromelane shards, (MGS 18 mm), moderate to high vesicularity, frequent highly vesicular accidental lithics, pl + ol phenocrysts	Moderately altered, most coarse ash are gel-palagonitized, scattered calcite cements in matrix and lining vesicles of accidentals (minor amygdaloidal), crescent shaped calcite cemented portions, very fine grained bladed amygdaloidal calcite lining vesicles	Low, rare granular alteration, (ABV 3)	
FR-13-149	N 43°09.691'	W 120°41.496'	1382	Fine grained, matrix supported hydrovolcanic ash-tuff from lower in sequence containing cm-scale elutriation pipes, blocky angular to sub-angular equant to sub-equant vitro-phyric fine-coarse ash and minor	Low alteration (~7% palagonitized), alteration of olivine to (iddingsite?) along margins and fracture/parting surfaces of solitary crystals in matrix	Low, rare granular-bubble alteration along vesicle surfaces, (ABV 1.3)	

Sample	Latitude	Longitude	Elevation (m)	Description	Abiotic Alteration	Bioalteration	Analyses
				lapilli sideromelane shards, some scalloped margins-some fracture bound surfaces-transecting vesicles, ~26% fresh glass, (MGS 7.1 mm), high crystallinity (~14%), pl>ol phenocrysts and crystal fragments, sieved pl, undercooled microlitic pl + px, moderately vesicular, rare vitro-phyric conchoidally fractured obsidian clasts			
FR-13-155	N 43°10.301'	W 120°42.037'	1372	Coarse grained, matrix supported hydrovolcanic pyroclastic lapilli-tuff from pyroclastic breccia-accidental rich, angular to sub-angular-sub-rounded fine-coarse ash and lapilli sideromelane shards, ~19% fresh glass, (MGS 4.2 mm), moderately vesicular, pl>>ol phenocrysts and crystal fragments,	Moderately altered (~13% gel-palagonite), fine bladed (~50 µm long) calcite lining walls of voids, traces of red oxides	Low-moderate, rare granular, minor simple curved and simple branching tubular types rooted on vesicles, (ABV 5)	
FR-13-156	N 43°09.649'	W 120°41.499'	1393	Coarse grained matrix supported hydrovolcanic lapilli-tuff, angular to sub-angular fine-coarse ahs and lapilli sideromelane shards,	Very low (sparse ~4% palagonitized)	Very low (ABV 1.3)	

Sample	Latitude	Longitude	Elevation (m)	Description	Abiotic Alteration	Bioalteration	Analyses
				~22% fresh glass, (MGS 12 mm), moderate-highly vesicular, pl>ol phenocrysts and crystal fragments, undercooled pl + px microlitic glass, consolidated matrix with transecting fractures, rare diatomite accidentals			
FR-13-157A	N 43°09.694'	W 120°46.637'	1319	Fine grained matrix supported hydrovolcanic ash-tuff , blocky angular to sub-angular mainly coarse and fine ash sideromelane shards with minor lapilli, ~28% fresh glass, (MGS 1.3 mm), low vesicularity, highly crystalline (~17% pl>>ol phenocrysts/glomerocrysts and crystal fragments, minor undercooling pl + px,	Moderately altered (~9% gel-palagonite), amygdaloidal calcite, extensive complete replacement of glass with calcite preserving primary texture/shape and enclosing unaltered phenocrysts (mostly pl laths), ~7% calcite	Low, mostly simple curved and minor simple branching/septae tubular types, minor granular/granular bubble-clast margins/fractures and vesicles, (ABV 3.3)	XRF
FR-13-157B	N 43°09.693'	W 120°46.637'	1319	Juvenile scoria bomb	-	N/A	
FR-13-158	N 43°09.675'	W 120°41.284'	1428	Medium grained matrix supported hydrovolcanic coarse ash-lapilli-tuff from horizontal bedding of tuff ring crest, blocky angular to sub-angular equant to elongate vitro-phyric sideromelane shards, ~18% fresh glass, (MGS 5.5 mm), low	Moderately altered (~10% gel-palagonite)-vesicle and margins, matrix alteration, rare red-brown oxidation (intergranular), calcite amygdales and vugs	Low, sparse simple curved/septae/ annulated-engorged/simple branching tubular types and minor granular bubble along mainly vesicles and fractures, some distinct >2 µm convoluted tubules	

Sample	Latitude	Longitude	Elevation (m)	Description	Abiotic Alteration	Bioalteration	Analyses
				vesicularity, highly crystalline (~18% pl>ol phenocrysts/glomerocrysts and undercooled pl + px microlites), rounded avesicular trachyitic accidental lithics, minor pumice		avoiding phenocrysts, (ABV 2.7)	
FR-13-159	N 43°09.606'	W 120°41.328'	1420	Medium grained matrix supported hydrovolcanic coarse-ash-lapilli-tuff from vertical bed near tuff ring crest, caliche surface coating, angular to sub-angular or sub-rounded sideromelane shards, moderately fractured, ~22% fresh glass, (MGS 6.8 mm), highly crystalline (~18% pl>undercooling pl + microlites>ol (phenocrysts crystal fragments), rare rounded trachyitic obsidian clasts	Moderate-high alteration (~15% gel-palagonitic) mainly along vesicles and within matrix, very deep red granular Fe-oxy-hydroxide alteration rimming vesicles in highly vesicular lapilli clasts-not observed in any other sample-may be associated with granular bioalteration-possibly reddened smectite grain replacement (RSGR) described by Walton and Schiffman (2003)-associated with minor gel-palagonite	Low, rare simple curved-convoluted/simple branching tubular and granular bubble types along vesicles or fractures, (ABV 2.3)	$\delta^{18}O$, $\delta^{13}C$
FR-13-160	N 43°09.595'	W 120°41.271'	1406	Matrix supported hydrovolcanic lapilli-tuff, angular to sub-angular or sub-rounded-rare scalloped margin coarse ash and lapilli vitro-phyric sideromelane shards in fine ash and calcite	Very low (< 1% palagonite), sparry and granular calcite cements in matrix	None observed, (ABV 0)	

Sample	Latitude	Longitude	Elevation (m)	Description	Abiotic Alteration	Bioalteration	Analyses
				cemented matrix, rare rounded accretionary lapilli, ~34% fresh glass, (MGS 9.5 mm), moderately to highly crystalline (~12%), moderately vesicular, rare rounded ~300 μm accretionary lapilli, pl>undercooling pl + px> ol phenocrysts and crystal fragments, rare diatomite clasts or disseminated in matrix			
FR-13-161	N 43°09.704'	W 120°41.257'	1426	Clast supported hydrovolcanic coarse ash-lapilli-tuff from near dike intrusion, angular to sub-angular or sub-rounded sideromelane shards, consolidated and fractured fine grained matrix, ~23% fresh glass, (MGS 7.8 mm), low vesicularity-many elongated pipe-like vesicles, highly crystalline (~ 29% pl>>>undercooled microlitic pl + px>>ol phenocrysts and glomerocrysts/crystal fragments	Highly altered (~17 % and ~10% amorphous gel- and granularly crystalline fibro-palagonite, respectively) - along vesicles/margins/fractures rare red oxides,	Moderate granular and granular-bubble and rare simple branching tubular alteration, (ABV 4.3)	

Sample	Latitude	Longitude	Elevation (m)	Description	Abiotic Alteration	Bioalteration	Analyses
FR-13-162	N 43°09.659'	W 120°41.056'	1475	Matrix supported hydrovolcanic coarse ash-tuff, angular to sub-angular vitro-phyric sideromelane shards, ~20% fresh glass, (MGS 6 mm), low vesicularity - regular circular shapes-micro-vesicular, high crystallinity (~14% pl>undercooled microlitic pl + px> ol phenocrysts/crystal fragments	Low (~7% gel-palagonite), rare red oxides	Moderate simple branching and rarer simple convoluted tubular alteration mainly rooted on vesicles-plagioclase and vesicle avoidance behaviour- some larger ~2 µm diameters and up to~50 µm long, rare granular-bubble alteration, (ABV 5.5)	
FR-13-163	N 43°09.669'	W 120°41.100'	1462	Very fine grained clast supported hydrovolcanic ash-tuff from alternating coarse and fine laminated layers, blocky angular to sub-angular avesicular coarse and fine ash sideromelane shards in very fine grained highly calcite cemented matrix moderately transected by fractures, ~37% fresh glass, (MGS 0.3 mm), very low vesicularity (< 2%), moderately to highly crystalline (~14% pl>undercooled microlitic pl + px> ol phenocrysts/crystal fragments, hopper olivine	Very low, (<2% gel-palagonite)-rarely found along clast margins showing clear colourless and clear yellow banded examples, matrix is infused with carbonates and some portion have distinct crescent-shaped and mottled appearance	Low, simple convoluted-curved/simple and complex network branching tubular types-some areas with clustered tubules radiating from diffuse single point connected to vesicle, rare granular-bubble type asymmetric along fractures connected to vesicles	

Sample	Latitude	Longitude	Elevation (m)	Description	Abiotic Alteration	Bioalteration	Analyses
FR-13-173-1	N 43°09.895'	W 120°41.243'	1414	Matrix supported pumiceous hydrovolcanic ash-tuff, angular to sub-angular fine to coarse ash and lapilli sideromelane shards-some fractures transecting vesicles-scalloped edges, very little fresh glass, (MGS 2 mm), low vesicularity, moderately crystalline (~13% albite twinned pl>undercooled microlitic pl + px> ol phenocrysts/crystal fragments, calcite cemented matrix, frequent pumice clasts, fractured matrix	Moderate to highly altered (~10% fibrously crystalline fibro-palagonite) - completely palagonitized clasts with radial fibrous vesicles rims and randomly oriented fibrous lath-like crystallites throughout, possible dendritic manganese oxide within calcite cemented matrix, calcite-filled fractures, ~18% calcite, large radial to finer grained calcite-filled pores in matrix (vugs)	Low, sparse simple curved-convoluted and simple branching tubular alteration mainly rooted asymmetrically along fractures and vesicles, vesicle avoidance-directionality, (ABV 2.3)	
FR-13-173-2	N 43°09.895'	W 120°41.243'	1414.5	Clast supported hydrovolcanic ash-tuff from above 173-1, angular to sub-angular fine to coarse ash and lapilli sideromelane shards, ~20% fresh glass, (MGS 7.3 mm), low vesicularity, > 300 µm pl>ol glomerocrysts, highly crystalline (~20% pl>>ol>undercooled pl + px microlites), open spaces between matrix and vesicle walls	Moderately to highly altered (~12% fibro-palagonite), completely altered lapilli-fibrously crystalline with radial vesicles rims/random fibrous-lath-like crystallites with unaltered pl and ol phenocrysts and glomerocrysts enclosed	Very low, rare simple curved-convoluted and possible terminal enlargement tubular alteration along vesicles, (ABV 0.7)	

Sample	Latitude	Longitude	Elevation (m)	Description	Abiotic Alteration	Bioalteration	Analyses
FR-13-173-3	N 43°09.895'	W 120°41.243'	1424	Matrix supported lapilli bearing fine ash tuff from above 173-2, blocky angular to sub-angular to sub-rounded fine to coarse ash and minor lapilli sideromelane shards, ~9% fresh glass, (MGS 17 mm vesicular lava clast) moderate to high vesicularity (~11% regular rounded-circular vesicles), swallow tail and albite twined pl, hopper ol, undercooled pl + px>pl phenocrysts>>ol phenocrysts and crystal fragments	Highly altered (~14% gel-palagonite), granularly crystalline fibro-palagonite along margins and vesicles-isopachous bands around vesicles, large > 400 µm optically continuous vug calcite with very fine grained bladed calcite on surface exposed to open space of pore, amygdaloidal calcite with mottled appearance, occasional red oxides	Moderate to high, frequent granular alteration beyond palagonite alteration fronts along margins and vesicles, (ABV 7.7)	
FR-13-174	N 43°09.943'	W 120°41.254'	1441	Coarse grained matrix supported hydrovolcanic lapilli tuff, blocky angular to sub-angular coarse ash and lapilli sideromelane shards, ~19% fresh glass, (MGS 21 mm), moderately vesicular (~11%), pl>>ol>undercooled pl + px microlites, ~1 mm ol>pl glomerocrysts, highly fractured ol crystal/fragments, spaces in matrix between vesicle wall and infilling	Highly altered (~15% and ~8% gel- and fibro-palagonite), isopachous regular banding/laminations around vesicles, altered olivine glomerocrysts (iddingsite?), amygdaloidal and vug calcite (~12%)	Moderate scattered granular alteration beyond palagonitic alteration front along margins and vesicles, (ABV 4)	

Sample	Latitude	Longitude	Elevation (m)	Description	Abiotic Alteration	Bioalteration	Analyses
				material			
FR-13-175A	N 43°09.988'	W 120°41.245'	1446	Matrix supported pumiceous and diatomaceous hydrovolcanic ash-tuff, blocky angular to sub-angular or sub-rounded sideromelane and scattered pumice clasts in fine grained matrix with disseminated diatomite and diatomite clasts, highest diatomite content, ~26% fresh glass, (MGS 4.9 mm), low vesicularity, low-moderate crystallinity (~9% pl>undercooled pl + px microlites>ol>Ti-magnetite)	Virtually unaltered, no visible palagonite or calcite/zeolite cements	Very low, rare granular, (ABV 0.7)	µXRD
FR-13-175B	N 43°09.988'	W 120°41.245'	1446	Coarse grained matrix supported hydrovolcanic lapilli-tuff from above 175A, angular to sub-angular coarse ash and lapilli sideromelane shards, ~40% fresh glass, (MGS 10.1 mm), moderately vesicular and crystalline, pl>>ol>undercooled pl + px microlites	Very low (<1% palagonitized), minor calcite	Very low to none, possibly sparse tubular types, (ABV 0)	

Sample	Latitude	Longitude	Elevation (m)	Description	Abiotic Alteration	Bioalteration	Analyses
FR-13-176	N 43°10.103'	W 120°40.929'	1480	Matrix supported hydrovolcanic lapilli-tuff, angular to sub-angular and scalloped edges with fractures transecting vesicle-sideromelane shards, ~37% fresh glass, (MGS 5.5 mm), low vesicularity, pl>undercooled pl + px microlites>ol phenocrysts and crystal fragments,	Low-moderate (~8% gel-palagonitized, fibrously crystalline fibro-palagonite with isopachous bands around vesicles and randomly oriented fibrous or lath-like crystallites in completely altered clasts, alteration along vesicle wall/margins/fractures, completely and partially calcite replaced clasts with primary textures/shapes preserved and unaltered pl laths enclosed	Low, simple curved-convoluted/simple and network branching tubular types with granular and granular-bubble alteration along fractures/vesicles, plagioclase and fracture avoidance behaviour, (ABV 2.3)	
FR-13-177	N 43°10.127'	W 120°40.886'	1504	Matrix supported hydrovolcanic coarse ash-lapilli-tuff, blocky angular to sub-angular or sub-rounded vitro-phyric sideromelane shards, scalloped edges-fracture bound, ~19% fresh glass, (MGS 6.4 mm), undercooled pl + px>pl >ol phenocrysts and crystal fragments, melt inclusion in olivine, consolidated fractured matrix, moderately vesicular-mostly rounded to oblong shapes, rare clast with stretched out pipe-like vesicles	Moderately altered (~12% gel-palagonite), granularly to partially fibrously crystalline fibro-palagonitic alteration of matrix-consolidated and desiccation-like fractured (contraction), gel-palagonite around vesicles and margins, slight isopachous rimming, calcite-filled fractures, vesicles (amygdaloidal) and voids (vugs) throughout matrix	High, frequent simple curved-convoluted and simple-network branching tubular alteration, minor septae bearing tubular, scattered granular and granular-bubble types along vesicles/fractures/margins, directional changes avoiding other vesicles/margins/tunnels/pl- crystals, often associated with gel-palagonite alteration fronts, some appear altered on interior, lengths >50 µm, some	SEM/BSE/EDS

Sample	Latitude	Longitude	Elevation (m)	Description	Abiotic Alteration	Bioalteration	Analyses
						bubble types rooted on calcite-sealed vesicles, (ABV 8.2)	
FR-13-178A	N 43°09.877'	W 120°40.740'	1530	Intrusive basaltic dike	-	N/A	XRF
FR-13-178B	N 43°09.877'	W 120°40.740'	1530	Intrusive basaltic dike	-	N/A	XRF
FR-13-179A	N 43°10.577'	W 120°40.696'	1407	Coarse grained matrix supported hydrovolcanic coarse-ash-lapilli tuff, angular to sub-angular sideromelane shards, ~28% fresh glass, (MGS 5.2 mm), undercooled pl + px>pl>ol phenocrysts and crystal fragments (~11% crystallinity), hopper ol, sieved-zoned pl, melt inclusions, variolitic textures	Low-moderately altered (~10% gel-palagonite) mainly along vesicles and margins, isopachous banding around vesicles, amygdaloidal calcite	Moderate simple curved-convoluted/simple-network branching tubular types occasionally rooted on calcite amygdales, scattered granular alteration at crystal-glass interface/vesicles, on location contains 'starburst' pattern of possible tubular alteration, tubular types exhibiting pl avoidance behaviour and common directionality	SEM/BSE/ EDS
FR-13-179B	N 43°10.577'	W 120°40.696'	1404	Very fine grained clast supported hydrovolcanic ash tuff, angular to sub-angular blocky mostly avesicular sideromelane shards, ~45% unaltered glass, (MGS 1.9 mm), pl>undercooled pl+ px microlites>ol phenocrysts and crystal fragments (~9%	Low (~7% gel-palagonite), mainly along clast margins with isopachous banding, slight alteration of matrix material	Low, rare simple curved tubular alteration from fractures and margins, sparse granular alteration (ABV 1)	

Sample	Latitude	Longitude	Elevation (m)	Description	Abiotic Alteration	Bioalteration	Analyses
				crystallinity), very low vesicularity (<3%)			
FR-13-180	N 43°09.966'	W 120°39.829'	1496	Medium grained matrix to clast supported hydrovolcanic coarse-ash-lapilli tuff, angular to sub-angular blocky fracture bound sideromelane shards with pervasive fractures throughout, ~24% fresh glass, (MGS 1.9 mm), undercooled pl+ px microlites>>pl>ol phenocrysts and crystal fragments, (~17% crystallinity, moderately vesicular	Low (~7% palagonitized), isopachous/banded vesicles rims up to ~50 µm thick, grainy crystalline fibro-palagonite mainly from vesicle walls and alteration-consolidation of matrix, amygdaloidal calcite	Low, occasional irregular granular fronts projecting from vesicles and along fractures, scattered simple-convoluted tubular types mainly rooted on fractures and vesicles, (ABV 1.7)	
FR-13-198	N 43°08.998'	W 120°39.767'	1527	Medium grained matrix supported hydrovolcanic coarse ash-lapilli tuff, angular to sub-angular blocky with some scalloped edge sideromelane pyroclast shards, ~15% fresh glass, (MGS 3.6 mm), undercooled pl+px microlites>pl>>ol>op phenocrysts and crystal fragments, hopper ol and sieved pl phenocrysts, low (~5%) vesicularity,	Moderately altered (~12% gel-palagonite), pyroclasts partially replaced by calcite with some primary textures preserved (vesicles/phenocrysts)-calcite is rougher and less regularly formed than in other samples with calcite replaced pyroclasts, amygdaloidal/vug and replacement calcite (~6%), very fine grained calcite	Low, mainly simple to convoluted or simple branching tubular types rooted on vesicles and fractures, rare simple tubular types extending beyond rough granular alteration fronts rooted on vesicles, examples of pl and vesicle avoidance, (ABV 2.7)	

Sample	Latitude	Longitude	Elevation (m)	Description	Abiotic Alteration	Bioalteration	Analyses

MGS: Maximum grain size in thin section; ABV: Average bioalteration value; pl: plagioclase; ol: olivine; px: pyroxene; op: opaques; crystallinity = pl + ol + op + px; pXRD: powder X-ray diffraction; µXRD: micro X-ray diffraction; SEM/BSE/EDS: scanning electron microscope imaging/backscatter electron imaging/energy dispersive spectroscopy; XRF: X-ray fluorescence spectroscopy; $\delta^{18}O$, $\delta^{13}C$: oxygen-18 and carbon-13 isotope geochemistry of carbonate cements (mass spectrometry)